Physiology and ecology of deep-sea *Bathymodiolus* symbioses

Dissertation
zur Erlangung des Grades eines
Doktors der Naturwissenschaften
- Dr. rer. nat. –

Dem Fachbereich Biologie /Chemie der
Universität Bremen
vorgelegt von

Målin Tietjen

Bremen
Dezember 2020

Die vorliegende Arbeit wurde vom April 2016 bis Dezember 2020 in der Abteilung Symbiose am Max-Planck-Institut für marine Mikrobiologie in Bremen unter der Leitung von Prof. Dr. Nicole Dubilier und Dr. Harald Gruber-Vodicka als direktem Betreuer angefertigt.

Gutachter:

Prof. Dr. Nicole Dubilier
Prof. Dr. Ute Hentschel Humeida

Tag des Promotionskolloquiums:

28. Januar 2021

Diese zur Veröffentlichung erstellte Version der Dissertation enthält Korrekturen.

“Do, or do not. There is not try.”

- Yoda -

Für Opa.

Contents

“Wikipedia is the best thing ever.
Anyone in the world can write anything they want about any subject.
So you know you are getting the best possible information.”
- Michael Scott -

Summary

The deep sea represents the largest ecosystem on Earth, and is characterised by permanent darkness, high pressure and low temperatures. Despite the seemingly harsh environmental conditions, the deep sea sustains a high biomass that is mostly concentrated around hydrothermal vents and cold seeps. In these 'oases of life', chemosynthesis, the process of converting chemical energy into biomass, enables certain animal groups to form dense populations. One of the dominant animals at hydrothermal vents and cold seeps are mussels of the genus *Bathymodiolus* that harbour bacterial symbionts in their gills. Depending on the composition of the surrounding vent and seep fluids, the mussels contain one or two bacterial types that use methane or sulphur compounds as energy sources for chemosynthesis to thrive and to feed their host animal.

Hydrothermal vents and cold seeps are highly dynamic ecosystems in which physico-chemical conditions can fluctuate over time. Understanding the degree of physiological adaptation of the deep-sea *Bathymodiolus* symbioses to such fluctuating conditions can shed light onto their ecological success in these rather extreme habitats. The research presented in my doctoral thesis focuses on the physiological adaptations of *Bathymodiolus* mussels and their chemosynthetic symbionts to short- and long-term limitations of chemical energy sources that sustain the metabolism of the symbiotic partners. Although numerous physiological studies have been conducted on the *Bathymodiolus* symbiosis, it was elusive to what extent the transcriptomes of host and symbionts in *Bathymodiolus* mussels were influenced by deep-sea sample recovery. With my thesis, I settled these uncertainties and uncovered that the expression profile of the host is largely unaffected by the sampling procedure, while the symbionts displayed strong physiological responses (Chapter II). Highly similar responses were also observed in an *in situ* displacement experiment, where *Bathymodiolus* mussels were removed from vent fluids for 10 days (Chapter IV).

Previous laboratory-based and *in situ* studies demonstrated that symbiont abundance is affected by the availability of their respective energy source. I used symbiont loss, induced by a long-term aquarium maintenance at low methane concentrations, to track transcriptomic responses of the host with respect to their symbiont load. I took advantage of this spatial distribution of the symbionts within the mussel gills, where symbionts locate in a distinct region from non-symbiotic cells. By separately analysing the transcriptomes of both gill regions, I was able to allocate host metabolic processes specifically to the symbiont-containing region and identified bacteriocytes as main drivers of gill immunity in bathymodiolin mussels with a fine-tuned ability to sense and respond to symbiont load (Chapter III). In summary, my studies unravel the natural physiological state of deep-sea *Bathymodiolus* mussels, how symbiont physiology is affected by changing environmental conditions, and how the mussels "control" their symbiont population in terms of numbers and potential bacterial invaders.

Zusammenfassung

Die Tiefsee ist das größte Ökosystem der Erde und wird von permanenter Dunkelheit, niedrigen Temperaturen und einem hohen Wasserdruck geprägt. Trotz dieser rauen Umweltbedingungen findet sich in der Tiefsee eine riesige Biomasse, die vor allem an Hydrothermalquellen und Cold-Seeps vorkommt. In diesen 'Oasen des Lebens' ermöglicht die Chemosynthese, ein Prozess in dem mit Hilfe chemischer Energie Biomasse generiert wird, einigen Tiergruppen eine hohe Populationsdichte. Eine der an solchen Quellen dominierenden Tiere sind Muscheln der Gattung *Bathymodiolus*, die in ihren Kiemen bakterielle Symbionten beherbergen. Abhängig von der chemischen Beschaffenheit des Meerwassers an diesen Quellen haben sie dabei einen oder zwei bakterielle Arten, die entweder Methan oder Schwefelverbindungen als Energiequelle für die Chemosynthese nutzen, um dort zu überleben und gleichzeitig ihren Wirten mit Nährstoffen zu versorgen.

Hydrothermalquellen und Cold-Seeps sind dynamische Ökosysteme, in denen sich die physikochemischen Bedingungen temporär ändern können. Ein tiefgehendes Verständnis über die physiologische Anpassungsfähigkeit der Tiefseemuscheln *Bathymodiolus* an solche fluktuierenden Bedingungen kann Erkenntnisse über ihren ökologischen Erfolg unter eher extremen Umweltbedingungen bringen. Im Rahmen meiner Doktorarbeit fokussiere ich mich auf die Physiologie der *Bathymodiolus* Muschel und ihrer chemosynthetischen Symbionten, und untersuche die Auswirkungen von Kurz- und Langzeit-Änderungen der physikochemischen Gegebenheiten, die normalerweise den Metabolismus der symbiontischen Partner aufrechterhalten. Denn obwohl schon zahlreiche Studien über die Physiologie der *Bathymodiolus* Muschel existieren, ist die Physiologie aller Partner unter natürlichen Bedingungen bislang nur bedingt erforscht. Hinzu kommt ein fehlendes Verständnis über den Umfang der Exprimierungsänderung im Wirt und im Symbionten, die bei der Beprobung von Muscheln aus der Tiefsee entstehen können. Mit meiner Doktorarbeit habe ich Teile dieser Unklarheiten aufklären können und gezeigt, dass die Physiologie des Wirtes bei der Erprobung aus der Tiefsee eher unbeeinträchtigt ist, sich allerdings die Expressionsprofile der Symbionten stark verändern und sie damit physiologische Anpassungen aufzeigen (Kapitel II). Sehr ähnliche physiologische Antworten der Partner konnten auch in einem Tiefseeexperiment gezeigt werden, in dem Muscheln für über 10 Tage von ihrer hydrothermalen Quelle entfernt worden sind (Kapitel IV).

Vorherige Labor- und *in situ*-basierte Studien haben gezeigt, dass sich die Symbiontenanzahl in Abhängigkeit der vorhandenen chemischen Energie verändert. Den Symbiontenverlust, induziert durch eine Langzeithälterung in Aquarien mit geringer Methankonzentration, habe ich genutzt um die Expressionsänderungen des Wirts in Abhängigkeit der Symbiontenanzahl zu analysieren. Dabei habe ich mir Zunutze gemacht, dass die Symbionten nur in einem bestimmten Teil der Kieme vorkommen, wohingegen andere Regionen und Zellen frei von Symbionten sind. Durch die separate Analyse der Transkriptome beider Regionen war es möglich zu identifizieren, welche metabolischen Prozesse des Wirts spezifisch für den Bereich sind, der die Symbionten beherbergt. Ich konnte verdeutlichen, dass die Bakteriozyten die Schlüsselzellen der Kiemenimmunität der *Bathymodiolus* Muscheln sind, mit einer sensiblen Fähigkeit zur Identifizierung und Antwort auf Symbiontenabundanzen (Kapitel III).

Zusammengefasst trägt meine Doktorarbeit zu einem besseren Verständnis bei, welche Physiologie die Tiefseeorganismen - in diesem Fall die *Bathymodiolus* Muschel - in ihrer natürlichen Umgebung haben, wie sich die Physiologie der Symbionten durch sich verändernde Umweltbedingungen beeinflusst, und auch wie die Muscheln ihre Symbiontenpopulation kontrolliert und sich vor anderen Bakterien in ihrer Umwelt schützt.

Chapter I | Introduction

The deep sea ecosystem

The oceans cover more than two-thirds of the Earth's surface, reaching average depths of 3,800 meters. Characterised by permanent darkness, high pressure and rather cold temperatures, the deep sea represents the largest ecosystem on Earth (Nybakken and Bertness, 2005). In spite of the seemingly harsh environmental conditions, the deep sea is home to a vast biodiversity (Ramírez Llodra and Billett, 2006). To study these deep-sea symbioses, state-of-the-art technology is required. This includes high-tech diving vehicles (e.g. remotely operated vehicles, ROVs), alongside high definition cameras and several instruments for measuring parameters *in situ* and sophisticated sampling equipment (Borin and Daffonchio, 2010).

The deep-sea can be divided into two major habitats, the heterotrophic and the chemosynthetic habitat (Ramírez Llodra and Billett, 2006). In the former, the animal communities depend on organic matter sinking down to the seafloor. In chemosynthetic habitats, the biota is sustained by microorganisms that use energy of reduced compounds to produce biomass (Jannasch, 1985).

Two of the known chemosynthetic habitats, hydrothermal vents and cold seeps, are of key importance for this thesis and are described in more detail in the following section.

Hydrothermal vents and cold seeps

Hydrothermal vents occur at the mid-ocean ridges at the periphery of continental plates (Rogers *et al.*, 2012; Figure 1). At these boundaries, new ocean crusts are forming as a result of seafloor-spreading (Van Dover, 2000). Through cracks and fissures that result from the spreading, seawater diffuses into the crust and is heated by an underlying hot source like magma (Tivey, 2007; Munn, 2020). The heated fluid moves upwards through the crust and re-emerges at the vents carrying dissolved chemicals that precipitate upon mixing with seawater and form the characteristic black plumes (German *et al.*, 2016). The hydrothermal vents also release volatiles like hydrogen sulphide, methane, carbon dioxide and hydrogen (Tivey, 2007;

Wankel *et al.*, 2011). High temperatures are characteristic for hydrothermal vents, where the plumes can reach temperature of more than 400°C (Perner *et al.*, 2014).

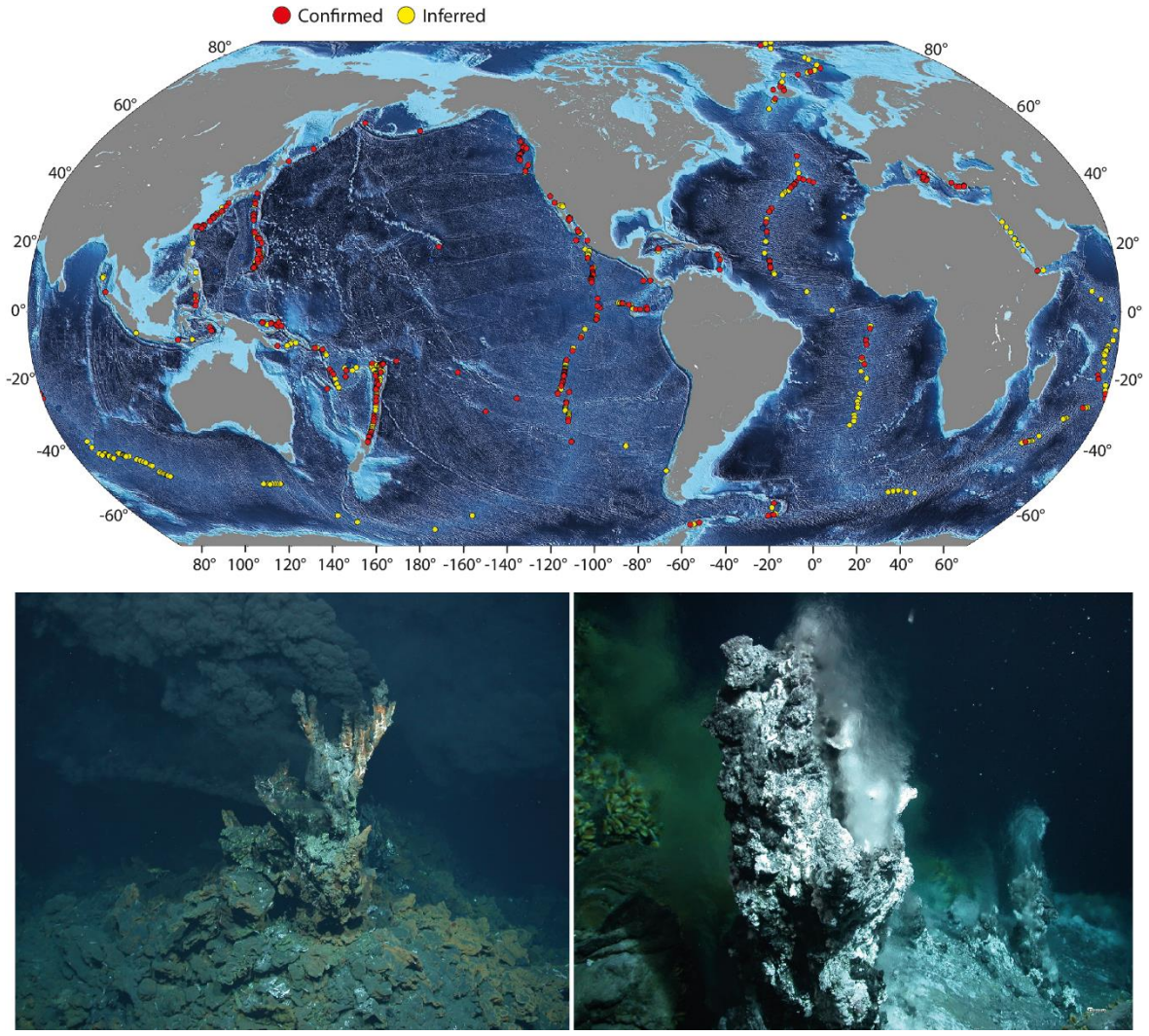

Figure 1: Map of hydrothermal vents around the globe. The map shows all known and predicted hydrothermal vents on Earth. Currently 666 vent fields have been confirmed and another 55 vents are inferred from plume data. Map was downloaded and modified from: https://doi.org/10.1594/PANGAEA.917894. Two examples of hydrothermal vents from the Mid-Atlantic Ridge showing a typical 'black smoker' chimney at the vent field Logatchev (left) and a hydrothermal venting at Menez Gwen (right). Both photographs © MARUM.

The first hydrothermal vents were discovered at the Galapagos Rift in 1977 (Weiss *et al.*, 1977). Since then, more and more hydrothermal systems are discovered around the world, with the most recent ones in 2016 and in 2018 ("Luso") in the Mid-Atlantic Ridge (https://vents-data.interridge.org/ventfield/luso).

In contrast to the hot hydrothermal vent ecosystems, cold seeps represent the colder chemosynthetic environments of the deep sea (Figure 2). In these habitats, low-temperature fluids are rich in reduced chemicals produced through microbial transformation, and represent the largest biomass and high productivity (Ristova *et al.*, 2015). Characteristic for cold seep ecosystems is the distinct bubbling of free and dissolved methane that strongly influence the the local carbon cycle and therefore also on the present organisms (Greinert *et al.*, 2010).

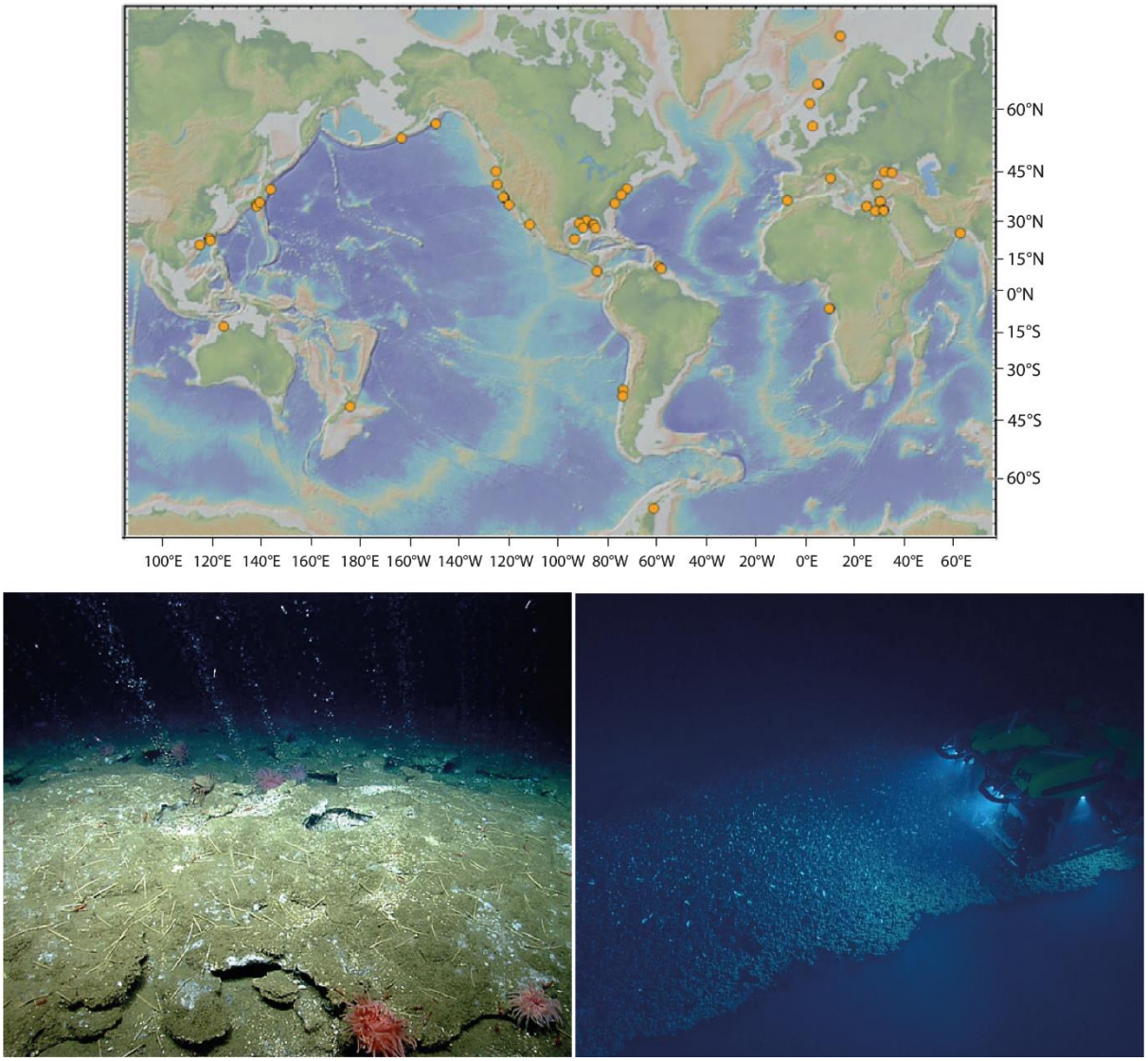

Figure 2: Map of cold seeps around the globe. Map of cold-seeps (orange dots) with hydrocarbon seepage. Map modified from Ruff (2020). Photographs of two cold-seeps in the North-Western Atlantic. Characteristic bubbling of methane at a cold seep in the off the Virginian shore (left; © NOAA Office of Ocean Exploration and Research), and an underwater brine pool characteristic for cold seeps in the Gulf of Mexico (right; © Ocean Exploration Trust).

Chemosynthesis enables life at hydrothermal vents and cold seeps

Many hydrothermal vents and cold seeps were found to contain large assemblages of animals including vestimentiferan worms, clams and mussels (Nybakken and Bertness, 2005; Figure 3). Because of the absence of light for primary production driven by photosynthesis, deep-sea animals must rely on other sources for nutrition. Several deep-sea animals live in symbiosis with bacteria that can use the chemical energy from vent and seep fluids to produce biomass (Dubilier *et al.*, 2008). In the process of chemosynthesis, reduced compounds such as

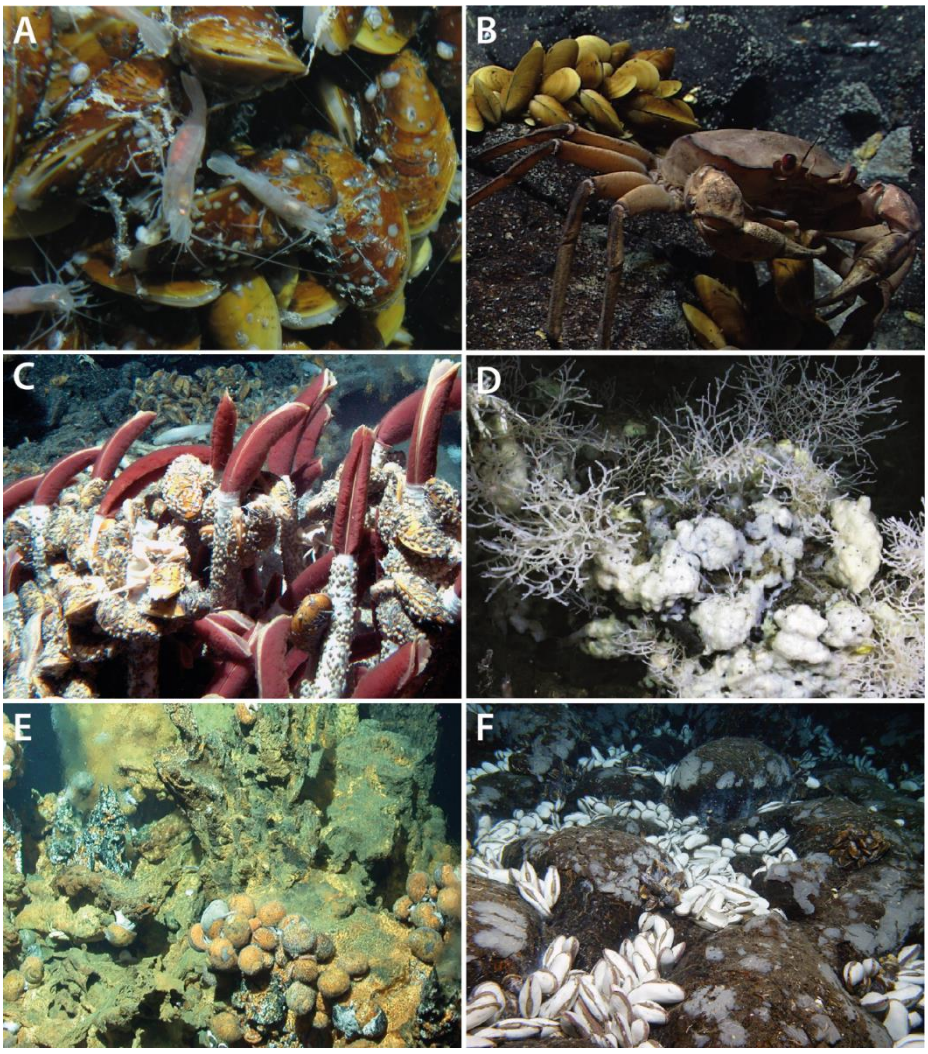

Figure 3: A glimpse of the biodiversity at hydrothermal vents and cold seeps. Examples of biota at hydrothermal vents (*A-C* and *E-F*) and cold seeps (D). ***A:*** Shrimps on a bathymodiolin mussel bed. ***B:*** Crab feeding off bathymodiolin mussels. ***C:*** Giant *Riftia* sp. tubeworms surrounded by bathymodiolin mussels. ***D:*** Two types of sponges from a cold seep in the Gulf of Mexico. ***E:*** Snails at a chimney. ***F:*** *Calyptogena* sp. clams. Images A, B, D and E © MARUM, images C and D © 2013 Dive and Discover™, Woods Hole Oceanographic Institution.

hydrogen sulphide, methane or hydrogen are oxidised by the bacterial symbionts to produce biomass (Petersen *et al.*, 2011; Hinzke *et al.*, 2019; Rubin-Blum *et al.*, 2019). Chemosynthesis builds the foundation for life in these habitats, which are commonly referred to as 'oases of life' (Jannasch, 1985; Van Dover, 2000). At hydrothermal vents and cold seeps, the animals harbouring chemosynthetic bacteria live adjacent to the energy-rich fluids and oxygenated water to ensure their survival (Stewart *et al.*, 2005). This close proximity to vent and seep fluids exposes the animals to highly variable physico-chemical conditions (Seston *et al.*, 2016).

The bathymodiolin symbiosis

The bathymodiolin mussel host

The most dominant genus of bathymodiolin mussels are those of the genus *Bathymodiolus*. *Bathymodiolus* mussels are globally distributed and have been found in deep-sea chemosynthetic habitats in the Pacific, Atlantic, and Indian Ocean, encompassing around 20 described species (Génio *et al.*, 2008). Only recently, three additional *Bathymodiolus* species have been identified in seeps from the Costa Rica margin (McCowin *et al.*, 2020).

At hydrothermal vents and cold seeps, bivalve mussels of the subfamily Bathymodiolinae (Bivalvia; Mytilidae) are one of the dominant macrofauna forming dense mussel beds in these habitats (Figure 4; Laming *et al.*, 2018). Typical for bivalves, bathymodiolin mussels are completely enclosed within a pair of shells that are opened or closed *via* adductor muscles (Barnes *et al.*, 2001). Through inhalant and exhalent siphons, the mussels draw seawater across the highly enlarged gills, which are the respiratory and feeding organs of the animals (Gosling, 2015)

The mytilid gill is organised in W-shaped filament stacks that are bilaterally symmetrical with dense ciliation that drives water flow (Cannuel *et al.*, 2009). In contrast to shallow-water mytilids, the ciliation of cells in bathymodiolin gills is concentrated towards the edge of the gill filament (Figure 5). This so-called ciliated edge is distinguishable from the rest of the gill filaments. The cells in this region contain a high number of mitochondria and show frontal, latero-frontal and lateral ciliation to produce the water currents (Fiala-Médioni *et al.*, 1986). Water is pumped through the animal to enable gas-exchanges *via* the gills (Gosling, 2015). *In situ* measurements of oxygen consumption in *Bathymodiolus* mussel showed that the respiration rate of these mussels was as high as in shallow-water mussels (Khripounoff *et al.*, 2017).

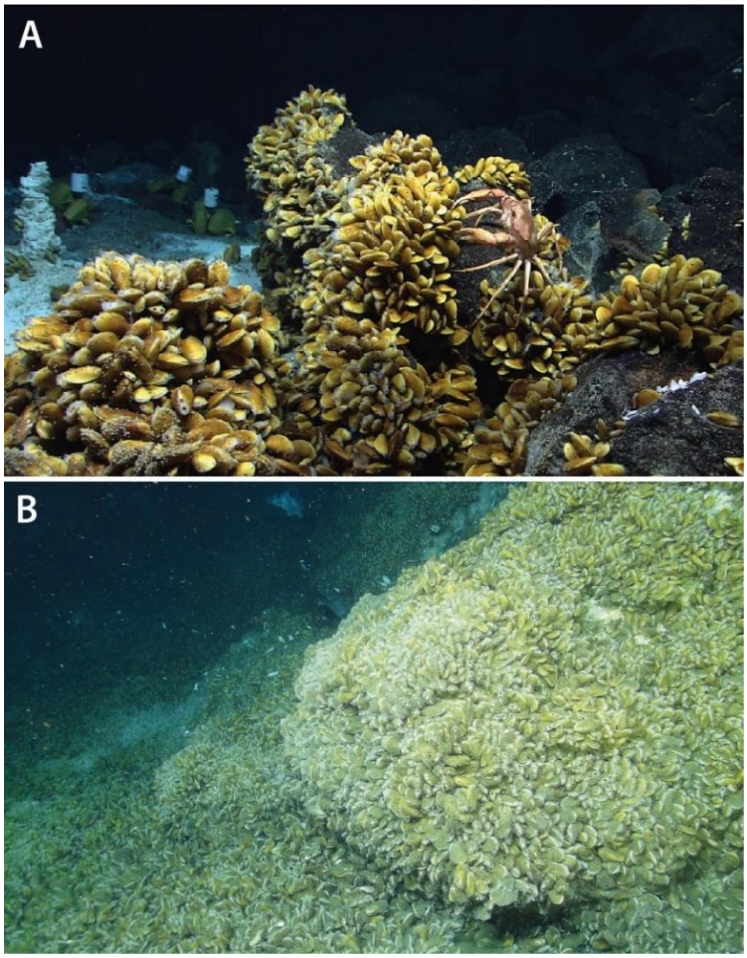

Figure 4: *Bathymodiolus* spp. mussels at hydrothermal vents and cold seeps. ***A:*** Mussels colonise dense patches close to diffuse fluids at hydrothermal vents in the Mid-Atlantic Ridge. Image © MARUM. ***B:*** Mussel bed at a cold seep on the US Atlantic coast. Image © Deepwater Canyons 2013 Expedition, NOAA-OER/BOEM/USGS.

One of the most striking features of bathymodiolin mussels are the highly enlarged gills. In fact, the surface of gills from symbiotic mytilid mussels is about 20-fold higher than in shallow-water relatives (Duperron *et al.*, 2016). In these organs, the mussels harbour chemosynthetic bacterial symbionts that provide nutrition for their host (Dubilier *et al.*, 2008). The colonisation of the mussel gill ensures access to seawater that contains energy sources from the hydrothermal vents (Distel *et al.*, 1995). In all known bathymodiolin species, chemosynthetic symbionts have been discovered (Petersen *et al.*, 2012). The symbionts are transmitted from the environment into the host gills (horizontal transmission) on the onset of the development of the gill tissue after metamorphosis (Wentrup *et al.*, 2014; Franke *et al.*, 2020).

Bathymodiolin mussels live in symbiosis with chemosynthetic bacteria

Two dominant Gammaproteobacteria associate with *Bathymodiolus* mussels, and depending on the environment, the mussels harbour either a methane-oxidising (methanotrophic) or a sulphur-oxidising (thiotrophic), or both symbionts in their gills (Riou *et al.*, 2008). Typically, the thiotrophic symbiont is the more dominant phylotype in such dual symbioses, and may be explained by higher abundance of sulphur compounds in the environment (Duperron *et al.*, 2016). The methanotrophic symbiont is a Type I methanothroph and uses methane as main carbon and energy source to assimilate biomass (Kochevar *et al.*, 1992; Petersen and Dubilier, 2009). Its closest free-living relative is *Methyloprofundus sedimenti* that has been isolated from whale fall sediments (Tavormina *et al.*, 2015). The thiotrophic symbiont can use a different reduced sulphur compounds as an energy source for chemoautotrophic carbon fixation (Duperron *et al.*, 2006). Like the symbionts of vesicomyid clams, the thiotrophic symbiont of *Bathymodiolus* mussels can also store elemental sulphur as energy source in the absence of an external sulphur source (Pruski *et al.*, 2002; Khripounoff *et al.*, 2017). The detailed metabolism of both symbiont has been reconstructed in previous literature (Figure 6), illustrating high metabolic interdependencies between host and symbionts.

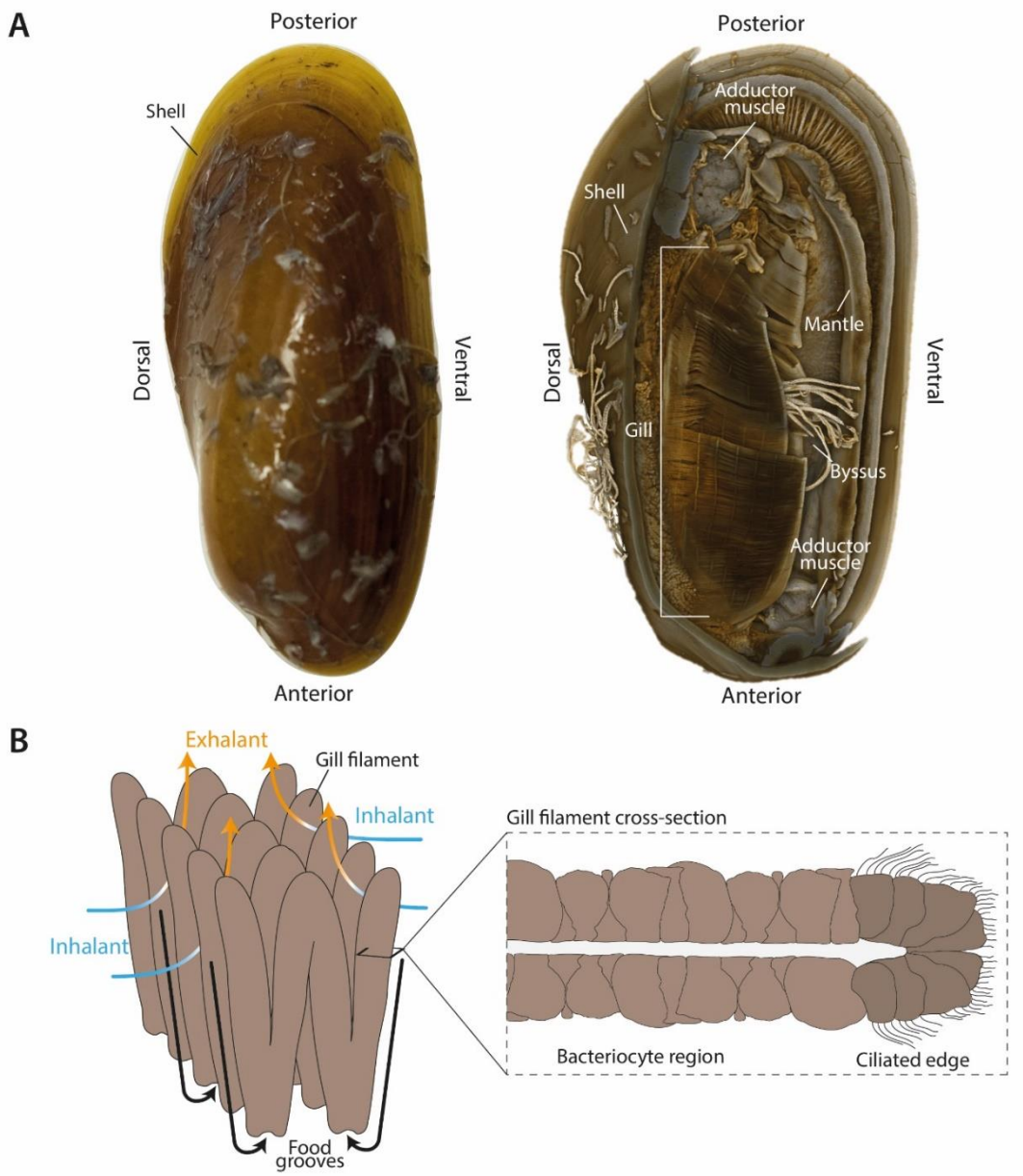

Figure 5: Morphology of *Bathymodiolus* mussels with emphasis on the gill. ***A:*** Side view of a closed *Bathymodiolus puteoserpentis* mussel (photograph) and a 3D volume rendering a *Bathymodiolus azoricus* mussel exposing the large gills, the mantle, and the adductor muscles (courtesy of Benedikt Geier). ***B***: Section of gill showing five W-shaped filaments (adapted from Gosling, 2015). Black arrows show particle transport along the filaments to the food grooves. Coloured arrows indicate water flow through the filaments from the inhalant (blue) to the exhalant (orange) chambers. Cross-section of gill filament shows the distinct gill regions of each filament. The gill filaments of *Bathymodiolus* spp. mussels are dominated by bacteriocytes that lack cilia and microvilli (bacteriocyte-region). Ciliated cells at the edge of each filament produce the currents for water and particle transport (ciliated edge).

Bathymodiolus symbioses represent nutritional interactions with their symbiont (e.g. Figure 6), in which the mussel host is dependent on the carbon provided by the symbionts. The dependency of chemosynthetic *vs*. photosynthetic derived nutrition can vary between sites and species (Riekenberg *et al.*, 2016). For example, in the cold seep species *B. childressi* from the Gulf of Mexico, stable isotope analyses revealed a dependency of phototrophic carbon and nutrition via filter-feeding, indicating that nutrients can be acquired from both chemo- and photosynthesis (Demopoulos *et al.*, 2019). The prerequisite of obtaining phototrophic carbon from the environment is a functional digestive system.

Although the gut of *Bathymodiolus* mussels is highly reduced, the mussels retained a functional feeding groove and labial palps (Kádár, Bettencourt, *et al.*, 2005; Franke *et al.*, 2020). Studies of mussel gut contents also indicate that the mussels also obtain their nutrition from organic matter (Kádár, Bettencourt, *et al.*, 2005). While the transfer of nutrients from symbionts to the host remains unresolved, it is likely that the mussel host obtains nutrition *via* lysosomal digestion of the symbionts. Lysosomal structures are repeatedly observed in mussel gill bacteriocytes, and indicate that intracellular digestion of symbionts *via* this route is common in *Bathymodiolus* mussels (Fiala-Médioni *et al.*, 1986; Streams *et al.*, 1997; Zheng *et al.*, 2017).

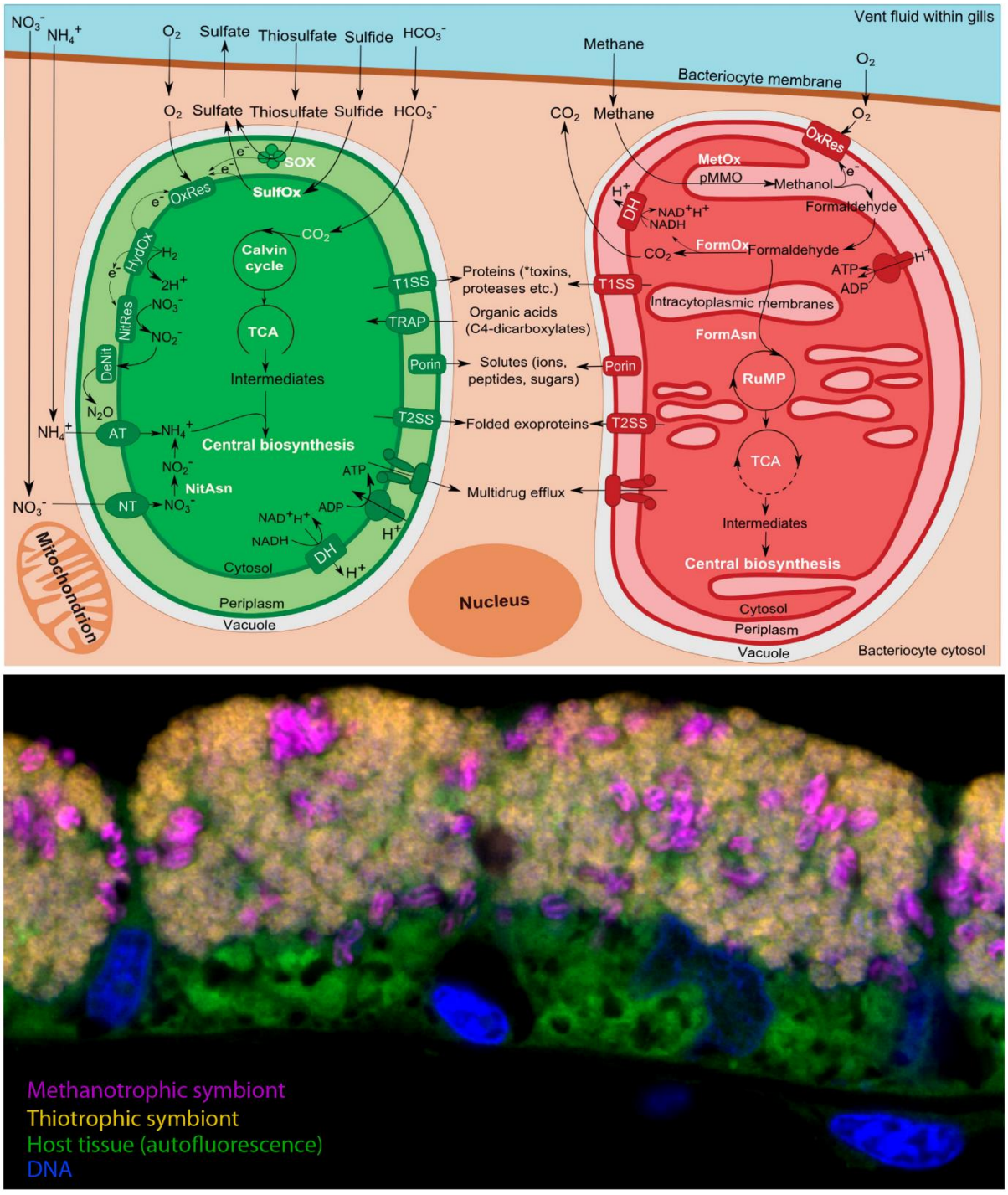

Figure 6: Metabolism and microscopy of the methanotrophic and thiotrophic symbionts of *Bathymodiolus* mussels. Upper panel shows metabolic reconstructions of the thiotrophic symbiont (left) and the methanotrophic symbiont (right) highlighting key metabolic processes and the exchange of compounds with their environment. Modified from Ponnudurai *et al.* (2017). Lower panel shows fluorescence *in situ* hybridisation image of a gill cross-section from a *B. azoricus* mussel, showing the co-occurrence of the methanotrophic (magenta) and thiotrophic (yellow) symbiont in host bacteriocytes (host cell in green and nuclei in blue). Image courtesy of Maximilian Franke.

Innate immune system of Bathymodiolus mussels

Intracellular digestion of symbionts does not only represent a nutritional process in bacteriocytes, but likely is also related to the innate immune system in *Bathymodiolus* mussels. For example, lysosomal symbiont digestion was shown to balance host physiology with symbiont load in insect bacteriocytes (Simonet *et al.*, 2018). As filter-feeding animals, bivalve mussels continuously pump seawater through their body cavities, and are thereby exposed to a pool of microorganisms in the water column (Canesi *et al.*, 2002). Mussel immunity is generally considered to be driven by hemocytes in the circulating hemolymph (Yang *et al.*, 2015; Castro *et al.*, 2018). Certain hemocyte types of *Bathymodiolus* spp. are considered to be professional phagocytes that eliminate invading microorganisms in the hemolymph (Tame *et al.*, 2015). However, hemocytes are rather scarce in comparison to other cells, and it is unlikely that hemocytes solely maintain immune levels required for the high number of symbionts or environmental bacteria. The gills of symbiotic bathymodiolin mussels are armoured with a range of proteins and metabolites that shape the innate immune response, and dictate which bacteria can invade and persist (Zheng *et al.*, 2017). For example, specific peptidoglycan recognition proteins were proposed to play a role in the defence against pathogens and in the regulation of the symbiosis (Ikuta *et al.*, 2019). With the exception of the pathogen *Ca*. Endonucleobacter 'bathymodioli', only the methane-oxidising symbiont appears to be able to colonise the *B. childressi* gill (Zielinski *et al.*, 2009), suggesting that these mussels are well-equipped to recognise their symbionts, and to eliminate potential pathogens.

Physiological studies of Bathymodiolus symbioses

Bathymodiolus symbioses are among the dominant fauna in hydrothermal vent and cold seep ecosystems, in which the mussel hosts are even considered as foundation species (Dubilier *et al.*, 2008; Kiel *et al.*, 2010). Because of their ecological relevance, it is of high interest to understand the physiological adaptations of such symbioses that allow them to thrive in these dynamic ecosystems. Over the last decades, several studies have been dedicated to understand potential physical, chemical and biological factors that influence bathymodiolin mussels. These included studies on their larval dispersal and succession (reviewed in Laming *et al.*, 2018), their development and growth (e.g. Franke *et al.*, 2020), and biological interactions with symbiotic and non-symbiotic bacteria (e.g. Barros *et al.*, 2016; Ponnudurai *et al.*, 2017) and other macrofauna (Hourdez and Jouin-Toulmond, 1998). All of these factors are interconnected, and fundamentally influenced by naturally occurring fluctuations of physico-chemical conditions at hydrothermal vents and cold seeps.

In several *in situ* and laboratory-based experiments, the influence of these fluctuating conditions have studied. For example, laboratory studies have investigated the effects of high metal concentrations and their toxicity in *Bathymodiolus* mussels as indicator for the physiological adaptation to hydrothermal vent fluids (Kádár, Costa, *et al.,* 2005; Company *et al.*, 2006; Martins *et al.,* 2017). In comparison, *in situ* based experiments have shed light onto the effects of changing environmental conditions in the natural environment. Translocation experiments with the cold-seep mussel *B. childressi* revealed that the environmental conditions affected mussel growth and fitness (Bergquist *et al.*, 2004). In another translocation experiment with the hydrothermal vent mussel *B. azoricus*, interruptions of hydrothermal fluid access revealed significant expression changes of over 1,000 genes in mussel gills after 7 days (Détrée *et al.*, 2019).

With the advances of 'omics' techniques, multiple levels of data can reveal the metabolic capabilities to endure the fluctuating environmental conditions of mussels in their natural habitat. For instance, metagenomic approaches could provide insights into the metabolic

potentials of the mussel symbionts, and how the environment may have shaped the presence of genes in these symbionts (Ansorge *et al.*, 2019). Alongside metagenomic studies, transcriptomic analyses are also used to explore the physiology of bathymodiolin mussels in their natural environment.

Aims of this thesis

The aim of my doctoral studies was to investigate physiological responses and adaptations of bathymodiolin hosts and symbionts to changing environmental conditions. In particular, I was interested in understanding the effects of short- and long-term limitations of chemical energy sources for the symbiosis. When I began my studies, our knowledge of the molecular processes in response to limitations of energy resources was restricted to few studies. Understanding the physiological adaptations of the bathymodiolin symbioses to naturally occurring fluctuations of physico-chemical conditions can shed light onto their ecological success in these rather extreme deep-sea habitats.

The method of choice throughout my studies was RNA-seq based transcriptomics, which is a state-of-the-art approach for high-throughput analyses on the function of organisms based on the expression of genes. Transcriptome-based investigations are highly advantageous on multiple levels. First and foremost, transcriptomics provides informative snapshots of the physiological state within an environmental context. Secondly, transcriptome-based analyses do not require a reference genome. This is beneficial for the analyses of mussel host transcriptomes, because only one reference genome is currently available for these species. And thirdly, the costs of RNA sequencing have decreased over the years while producing even better quality libraries. On top of this, subsequent data analyses have progressed enormously and have increased our confidence in transcriptome-based biological interpretations. Nonetheless, transcriptomics of the eukaryotic deep-sea mussels is underexplored, and a considerable part of my doctoral studies involved the quality check of different transcriptomic analyses. I established a standard operation procedure for host transcriptomics that enabled

me to investigate my research questions. Through the identification of expressed genes during these periods of limited energy resources, I gained insights into the physiological processes of the symbiotic partners. The specific research questions that were addressed in the next three chapters of my thesis are introduced below.

Do the transcriptomes of on-board fixed deep-sea organisms reflect their natural physiology?

In the past decades, several transcriptomic studies have been conducted to understand the physiology of deep-sea bacteria and animals. In most of these studies, samples were collected alive from great depths and were processed on board for further analyses. The time interval between sample collection and sample recovery on the research vessel can often take hours. Realistically, the samples are also not immediately processed, but may be stored in buckets with surface seawater for a few hours until they are eventually fixed for transcriptome analyses. Within this time frame, it is possible that depressurisation or temperature changes occurring during the ascent to the surface influence gene expression, and that the on-board stabilised transcriptomes do not reflect the physiology of organisms in their natural habitat. Before my doctoral studies, it was elusive if and to which extent host and symbiont transcriptomes of *Bathymodiolus* symbioses were influenced by sample recovery and on-board storage. In fact, only a handful of studies have employed deep-sea *in situ* fixation techniques to understand the natural physiology of their study organisms. It was therefore of great interest to settle these uncertainties because it may lay the foundation for planning future research of deep-sea organisms, and may challenge hypotheses on the physiology of on-board fixed deep-sea organisms.

To address this, I analysed *in situ* stabilised transcriptomes of host and symbionts, and compared them to on-board fixed samples. Intriguingly, I could not detect any changes of gene expression in the transcriptomes of the host gills. In contrast, both the methanotrophic and thiotrophic symbiont showed major transcriptome changes and revealed similar but also

dissimilar responses to sample recovery and on-board fixation. This study does not only extend our understanding of the different physiological responses of deep-sea organisms to the sampling procedure, but also reveals the short-term survival strategies of the symbionts of *Bathymodiolus* mussels to fluctuating environmental conditions such as limitations of oxygen, methane and sulphide, which are known to occur regularly at hydrothermal vents. The results of this study were assessed in chapter II.

What are the long-term effects of limitation of the energy source for the symbiosis?

Limited access to chemical energy resources may have a significant impact on *Bathymodiolus* symbioses. To reveal the long-term effects of symbiont loss in *Bathymodiolus* symbioses, I analysed the metagenomes and transcriptomes of mussels that were maintained in aquaria for several years with low methane concentrations, a key energy and carbon source for their symbionts. The metagenome analyses I conducted revealed a substantial drop of symbiont numbers, which was confirmed through transmission electron microscopy and fluorescence *in situ* hybridisation images provided by my colleagues. Interestingly, we also observed much less lysosomal structures in gill bacteriocytes in the near absence of symbionts.

Based on these observations, my initial aim was to investigate if the low symbiont number in gill bacteriocytes could be attributed to the expression of lysozymes, a specific group of enzymes that hydrolyse bacterial cell walls. Previous studies have found evidence for lysozyme involvement in host-symbiont interactions. While this research goal was highly exciting at first, I soon discovered that lysozymes likely do not play the dominant role in the intracellular digestion of symbionts in *Bathymodiolus* mussels (preliminary results of lysozyme expression and distribution in gills in the appendix of chapter III). As a consequence, I adapted my research aim and started to investigate alternative mechanisms in host bacteriocytes that might be involved in controlling symbiont populations under low-energy conditions.

I employed gene co-expression network analyses to systematically investigate gene groups that link symbiont abundances with cellular processes of host bacteriocytes. By reconstructing the physiology of symbiont-hosting bacteriocytes over a cycle of symbiont depletion and symbiont re-acquisition, mediated by changing methane concentrations in the aquaria, I identified gene groups involved in the recognition and lysosomal digestion of symbionts. The results of the long-term husbandry of mussels in low methane concentrations are described in chapter III.

How do host and symbionts cope with short-term limitations of hydrothermal access?

At hydrothermal vents, the symbionts of *Bathymodiolus* mussels are dependent on reduced compounds from vent fluids. Dynamic mixing of these vent fluids with seawater can result in short-term limitations of reduced chemical energy for the symbionts. The potential physiological stress imposed on the organisms by such fluctuating conditions is currently not well understood. A previous doctoral thesis has investigated host-symbiont interactions of displaced *B. azoricus* mussels based on quantitative PCR (qPCR) analyses. The data resulting from this study showed symbiont depletion within days of displacement from the original mussel bed.

In an *in situ* experiment conducted on a research cruise in 2016, fluid access was manipulated through displacement of mussels for several days. The aim of this experiment was to investigate the effects of fluctuating access to reduced chemical energy source like methane and sulphur in the hydrothermal fluids. To investigate the impacts of limited fluid access on the physiological response of host and symbionts, I analysed the transcriptomes of host and symbionts from displaced mussels, and compared them to mussels from the natural mussel bed. The results of this study are described in chapter IV.

References

Ansorge, R., Romano, S., Sayavedra, L., Porras, M. Á. G., *et al.* (2019) 'Functional diversity enables multiple symbiont strains to coexist in deep-sea mussels', *Nature Microbiology*, 4, pp. 2487–2497. doi: 10.1038/s41564-019-0572-9.

Barnes, R. S. K., Calow, P., Olive, P. J. W., Golding, D. W., *et al.* (2001) *The Invertebrates: A Synthesis*. Third Edit. Blackwell Science Ltd.

Barros, I., Mendes, S. and Rosa, D. (2016) 'Vibrio diabolicus Immunomodulatory Effects on Bathymodiolus azoricus During Long-term Acclimatization at Atmospheric Pressure', *Journal of Aquaculture Research & Development*, 7. doi: 10.4172/2155-9546.1000464.

Bergquist, D. C., Fleckenstein, C., Szalai, E. B., Knisel, J., *et al.* (2004) 'Environment drives physiological variability in the cold seep mussel Bathymodiolus childressi', *Limnology and Oceanography*, 49, pp. 706–715. doi: 10.4319/lo.2004.49.3.0706.

Borin, S. and Daffonchio, D. (2010) 'Deep Sea Sampling, Sample Work-up and Analysis', in *Handbook of Hydrocarbon and Lipid Microbiology*. Springer Berlin Heidelberg.

Canesi, L., Gallo, G., Gavioli, M. and Pruzzo, C. (2002) 'Bacteria-hemocyte interactions and phagocytosis in marine bivalves', *Microscopy Research and Technique*, 57, pp. 469–476. doi: 10.1002/jemt.10100.

Cannuel, R., Beninger, P. G., McCombie, H. and Boudry, P. (2009) 'Gill development and its functional and evolutionary implications in the blue mussel Mytilus edulis (Bivalvia: Mytilidae)', *Biological Bulletin*, 217, pp. 173–188. doi: 10.1086/BBLv217n2p173.

Castro, J. M., Bianchi, V. A., Pascual, M. M., Almeida, C., *et al.* (2018) 'Immune and biochemical responses in hemolymph and gills of the Patagonian freshwater mussel Diplodon chilensis, against two microbiological challenges: Saccharomyces cerevisiae and Escherichia coli', *Journal of Invertebrate Pathology*, 157, pp. 36–44. doi: 10.1016/j.jip.2018.08.005.

Company, R., Serafim, A., Cosson, R., Camus, L., *et al.* (2006) 'The effect of cadmium on antioxidant responses and the susceptibility to oxidative stress in the hydrothermal vent mussel Bathymodiolus azoricus', *Marine Biology*, 148, pp. 817–825. doi: 10.1007/s00227-005-0116-0.

Demopoulos, A. W. J., McClain-Counts, J. P., Bourque, J. R., Prouty, N. G., *et al.* (2019) 'Examination of Bathymodiolus childressi nutritional sources, isotopic niches, and food-web linkages at two seeps in the US Atlantic margin using stable isotope analysis and mixing models', *Deep-Sea Research Part I: Oceanographic Research Papers*, 148, pp. 53–66. doi: 10.1016/j.dsr.2019.04.002.

Détrée, C., Haddad, I., Demey-thomas, E., Vinh, J., *et al.* (2019) 'Global host molecular perturbations upon in situ loss of bacterial endosymbionts in the deep-sea mussel Bathymodiolus azoricus assessed using proteomics and transcriptomics', pp. 1–14.

Distel, D. L., Lee, H. K. and Cavanaugh, C. M. (1995) 'Intracellular coexistence of methano- and thioautotrophic bacteria in a hydrothermal vent mussel.', *Proceedings of the National Academy of Sciences of the United States of America*, 92, pp. 9598–9602. doi: 10.1073/pnas.92.21.9598.

Van Dover, C. L. (2000) *The Ecology of Deep-Sea Hydrothermal Vents*. Princeton Univ. Press, New Jersey.

Dubilier, N., Bergin, C. and Lott, C. (2008) 'Symbiotic diversity in marine animals : the art of harnessing chemosynthesis', *Nature Reviews Microbiology*, 6, pp. 725–740. doi: 10.1038/nrmicro1992.

Duperron, S., Bergin, C., Zielinski, F., Blazejak, A., *et al.* (2006) 'A dual symbiosis shared by two mussel species, Bathymodiolus azoricus and Bathymodiolus puteoserpentis (Bivalvia: Mytilidae), from hydrothermal vents along the northern Mid-Atlantic Ridge', *Environmental Microbiology*, 8, pp. 1441–1447. doi: 10.1111/j.1462-2920.2006.01038.x.

Duperron, S., Quiles, A., Szafranski, K. M., Léger, N., *et al.* (2016) 'Estimating Symbiont Abundances and Gill Surface Areas in Specimens of the Hydrothermal Vent Mussel Bathymodiolus puteoserpentis Maintained in Pressure Vessels', *Frontiers in Marine Science*, 3, pp. 1–12. doi: 10.3389/fmars.2016.00016.

Fiala-Médioni, A., Métivier, C., Herry, A. and Le Pennec, M. (1986) 'Ultrastructure of the gill of hydrothermal-vent mytilid Bathymodiolus sp.', 92, pp. 65–72.

Franke, M., Geier, B., Hammel, J. U., Dubilier, N., *et al.* (2020) 'Becoming symbiotic – the symbiont acquisition and the early development of bathymodiolin mussels', *bioRxiv*.

Génio, L., Johnson, S. B., Vrijenhoek, R. C., Cunha, M. R., *et al.* (2008) 'New record of "Bathymodiolus" mauritanicus Cosel 2002 from the Gulf of Cadiz (NE Atlantic) mud volcanoes', *Journal of Shellfish Research*, 27, pp. 53–61. doi: 10.2983/0730-8000(2008)27[53:NROBMC]2.0.CO;2.

German, C. R., Casciotti, K. A., Dutay, J. C., Heimbürger, L. E., *et al.* (2016) 'Hydrothermal impacts on trace element and isotope ocean biogeochemistry', *Philosophical Transactions of the Royal Society A: Mathematical, Physical and Engineering Sciences*, 374, pp. 0–2. doi: 10.1098/rsta.2016.0035.

Gosling, E. (2015) *Marine Bivalve Molluscs*. Chichester, UK: John Wiley & Sons, Ltd.

Greinert, J., McGinnis, D. F., Naudts, L., Linke, P., *et al.* (2010) 'Atmospheric methane flux from bubbling seeps: Spatially extrapolated quantification from a Black Sea shelf area', *Journal of Geophysical Research: Oceans*, 115, pp. 1–18. doi: 10.1029/2009JC005381.

Hinzke, T., Kleiner, M., Breusing, C., Felbeck, H., *et al.* (2019) 'Host-microbe interactions in the chemosynthetic *Riftia pachyptila* symbiosis', *mBio*, 10, pp. 1–20. doi: 10.1128/mBio.02243-19.

Hourdez, S. and Jouin-Toulmond, C. (1998) 'Functional anatomy of the respiratory system of Branchipolynoe species (Polychaeta, Polynoidae), commensal with Bathymodiolus species (Bivalvia, Mytilidae) from deep-sea hydrothermal vents', *Zoomorphology*, 118, pp. 225–233. doi: 10.1007/s004350050071.

Ikuta, T., Tame, A., Saito, M., Aoki, Y., *et al.* (2019) 'Identification of cells expressing two peptidoglycan recognition proteins in the gill of the vent mussel, Bathymodiolus septemdierum', *Fish and Shellfish Immunology*, 93, pp. 815–822. doi: 10.1016/j.fsi.2019.08.022.

Jannasch, H. W. (1985) 'The chemosynthetic support of life and the microbial diversity at deep-sea hydrothermal vents', *Proceedings of the Royal Society B*, 225, pp. 277–297.

Kádár, E., Costa, V., Santos, R. S. and Lopes, H. (2005) 'Behavioural response to the bioavailability of inorganic mercury in the hydrothermal mussel Bathymodiolus azoricus', *Journal of Experimental Biology*, 208, pp. 505–513. doi: 10.1242/jeb.01415.

Kádár, E., Bettencourt, R., Costa, V., Santos, R. S., *et al.* (2005) 'Experimentally induced endosymbiont loss and re-acquirement in the hydrothermal vent bivalve Bathymodiolus azoricus', *Journal of Experimental Marine Biology and Ecology*, 318, pp. 99–110. doi: 10.1016/j.jembe.2004.12.025.

Khripounoff, A., Caprais, J. C., Decker, C., Le Bruchec, J., *et al.* (2017) 'Respiration of bivalves from three different deep-sea areas: Cold seeps, hydrothermal vents and organic carbon-rich sediments',

Deep-Sea Research Part II: Topical Studies in Oceanography, 142, pp. 233–243. doi: 10.1016/j.dsr2.2016.05.023.

Kiel, S., Landman, N. and Harries, P. (2010) *The Vent and Seep Biota: Aspects from Microbes to Ecosystems*.

Kochevar, R. E., Childress, J. J., Fisher, C. R. and Minnich, E. (1992) 'The methane mussel: roles of symbiont and host in the metabolic utilization of methane', *Marine Biology*, 112, pp. 389–401.

Laming, S. R., Gaudron, S. M. and Duperron, S. (2018) 'Lifecycle Ecology of Deep-Sea Chemosymbiotic Mussels: A Review', *Frontiers in Marine Science*, 5. doi: 10.3389/fmars.2018.00282.

Martins, I., Goulart, J., Martins, E., Morales-Román, R., *et al.* (2017) 'Physiological impacts of acute Cu exposure on deep-sea vent mussel Bathymodiolus azoricus under a deep-sea mining activity scenario', *Aquatic Toxicology*, 193, pp. 40–49. doi: 10.1016/j.aquatox.2017.10.004.

McCowin, M. F., Feehery, C. and Rouse, G. W. (2020) 'Spanning the depths or depth-restricted: Three new species of Bathymodiolus (Bivalvia, Mytilidae) and a new record for the hydrothermal vent Bathymodiolus thermophilus at methane seeps along the Costa Rica margin', *Deep-Sea Research Part I: Oceanographic Research Papers*, 164, p. 103322. doi: 10.1016/j.dsr.2020.103322.

Munn, C. B. (2020) *Marine Microbiology: Ecology and Applications*. 3rd Editio. Edited by C. B. Munn. Boca Raton: CRC Press.

Nybakken, J. W. and Bertness, M. D. (2005) *Marine Biology: An ecological approach*. sixth Edit. Edited by C. Bridges et al. San Francisco: Pearson Educationm Inc,. Benjamin Cummings.

Perner, M., Gonnella, G., Kurtz, S. and LaRoche, J. (2014) 'Handling temperature bursts reaching 464°C: Different microbial strategies in the sisters peak hydrothermal chimney', *Applied and Environmental Microbiology*, 80, pp. 4585–4598. doi: 10.1128/AEM.01460-14.

Petersen, J. M., Zielinski, F. U., Pape, T., Seifert, R., *et al.* (2011) 'Hydrogen is an energy source for hydrothermal vent symbioses', *Nature*, 476, pp. 176–180. doi: 10.1038/nature10325.

Petersen, J. M., Wentrup, C., Verna, C., Knittel, K., *et al.* (2012) 'Origins and evolutionary flexibility of chemosynthetic symbionts from deep-sea animals', *Biological Bulletin*, 223, pp. 123–137. doi: 10.1086/BBLv223n1p123.

Petersen, J. M. and Dubilier, N. (2009) 'Methanotrophic symbioses in marine invertebrates', *Environmental Microbiology Reports*, 1, pp. 319–335. doi: 10.1111/j.1758-2229.2009.00081.x.

Ponnudurai, R., Kleiner, M., Sayavedra, L., Petersen, J. M., *et al.* (2017) 'Metabolic and physiological interdependencies in the Bathymodiolus azoricus symbiosis', *ISME Journal*, 11, pp. 463–477. doi: 10.1038/ismej.2016.124.

Pruski, A. M., Rousse, N., Fiala-Médioni, A. and Boulègue, J. (2002) 'Sulphur signature in the hydrothermal vent mussel Bathymodiolus azoricus from the Mid-Atlantic Ridge', *Journal of the Marine Biological Association of the United Kingdom*, 82, pp. 463–468. doi: 10.1017/S0025315402005726.

Ramírez Llodra, E. and Billett, D. S. M. (2006) 'Deep Sea Ecosystems: Pristine Biodiversity', in Duarte, C. M. (ed.) *The Exploration of marine biodiversity: scientific and technological challenges*. Bilbao, Spain: Fundacion BBVA, pp. 63–92.

Riekenberg, P. M., Carney, R. S. and Fry, B. (2016) 'Trophic plasticity of the methanotrophic mussel Bathymodiolus childressi in the Gulf of Mexico', *Marine Ecology Progress Series*, 547, pp. 91–106.

doi: 10.3354/meps11645.

Riou, V., Halary, S., Duperron, S., Bouillon, S., *et al.* (2008) 'Influence of CH4 and H2S availability on symbiont distribution, carbon assimilation and transfer in the dual symbiotic vent mussel Bathymodiolus azoricus', *Biogeosciences*, 5, pp. 1681–1691. doi: 10.5194/bg-5-1681-2008.

Ristova, P. P., Wenzhöfer, F., Ramette, A., Felden, J., *et al.* (2015) 'Spatial scales of bacterial community diversity at cold seeps (Eastern Mediterranean Sea)', *ISME Journal*, 9, pp. 1306–1318. doi: 10.1038/ismej.2014.217.

Rogers, A. D., Tyler, P. A., Connelly, D. P., Copley, J. T., *et al.* (2012) 'The discovery of new deep-sea hydrothermal vent communities in the Southern ocean and implications for biogeography', *PLoS Biology*, 10. doi: 10.1371/journal.pbio.1001234.

Rubin-Blum, M., Antony, C. P., Sayavedra, L., Martínez-Pérez, C., *et al.* (2019) 'Fueled by methane: deep-sea sponges from asphalt seeps gain their nutrition from methane-oxidizing symbionts', *ISME Journal*, 13, pp. 1209–1225. doi: 10.1038/s41396-019-0346-7.

Seston, S. L., Beinart, R. A., Sarode, N., Shockey, A. C., *et al.* (2016) 'Metatranscriptional response of chemoautotrophic Ifremeria nautilei endosymbionts to differing sulfur regimes', *Frontiers in Microbiology*, 7, pp. 1–18. doi: 10.3389/fmicb.2016.01074.

Simonet, P., Gaget, K., Balmand, S., Lopes, M. R., *et al.* (2018) 'Bacteriocyte cell death in the pea aphid/Buchnera symbiotic system', *Proceedings of the National Academy of Sciences of the United States of America*, 115, pp. E1819–E1827. doi: 10.1073/pnas.1720237115.

Stewart, F. J., Newton, I. L. G. and Cavanaugh, C. M. (2005) 'Chemosynthetic endosymbioses: Adaptations to oxic-anoxic interfaces', *Trends in Microbiology*. Elsevier Current Trends, pp. 439–448. doi: 10.1016/j.tim.2005.07.007.

Streams, M. E., Fisher, C. R. and Fiala-Médioni, A. (1997) 'Methanotrophic symbiont location and fate of carbon incorporated from methane in a hydrocarbon seep mussel', *Marine Biology*, 129, pp. 465–476. doi: 10.1007/s002270050187.

Tame, A., Yoshida, T., Ohishi, K. and Maruyama, T. (2015) 'Phagocytic activities of hemocytes from the deep-sea symbiotic mussels Bathymodiolus japonicus, B. platifrons, and B. septemdierum', *Fish and Shellfish Immunology*, 45, pp. 146–156. doi: 10.1016/j.fsi.2015.03.020.

Tavormina, P. L., Hatzenpichler, R., McGlynn, S., Chadwick, G., *et al.* (2015) 'Methyloprofundus sedimenti gen. nov., sp. nov., an obligate methanotroph from ocean sediment belonging to the "deep sea-1" clade of marine methanotrophs', *International Journal of Systematic and Evolutionary Microbiology*, 65, pp. 251–259. doi: 10.1099/ijs.0.062927-0.

Tivey, M. K. (2007) 'Generation of Seafloor Hydrothermal Vent Fluids and associated Mineral Deposits', *Oceanography*, 20, pp. 50–65.

Wankel, S. D., Germanovich, L. N., Lilley, M. D., Genc, G., *et al.* (2011) 'Influence of subsurface biosphere on geochemical fluxes from diffuse hydrothermal fluids', *Nature Geoscience*, 4, pp. 461–468. doi: 10.1038/ngeo1183.

Weiss, R. F., Lonsdale, P., Lupton, J. E., Bainbridge, A. ., *et al.* (1977) 'Hydrothermal plumes in the Galapagos Rift', *Nature*, 267, pp. 600–603.

Wentrup, C., Wendeberg, A., Schimak, M., Borowski, C., *et al.* (2014) 'Forever competent: Deep-sea bivalves are colonized by their chemosynthetic symbionts throughout their lifetime', *Environmental*

Microbiology, 16, pp. 3699–3713. doi: 10.1111/1462-2920.12597.

Yang, H. S., Hong, H. K., Donaghy, L., Noh, C. H., *et al.* (2015) 'Morphology and Immune-related activities of hemocytes of the mussel Mytilus coruscus (Gould, 1861) from East Sea of Korea', *Ocean Science Journal*, 50, pp. 77–85. doi: 10.1007/s12601-015-0006-4.

Zheng, P., Wang, M., Li, C., Sun, X., *et al.* (2017) 'Insights into deep-sea adaptations and host – symbiont interactions : A comparative transcriptome study on Bathymodiolus mussels and their coastal relatives', pp. 5133–5148. doi: 10.1111/mec.14160.

Zielinski, F. U., Pernthaler, A., Duperron, S., Raggi, L., *et al.* (2009) 'Widespread occurrence of an intranuclear bacterial parasite in vent and seep bathymodiolin mussels', *Environmental Microbiology*, 11, pp. 1150–1167. doi: 10.1111/j.1462-2920.2008.01847.x.

List of publications and contributions

Manuscripts included in this thesis:

1. **Målin Tietjen,** Christian Borowski, Rebecca Ansorge, Miguel Ángel González Porras, Nikolaus Leisch, Nicole Dubilier and Harald R. Gruber-Vodicka (2020). *In situ* fixation reveals (dis)similar survival strategies of two endosymbionts in a deep-sea mussel host. **(Chapter II)**

   Manuscript in preparation.

2. **Målin Tietjen,** Nikolaus Leisch, Maximilian Franke, Claas Hiebenthal, Frank Melzner, Thorsten Reusch, Nicole Dubilier and Harald R. Gruber-Vodicka (2020). Lysosomal symbiont digestion shapes innate immunity and fuels the metabolism of bacteriocytes in a deep-sea mussel host. **(Chapter III)**

   Manuscript in preparation.

3. **Målin Tietjen,** Christian Borowski, Nicole Dubilier and Harald Gruber-Vodicka (2020). Deep-sea *Bathymodiolus* mussels are resistant to short-term limitations of hydrothermal access. **(Chapter IV)**

   Manuscript in preparation.

Contributions to publications not included in this thesis:

4. Oliver Jäckle, Brandon K. B. Seah, **Målin Tietjen**, *et al.* (2019). Chemosynthetic symbiont with a drastically reduced genome serves as primary energy storage in the marine flatworm *Paracatenula. PNAS, 116, pp. 8505-8514, doi: 10.1073/pnas.1818995116.*

   Contribution: *Assembly and annotation of a host de novo transcriptome.*

5. Oliver Jäckle, **Målin Tietjen**, Harald Gruber-Vodicka (2018). The role of endosymbionts in rostrum regeneration of the marine flatworm *Paracatenula* sp. standrea.

   Contribution: *Development of strategy and analysis for symbiont transcriptomics.*

   Manuscript in preparation.

6. Miguel Ángel González Porras, Adrien Assié, **Målin Tietjen**, *et al.* (2020). The hungry nucleus: The nutritional demands of a chitinolytic intranuclear parasite trigger its host cell to upregulate sugar import.

   Contribution: *Development of strategy for host and pathogen transcriptome analyses.*

   Manuscript in preparation.

Chapter II

In situ fixation reveals (dis)similar survival strategies of two endosymbionts in a deep-sea mussel host

Målin Tietjen[1,2], Christian Borowski[1,2], Rebecca Ansorge[1,3], Nikolaus Leisch[1], Miguel Ángel González Porras[1], Nicole Dubilier[1,2] and Harald R. Gruber-Vodicka[1]

[1] Max Planck Institute for Marine Microbiology, Bremen, Germany

[2] MARUM – Center for Marine Environmental Sciences of the University of Bremen, Germany

[3] Quadram Institute Bioscience, Norwich, United Kingdom

Author contributions: *ND, CB, HRGV and MT designed the study, ND and CB coordinated sampling strategy, ND, CB and RA processed on-board samples, MT performed nucleotide extractions, MT and HRGV conceived data analyses, RA performed symbiont genome binning, MÁGP conducted FISH and imaging, NL performed TEM and imaging, MT analysed the data and wrote the manuscript with contributions of RA and HRGV.*

This manuscript is in preparation and has not been reviewed by all authors.

Abstract

Deep-sea hydrothermal vents are highly dynamic ecosystems in which physico-chemical conditions can fluctuate within short periods of time. The physiological adaptations of organisms that thrive in these extreme ecosystems is not well understood. One of the major limiting factors for studying the natural physiology of deep-sea organisms is sample collection. The sampling procedures, including recovery from thousands of meters depth and subsequent processing on board, may already cause changes of gene expression, and thereby mask the natural physiology of the organisms. We wanted to understand the effects of deep-sea sampling on the transcriptome of the most dominant organisms at hydrothermal vents on the Mid-Atlantic Ridge, the mussel *Bathymodiolus puteoserpentis* that harbours a methanotrophic and a thiotrophic symbionts in its gills. To obtain the natural transcriptomes of host and symbionts, we developed and employed the *in situ* fixation device 'IDEFIX'. We compared the transcriptomes of *in situ* fixed samples with those samples fixed on-board immediately after recovery, and after 6, 24 and 48 hours of on-board storage. While the mussel host only displayed minor transcriptome changes throughout our experiment, the two endosymbionts revealed substantial changes in all on-board fixed mussels. In both symbionts, we observed similarly high expression of nitrate respiration that indicate a shared adaption to cope with short-term limitations of oxygen. Yet, we also detected dissimilar strategies in the two symbionts, including energy investment and cell elongation in the methanotrophic symbiont, and energy conservation reflected by overall lower mRNA abundance in the thiotrophic symbiont. Our study contributes to the understanding of the physiological responses in deep-sea organisms to sampling procedures, and exposes distinct physiological strategies of deep-sea symbionts to changing environmental conditions. Based on our findings in the presented study, we propose to stabilise the mRNA of deep-sea organisms at their natural location to avoid biases in transcriptome analyses and subsequent interpretations on their physiology.

Introduction

With the discovery of the "oases of life" at hydrothermal vents in 1977, the deep sea was no longer considered to be an uninhabitable environment. Rather, hydrothermal vents are recognised as areas of high primary production that are populated by animals from different phyla (Van Dover, 2000). To thrive in these habitats, many animals depend on chemosynthetic bacterial symbionts that use chemical energy from vent fluids to produce biomass (Dubilier *et al.*, 2008). Life at hydrothermal vents is challenged by dynamic mixing of seawater with hydrothermal fluids resulting in highly variable physico-chemical conditions for the organisms (Seston *et al.*, 2016). This includes periods of low oxygen concentrations and limited access to reduced chemical energy for the symbionts. The potential physiological stress imposed on the organisms by these fluctuating conditions is currently not well understood due to difficulties of replicating hydrothermal vent environments in the laboratory.

One of the major limiting factors for studying the physiological response of organisms to these fluctuating conditions lies within the sample collection from the deep sea (Sanders *et al.*, 2013). The recovery of samples from thousands of meters depths can take several hours, and realistically, subsequent preservation of all samples may take between 2 and 8 hours after recovery. During this time, several factors including depressurisation or temperature changes may alter gene expression in the organisms (Steiner *et al.*, 2019). Gene expression changes may be the result of varying mRNA stability and turnover, which may be influenced and regulated by many different processes in animals and bacteria (e.g. Chan *et al.*, 2018; Boël *et al.*, 2016). Overall, the mRNA of animals is much more stable than in bacteria, in which mRNA stability can also differ considerably between bacterial taxa (Dressaire *et al.*, 2013). It is therefore of great interest to understand potential gene expression changes that may occur during sample recovery to reveal the natural physiology of the deep-sea organisms.

In recent years, the importance for *in situ* fixation of deep-sea organisms has been recognised, and studies that investigate potential biases introduced by sample recovery are emerging. For example, *in situ* fixation of free-living bacteria communities provided insights into their

natural activities in the deep ocean, and increased rates of nitrate reduction and higher abundances of transcripts for heat-shock proteins were detected in on-board processed samples (Fortunato *et al.*, 2020). Similar studies also revealed effects of on-board fixation on bacterial symbionts in animal hosts. In the deep-sea galatheid squat lobster *Shinkaia crosnieri*, *in situ* fixation provided insights into the physiology of the ectosymbiotic community revealing differences in the expression of *in situ* and on-board fixed samples (Motoki *et al.*, 2020).

However, it remains unresolved how the sampling procedure affects the specific physiological and cellular processes in tissues of deep-sea animals that house endosymbionts. To address this, we performed an *in situ* fixation experiment on the deep-sea mussel *Bathymodiolus puteoserpentis* (superorder Pteriomorphia, subfamily Bathymodiolinae; González *et al.*, 2015; Duperron *et al.*, 2009) that commonly dominate the fauna at hydrothermal vents on the Northern Mid-Atlantic Ridge (Wendeberg *et al.*, 2012). The mussels form dense patches in areas with indirect hydrothermal input (diffuse fluids). These fluids are characterised by colder temperatures through mixing with ambient seawater (Bemis *et al.*, 2012). *B. puteoserpentis* mussels live in symbiosis with two primary chemosynthetic Gammaproteobacteria, a methane-oxidising and a sulphur-oxidising symbiont (Duperron *et al.*, 2006). The methane-oxidising symbiont (hereon after referred to 'methanotrophic symbiont') of *B. puteoserpentis* is closely related to *Methyloprofundus sedimenti*, an aerobic methane-oxidising species isolated from a deep-sea whale fall (Geier *et al.*, 2020; Tavormina *et al.*, 2015). Similar to its free-living relative, the methanotrophic symbiont uses methane or methanol as carbon and energy source (Wendeberg *et al.*, 2012; Tavormina *et al.*, 2017). The sulphur-oxidising symbiont (hereon after referred to 'thiotrophic symbiont') falls within the SUP05 cluster of the *Thioglobaceae* family and is capable of the oxidation of reduced sulphur to fuel CO_2 fixation (Ansorge *et al.*, 2019). Both endosymbionts reside in epithelial gills cells, the so-called bacteriocytes (Duperron *et al.*, 2006). Within these bacteriocytes, the symbionts have continuous access to oxidised (oxygen and nitrate) and reduced compounds (sulphide and methane) to meet their nutritional needs.

To understand the impact of sample recovery on the physiology of host and symbionts in the *Bathymodiolus* symbiosis, we developed and employed an *in situ* fixation device to obtain the natural transcriptome state at their mussel bed. From the same mussel bed, we collected additional mussels and stabilised them on-board at different time points after recovery to track how the physiological response of host and symbionts changes over time. Notably, we could not detect any changes in host transcriptomes. In contrast, we found significant gene expression changes in the methanotrophic and thiotrophic symbiont during sample recovery and on-board storage. This study adds to our understanding of the physiological responses in deep-sea organisms to the sampling procedure, and reveals distinct survival strategies of symbiotic deep-sea bacteria to fluctuating environmental conditions.

Materials & Methods

Sample collection and fixation strategy

Bathymodiolus puteoserpentis mussels were collected during the FS Meteor cruise M126 ("BigMAR") in 2016 from the Ash Lighthouse mussel bed (13°30'48.5856"N, 44°57'46.872"W) of the hydrothermal vent field Semenov-2 at a depth of 2446.7 m in the Northern Mid-Atlantic Ridge (Supplementary Figure 1A). To obtain the natural physiological state of host and symbionts, we developed the In Depth Fixation Device (IDEFIX) to stabilise the nucleotides and proteins of host and symbionts directly at the mussel bed (Supplementary Figure 1B). IDEFIX consisted of four numbered chambers, each filled with the dense stabilising solution RNAlater that reliably preserves nucleotides and proteins of organisms including deep-sea mussels (Kruse *et al.*, 2017; Mat *et al.*, 2020). Heavy lids on each IDEFIX chamber could be opened and closed by the ROV arm *via* so-called "monkey fists" on the lids. The chambers were built onto a specialised tray with a steel-comb that was used to separate single mussels from byssus-clotted clumps. The ROV pilot carefully cracked the shells of individual specimens above the IDEFIX chambers and dropped them into the fixative to stabilise the whole mussel instantly. These *in situ* fixed specimens are referred to is0 samples throughout this study.

To reveal the effects of mussel recovery and on-board storage on host and symbiont, we also collected mussels and fixed them at different time points on board. While some mussels were fixed right next to the ROV as soon as they were recovered on board (2-hours post collection from the mussel bed), others were stored in buckets at 4°C for 6 h, 24 h and 48 h until they were cracked and fixed as whole mussels in RNAlater. We hereon refer to the different on-board fixation time points as “ob2”, “ob8”, “ob26” and “ob50” samples, representative of their time of fixation since collection from the mussel bed. To decipher if the main driver for a changing transcriptome of the symbiosis was the handling of mussels or the removal of vent fluids, we collected additional mussels in enclosed mesh cages. These cages were displaced about 65 m away from the original mussel bed (13°30'46.8468"N, 44°57'46.3788"W). We re-collected one cage after 24 h and fixed mussels with IDEFIX and another after 48 h and fixed mussels with IDEFIX (Supplementary Figure 1C). These samples are referred to as “dis24” and “dis48” samples in this study.

A detailed list of specimens used in this study including exact times of the individual fixation points are listed in the Supplementary Table 1. The fixed mussels were then stored in individual bags at -80°C until dissection and extraction of nucleic acids and proteins in the Bremen laboratory.

Specimen dissection and nucleotide extractions

For each fixation time point, five mussels of the same size ranges were selected. The deep-frozen mussels were dissected quickly while thawing on an ice tray. Pieces of the symbiont-containing gills were cut from the mussels and immediately placed into the buffering solution of the nucleotide extraction kit. Each sample was subjected to nucleic acid and protein extractions using the AllPrep® DNA/RNA/Protein Mini Kit (QIAGEN, Hilden, Germany) following the manufacturers guidelines with minor amendments to the protocol: The RNA was incubated in 100 µl RNase-free water at room temperature for 10 min before elution to increase the yield.

Transcriptome sequencing, host de novo transcriptome assembly and functional annotation

RNA library preparation and sequencing were performed at the Max Planck Genome Center Cologne, Germany (https://mpgc.mpipz.mpg.de/home/). The RNA samples were subjected to a dual RNA-Seq approach to sequence polyA-tail enriched RNA libraries and total RNA libraries. For polyA enrichment with NEBNext poly(A) mRNA Magnetic Isolation Module (New England Biolabs, Germany), 500 ng of total RNA per sample were used. Libraries were prepared with NEBNext Ultra Directional RNA Library Prep Kit for Illumina (New England Biolabs, Frankfurt am Main, Germany) with 12 cycles of PCR amplification. For total RNA libraries, 35 ng total RNA was used for library preparation with NEBNext Ultra Directional RNA Library Prep Kit for Illumina (New England Biolabs, Frankfurt am Main, Germany) with 10 cycles of PCR amplification. The quality and quantity of all RNA libraries were assessed at all steps using the TapeStation system (Agilent Technologies, USA) and fluorometry using Invitrogen Qubit (Thermo Fisher Scientific, USA). The libraries were immobilized and processed onto a flow cell with a cBot (Illumina, USA) and sequenced on HiSeq3000 system (Illumina, USA) to a minimum depth of 7 million reads. Read lengths of 150 bp single-end reads were sequenced for total RNA libraries, while polyA-tail enriched libraries were sequenced as paired-end reads (see Supplementary Table 1 for sequencing details).

All libraries were adaptor- and quality-trimmed (Q=2) using BBDuk v38.06 (http://sourceforge.net/projects/bbmap/). To generate a host *de novo* transcriptome assembly, all polyA-tail enriched libraries were combined and assembled with Trinity v2.5.1 (Grabherr *et al.*, 2011). Assembly statistics and completeness were assessed with utility scripts of the Trinity package v2.5.1 (Haas *et al.*, 2013) and BUSCO v3 (Simão *et al.*, 2015) using the metazoan database odb09 (accessed on 5th February 2019). To remove redundant sequences, transcripts were clustered to 97% identity using VSEARCH (Rognes *et al.*, 2016). Contaminating reads (e.g. plants, fungi, non-symbiotic bacteria) were filtered out with

MEGAN6 v6.10.3 (Huson *et al.*, 2016) based on their taxonomic origin determined by the closest hits from NCBI blast v2.2.28 searches against nr (db version 20150811).

For functional annotation of the *B. puteoserpentis* transcriptome, the annotation pipeline of Trinotate v3.0.1 (https://github.com/Trinotate/Trinotate.github.io/; e.g. Bryant *et al.*, 2017) was applied to the 'cleaned' *de novo* assembly. Additionally, a cloud-based InterProScan was run in Blast2GO v5.2.5 (Conesa *et al.*, 2005) using the following databases: CDD (Marchler-Bauer *et al.*, 2017), HAMAP (Pedruzzi *et al.*, 2015), HMMPanther (Mi *et al.*, 2019) , HMMPfam (El-Gebali *et al.*, 2019), HMMPIR (Wu *et al.*, 2004), FPrintScan (Attwood *et al.*, 2012), BlastProDom (Servant *et al.*, 2002), ProfileScan (Sigrist *et al.*, 2013), PatternScan (Sigrist *et al.*, 2013), Gene3D (Lewis *et al.*, 2018), SFLD (Akiva *et al.*, 2014), Superfamily (Oates *et al.*, 2015), MobiDBLite (Piovesan *et al.*, 2018).

Metagenome sequencing, symbiont binning and functional annotation

DNA library preparation and sequencing were performed at the Max Planck Genome Center Cologne, Germany (https://mpgc.mpipz.mpg.de/home/). Metagenome libraries from two *B. puteoserpentis* specimens collected from the mussel bed Quest at the Logatchev vent field (13°30'48.5856"N, 44°57'46.872"W) during the "BigMAR" M126 cruise were used to generate symbiont reference genomes due to poor quality of DNA libraries from the Ash Lighthouse mussel bed (details in Sayavedra, 2016). For symbiont binning, sequencing adaptors and phiX internal Illumina standard sequences were removed and reads were quality filtered (Q=2) with BBDuk v38.06. For genome binning of the thiotrophic symbiont, the metagenome library was assembled with SPAdes v3.10.1 (Bankevich *et al.*, 2012), and binned with MetaBAT 2 v2.10.2 (Kang *et al.*, 2019). The quality of the genome bins were assessed with CheckM v1.0.7 (Parks *et al.*, 2015) and annotated with RAST v2.0 (Aziz *et al.*, 2008) using ClassicRAST (accessed 1st August 2019). Clusters of Orthologous Genes (COG) were assigned to the genomes of both symbionts with eggnog-mapper v2 (Huerta-Cepas *et al.*, 2019), and BlastKOALA v2.2 (Kanehisa *et al.*, 2016) was used to assign KEGG pathway modules.

Differential gene expression analyses

For both symbionts, gene expression was quantified with kallisto v0.46.0 (Bray *et al.*, 2016) using the cleaned mRNA reads of the total RNA libraries, and the metagenome-assembled genome bin as reference. Host genes were also quantified with kallisto v0.46.0 (Bray *et al.*, 2016) using the cleaned mRNA reads of the polyA-enriched RNA libraries and the *B. puteoserpentis de novo* transcriptome assembly as reference. For subsequent differential gene expression analyses, raw gene count matrices were generated with utility scripts of the Trinity v2.5.1 package (Haas *et al.*, 2013) for pairwise comparisons between gill samples of *in situ* fixed mussels and ob2, ob8, ob26, ob50, dis24, and dis48. To identify differentially expressed genes with highest certainty, we applied a two-part approach for differential gene expression analyses using R v3.5.3 (R Core Team, 2019). We used the count-data approach by edgeR v3.24.3 implemented in the utility scripts of the Trinity package v2.8.4 (Haas *et al.*, 2013). We also applied the compositional data approach by ALDEx2 v1.14.1 (Fernandes *et al.*, 2013). Only if the False-Discovery Rate (FDR) of a gene was below 5% in both approaches, statistical significance was accepted.

Results & Discussion

Differential gene expression analyses revealed dissimilar transcriptome changes in host and symbionts

We wanted to assess whether expression profiles of the mussel host *B. puteoserpentis* and its symbionts changed in response to sample recovery and on-board storage compared to their *in situ* transcriptome at the mussel bed. This is of particular importance because most transcriptomic studies of deep-sea samples have been conducted with samples that were fixed on board due to the difficulties of fixing these samples *in situ* (Sanders *et al.*, 2013). To determine the transcriptome changes of host and symbionts, we performed differential gene expression analyses, and accepted differential gene expression if the False-Discovery Rate (FDR) was below 5% in both analyses that we applied (edgeR and ALDEx2). In spite of the conservative cut-off, we detected distinct transcriptome changes in response to sample recovery and on-board storage in the symbiotic partners of the *B. puteoserpentis* symbiosis.

Our experimental setup included mussels that were fixed *in situ* (is0), along with four distinct time points of on-board fixation up to 50 hours after collection from the mussel bed (ob2, ob8, ob26 and ob50). In addition, we analysed mussels that were displaced from the original mussel bed to a location without diffuse fluids and that were fixed at the seafloor at two different time points (dis24 and dis48) to control the effects of the removal of the energy source. Our results show that deep-sea sample recovery and on-board storage had minor impact on the gill transcriptome of the host (Supplementary Figure 2). We did not observe significant gene expression changes in ob2 and ob8 mussels compared to *in situ* their transcriptome. In ob26 and ob50 samples, only few genes showed significant expression changes compared to the *in situ* transcriptome. No differential gene expression was detected for displaced mussels dis24 and dis48 compared to the *in situ* samples (Supplementary Figure 2). We hypothesise that the few transcriptome changes in ob26 and ob50 were likely not caused by limited access to vent fluids. It is possible that other factors, such as differences of

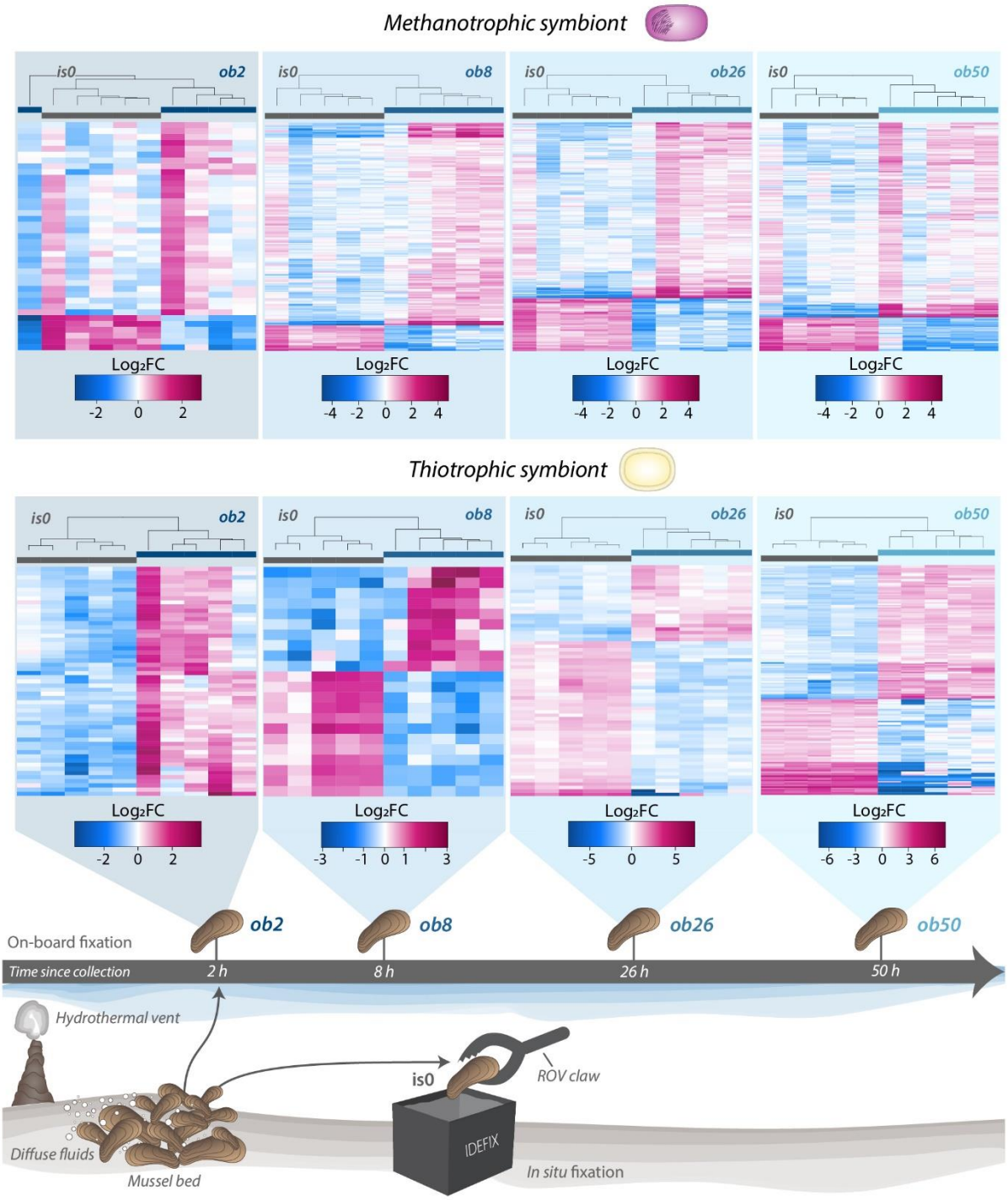

Figure 1: Differential gene expression between *in situ* and on-board fixed transcriptomes of the methanotrophic and thiotrophic symbiont. Sampling scheme showing the *in situ* fixation strategy and the different fixation time points of on-board samples. Heatmaps for every on-board fixation time point show an increasing number of differentially expressed genes compared to *in situ* fixed samples in both symbionts, and distinct clustering of each sampling time point. Number of differentially expressed genes: ob2 = 39 genes, ob8 = 213 genes, ob26 = 295 genes, ob50 = 290 genes (methanotrophic symbiont), ob2 = 55 genes, ob8 = 22 genes, ob26 = 67 genes, ob50 = 169 genes (thiotrophic symbiont).

atmospheric pressure compared to pressure at around 2440 m depth, induced these minor changes in on-board fixed samples. Based on previous assumptions that *B. puteoserpentis* might be susceptible to depressurisation because of their occurrence at high depths (Duperron *et al.*, 2016), it is striking that we could only observe such minor expression changes in the gill transcriptomes of the host.

In contrast to the host, the symbionts of *B. puteoserpentis* revealed substantial transcriptome changes, already within two hours after collection from the mussel bed (ob2; Figure 1). In both symbionts, the number of differentially expressed genes increased continuously with prolonged on-board storage or displacement (Figure 1 and Supplementary Figure 3). The majority of these genes were higher expressed in on-board fixed samples and in displaced samples compared to the *in situ* samples (Supplementary Table 3 and 4). In spite of these overall similarities, we identified substantial differences between the two symbionts.

In the methanotrophic symbiont, we found a notably high number of genes that were differentially expressed in each on-board fixation time point compared to the *in situ* transcriptome (Supplementary Figure 5A; Supplementary Figure 5B includes dis24 and dis48 samples). This effect was most prominent in the intersection of ob8, ob26 and ob50 samples with 113 genes, and suggests a baseline response of the methanotrophic symbiont that was induced within 8 hours after collection from the mussel bed. This transcriptome pattern was also reflected by the COG categories attributed to the differentially expressed genes (Supplementary Figure 4 and Supplementary Table 3). The number of genes per COG category that were up- or downregulated increased consistently with prolonged on-board storage. Based on these observations, we hypothesise that the methanotrophic symbiont displayed a stable and homogeneous transcriptomic response to the on-board conditions.

In contrast to the methanotrophic symbiont, the number of differentially expressed genes shared between on-board fixed samples was much lower in the thiotrophic symbiont and encompassed only 11 genes at the intersection ob8, ob26 and ob50 samples (Supplementary Figure 5A; Supplementary Figure 5B includes dis24 and dis48 samples). Overall, the number

of shared genes between on-board fixed samples was also rather patchy and resembled a heterogeneous transcriptome pattern. The distribution of differentially expressed genes assigned to COG categories was similarly inconsistent (Supplementary Figure 4 and Supplementary Table 3). We hypothesise that this observed transcriptome response could be result of high strain variability of the thiotrophic symbiont in *B. puteoserpentis*. Throughout its distribution along the Northern Mid-Atlantic Ridge, *B. puteoserpentis* harbours a versatile pool of strains of the thiotrophic symbiont. The highest number of strains was predicted to co-exist in individuals from the hydrothermal vent field Semenov-2, from which we collected the mussels in this study (Ansorge *et al.*, 2019). For methanotrophic symbionts of *Bathymodiolus* mussels, the overall strain diversity is likely much lower (Romero Picazo *et al.*, 2019). The range of physiological capabilities reflected by symbiont strain variability may explain the homogeneous gene expression changes of the methanotrophic symbiont *versus* the heterogeneous gene expression changes of the thiotrophic symbiont. The number of differentially expressed genes in the symbiotic partners indicate that the transcriptomes of *B. puteoserpentis* symbionts were considerably more affected by sample recovery and extended on-board storage than their mussel host.

Symbiont transcriptome patterns reflect mRNA synthesis and degradation

The discrepancy between host and symbiont gene expression changes may be a result of dissimilar mRNA synthesis and degradation between bacteria and eukaryotes. In the mussel host, we detected significant expression changes of only few genes in ob26 and ob50 samples. In general, eukaryotic transcription involves complex and energy-demanding molecular processes including post-transcriptional modifications (Janga *et al.*, 2009). Not only is the synthesis of mRNA highly regulated in eukaryotes, but also the degradation of mRNA molecules involves complex and very much coordinated processes (Chan *et al.*, 2018; Cramer, 2019). It is therefore not surprising that the mussel host maintained a stable transcriptome throughout the experiment. In contrast, fast synthesis and degradation of mRNA might be essential for the symbionts to quickly adapt to changing environmental conditions (Dressaire

et al., 2013; Laalami, Zig and Putzer, 2014). To investigate if this turnover of mRNA would explain the gene expression changes observed in both symbionts in on-board fixed samples, we looked for possible changes of transcription regulation and for overall mRNA degradation.

We found significant changes in the expression of key bacterial transcription factors in on-board fixed samples, which revealed similarities but also dissimilarities in the regulation of transcription between the methanotrophic and thiotrophic symbiont (Table 1). In both symbionts, we observed a significantly lower expression of the transcription termination factor Rho in ob26 samples compared to the *in situ* transcriptome. The transcription terminator Rho is responsible for the dissociation of RNA polymerases from the template DNA, which is thought to be the primary process of transcription termination in bacteria (Peters *et al.*, 2011). In the methanotrophic symbiont, we also identified significantly lower expression of the Rho co-factor NusA in ob26 samples. NusA supports the formation and stabilisation of RNA molecules during transcription termination (Chen *et al.*, 2019). In the thiotrophic symbiont, we identified the Rho co-factor NusG that was significantly lower expressed in ob8 and ob26 of the thiotrophic symbiont (Table 1). Together with Rho, the co-factor NusG suppresses antisense transcription to prevent an accumulation of antisense transcripts (Peters *et al.*, 2012). It is possible that the significantly lower expression of Rho and NusG in the thiotrophic symbiont could cause an uncontrolled transcription of antisense RNA. The significantly lower expression of transcription termination by Rho and its co-factors NusA in the methanotrophic symbiont and NusG in the thiotrophic symbiont suggest a change in the regulation of gene expression.

We also detected significant changes of gene expression for RNA polymerase sigma factors in both symbionts of on-board fixed samples. However, the expression changes followed a dissimilar pattern in the two symbionts (Table 1). In general, sigma factors guide the RNA polymerases to specific promotor sequences and thereby regulate expression of certain genes in bacteria (Wo, 1998). In the methanotrophic symbiont, we observed upregulation of RNA polymerase sigma factors RpoN and RpoH within 8 hours after collection from the mussel bed

(Table 1). RpoH has been determined as key regulator of heat-shock proteins and chaperones in *Escherichia coli* (Narberhaus and Balsiger, 2003). RpoN has regulatory roles for the transcription of genes involved in several metabolic processes including nitrogen metabolism (Lardi *et al.*, 2015). Besides these two sigma factors, we also found significantly higher expression of a Crp/Fnr family protein in ob26 and ob50 samples of the methanotrophic symbiont. Crp/Fnr family proteins have been associated with transcriptional regulation in response to a range of intracellular and environmental factors including oxidative and nitrosative stress, and temperature changes (Körner *et al.*, 2003). We hypothesise that RpoH, RpoN and the Crp/Fnr protein were key drivers of the gene regulation observed in the methanotrophic symbiont of on-board samples.

Table 1: Expression of transcription regulators in methanotrophic and thiotrophic symbionts. In the methanotrophic symbiont, two RNA polymerase sigma factors and one Crp/Fnr transcription regulators were upregulated relative to *in situ* transcriptomes, while sigma factor RpoD, a putative transcriptional regulator, a transcription termination factor, and a transcription anti-termination factor were downregulated in the thiotrophic symbiont. Average log_2FCs relative to *in situ* (n=5).

Methanotrophic symbiont

Gene	Annotation	Log₂FC relative to *in situ* transcriptome			
		ob2	ob8	ob26	ob50
rpoN	RNA polymerase sigma-54 factor RpoN		0.60	0.64	0.45
rpoH	RNA polymerase sigma factor RpoH		0.67	1.16	0.96
rhoXY	Transcription termination factor Rho			-1.77	
nusA	Transcription termination protein NusA			-1.63	
fnrX	Transcriptional regulator Crp/Fnr family			1.56	0.91

Thiotrophic symbiont

Gene	Annotation	Log₂FC relative to *in situ* transcriptome			
		ob2	ob8	ob26	ob50
rpoD	RNA polymerase sigma factor RpoD		-0.98		
nusG	Transcription termination protein NusG		-2.12	-2.34	
rhoXY	Transcription termination factor Rho			-0.96	
ptrX	Putative transcriptional regulator				-3.82

In contrast to the methanotrophic symbiont, the expression of transcription regulators was significantly lower and generally less consistent in the thiotrophic symbiont of on-board samples (Table 1). We detected lower expression of the RNA polymerase sigma factor RpoD in ob8 samples. RpoD regulates the transcription of housekeeping genes under 'normal' conditions in many bacteria (Miura *et al.*, 2015). Besides RpoD, we also found significantly lower expression of a putative transcriptional regulator in ob50 samples of the thiotrophic symbiont. Both RpoD and the putative transcriptional regulator were correlated with the downregulation of several genes in the thiotrophic symbiont that maintain the metabolism in no-stress conditions. However, as the expression pattern of these two transcription regulators was rather inconsistent throughout the on-board fixation time points, it is difficult to interpret their effect on the overall transcriptomic response of the thiotrophic symbiont. In summary, the differences in the expression of the transcriptional regulators between the methanotrophic and thiotrophic symbiont indicate a dissimilar transcriptomic response to on-board storage.

To identify if the overall expression of genes was affected by differential expression of transcriptional regulators, we plotted the expression of single genes in fixation time point of our experiment (Supplementary Figure 6A, 6B and 6C). In the methanotrophic symbiont, we found a large number of intersecting genes that were expressed in all fixation time points. Out of 3,164 predicted genes, 2,452 genes were constitutively expressed in the methanotrophic symbiont (Supplementary Figure 6B). Only a small number of additional genes were expressed at individual time points, and the highest number of genes was expressed in the *in situ* transcriptome. In the thiotrophic symbiont, the overall number of constitutively expressed genes was much lower. Here only 1,406 genes were expressed out of 2,367 predicted genes. Similar to the methanotrophic symbiont, we also detected the highest number of expressed genes in *in situ* samples. The slight differences in the total expression of genes at each fixation time point suggests a turnover of symbiont mRNA that was likely mediated by a small set of transcription regulators.

Such a turnover of mRNA needs transcription regulators to select expressed genes, but is also highly influenced by the degradation of mRNA. In general, degradation of mRNA may be an adaptation by bacteria to facilitate quick responses to a changing environment (Dressaire *et al.*, 2013). We therefore also wanted to track if the dissimilar transcriptome pattern between methanotrophic and thiotrophic symbiont could be explained differences in mRNA degradation. For this, we analysed the total number of mRNA reads per fixation time point that could be mapped to the methanotrophic and thiotrophic symbiont genomes. We found that the overall abundance of mRNA reads remained relatively stable in the methanotrophic symbiont (Supplementary Figure 7). In the thiotrophic symbiont, we observed a much greater decrease of mRNA reads with extended on-board storage (Supplementary Figure 7). This considerably steeper decrease of mRNA in thiotrophic symbiont from on-board fixed samples may be the result of the downregulation of the Rho-NusG transcription termination described before. A lower abundance of Rho-NusG can lead to an accumulation of antisense transcripts, which in return might favour stimulate the degradation of mRNA (Peters *et al.*, 2012). We conclude that the overall stability of mRNA, measured by consistency of expressed genes and total mRNA read abundance, was higher in the methanotrophic symbiont. In contrast, the mechanisms that drove mRNA degradation were much more pronounced in the thiotrophic symbiont.

Based on these results, we propose that the changing environmental factors induced by sample recovery and on-board fixation had a much greater effect on the symbiont transcriptome than on the mussel host transcriptome. Our results show that the regulation of transcription is affected in both symbionts as soon as they are removed from their natural habitat. This likely results in a cascade of changes in the transcription of many functional mechanisms allowing the symbionts to quickly react to the changes in their environment. The high number of differentially expressed genes in symbionts of on-board samples compared to the *in situ* transcriptome can likely be explained by fast mRNA turnover through changes in gene transcription affecting mRNA synthesis and through mRNA degradation. Compared to their

mussel host, the symbionts are much more affected by the present environmental conditions, and both adapt their transcription quickly to respond.

High expression of stress proteins in on-board stored symbionts

The strongest expression changes in both symbionts was observed for heat-shock proteins and chaperones in on-board stored samples (Table 2). In the methanotrophic symbiont, several heat-shock proteins and chaperones were highly upregulated within 8 hours since collection from the mussel bed. All of these genes remained significantly higher expressed in ob26 and ob50 samples. Among them were four different heat-shock proteins of the Hsp20 family. The change of expression for these Hsp20 proteins ranged between 5 and 42-fold increases in on-board fixed samples compared to the is0 samples, and largely increased with progressing on-board storage. In the thiotrophic symbiont, we also detected significantly higher expression of an Hsp20 protein in ob26 and ob50 samples relative to is0 samples. However, the expression change for this Hsp20 was generally lower compared to the Hsp20 proteins of the methanotrophic symbiont, with 3.5 to 10.8-fold increases at the same fixation time points. Hsp20 family proteins (also known as small heat-shock proteins) are recognised for their involvement in protein folding under diverse stress conditions (Obuchowski and Liberek, 2020).

Out of all heat-shock proteins and chaperones detected, we found the highest expression for the heat-shock protein DnaK in ob8, ob26 and ob50 samples of the methanotrophic symbiont, exceeding more than a 70-fold higher expression in all on-board fixed samples (Table 2). DnaK was also significantly higher expressed in on-board samples of the thiotrophic symbiont compared to the *in situ* samples. Similar to the Hsp20 protein, DnaK showed much lower expression changes in the thiotrophic symbiont compared to the methanotrophic symbiont of 11.5-fold. DnaK is one of the key heat-shock proteins in bacteria, belongs to the Hsp70 family and has several associated co-chaperones (Rosenzweig *et al.*, 2019). We also identified several such linked genes that co-function with DnaK in the DnaK chaperone system and that were significantly higher expressed in on-board fixed samples compared to the *in situ* fixed

samples. These included the co-chaperone CbpA (DnaJ homolog) and CbpM in the methanotrophic symbiont, and the DnaK co-chaperone GrpE in the thiotrophic symbiont (Table 2; Doyle, Hoskins and Wickner, 2007). The DnaK chaperone system is involved in a wide range of key cellular functions such as resistance to heat shock and many other (Chae *et al.*, 2004; Tomoyasu *et al.*, 2012). We hypothesise that the DnaK chaperone system is employed by both symbionts as a protective response to the conditions induced through sample recovery and on-board storage.

Table 2: Expression of heat-shock proteins and chaperones in methanotrophic and thiotrophic symbiont. Relative to *in situ* transcriptomes, nine heat-shock proteins and chaperones were significantly higher expressed in the methanotrophic symbiont, six were significantly higher expressed in the thiotrophic symbiont. No differential expression of these proteins were found in ob2 samples of the methanotrophic symbiont. Average log_2FCs relative to *in situ* (n=5).

Methanotrophic symbiont

Gene	Annotation	Log₂FC relative to *in situ* transcriptome			
		ob2	ob8	ob26	ob50
cbpA	DnaJ-class molecular chaperone CbpA		3.59	3.85	3.72
cbpM	Chaperone-modulator protein CbpM		2.33	2.01	2.48
clpB	***Chaperone ClpB***		***3.64***	***3.85***	***3.99***
dnaK	***Chaperone protein DnaK***		***6.28***	***6.46***	***6.54***
hsp20A	Heat shock protein Hsp20 family		4.73	5.16	5.42
hsp20B	Heat shock protein Hsp20 family		4.70	4.98	5.25
hsp20C	Heat shock protein Hsp20 family		2.57	3.19	2.39
hsp20D	Heat shock protein Hsp20 family		2.69	2.66	2.92

Thiotrophic symbiont

Gene	Annotation	Log₂FC relative to *in situ* transcriptome			
		ob2	ob8	ob26	ob50
clpB	***Chaperone ClpB***	***1.88***	***2.44***	***3.12***	***5.04***
dnaK	***Chaperone protein DnaK***	***1.48***		***2.30***	***3.53***
grpE	Heat shock protein GrpE				1.46
hscA	Chaperone protein HscA			-1.30	-1.64
htpG	Chaperone protein HtpG			2.06	3.33
hsp20A	Heat shock protein Hsp20 family			1.83	3.44

The remarkably high expression of such heat-shock proteins and chaperones in both symbionts indicates a strong response to the changing environmental conditions induced during sample recovery and on-board storage. A recent study showed higher expression of heat-shock proteins in free-living deep-sea thiotrophic Epsilonproteobacteria in on-board incubated samples (Fortunato *et al.*, 2020). It is possible that the upregulation of heat-shock proteins is a common response of deep-sea bacteria to depressurisation. In the methanotrophic symbiont, the high expression of the RNA polymerase sigma factor RpoH likely regulated the extreme heat-shock response (Table 1; Narberhaus and Balsiger, 2003).

While the upregulation of heat-shock proteins might represent a typical response to unfavourable environmental conditions, it may also indicate a strategy of the symbionts to survive in the host bacteriocyte. For example, ClpB was found to be essential for cell survival during extreme heat stress, but has been associated with symbionts to escape intracellular digestion by the host (Doyle *et al.*, 2007; Neckers and Tatu, 2008). Intracellular digestion of symbionts *via* lysosomes has been identified to be an important process for controlling symbiont abundance in the cold-seep mussel *B. childressi* (Tietjen *et al.*, 2020). It is intriguing to speculate that the symbionts of *B. puteoserpentis* use these heat-shock proteins to avoid lysosomal digestion by the host. In fact, the epibionts of the deep-sea lobster showed no expression changes for the ClpB coding genes, and might be because these symbionts are not prone to lysosomal digestion as epibionts (Motoki *et al.*, 2020). The involvement of heat-shock proteins in host-symbiont interactions has yet to be demonstrated for chemosynthetic symbioses, and is a promising prime target for future research.

Nitrate respiration supports oxygen demand of symbionts during on-board storage

Sample recovery and on-board storage induced a temporal interruption of oxygen supply for the symbionts of *B. puteoserpentis* when the mussels closed their shells. While the genes for oxygen respiration such as cytochrome-c oxidase were expressed in all conditions, we detected significant upregulation of nitrate respiration (dissimilatory nitrate reduction) in the symbionts within 2 hours after collection from the mussel bed. The methanotrophic symbiont

showed first signs of increased nitrate respiration in ob2 samples through upregulation of the nitrate/nitrite transporter NarK and the dissimilatory nitrite reductase Nir (Figure 2 and Supplementary Table 3). With extended on-board storage, the methanotrophic symbiont increased the expression for nitrate respiration (Nir, NarG and NarH). A similar pattern was observed for the thiotrophic symbiont, however upregulation of these NarK, NarG and NarH occurred later (Figure 2 and Supplementary Table 4). The significantly higher expression of genes involved in nitrate respiration suggest a higher demand for additional electron acceptors besides oxygen in on-board fixed samples. In the displaced samples dis24 and dis48, the methanotrophic symbiont also showed higher expression of NarK, and dissimilatory nitrate reduction *via* NarG and NarH (Supplementary Table 3). However, unlike in the methanotrophic symbiont, the genes for nitrate respiration (NarG and NarH) were lower expressed in dis24 and dis48 samples of the thiotrophic symbiont (Supplementary Table 4). Instead, genes for assimilatory nitrate reductase together with the NarK were significantly upregulated, and suggest that oxygen was not as limited in the displaced mussels as in the on-board stored mussels.

The use of nitrate as alternative electron acceptor for energy synthesis is widespread in free-living and symbiotic chemosynthetic bacteria (Hentschel *et al.*, 1993; Moreno-Vivián *et al.*, 1999). Although nitrate respiration has a lower energy yield than oxygen, this electron acceptor is more favourable for energy synthesis over other sources like fermentation (Thauer *et al.*, 1977). The genomes of the methanotrophic and thiotrophic symbiont of *B. puteoserpentis* indicated the potential to use nitrate as alternative terminal electron acceptor to oxygen in the respiratory process. However, the genome of both symbionts only encoded an incomplete denitrification pathway to produce nitrite, nitric oxide and dinitrogen oxide, but not dinitrogen. It is possible that upon increased respiration of nitrate by both symbionts, cytotoxic nitric oxide accumulates in the gill bacteriocytes. In the methanotrophic symbiont, we detected significant upregulation of the transcriptional regulator NnrS in ob8, ob26 and ob50, and also in dis24 and dis48 samples (Supplementary Table 3). NnrS was found

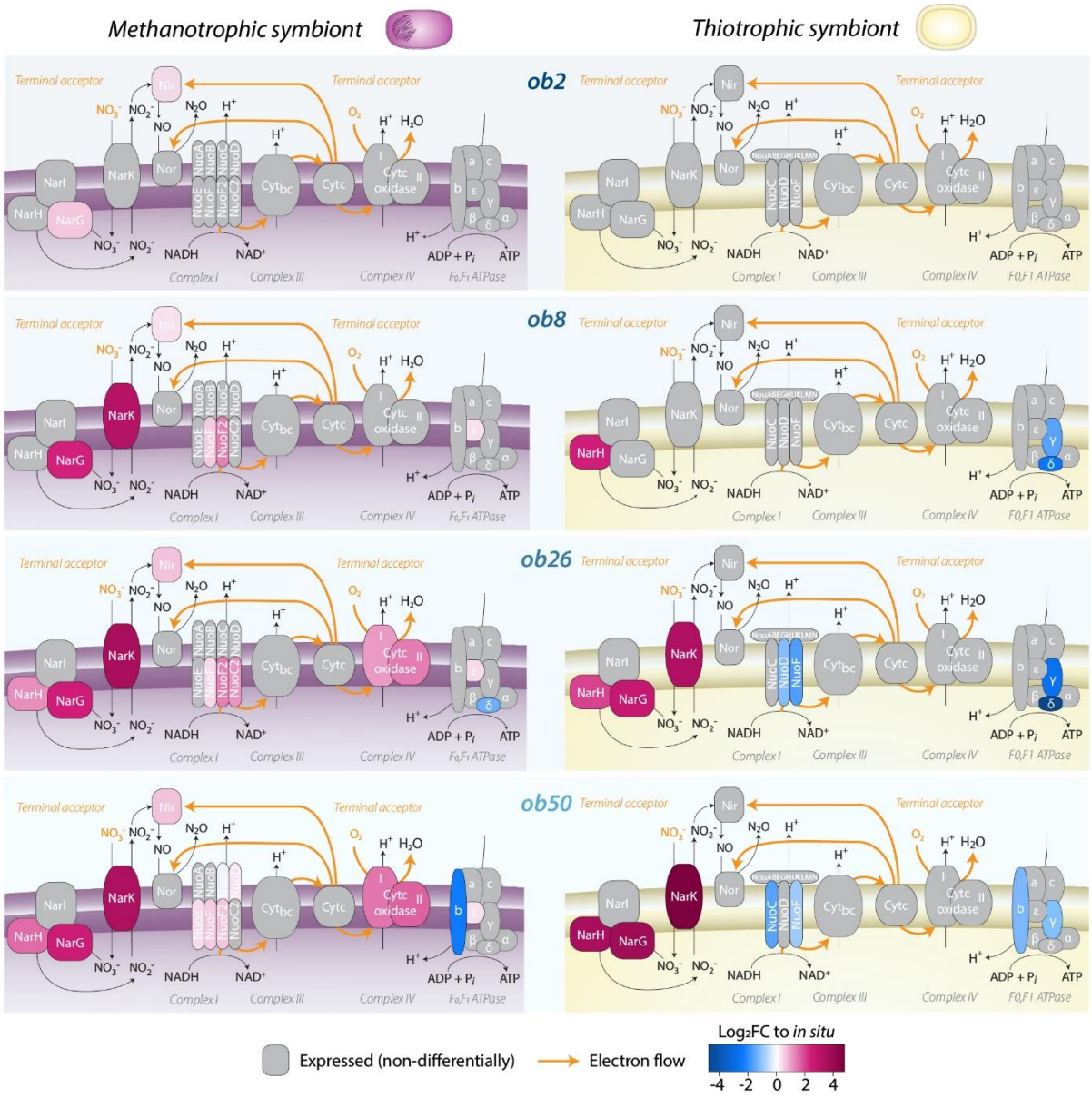

Figure 2: Nitrate respiration supports energy synthesis in both symbionts of on-board fixed mussels. Schematic of possible electron transport chain of the methanotrophic (purple cell membrane) and thiotrophic (yellow cell membrane) symbiont that use oxygen and nitrate as terminal electron acceptors through redox reductions, which possibly involve the same enzymes of complex I and II for this process (Chen and Strous, 2013). Grey proteins indicate non-differential expression, blue or red colouration represent log_2FCs compared to *in situ* samples. Orange arrows indicate proposed electron flow. The methanotrophic symbiont responds quickly to changing environmental conditions and shows upregulation of dissimilatory nitrate respiration genes in ob2 samples. The thiotrophic symbiont shows first signs of this response in ob8 samples.

to be involved in the protection of proteins that contain iron-sulphur clusters from inhibition by nitric oxide (Stern *et al.*, 2013). We did not detect significant upregulation of an analogous protective protein to nitric oxide in the transcriptomes of the thiotrophic symbiont.

In the methanotrophic symbiont, nitrate respiration is likely an adaption for oxygen-low conditions to retain a functioning methane oxidation pathway similar to free-living methanotrophic bacteria (Kits, Klotz and Stein, 2015). Denitrification has been linked to methane oxidation in the absence of oxygen, however the mechanisms that couple methane oxidation to nitrate reduction are unresolved (Chistoserdova *et al.*, 2009). Our data shows the link between nitrate respiration and methane oxidation through significantly higher expression of particulate methane monoxygenase, suggesting a high oxygen-dependency of the methanotrophic symbiont (Supplementary Figure 8 and Supplementary Note 1). Supporting this evidence for a higher oxygen dependency was the significantly higher expression of the protein NtrY in ob8 and dis48 samples. NtrY is a haem-binding histidine kinase that, in the absence of oxygen, induces a signalling cascade that regulates the expression of nitrogen respiration enzymes (Carrica *et al.*, 2012). In addition, the significantly higher expression for the RNA polymerase sigma factor RpoN described before likely also regulates the transcription of genes involved in nitrogen metabolism (Lardi *et al.*, 2015). Taken together, it appears that the methanotrophic symbiont is highly sensitive to oxygen limitations, and has a fine-tuned regulatory mechanism that allows it to quickly use nitrate as an alternative terminal electron acceptor instead of oxygen.

Nitrate respiration in the thiotrophic symbiont of *Bathymodiolus* spp. mussels has been described in previous studies (Ponnudurai *et al.*, 2017). In fact, the use of nitrate as alternative electron acceptor is reported for distantly related thiotrophic symbionts of several other marine invertebrate hosts from hydrothermal vents and also from reduced shallow water sediments, suggesting that this a common trait among sulphur-oxidising symbionts. For example, the sulphur-oxidising symbionts of Stilbonematinae were shown to use nitrate as alternative electron acceptor, which enables their nematode host to move into the deeper

anoxic sediments (Hentschel *et al.*, 1999). In the hydrothermal vent snail *Alviniconcha*, the thiotrophic symbionts were proposed to use nitrate as alternative electron acceptor to avoid competition with their host, and showed upregulation of nitrate respiration after treatment with hydrogen sulphide and nitrate (Breusing *et al.*, 2020). In symbionts of the tubeworm *Ridgeia piscesae,* the use of nitrate as electron acceptor was proposed to be linked to sulphide oxidation (Liao *et al.*, 2014). We also detected such a higher expression of sulphur oxidation pathways in on-board fixed samples that may be linked to increased nitrate respiration in the thiotrophic symbiont (Supplementary Note 1 and Supplementary Figure 8).

In the natural environment, short-term limitation of oxygen is expected to occur frequently for symbionts of *Bathymodiolus* mussels. By drawing seawater through the gill filaments, the mussels supply the symbionts with oxygen. In our experiment, oxygen limitation was likely induced by the mussel host through the immediate closing of their valves upon contact with ROV arm during collection. It is likely that the mussels show this protective behaviour frequently in their natural habitat to avoid predation by other macrofauna such as crustaceans that co-occur at the mussel bed (Micheli *et al.*, 2002). In our experiment, oxygen was likely re-introduced into the system after 24 hours of on-board storage. We found significant upregulation of cytochrome-c oxidase of the respiratory chain complex IV in the methanotrophic symbiont in ob26 and ob50 samples (Figure 2), suggesting that the mussel host started normal respiratory activity with the flow of oxygen-rich water through the body cavities. Recent studies revealed that *Bathymodiolus* mussels interrupt the flow of water through their gills by closing their valves in biological rhythms (Mat *et al.*, 2020). The mussels not only close their valves because of stimuli by predators, but also because of tidal and daily rhythms that influence the behaviour and physiology of the mussels (Mat *et al.*, 2020). Consequently, the symbionts of *Bathymodiolus* mussels must be able to cope with frequent periods of interrupted oxygen flow through the gills. An additional abiotic cause for short-term oxygen limitations in the *Bathymodiolus* system is the dynamic mixing of anoxic hydrothermal vent effluents with the oxygen-rich seawater (Arndt *et al.*, 2001; Seston *et al.*, 2016). The upregulation of nitrate respiration in both symbionts in our study appears to be an

adaption to cope with these short-term fluctuations of oxygen in the natural environment of the symbiosis.

Cell elongation in the methanotrophic symbiont enhances nutrient uptake

Although the methanotrophic and thiotrophic symbiont shared similar responses to sample recovery and on-board storage, we also observed a striking difference between these two symbionts. The methanotrophic symbiont showed significant upregulation of genes involved in the synthesis of cytoplasmic peptidoglycan precursors within two hours after collection from the *in situ* environment (Figure 3). With exception of MurA, all genes involved in the synthesis of peptidoglycan precursors were upregulated in the on-board fixed mussels and showed increasing expression over time (Figure 3). We also observed higher expression of some of these genes in displaced samples (Supplementary Table 3), suggesting that this response of the symbionts was not related to pressure changes but rather to limitations of vent fluids and substrates. In bacteria, cell shape and size is largely determined by peptidoglycan (Monds *et al.*, 2014). We therefore hypothesise that the upregulation of cell wall synthesis genes was linked to cell enlargement of the methanotrophic symbiont (Figure 3). Although we could not perform microscopy imaging with our RNAlater fixed specimens to show cell elongation, we acquired microscopy images of other *B. puteoserpentis* mussels that were incubate with EdU for 46 hours before fixation, and of *B. childressi* mussels that were starved for 48 hours before fixation (Supplementary Figure 9). In these mussels, cell elongation of the methanotrophic symbiont was apparent, and suggests that this is a shared response between methanotrophic symbiont of different *Bathymodiolus* hosts.

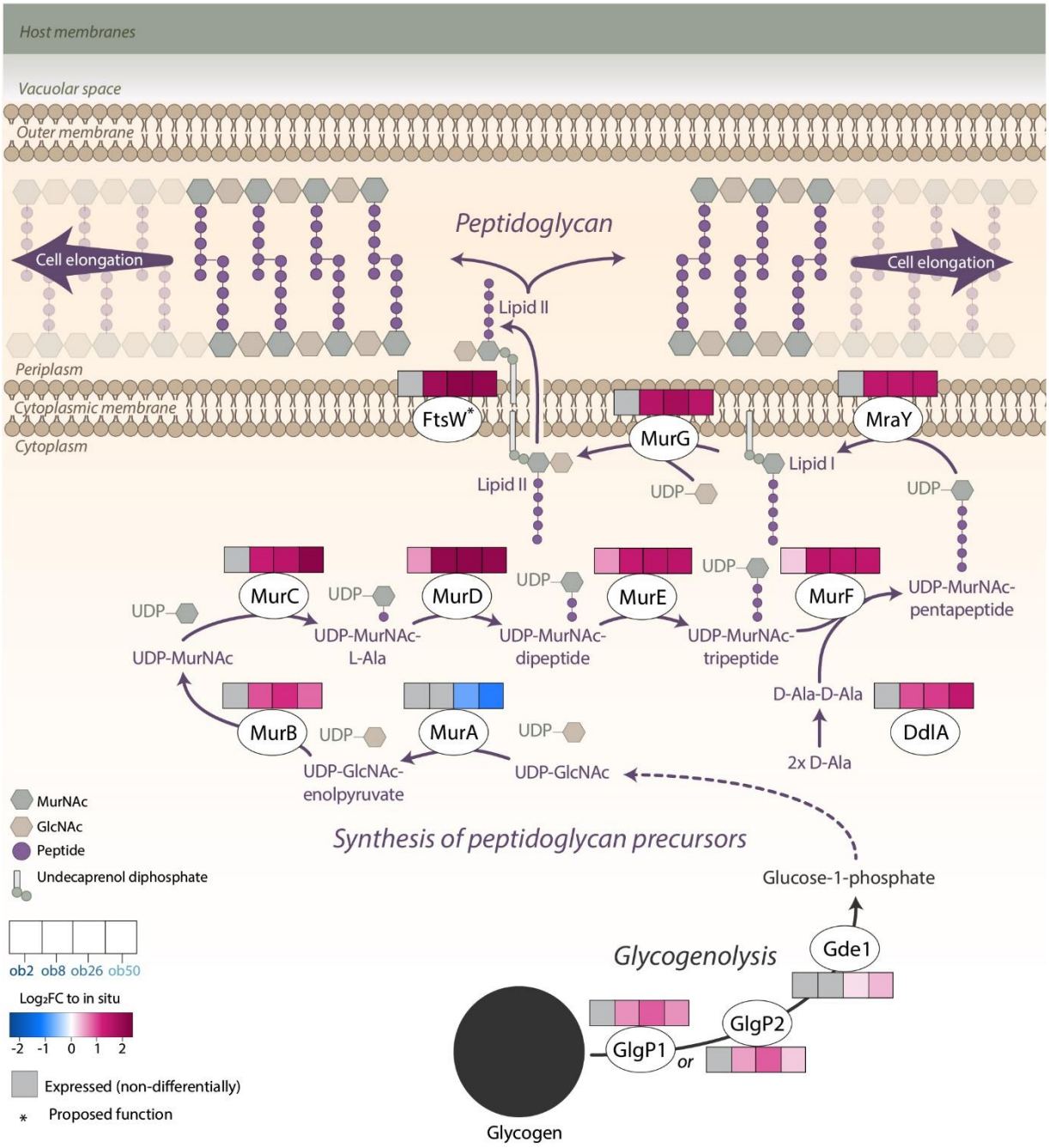

Figure 3: Upregulation of peptidoglycan synthesis for cell elongation in the methanotrophic symbiont. The methanotrophic symbiont degrades glycogen *via* glycogenolysis to access stored glucose, e.g. to generate UDP-GlcNAc for peptidoglycan synthesis. The intracellular precursors of peptidoglycan are produced by multiple enzymes resulting in lipid II that is flipped across the cytoplasmic membrane into the periplasm. The resulting peptidoglycan is likely added to the peptidoglycan layer to for cell elongation. Coloured boxes illustrate relative expression changes (log_2 fold-changes) of on-board fixed samples compared to the *in situ* fixed samples. FtsW likely has "flippase"-like functions as found in Taguchi *et al.* (2019).

Many bacteria elongate their cells in response to diverse environmental stressors (Wehrens *et al.*, 2018). In the marine heterotroph *Pseudovibrio* sp., cell elongation was observed as a response to limiting phosphate starvation (Romano *et al.*, 2015). While we cannot determine the trigger for cell elongation in the methanotrophic symbiont with our data, we hypothesise that the limitation of methane is one key factor. Cell elongation during methane depletion could be a strategy to maximise growth rate when environmental conditions become favourable again. It has been demonstrated that larger cells can reach their maximal growth rate much quicker than smaller cells (Monds *et al.*, 2014). Cell elongation or filamentation has not been documented for *Methyloprofundus sedimenti* over the course of a 96-hour methane-starvation experiment (Tavormina *et al.*, 2017). However, filamentation has been reported for a free-living methylotroph in response to UV radiation (Williams and Shimmin, 1978). While it is still unknown how these changes in cell shapes are triggered and regulated, there are several possible advantages of developing large surface areas when enclosed in a host cell under stress conditions, including the avoidance of phagocytosis (Yang *et al.*, 2016). It is also possible that the methanotrophic symbiont of *B. puteoserpentis* uses cell elongation as a strategy to increase the surface for diffusion of oxygen and methane through the membranes. In this way, the methanotrophic symbiont could gain a competitive advantage over the thiotrophic symbiont to access oxygen.

It remains to be resolved why we detected significant downregulation of MurA, which is one of two known enzymes that facilitate the production of UDP-GlcNAc as first committed step of peptidoglycan biosynthesis (Barreteau *et al.*, 2008). The genome of the methanotrophic symbiont did not encode the other known enzyme, MurZ, that mediates the synthesis of UDP-GlcNAc (Rismondo *et al.*, 2017). It is possible that UDP-GlcNAc is re-transferred from the periplasm into the cytosol as a result of peptidoglycan recycling (Park and Uehara, 2008). In addition, MurA was not encoded on the same operon or in close proximity as all other proteins of peptidoglycan biosynthesis in our metagenome-assembled genome bin, and it is possible that MurA is transcribed by different sigma-factors.

Because the symbionts are removed from their energy source in vent fluids, the methanotrophic symbiont requires additional energy and carbon to produce peptidoglycan precursors as part of cell elongation. The methanotrophic symbiont encoded pathways for glycogen synthesis, storage and degradation, and appears to rely on this self-storage as energy source as suggested for other bacterial species (Sekar *et al.*, 2019). We detected significantly higher expression of glycogen degradation in on-board samples of the methanotrophic symbiont (Figure 3). It is likely that the break-down of glycogen (glycogenolysis) served as nutrient resource to support both cell survival and cell elongation in the methanotrophic symbiont under energy-limited conditions.

Conclusion

Hydrothermal vents are highly dynamic ecosystems in which emission rates and composition of fluids can fluctuate within short-periods of time. At the same time, these remote oases are just as influenced by tidal rhythms as shallow-water ecosystems. It is assumed that the symbionts occupy a more sheltered habitat within the mussel host that provides a stable environment for the symbionts. In our study, the recovery of deep-sea *Bathymodiolus* mussels and their on-board storage, as well as the displacement experiment at least partially resembled naturally occurring interruptions of energy-rich water flow in the system. In contrast to the hypothesis of a shelter status for endosymbionts, not the host, but the symbionts responded at the transcriptomic level. In addition, the high number of genes that were only differentially expressed in displaced samples suggests that the sample recovery and on-board storage triggered a distinct response, suggesting the capability for both symbiont to tightly regulate expression based on environmental stimuli.

While we could not detect significant gene expression changes in the host gills, it is important to consider that not all responses to stress manifest at the cellular level in animals, but can also be counteracted by behavioural adaptations including the closing of shells. This behavioural response has an effect on the symbionts enclosed within tissues of their mussel host. In the gills of the mussel host, the symbionts are not only influenced by the physico-

chemical environment of the hydrothermal vent, but also by host behaviour that determines water flow and thus oxygen and chemical energy supply. It is intriguing to speculate that endosymbionts of bivalve mussels might even need to be more flexible to cope with oxygen and energy limitations than free-living bacteria. Sustaining a versatile metabolism, for instance by using alternative electron acceptors, is essential to ensure survival in these fluctuating environments and has been described for intracellular pathogens. In a similar manner as well-adapted pathogens, the symbionts appear to have been selected to minimise competition with their host. A hallmark for symbionts on all parts of the mutualist to pathogen spectrum therefore appears to be a flexible metabolism to survive nutritional deprivation, and temporarily low oxygen concentrations. This selection for flexibility is also connected to competitive adaptations between the symbionts to acquire essential resources. For example, the methanotrophic symbiont displayed cell elongation to enhance diffusion of oxygen, nitrate and methane traces, requiring investment of own glucose stores. In contrast, the thiotrophic symbiont appeared to downregulate gene transcription to conserve energy, which was reflected by lower overall lower mRNA abundance. These dissimilar survival strategies temporarily resolve the competition, however, these strategies are probably only viable for a short period of time because symbiont loss was already detectable after 7 days of displacement in the deep-sea mussel *B. azoricus* (Détrée *et al.*, 2019).

We propose that studies on the physiology of deep-sea symbioses should base interpretations on *in situ* fixed organisms. Although we could not detect clear changes in the host transcriptome, we found substantial transcriptome changes in both symbiont. The on-board fixed samples did not reflect their natural physiology, and it is likely that both results from expression analyses or from further experiments are constrained by the stress response the symbionts are displaying.

Acknowledgements

We thank the Deutsche Forschungsgemeinschaft (DFG, German Research Foundation) for funding under Germany's Excellence Strategy EXC-2077-390741603. Special thanks go to the captain, crew and research team from the Meteor M126 research cruise in 2016, particularly to Volker Ratmeyer for input on the IDEFIX construction and the remaining ROV team from the MARUM for excellent operation of the ROV during IDEFIX fixation. We also acknowledge the help of Georg Herz and the MPI Bremen mechanic workshop for IDEFIX construction. We thank Bruno Hüttel und Lisa Czaja-Hasse from the Max Planck Genome Center in Cologne for their great technical support during library preparation and sequencing. We thank Silke Wetzel, Dolma Michellod for their assistance during sample collection and processing. We also thank Maxim Rubin-Blum, Lizbeth Sayavedra, Chakkiath Paul Antony, and the Symbiosis Department for scientific input and discussions.

Chapter II: Supplementary Note

Supplementary Note – Upregulation of methane- and sulphur-oxidation

In addition to an increased expression of nitrate respiration, the methanotrophic and the thiotrophic symbiont exhibited significant changes of gene expression for their specific metabolism of methane and sulphur, respectively. In the methanotrophic symbiont, we detected higher expression of all subunits of the particulate methane monoxygenase (PmoA, PmoB and PmoC), in ob8, ob26 and ob50 samples in spite of the removal of mussels from the methane source (Supplementary Figure 8 and Supplementary Table 3). In both displacement samples, only PmoC was significantly higher expressed. In the absence of hydrothermal vent fluids, the upregulation of the methane monoxygenase may be the result of scavenging trace methane in the mussel tissues, analogous to what has been proposed in starved *Methyloprofundus sedimenti* (Tavormina *et al.*, 2017). However, we also observed lower expression of the methanol-oxidising XoxF after 24 hours of on-board storage (Supplementary Figure 8), which suggests that high expression of methane oxidation is not necessarily related to the availability of methane in mussel tissues. Rather, higher expression of methane monoxygenase could be a strategy to accumulate mRNA transcripts for quick translation or to increase the amount of enzymes available to occupy the larger membrane space in the elongated cells. Both would be viable strategies to jumpstart growth upon replenishment of methane to the mussel (Tavormina *et al.*, 2017).

Methanol, the product of methane oxidation by the methanotrophic symbiont *via* particulate methane monoxygenase, could diffuse out of the cells to be oxidised to formaldehyde by the thiotrophic symbiont through methanol dehydrogenase XoxF (Sayavedra, 2016). We detected significantly higher expression of XoxF in the thiotrophic symbiont of ob2 and ob50 samples, suggesting that the thiotrophic symbiont utilises additional energy and carbon resources in the absence of vent fluids. Although our transcriptome data could not resolve the full pathway of methanol oxidation to carbon assimilation, we also found significantly higher expression of formate dehydrogenase FDH-O to produce carbon dioxide (Supplementary Figure 8 and

Supplementary Table 4). It is tempting to speculate that both symbionts compete for methanol produced by the methanotrophic symbiont in conditions where the primary substrates for energy metabolism of either symbiont is limited.

In the thiotrophic symbiont, we also observed significant changes of expression of genes that are part of sulphur oxidation pathways in on-board stored samples (Supplementary Figure 8 and Supplementary Table 4). Both, the Sox-complex for thiosulphate oxidation, and the reverse-acting dissimilatory sulphite reductase complex (Dsr-complex) for hydrogen sulphide oxidation were present in the genome of the *B. puteoserpentis* symbiont. We found higher expression of genes involved of the Sox-complex SoxY, SoxA and SoxX in ob2 and ob50 samples compared to the *in situ* transcriptomes, which could indicate higher availability of thiosulphate in these samples. In addition, we found significantly lower expression of genes (DsrM, DsrK, DsrO) that are part of the membrane-bound Dsr-complex in ob26 and ob50 samples. In comparison, the thiotrophic symbiont of the related host species *B. azoricus* had a higher expression of proteins for the Sox-complex to oxidise thiosulphate than proteins of the Dsr-complex for hydrogen sulphide oxidation, suggesting that thiosulphate is of high importance in the *B. azoricus* habitat (Ponnudurai *et al.*, 2017).

Interestingly, we found significantly higher expression of hydrogen sulphide oxidation proteins DsrA and DsrB in ob50 samples alongside SoxY and SoxA. The upregulation of DsrA and DsrB indicates high availability of hydrogen sulphide at later stages of on-board storage. In the Pacific vent mussel *B. thermophilus,* accumulation of hydrogen sulphide was detected after several hours of anoxia, and was found to be produced by the thiotrophic symbiont (Arndt *et al.*, 2001). It is possible that the thiotrophic symbiont of *B. puteoserpentis* also generated hydrogen sulphide in on-board stored mussels. The hydrogen sulphide may be produced from own elemental sulphur stores in the thiotrophic symbiont, as has been reported for the symbionts of *B. azoricus* (Kádár *et al.*, 2005). It is likely that variations in the presence of sulphur compounds and a delayed turnover of own sulphur storages influences the expression of genes for sulphur pathways.

References

Akiva, E., Brown, S., Almonacid, D. E., Barber, A. E., *et al.* (2014) 'The Structure-Function Linkage Database', *Nucleic Acids Research*, 42, pp. 521–530. doi: 10.1093/nar/gkt1130.

Ansorge, R., Romano, S., Sayavedra, L., Porras, M. Á. G., *et al.* (2019) 'Functional diversity enables multiple symbiont strains to coexist in deep-sea mussels', *Nature Microbiology*, 4, pp. 2487–2497. doi: 10.1038/s41564-019-0572-9.

Arndt, C., Gaill, F. and Felbeck, H. (2001) 'Anaerobic sulfur metabolism in thiotrophic symbioses', *Journal of Experimental Biology*, 204, pp. 741–750.

Attwood, T. K., Coletta, A., Muirhead, G., Pavlopoulou, A., *et al.* (2012) 'The PRINTS database: A fine-grained protein sequence annotation and analysis resource-its status in 2012', *Database*, 2012, pp. 1–9. doi: 10.1093/database/bas019.

Aziz, R. K., Bartels, D., Best, A., DeJongh, M., *et al.* (2008) 'The RAST Server: Rapid annotations using subsystems technology', *BMC Genomics*, 9, pp. 1–15. doi: 10.1186/1471-2164-9-75.

Bankevich, A., Nurk, S., Antipov, D., Gurevich, A. A., *et al.* (2012) 'SPAdes: A new genome assembly algorithm and its applications to single-cell sequencing', *Journal of Computational Biology*, 19, pp. 455–477. doi: 10.1089/cmb.2012.0021.

Barreteau, H., Kovač, A., Boniface, A., Sova, M., *et al.* (2008) 'Cytoplasmic steps of peptidoglycan biosynthesis', *FEMS Microbiology Reviews*, 32, pp. 168–207. doi: 10.1111/j.1574-6976.2008.00104.x.

Bemis, K., Lowell, R. P. and Farough, A. (2012) 'Diffuse flow on and around hydrothermal vents at mid-Ocean ridges', *Oceanography*, 25, pp. 183–191. doi: 10.5670/oceanog.2012.16.

Boël, G., Letso, R., Neely, H., Price, W. N., *et al.* (2016) 'Codon influence on protein expression in *E. coli* correlates with mRNA levels', *Nature*, 529, pp. 358–363. doi: 10.1038/nature16509.

Bray, N. L., Pimentel, H., Melsted, P. and Pachter, L. (2016) 'Near-optimal probabilistic RNA-seq quantification', 34, pp. 525–527. doi: 10.1038/nbt.3519.

Breusing, C., Mitchell, J., Delaney, J., Sylva, S. P., *et al.* (2020) 'Physiological dynamics of chemosynthetic symbionts in hydrothermal vent snails', *ISME Journal*, 14, pp. 2568–2579. doi: 10.1038/s41396-020-0707-2.

Bryant, D. M., Johnson, K., DiTommaso, T., Tickle, T., *et al.* (2017) 'A Tissue-Mapped Axolotl De Novo Transcriptome Enables Identification of Limb Regeneration Factors', *Cell Reports*, 18, pp. 762–776. doi: 10.1016/j.celrep.2016.12.063.

Carrica, M. del C., Fernandez, I., Martí, M. A., Paris, G., *et al.* (2012) 'The NtrY/X two-component system of Brucella spp. acts as a redox sensor and regulates the expression of nitrogen respiration enzymes', *Molecular Microbiology*, 85, pp. 39–50. doi: 10.1111/j.1365-2958.2012.08095.x.

Chae, C., Sharma, S., Hoskins, J. R. and Wickner, S. (2004) 'CbpA, a DnaJ homolog, is a DnaK co-chaperone, and its activity is modulated by CbpM', *Journal of Biological Chemistry*, 279, pp. 33147–33153. doi: 10.1074/jbc.M404862200.

Chan, L. Y., Mugler, C. F., Heinrich, S., Vallotton, P., *et al.* (2018) 'Non-invasive measurement of mRNA decay reveals translation initiation as the major determinant of mRNA stability', *eLife*, 7, pp. 1–32. doi: 10.7554/eLife.32536.

Chen, J., Morita, T. and Gottesman, S. (2019) 'Regulation of transcription termination of small RNAs and by small RNAs: Molecular mechanisms and biological functions', *Frontiers in Cellular and Infection Microbiology*, 9, pp. 1–9. doi: 10.3389/fcimb.2019.00201.

Chistoserdova, L., Kalyuzhnaya, M. G. and Lidstrom, M. E. (2009) 'The expanding world of methylotrophic metabolism', *Annual Review of Microbiology*, 63, pp. 477–499. doi: 10.1146/annurev.micro.091208.073600.

Conesa, A., Götz, S., García-Gómez, J. M., Terol, J., *et al.* (2005) 'Blast2GO: A universal tool for annotation, visualization and analysis in functional genomics research', *Bioinformatics*, 21, pp. 3674–3676. doi: 10.1093/bioinformatics/bti610.

Cramer, P. (2019) 'Organization and regulation of gene transcription', *Nature*. doi: 10.1038/s41586-019-1517-4.

Détrée, C., Haddad, I., Demey-thomas, E., Vinh, J., *et al.* (2019) 'Global host molecular perturbations upon in situ loss of bacterial endosymbionts in the deep-sea mussel *Bathymodiolus azoricus* assessed using proteomics and transcriptomics', pp. 1–14.

Van Dover, C. L. (2000) *The Ecology of Deep-Sea Hydrothermal Vents*. Princeton Univ. Press, New Jersey.

Doyle, S. M., Hoskins, J. R. and Wickner, S. (2007) 'Collaboration between the ClpB AAA+ remodeling protein and the DnaK chaperone system', *Proceedings of the National Academy of Sciences of the United States of America*, 104, pp. 11138–11144. doi: 10.1073/pnas.0703980104.

Dressaire, C., Picard, F., Redon, E., Loubière, P., *et al.* (2013) 'Role of mRNA Stability during Bacterial Adaptation', *PLoS ONE*, 8. doi: 10.1371/journal.pone.0059059.

Dubilier, N., Bergin, C. and Lott, C. (2008) 'Symbiotic diversity in marine animals : the art of harnessing chemosynthesis', *Nature Reviews Microbiology*, 6, pp. 725–740. doi: 10.1038/nrmicro1992.

Duperron, S., Bergin, C., Zielinski, F., Blazejak, A., *et al.* (2006) 'A dual symbiosis shared by two mussel species, *Bathymodiolus azoricus* and *Bathymodiolus puteoserpentis* (Bivalvia: Mytilidae), from hydrothermal vents along the northern Mid-Atlantic Ridge', *Environmental Microbiology*, 8, pp. 1441–1447. doi: 10.1111/j.1462-2920.2006.01038.x.

Duperron, S., Lorion, J., Samadi, S., Gros, O., *et al.* (2009) 'Symbioses between deep-sea mussels (Mytilidae: Bathymodiolinae) and chemosynthetic bacteria: diversity, function and evolution', *Comptes Rendus - Biologies*, 332, pp. 298–310. doi: 10.1016/j.crvi.2008.08.003.

Duperron, S., Quiles, A., Szafranski, K. M., Léger, N., *et al.* (2016) 'Estimating Symbiont Abundances and Gill Surface Areas in Specimens of the Hydrothermal Vent Mussel *Bathymodiolus puteoserpentis* Maintained in Pressure Vessels', *Frontiers in Marine Science*, 3, pp. 1–12. doi: 10.3389/fmars.2016.00016.

El-Gebali, S., Mistry, J., Bateman, A., Eddy, S. R., *et al.* (2019) 'The Pfam protein families database in 2019', *Nucleic Acids Research*, 47, pp. D427–D432. doi: 10.1093/nar/gky995.

Fernandes, A. D., Macklaim, J. M., Linn, T. G., Reid, G., *et al.* (2013) 'ANOVA-Like Differential Expression (ALDEx) Analysis for Mixed Population RNA-Seq', *PLoS ONE*, 8. doi: 10.1371/journal.pone.0067019.

Fortunato, C. S., Butterfield, D. A., Larson, B., Lawrence-Slavas, N., *et al.* (2020) 'Seafloor incubation experiment with deep-sea hydrothermal vent fluid reveals effect of pressure 2 and lag time on autotrophic microbial communities', *bioRxiv*, pp. 1–36. doi: https://doi.org/10.1101/2020.11.11.378315.

Geier, B., Sogin, E. M., Michellod, D., Janda, M., *et al.* (2020) 'Spatial metabolomics of in situ host-microbe interactions at the micrometer scale', *Nature Microbiology*, 5. doi: 10.1038/s41564-019-0664-6.

González, V. L., Andrade, S. C. S., Collins, T. M., Dunn, C. W., *et al.* (2015) 'A phylogenetic backbone for Bivalvia: an RNA-seq approach', *Proceedings of the Royal Society B: Biological Sciences*, 282, p. 20142332. doi: 10.1098/rspb.2014.2332.

Grabherr, M. G., Haas, B. J., Yassour, M., Levin, J. Z., *et al.* (2011) 'Full-length transcriptome assembly from RNA-Seq data without a reference genome', *Nature Biotechnology*, 29, pp. 644–652. doi: 10.1038/nbt.1883.

Haas, B. J., Papanicolaou, A., Yassour, M., Grabherr, M., *et al.* (2013) 'De novo transcript sequence reconstruction from RNA-seq using the Trinity platform for reference generation and analysis', *Nature Protocols*, 8, pp. 1494–1512. doi: 10.1038/nprot.2013.084.

Hentschel, U., Berger, E. C., Bright, M., Felbeck, H., *et al.* (1999) 'Metabolism of nitrogen and sulfur in ectosymbiotic bacteria of marine nematodes (Nematoda, Stilbonematinae)', *Marine Ecology Progress Series*, 183, pp. 149–158. doi: 10.3354/meps183149.

Hentschel, U., Cary, S. C. and Felbeck, H. (1993) 'Nitrate respiration in chemoautotrophic symbionts of the bivalve *Lucinoma aequizonata'*, *Marine Ecology Progress Series*, 94, pp. 35–41. doi: 10.3354/meps094035.

Huerta-Cepas, J., Szklarczyk, D., Heller, D., Hernández-Plaza, A., *et al.* (2019) 'EggNOG 5.0: A hierarchical, functionally and phylogenetically annotated orthology resource based on 5090 organisms and 2502 viruses', *Nucleic Acids Research*, 47, pp. D309–D314. doi: 10.1093/nar/gky1085.

Huson, D. H., Beier, S., Flade, I., Górska, A., *et al.* (2016) 'MEGAN Community Edition - Interactive Exploration and Analysis of Large-Scale Microbiome Sequencing Data', *PLoS Computational Biology*, 12, pp. 1–12. doi: 10.1371/journal.pcbi.1004957.

Janga, S. C., Salgado, H. and Martínez-Antonio, A. (2009) 'Transcriptional regulation shapes the organization of genes on bacterial chromosomes', *Nucleic Acids Research*, 37, pp. 3680–3688. doi: 10.1093/nar/gkp231.

Kádár, E., Bettencourt, R., Costa, V., Santos, R. S., *et al.* (2005) 'Experimentally induced endosymbiont loss and re-acquirement in the hydrothermal vent bivalve *Bathymodiolus azoricus'*, *Journal of Experimental Marine Biology and Ecology*, 318, pp. 99–110. doi: 10.1016/j.jembe.2004.12.025.

Kanehisa, M., Sato, Y. and Morishima, K. (2016) 'BlastKOALA and GhostKOALA: KEGG Tools for Functional Characterization of Genome and Metagenome Sequences', *Journal of Molecular Biology*, 428, pp. 726–731. doi: 10.1016/j.jmb.2015.11.006.

Kang, D. D., Li, F., Kirton, E., Thomas, A., *et al.* (2019) 'MetaBAT 2: An adaptive binning algorithm for robust and efficient genome reconstruction from metagenome assemblies', *PeerJ*, 2019, pp. 1–13. doi: 10.7717/peerj.7359.

Kits, K. D., Klotz, M. G. and Stein, L. Y. (2015) 'Methane oxidation coupled to nitrate reduction under hypoxia by the Gammaproteobacterium *Methylomonas denitrificans* , sp. nov. type strain FJG1', *Environmental Microbiology*, 17, pp. 3219–3232. doi: 10.1111/1462-2920.12772.

Körner, H., Sofia, H. J. and Zumft, W. G. (2003) 'Phylogeny of the bacterial superfamily of Crp-Fnr transcription regulators: Exploiting the metabolic spectrum by controlling alternative gene programs', *FEMS Microbiology Reviews*, 27, pp. 559–592. doi: 10.1016/S0168-6445(03)00066-4.

Kruse, C. P. S., Basu, P., Luesse, D. R. and Wyatt, S. E. (2017) 'Transcriptome and proteome responses in RNAlater preserved tissue of Arabidopsis thaliana', *PLoS ONE*, 12, pp. 1–10. doi: 10.1371/journal.pone.0175943.

Laalami, S., Zig, L. and Putzer, H. (2014) 'Initiation of mRNA decay in bacteria', *Cellular and Molecular Life Sciences*, 71, pp. 1799–1828. doi: 10.1007/s00018-013-1472-4.

Lardi, M., Aguilar, C., Pedrioli, A., Omasits, U., *et al.* (2015) 'σ54-Dependent response to nitrogen limitation and virulence in *Burkholderia cenocepacia* strain H111', *Applied and Environmental Microbiology*, 81, pp. 4077–4089. doi: 10.1128/AEM.00694-15.

Lewis, T. E., Sillitoe, I., Dawson, N., Lam, S. D., *et al.* (2018) 'Gene3D: Extensive prediction of globular domains in proteins', *Nucleic Acids Research*, 46, pp. D435–D439. doi: 10.1093/nar/gkx1069.

Liao, L., Wankel, S. D., Wu, M., Cavanaugh, C. M., *et al.* (2014) 'Characterizing the plasticity of nitrogen metabolism by the host and symbionts of the hydrothermal vent chemoautotrophic symbioses *Ridgeia piscesae*', *Molecular Ecology*, 23, pp. 1544–1557. doi: 10.1111/mec.12460.

Marchler-Bauer, A., Bo, Y., Han, L., He, J., *et al.* (2017) 'CDD/SPARCLE: Functional classification of proteins via subfamily domain architectures', *Nucleic Acids Research*, 45, pp. D200–D203. doi: 10.1093/nar/gkw1129.

Mat, A. M., Sarrazin, J., Markov, G. V, Apremont, V., *et al.* (2020) 'Biological rhythms in the deep-sea hydrothermal mussel *Bathymodiolus azoricus*', *Nature Communications*, 11. doi: 10.1038/s41467-020-17284-4.

Mi, H., Muruganujan, A., Ebert, D., Huang, X., *et al.* (2019) 'PANTHER version 14: More genomes, a new PANTHER GO-slim and improvements in enrichment analysis tools', *Nucleic Acids Research*, 47, pp. D419–D426. doi: 10.1093/nar/gky1038.

Micheli, F., Peterson, C. H., Mullineaux, L. S., Fisher, C. R., *et al.* (2002) 'Predation structures communities at deep-sea hydrothermal vents', *Ecological Monographs*, 72, pp. 365–382. doi: 10.1890/0012-9615(2002)072[0365:PSCADS]2.0.CO;2.

Miura, C., Komatsu, K., Maejima, K., Nijo, T., *et al.* (2015) 'Functional characterization of the principal sigma factor RpoD of phytoplasmas via an in vitro transcription assay', *Scientific Reports*, 5, pp. 3–5. doi: 10.1038/srep11893.

Monds, R. D., Lee, T. K., Colavin, A., Ursell, T., *et al.* (2014) 'Systematic Perturbation of Cytoskeletal Function Reveals a Linear Scaling Relationship between Cell Geometry and Fitness', *Cell Reports*, 9, pp. 1528–1537. doi: 10.1016/j.celrep.2014.10.040.

Moreno-Vivián, C., Cabello, P., Martínez-Luque, M., Blasco, R., *et al.* (1999) 'Prokaryotic nitrate reduction: molecular properties and functional distinction among bacterial nitrate reductases', *Journal of Bacteriology*, 181, pp. 6573–6584.

Motoki, K., Watsuji, T., Takaki, Y., Takai, K., *et al.* (2020) ' Metatranscriptomics by In Situ RNA Stabilization Directly and Comprehensively Revealed Episymbiotic Microbial Communities of Deep-Sea Squat Lobsters ', *mSystems*, 5, pp. 1–16. doi: 10.1128/msystems.00551-20.

Narberhaus, F. and Balsiger, S. (2003) 'Structure-function studies of *Escherichia coli* RpoH (σ32) by in vitro linker insertion mutagenesis', *Journal of Bacteriology*, 185, pp. 2731–2738. doi: 10.1128/JB.185.9.2731-2738.2003.

Neckers, L. and Tatu, U. (2008) 'Molecular Chaperones in Pathogen Virulence: Emerging New Targets for Therapy', *Cell Host and Microbe*, 4, pp. 519–527. doi: 10.1016/j.chom.2008.10.011.

Oates, M. E., Stahlhacke, J., Vavoulis, D. V., Smithers, B., *et al.* (2015) 'The SUPERFAMILY 1.75 database in 2014: A doubling of data', *Nucleic Acids Research*, 43, pp. D227–D233. doi: 10.1093/nar/gku1041.

Obuchowski, I. and Liberek, K. (2020) 'Small but mighty: a functional look at bacterial sHSPs', *Cell Stress and Chaperones*, 25, pp. 593–600. doi: 10.1007/s12192-020-01094-0.

Park, J. T. and Uehara, T. (2008) 'How Bacteria Consume Their Own Exoskeletons (Turnover and Recycling of Cell Wall Peptidoglycan)', *Microbiology and Molecular Biology Reviews*, 72, pp. 211–227. doi: 10.1128/mmbr.00027-07.

Parks, D. H., Imelfort, M., Skennerton, C. T., Hugenholtz, P., *et al.* (2015) 'CheckM: Assessing the quality of microbial genomes recovered from isolates, single cells, and metagenomes', *Genome Research*, 25, pp. 1043–1055. doi: 10.1101/gr.186072.114.

Pedruzzi, I., Rivoire, C., Auchincloss, A. H., Coudert, E., *et al.* (2015) 'HAMAP in 2015: Updates to the protein family classification and annotation system', *Nucleic Acids Research*, 43, pp. D1064–D1070. doi: 10.1093/nar/gku1002.

Peters, J. M., Mooney, R. A., Grass, J. A., Jessen, E. D., *et al.* (2012) 'Rho and NusG suppress pervasive antisense transcription in Escherichia coli', *Genes and Development*, 26, pp. 2621–2633. doi: 10.1101/gad.196741.112.

Peters, J. M., Vangeloff, A. D. and Landick, R. (2011) 'Bacterial transcription terminators: The RNA 3′-end chronicles', *Journal of Molecular Biology*, 412, pp. 793–813. doi: 10.1016/j.jmb.2011.03.036.

Piovesan, D., Tabaro, F., Paladin, L., Necci, M., *et al.* (2018) 'MobiDB 3.0: More annotations for intrinsic disorder, conformational diversity and interactions in proteins', *Nucleic Acids Research*, 46, pp. D471–D476. doi: 10.1093/nar/gkx1071.

Ponnudurai, R., Kleiner, M., Sayavedra, L., Petersen, J. M., *et al.* (2017) 'Metabolic and physiological interdependencies in the *Bathymodiolus azoricus* symbiosis', *ISME Journal*, 11, pp. 463–477. doi: 10.1038/ismej.2016.124.

R Core Team (2019) *R: A language and environment for statistical computing*., *R Foundation for Statistical Computing, Vienna, Austria*.

Rismondo, J., Bender, J. K. and Halbedel, S. (2017) 'Suppressor Mutations Linking gpsB with the First Committed Step of Peptidoglycan Biosynthesis in *Listeria monocytogenes*', *Journal of Bacteriology*, 199, pp. 1–16.

Rognes, T., Flouri, T., Nichols, B., Quince, C., *et al.* (2016) 'VSEARCH: A versatile open source tool for metagenomics', *PeerJ*, 2016, pp. 1–22. doi: 10.7717/peerj.2584.

Romano, S., Schulz-Vogt, H. N., González, J. M. and Bondarev, V. (2015) 'Phosphate limitation induces drastic physiological changes, virulence-related gene expression, and secondary metabolite production in Pseudovibrio sp. strain FO-BEG1', *Applied and Environmental Microbiology*, 81, pp. 3518–3528. doi: 10.1128/AEM.04167-14.

Romero Picazo, D., Dagan, T., Ansorge, R., Petersen, J. M., *et al.* (2019) 'Horizontally transmitted symbiont populations in deep-sea mussels are genetically isolated', *ISME Journal*, 13, pp. 2954–2968. doi: 10.1038/s41396-019-0475-z.

Rosenzweig, R., Nillegoda, N. B., Mayer, M. P. and Bukau, B. (2019) 'The Hsp70 chaperone network', *Nature Reviews Molecular Cell Biology*. doi: 10.1038/s41580-019-0133-3.

Sanders, J. G., Beinart, R. A., Stewart, F. J., Delong, E. F., *et al.* (2013) 'Metatranscriptomics reveal differences in in situ energy and nitrogen metabolism among hydrothermal vent snail symbionts', *The ISME Journal*, 7, pp. 1556–1567. doi: 10.1038/ismej.2013.45.

Sayavedra, L. (2016) 'Host-symbiont interactions and metabolism of chemosynthetic symbiosis in deep-sea *Bathymodiolus* mussels', *PhD Thesis*, pp. 1–244.

Sekar, K., Linker, S. M., Nguyen, J., Grünhagen, A., *et al.* (2019) 'Bacterial glycogen provides short-term benefits in changing environments'. doi: 10.1128/AEM.00049-20.

Servant, F., Bru, C., Carrère, S., Courcelle, E., *et al.* (2002) 'ProDom: automated clustering of homologous domains.', *Briefings in bioinformatics*, 3, pp. 246–251. doi: 10.1093/bib/3.3.246.

Seston, S. L., Beinart, R. A., Sarode, N., Shockey, A. C., *et al.* (2016) 'Metatranscriptional response of chemoautotrophic *Ifremeria nautilei* endosymbionts to differing sulfur regimes', *Frontiers in Microbiology*, 7, pp. 1–18. doi: 10.3389/fmicb.2016.01074.

Sigrist, C. J. A., De Castro, E., Cerutti, L., Cuche, B. A., *et al.* (2013) 'New and continuing developments at PROSITE', *Nucleic Acids Research*, 41, pp. 344–347. doi: 10.1093/nar/gks1067.

Simão, F. A., Waterhouse, R. M., Ioannidis, P., Kriventseva, E. V., *et al.* (2015) 'BUSCO: Assessing genome assembly and annotation completeness with single-copy orthologs', *Bioinformatics*, 31, pp. 3210–3212. doi: 10.1093/bioinformatics/btv351.

Steiner, P. A., De Corte, D., Geijo, J., Mena, C., *et al.* (2019) 'Highly variable mRNA half-life time within marine bacterial taxa and functional genes', *Environmental Microbiology*, 21, pp. 3873–3884. doi: 10.1111/1462-2920.14737.

Stern, A. M., Liu, B., Bakken, L. R., Shapleigh, J. P., *et al.* (2013) 'A novel protein protects bacterial iron-dependent metabolism from nitric oxide', *Journal of Bacteriology*, 195, pp. 4702–4708. doi: 10.1128/JB.00836-13.

Taguchi, A., Welsh, M. A., Marmont, L. S., Lee, W., *et al.* (2019) 'FtsW is a peptidoglycan polymerase that is functional only in complex with its cognate penicillin-binding protein', *Nature Microbiology*, 4, pp. 587–594. doi: 10.1038/s41564-018-0345-x.

Tavormina, P. L., Hatzenpichler, R., McGlynn, S., Chadwick, G., *et al.* (2015) '*Methyloprofundus sedimenti* gen. nov., sp. nov., an obligate methanotroph from ocean sediment belonging to the "deep sea-1" clade of marine methanotrophs', *International Journal of Systematic and Evolutionary Microbiology*, 65, pp. 251–259. doi: 10.1099/ijs.0.062927-0.

Tavormina, P. L., Kellermann, M. Y., Antony, C. P., Tocheva, E. I., *et al.* (2017) 'Starvation and recovery in the deep-sea methanotroph *Methyloprofundus sedimenti*', *Molecular Microbiology*, 103, pp. 242–252. doi: 10.1111/mmi.13553.

Thauer, R. K., Jungermann, K. and Decker, K. (1977) 'Energy Conservation in Chemotrophic Anaerobic Bacteria', *Bacteriological Reviews*, 41, pp. 100–180. doi: 10.1108/eb027807.

Tietjen, M., Leisch, N., Franke, M., Hiebenthal, C., *et al.* (2020) *Lysosomal digestion of symbionts shapes innate immunity and fuels the metabolism of bacteriocytes in a deep-sea mussel host*. Manuscript in prep.

Tomoyasu, T., Tabata, A., Imaki, H., Tsuruno, K., *et al.* (2012) 'Role of *Streptococcus intermedius* DnaK chaperone system in stress tolerance and pathogenicity', *Cell Stress and Chaperones*, 17, pp. 41–55. doi: 10.1007/s12192-011-0284-4.

Wehrens, M., Ershov, D., Rozendaal, R., Walker, N., *et al.* (2018) 'Size Laws and Division Ring Dynamics in Filamentous *Escherichia coli* cells', *Current Biology*, 28, pp. 972-979.e5. doi: 10.1016/j.cub.2018.02.006.

Wendeberg, A., Zielinski, F. U., Borowski, C. and Dubilier, N. (2012) 'Expression patterns of mRNAs for methanotrophy and thiotrophy in symbionts of the hydrothermal vent mussel *Bathymodiolus puteoserpentis*', *ISME Journal*, 6, pp. 104–112. doi: 10.1038/ismej.2011.81.

Williams, E. and Shimmin, M. A. (1978) 'Radiation-induced filamentation in obligate methylotrophs', 4, pp. 137–141.

Wo, M. M. S. M. (1998) 'Eubacterial sigma-factors', 22.

Wu, C. H., Nikolskaya, A., Huang, H., Yeh, L. S. L., *et al.* (2004) 'PIRSF: family classification system at the Protein Information Resource', *Nucleic Acids Research*, 32, pp. 112D – 114. doi: 10.1093/nar/gkh097.

Yang, D. C., Blair, K. M. and Salama, N. R. (2016) 'Staying in Shape: the Impact of Cell Shape on Bacterial Survival in Diverse Environments', *Microbiology and molecular biology reviews*, 80, pp. 187–203. doi: 10.1128/MMBR.00031-15.Address.

Chapter II: Supplementary Tables and Figures

All Supplementary Tables of this chapter are deposited on the provided CD-ROM.

Supplementary Figures

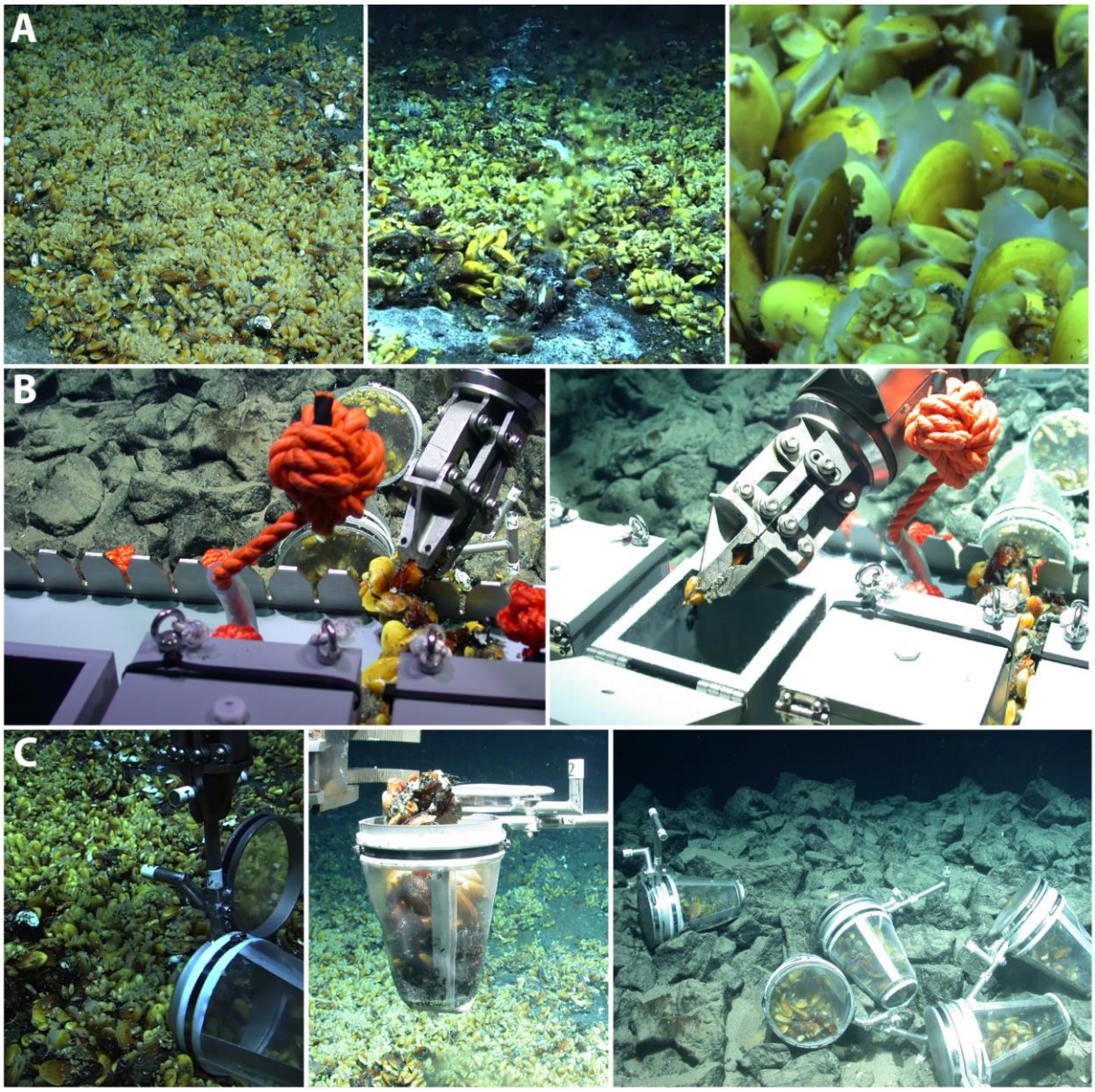

Supplementary Figure 1: Sample collection and experimental setup. ***A:*** *Bathymodiolus puteoserpentis* mussels form dense patches at the Ash Lighthouse mussel bed. Diffuse hydrothermal vent fluids are visible through the shimmering water. Undisturbed mussels have open shells for filtration of seawater. ***B:*** Deployment of IDEFIX for *in situ* fixation of mussels. Individual mussels are separated from byssus-clotted mussel clumps with the help of the steel comb and are cracked by the ROV arm. Mussels are then dropped into the RNAlater-containing boxes. ***C:*** Displacement of mussels from the Ash Lighthouse mussel bed. Mussels are collected in mesh cages from the mussel bed and displaced to a site without diffuse fluids. Cages are re-collected after 1 and 2 days of displacement and fixed with IDEFIX. © MARUM Center for Marine Environmental Sciences.

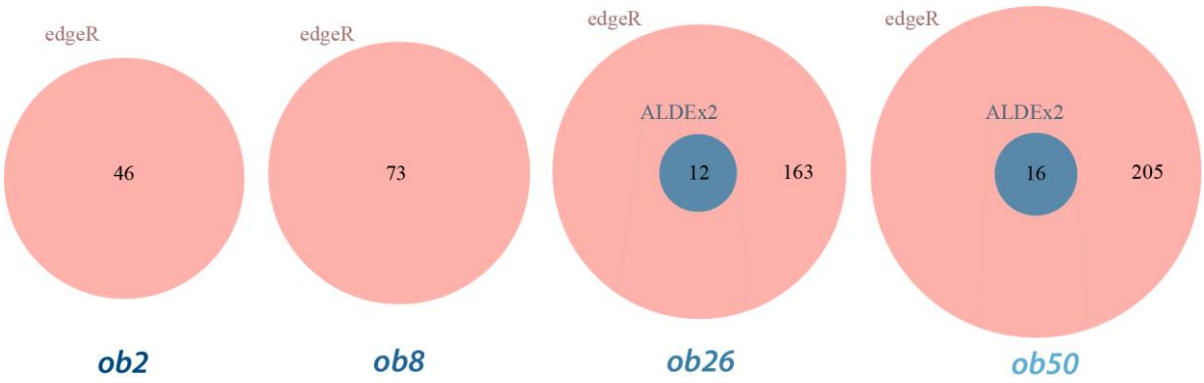

Supplementary Figure 2: Differential gene expression in the *Bathymodiolus puteoserpentis* mussel host. Venn diagram shows the number of differentially expressed genes (FDR < 0.05) that were detected by edgeR and ALDEx2 in on-board fixed mussels. Only in samples ob26 and ob50 both methods found differential gene expression.

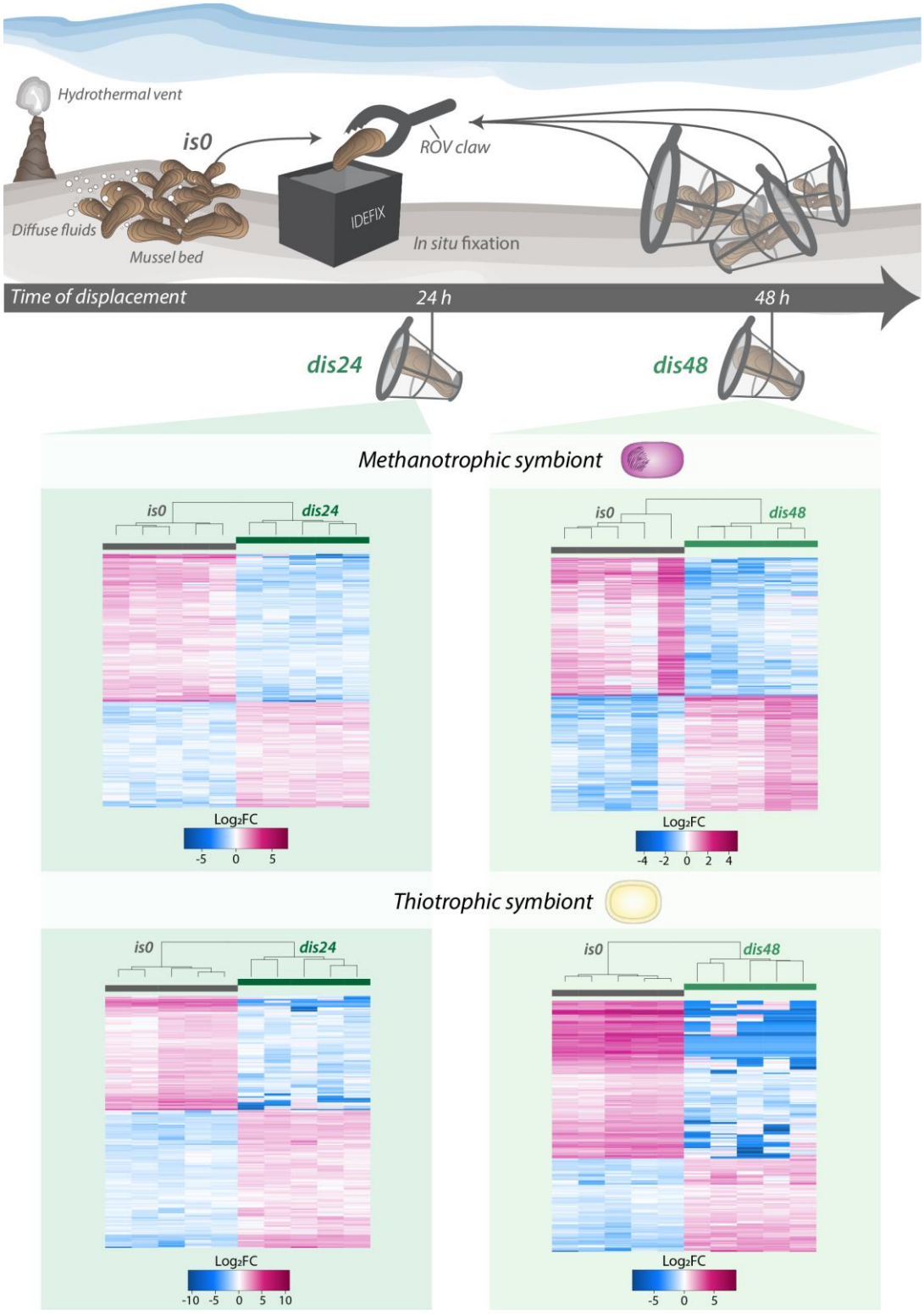

Supplementary Figure 3: Differential gene expression of displaced and *in situ* fixed symbionts. Sampling scheme illustrates the displacement of mussels in mesh cages and the IDEFIX fixation strategy for all samples. Heatmaps for both displacement fixation time points show an increasing number of differentially expressed genes compared to *in situ* fixed samples in both symbionts, and distinct clustering of each sampling time point. Number of differentially expressed genes: dis24 = 418 genes, dis48 = 581 genes (methanotrophic symbiont), and dis24 = 225 genes, dis48 = 240 genes (thiotrophic symbiont).

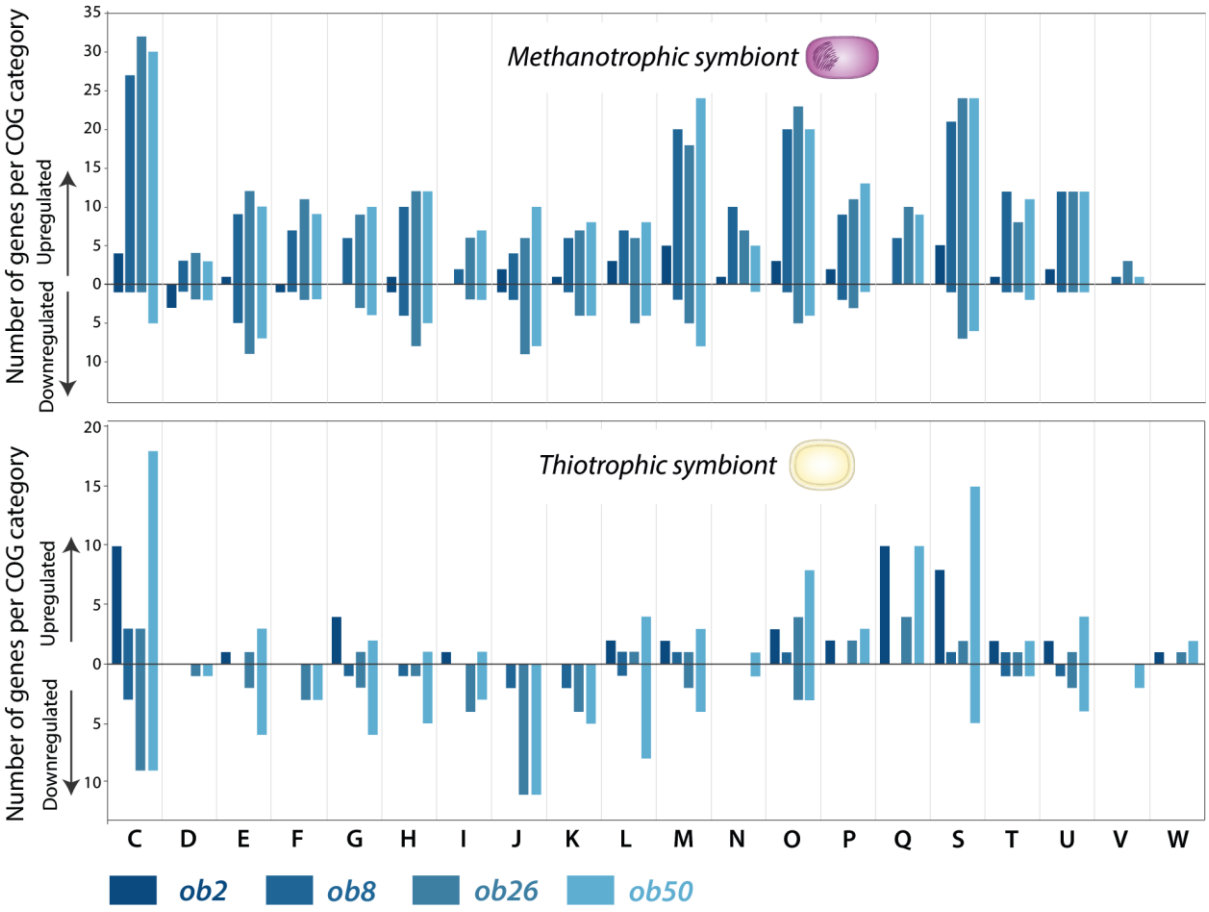

Supplementary Figure 4: Up- and downregulation of differentially expressed genes per COG category. Distribution of COG categories in the methanotrophic and thiotrophic symbiont of on-board fixed samples compared to the *in situ* transcriptome. Individual bars indicate the number of differentially expressed genes (FDR < 0.05) that were up- or downregulated in each on-board sample compared to the *in situ* fixed samples. COG categories were determined with eggnogg mapper V2. Note that not all differentially expressed genes could be attributed to a COG category.

C: Energy production and conversion, D: Cell cycle, E: Amino acid transport and metabolism, F: Nucleotide transport and metabolism, G: Carbohydrate transport and metabolism, H: Coenzyme transport and metabolism, I: Lipid transport and metabolism, J: Translation, ribosomal structure and biogenesis, K: Transcription, L: Replication, recombination and repair, M: Cell envelope biosynthesis, N: Cell motility, O: Posttranslational modification, protein turnover and chaperones, P: Inorganic ion transport, Q: Secondary metabolite biosynthesis, transport and catabolism, S: unknown, T: Signal transduction mechanisms, U: Intracellular trafficking, secretion and vesicular transport, V: Defence mechanisms, W: Extracellular structures.

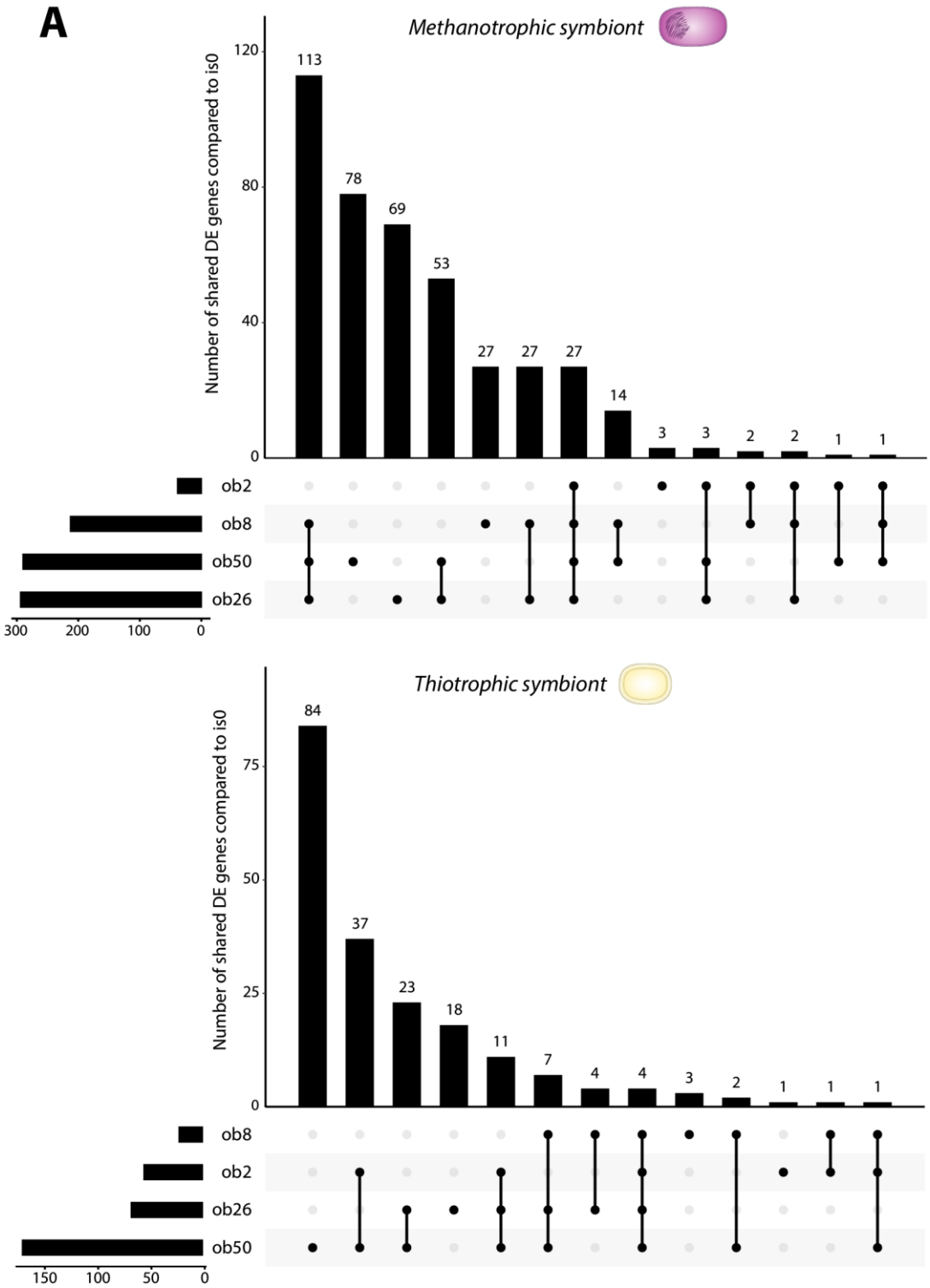

Supplementary Figure 5A: Number of shared differentially expressed genes in on-board fixed samples relative to *in situ* samples. UpSetR plots for methanotrophic and thiotrophic symbiont showing intersections between differentially expressed genes (FDR < 0.05) of on-board fixation time points. Bar chart on the left indicates the total number of differentially expressed (DE) genes for each fixation time point. Intersection size between fixation time points is indicated in the upper bar chart. Connected dots indicate the fixation time points considered for each intersection.

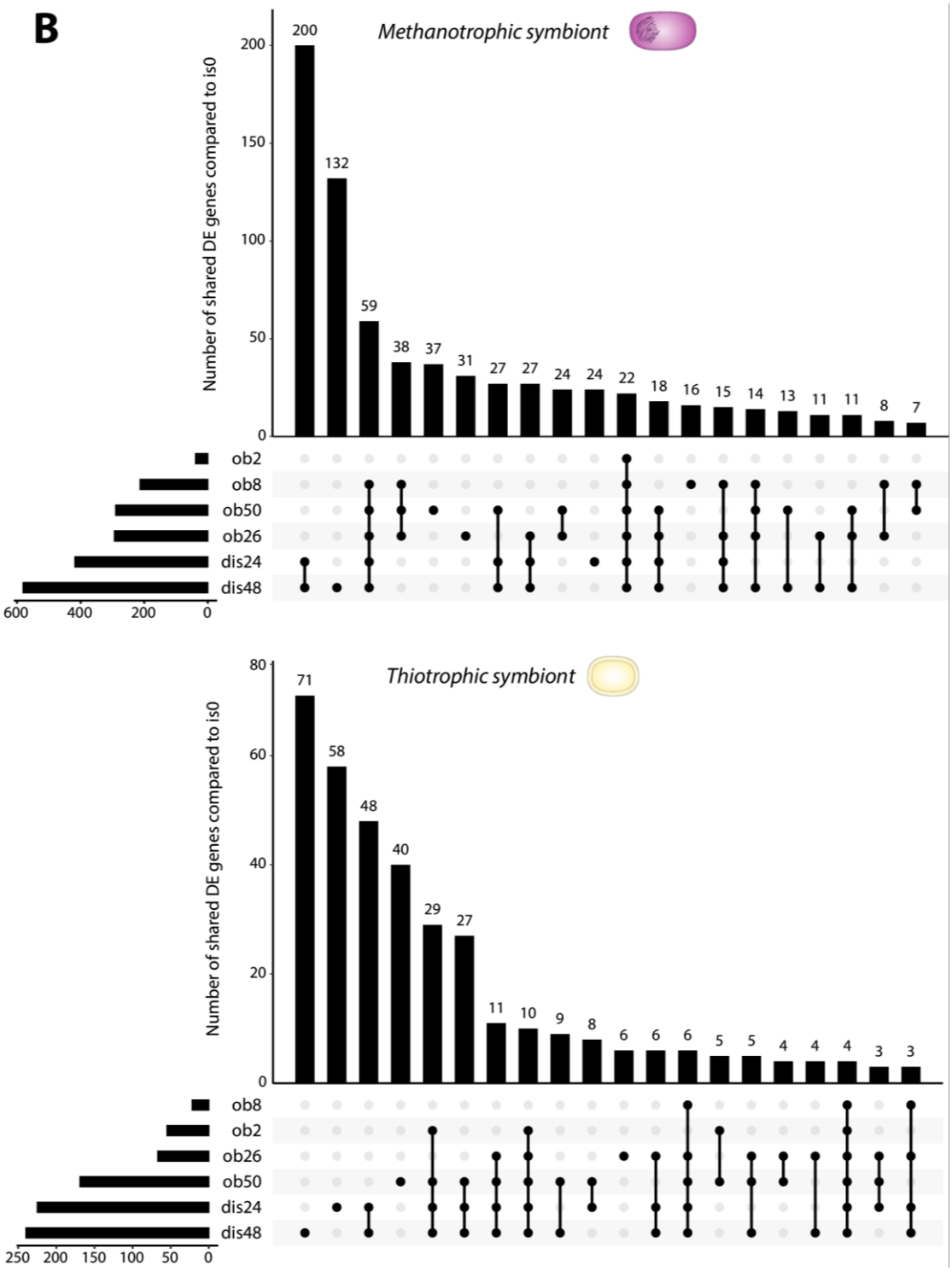

Supplementary Figure 5B: Number of shared differentially expressed genes in all fixation time points relative to *in situ* samples. UpSetR plots for methanotrophic and thiotrophic symbiont showing intersections between differentially expressed (DE) genes (FDR < 0.05) of all fixation time points. Bar chart on the left indicates the total number of differentially expressed genes for each fixation time point. Intersection size between fixation time points is indicated in the upper bar chart. Connected dots indicate the fixation time points considered for each intersection.

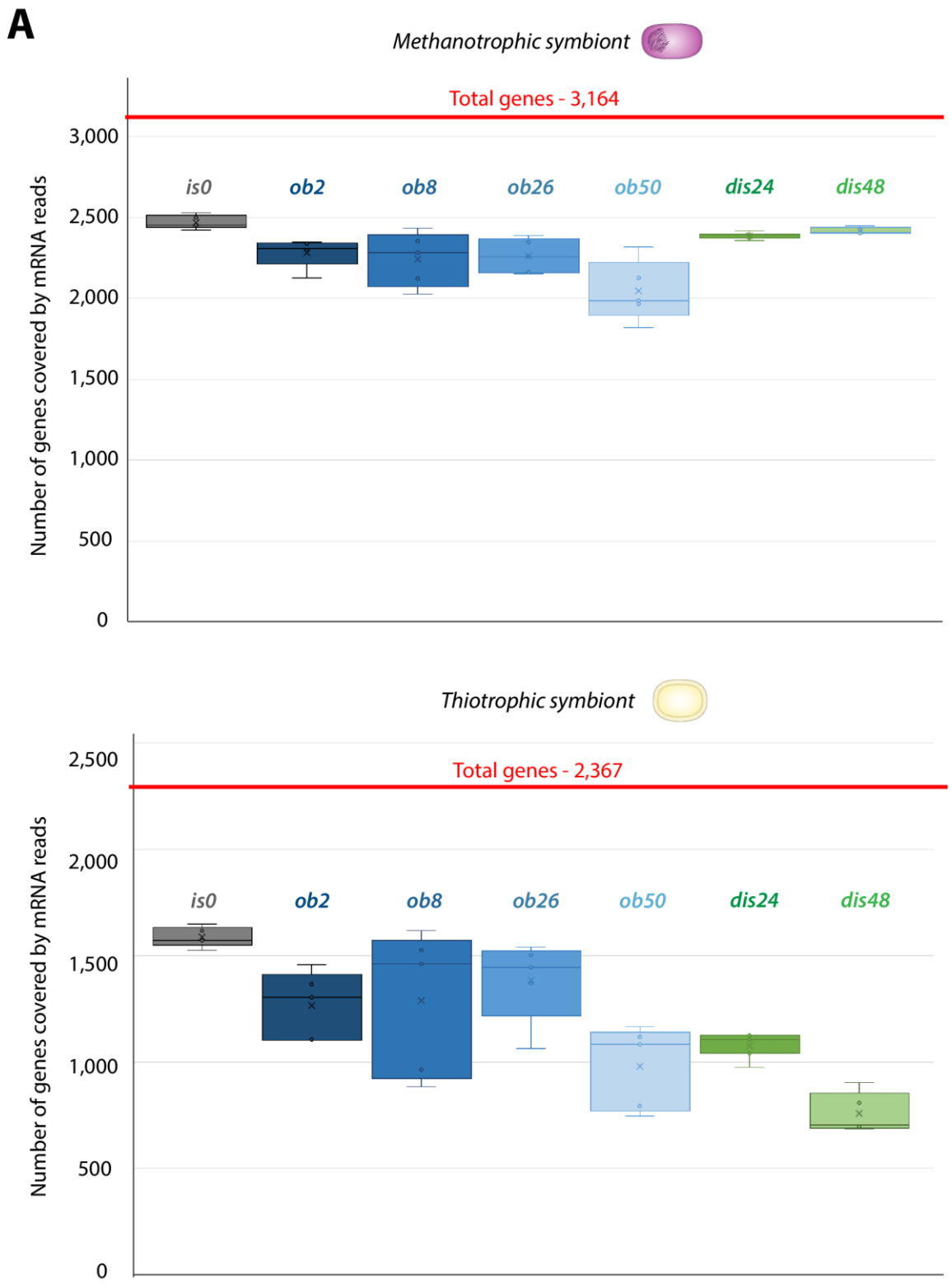

Supplementary Figure 6A: Number of expressed genes in the methanotrophic and thiotrophic symbiont of all fixation time points. Boxplots indicate the range of expressed genes represented by transcript per millions (TPM > 0) in the methanotrophic and thiotrophic symbiont for each fixation time point (n=5).

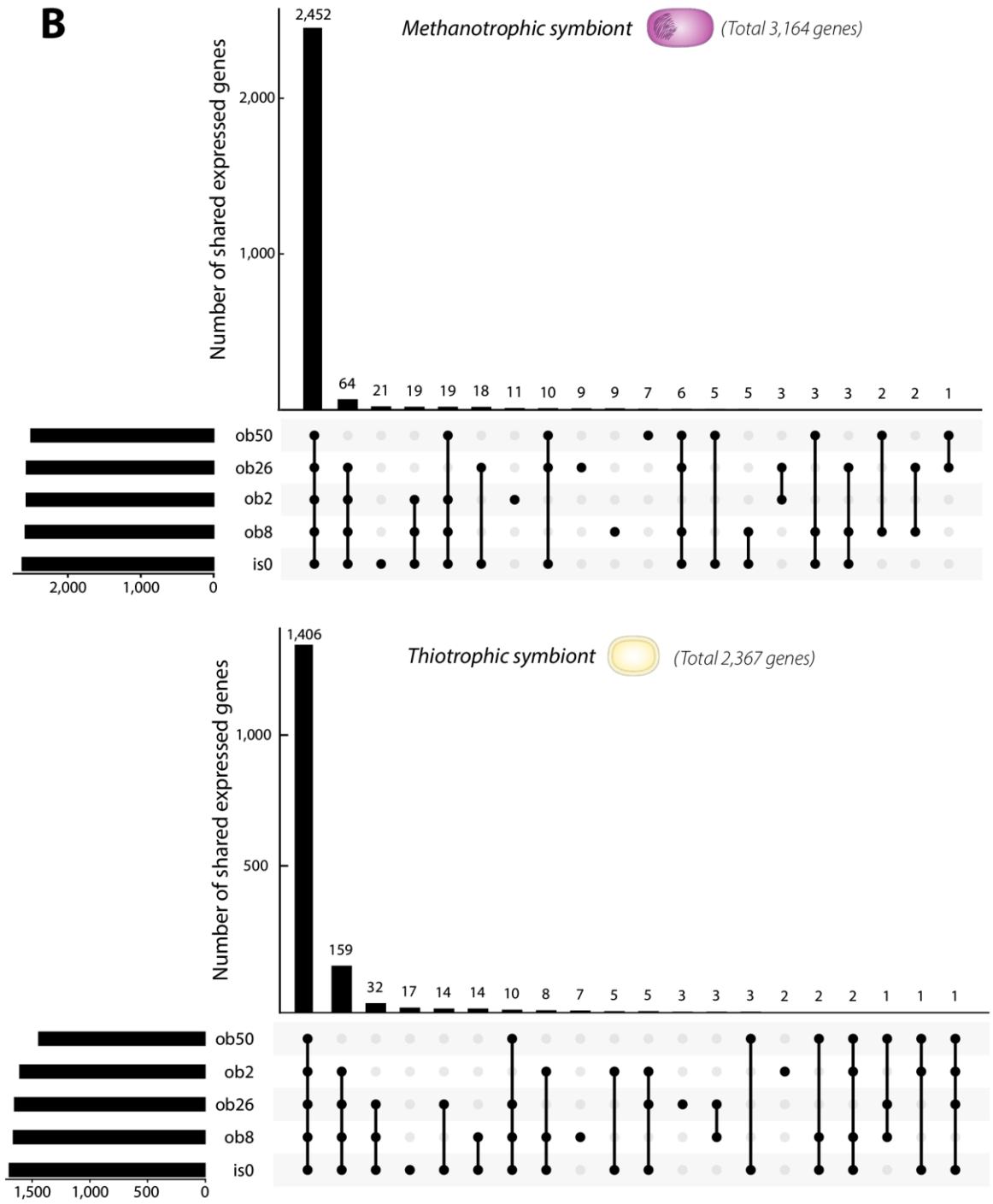

Supplementary Figure 6B: Cumulative numbers of expressed genes shared in *in situ* and on-board fixed samples. UpSetR plots for methanotrophic and thiotrophic symbiont showing intersections between expressed genes of *in situ* and on-board fixation time points. Bar chart on the left indicates the total number of expressed genes for each fixation time point (cumulative number, n=5). Intersection size between fixation time points is indicated in the upper bar chart. Connected dots indicate the fixation time points considered for each intersection.

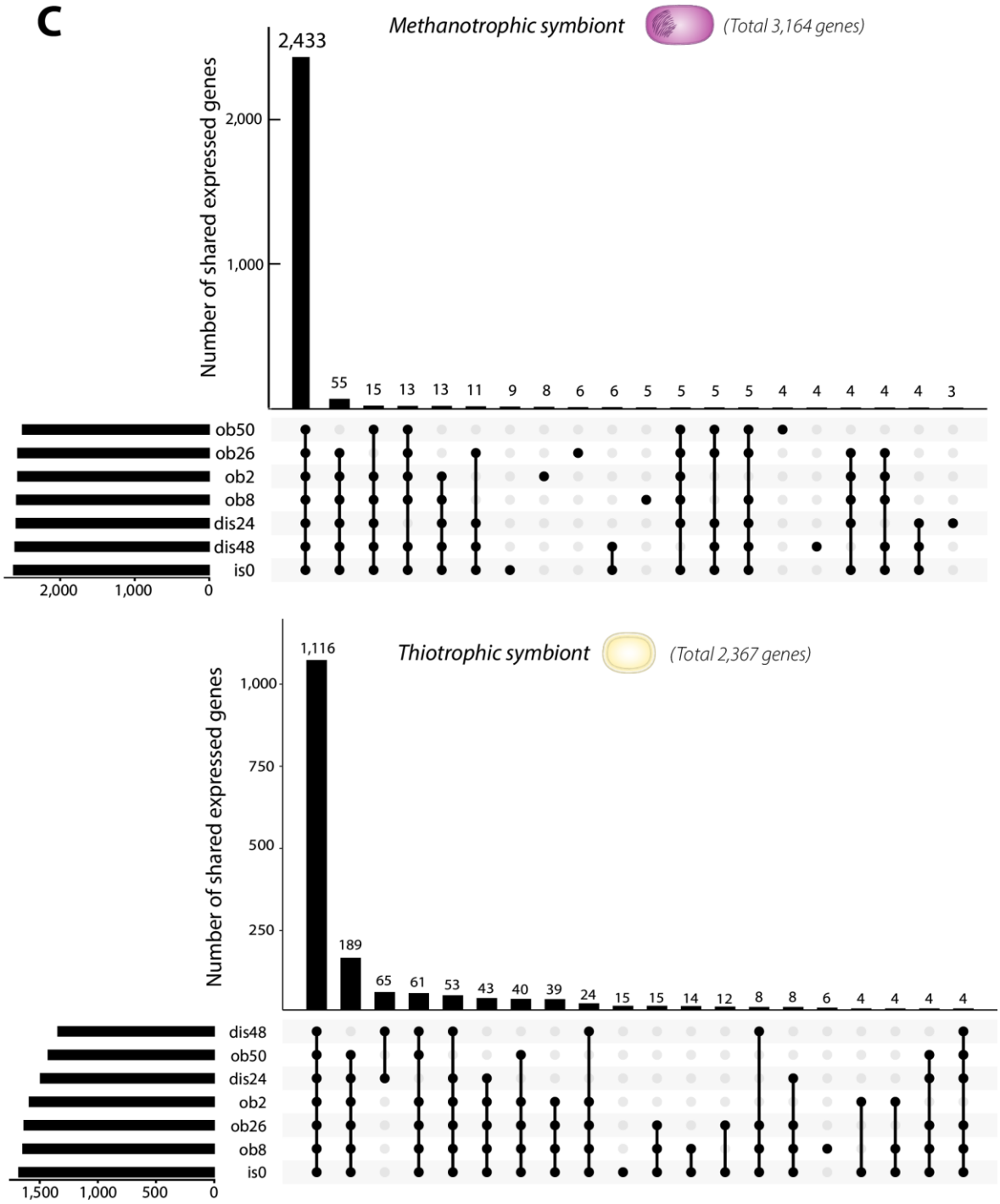

Supplementary Figure 6C: Cumulative numbers of expressed genes shared in *in situ*, on-board and displacement samples. UpSetR plots for methanotrophic and thiotrophic symbiont showing intersections between expressed genes of *in situ,* on-board and displacement fixation time points. Bar chart on the left indicates the total number of expressed genes for each fixation time point (cumulative number, n=5). Intersection size between fixation time points is indicated in the upper bar chart. Connected dots indicate the fixation time points considered for each intersection.

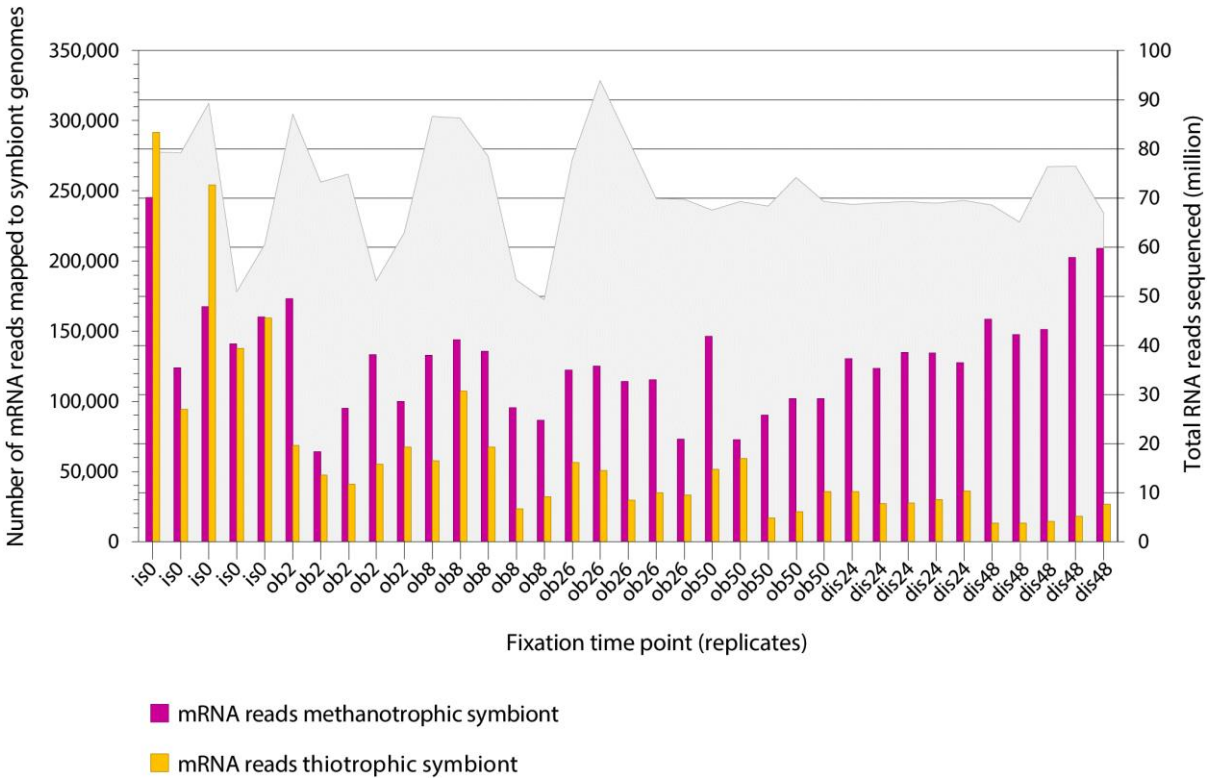

Supplementary Figure 7: Symbiont mRNA read coverage per fixation time point replicate. Coloured bars indicate the number of mRNA reads mapped to symbiont genomes (left axis). Grey filled line shows the number of total RNA reads sequenced for individual replicate (right axis). Number of mapped mRNA reads for thiotrophic symbiont decreases with extended on-board storage, while number of mapped mRNA reads for methanotrophic symbiont remains relatively stable.

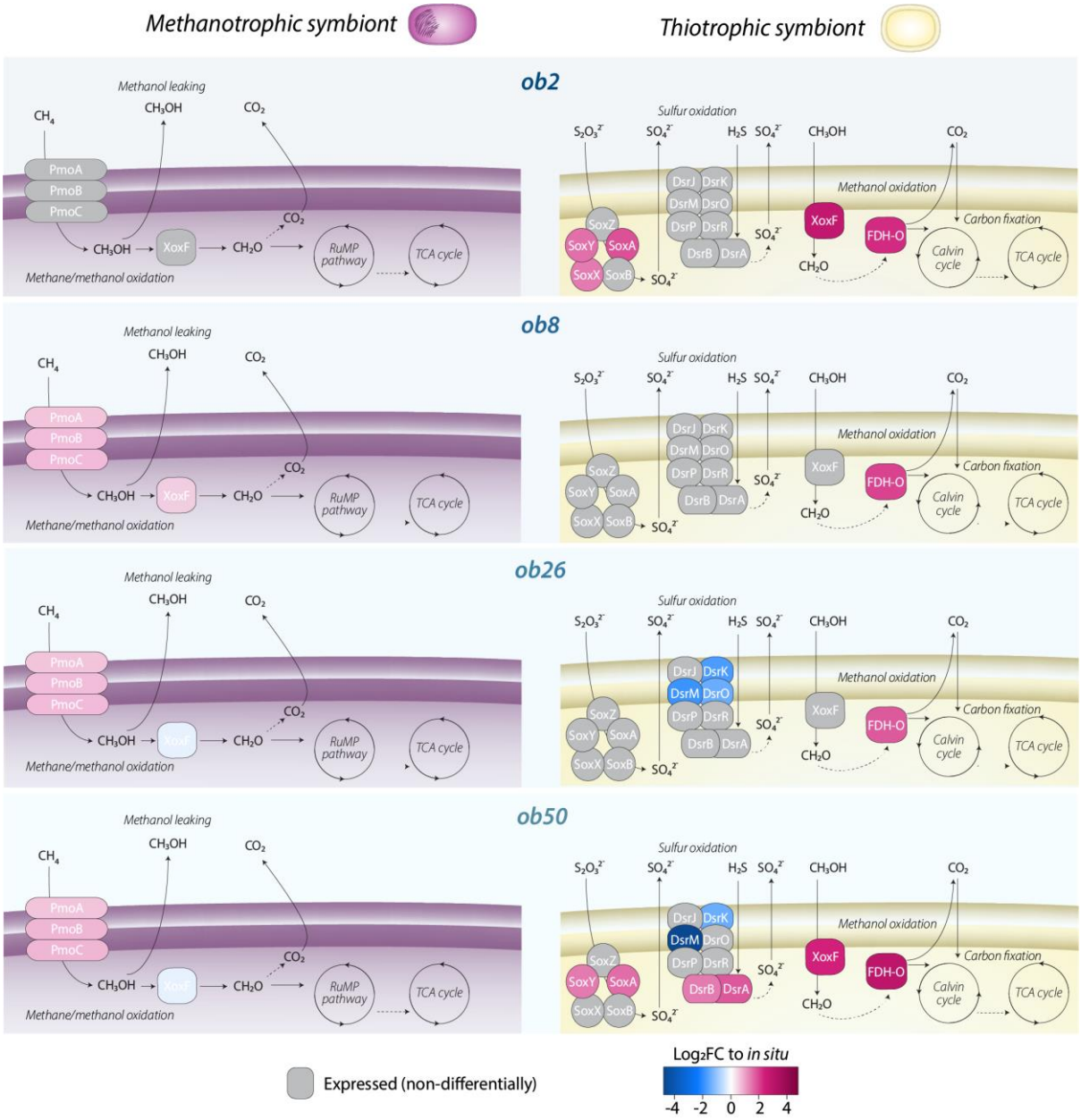

Supplementary Figure 8: Expression changes of energy pathways in the methanotrophic and thiotrophic symbiont of on-board fixed samples. Both metabolic reconstructions show key genes for energy synthesis in both symbionts in ob2, ob8, ob26 and ob50 samples (top to bottom) after on-board fixation. Coloured proteins show significant gene expression changes (FDR < 0.05) relative to the *in situ* fixation samples (log2 fold-changes), grey proteins indicate non-differential expression of these proteins compared to *in situ* fixation samples.

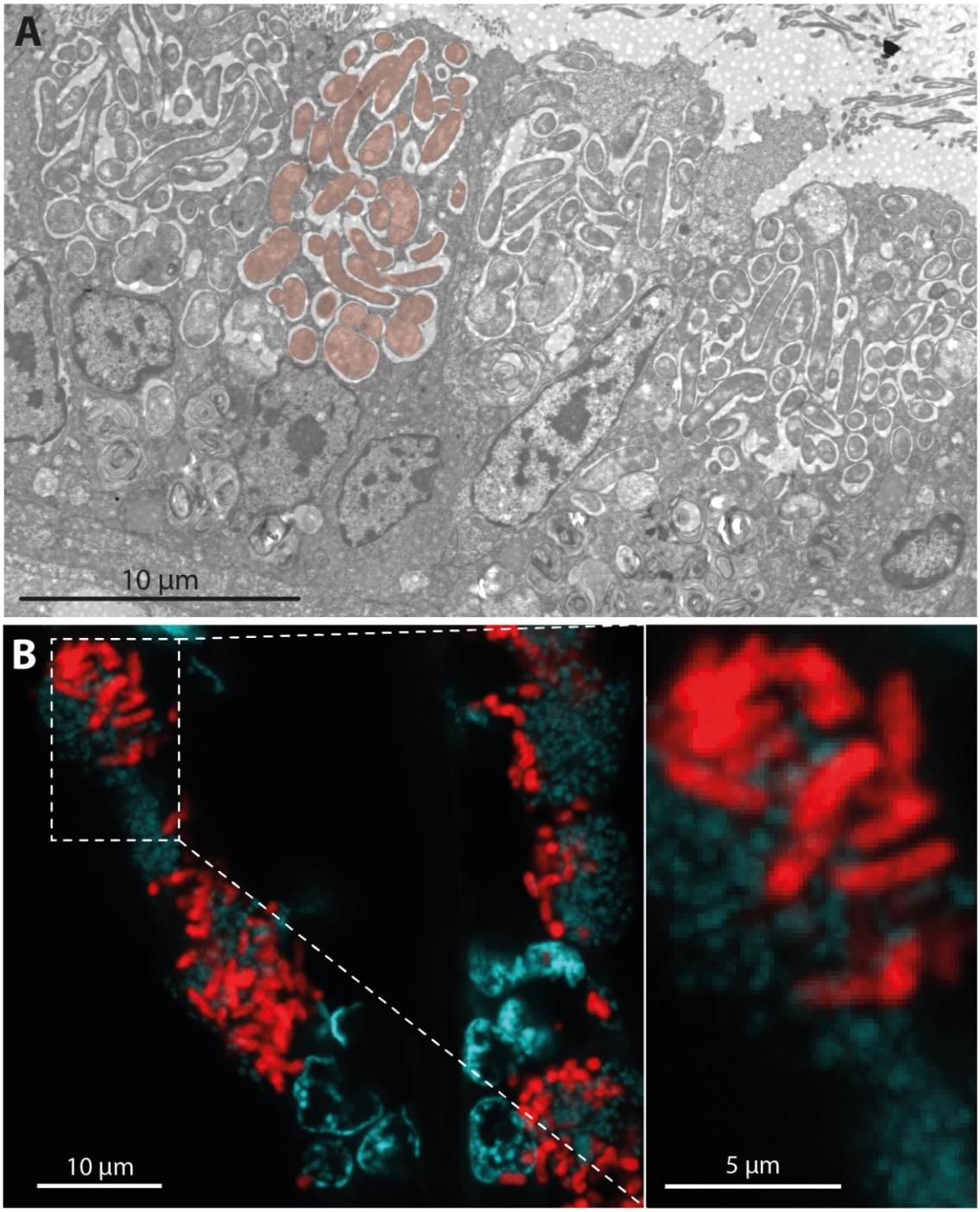

Supplementary Figure 9: Cell elongation in the methanotrophic symbiont of *Bathymodiolus* spp. mussels. ***A*****:** Transmission electron microscopy image of a gill cross-section from a *Bathymodiolus childressi* specimen collected from the Gulf of Mexico. This specimen was subjected to a 48-hour starvation experiment during the research cruise, where mussels were maintained in surface seawater without methane input. Among the methanotrophic symbiont cells, several showed elongation (red = methanotrophic symbionts observed in a single bacteriocyte). ***B:*** Fluorescence *in situ* hybridisation image of a longitudinal gill section from a *Bathymodiolus puteoserpentis* specimen collected from the Mid-Atlantic Ridge during the M126 cruise. This specimen was subjected a 46-hour EdU incubation experiment that was designed to track cell division in these mussels. The methanotrophic symbiont (red) appeared as elongated cells within bacteriocytes (red = specific FISH probe for methanotrophic symbiont, cyan = DAPI).

Chapter III

Lysosomal symbiont digestion shapes innate immunity and fuels the metabolism of bacteriocytes in a deep-sea mussel host

Målin Tietjen[1,2,*], Nikolaus Leisch[1,*], Maximilian Franke[1], Claas Hiebenthal[3], Frank Melzner[3], Thorsten Reusch[3], Nicole Dubilier[1,2], and Harald R. Gruber-Vodicka[1]

[1] Max Planck Institute for Marine Microbiology, Bremen, Germany

[2] MARUM – Center for Marine Environmental Sciences of the University of Bremen, Germany

[3] GEOMAR – Helmholtz Centre for Ocean Research Kiel, Germany

* These authors contributed equally

Author contribution: *NL, HRGV and MT designed the study, ND coordinated mussel collection and transfer to aquaria, CH, FM and TR built and maintained aquaria, NL and MT sampled aquaria specimens, NL performed gill region microdissection and TEM, MT performed nucleotide extractions, MT, NL and HRGV conceived data analyses, MT performed metagenome and transcriptome analyses, MF performed fluorescence imaging, MT wrote first draft, MT and HRGV wrote the manuscript with revisions from NL and contributions from ND.*

This manuscript is in preparation and has not been reviewed by all authors.

Abstract

Understanding the physiology of symbiotic systems within foundation species is of high interest as they shape and structure ecosystems. A common limitation for studying the physiological interplay of organisms within such symbiotic systems is that neither host nor symbionts can be cultivated, preventing straightforward analyses of biological processes linked to symbiont presence. The cold-seep mussel *B. childressi* contains chemosynthetic methane-oxidising symbionts in the bacteriocyte region of its gills, while the ciliated edge is typically symbiont-free. Previous studies on host-symbiont interactions in bathymodiolin mussels were so far, however, limited to whole gill filament transcriptome analyses, without the possibility to allocate host metabolic processes specifically to the symbiont-containing region. To overcome this, we separately analysed the transcriptomes of the symbiotic bacteriocyte region and the non-symbiotic ciliated edge region from the same mussel gills. By combining gene co-expression networks and differential gene expression analyses, we disentangled the cellular processes specific to symbiont-containing gill regions, and identified a selected set of host genes that could be linked to symbiont abundance. We could track the targeted breakdown, uptake and storage of symbiont biomass that fuels the host metabolism. Our findings suggest that bacteriocytes are the main drivers of gill immunity in bathymodiolin mussels with a fine-tuned ability to sense and respond to symbiont abundance. We demonstrate that unbiased gene co-expression networks provide detailed insight into the most relevant details in the physiology of symbiotic bathymodiolin hosts. For the first time, we could gain insights into the molecular processes specific to symbiont-containing gill regions, and could resolve physiological adaptations of bacteriocytes to the symbiosis.

Introduction

Mytilid mussels (superorder Pteriomorphia, family Mytilinae; González *et al.*, 2015) represent one of the most economically and ecologically relevant groups of marine animals. Having evolved large gills that serve as efficient feeding and respiratory organs, mytilids have successfully colonised various ecosystems world-wide including the deep sea (Gosling, 2015). However, filter-feeding in deep-sea environments is not always sufficient to sustain large mussel beds as only a minor fraction phototrophy-derived carbon reaches the deep sea (Duperron *et al.*, 2009). Instead, the deep-sea mytilid representatives of the subfamily Bathymodiolinae largely rely on chemosynthetic bacteria that supply their nutrition (Assié *et al.*, 2020). Despite the fact that bathymodiolin mussels often dominate the fauna at cold seeps and hydrothermal vents as keystone species forming large mussel beds, it is still unclear how much the mussels depend on their symbionts that colonise their gills, and how symbiont-derived nutrients are metabolised by the host. This has been particularly difficult to assess as only a handful of bathymodiolin species including *Bathymodiolus childressi* (also known as *Gigantidas childressi;* Thubaut *et al.*, 2013*;* Xu *et al.*, 2019) have been maintained in aquaria over longer periods of time that allow experimental manipulation (e.g. Dattagupta *et al.*, 2007; Barros *et al.*, 2015; Yu *et al.*, 2019).

Bathymodiolin gills can be divided into two distinct regions based on the ultrastructure of the epithelial cells along single filaments. The largest region is dominated by symbiont-containing bacteriocytes and is surrounded by the ciliated edge, the region with densely ciliated cells that contain numerous mitochondria and frontal, latero-frontal and lateral cilia (Fiala-Médioni *et al.*, 1986; Gosling, 2015). The cold-seep species *Bathymodiolus childressi* from the Gulf of Mexico harbours a methane-oxidising symbiont within non-ciliated bacteriocytes. In these bacteriocytes, multiple symbionts are located in vacuolar-like housing structures that are found in all symbiotic bathymodiolin mussels (Wentrup *et al.*, 2014). The symbiont of *B. childressi* is a Type I methanothroph (*Methylococcaceae*) that uses methane as carbon and energy source like its closest free-living relative *Methyloprofundus sedimenti* (Petersen and

Dubilier, 2009; Tavormina *et al.*, 2015; Riekenberg *et al.*, 2016). Both *M. sedimenti* and the symbiont of *B. childressi* contain intracytosolic membrane stacks and storage granules, which are characteristic for Type I methanothrophs (Tavormina *et al.*, 2015; Petersen and Dubilier, 2009). The symbiont of *B. childressi* oxidises methane *via* a particulate methane monooxygenase (Petersen and Dubilier, 2009; Ponnudurai *et al.*, 2017), and likely assimilates methane with high efficiency by converting up to 80% of into biomass (Kochevar *et al.*, 1992).

The close association with symbionts and the frequent encounter with environmental microorganisms requires a functioning innate immunity to eliminate potential pathogens (Canesi *et al.*, 2002). In bathymodiolin mussels, innate immunity is proposed to be mediated by recognition of bacterial molecular patterns that are typically detected by a range of host membrane proteins (Mogensen, 2009; Zheng *et al.*, 2017). However, it is still unclear how bathymodiolin hosts can distinguish symbionts from other bacteria. Not only the detection, but also the elimination of bacteria through phagocytosis and subsequent lysosomal digestion plays important immune role in bathymodiolin mussels (Yu *et al.*, 2019). Lysosomal digestion of symbionts in bacteriocytes also supports the nutrient acquisition in bathymodiolin hosts to meet their nutritional requirements (Zheng *et al.*, 2017). Such phagolysosomal processes have repeatedly been reported for several bathymodiolin species, but the underlying molecular processes involved in symbiont digestion have not yet been resolved.

We wanted to gain insights into the molecular processes in *B. childressi* bacteriocytes that can be linked to symbiont presence. For this, we experimentally manipulated the symbiont abundance in bacteriocytes and obtained distinct physiological states of bacteriocytes reflecting symbiont load. To reveal the molecular processes occurring specifically within bacteriocytes, we separated the bacteriocyte gill region from ciliated edge of the same mussels and applied unbiased and systematic gene co-expression networks (GCNs) in combination with differential gene expression analyses. Transcriptome analyses with GCNs offer great potential for identifying gene clusters involved in prevailing or highly adaptable cellular processes, especially when analysing multiple experimental conditions in parallel (Carter *et*

al., 2004; Feng *et al.*, 2012). Particularly in non-model animals like bivalves, GCNs have the potential to reveal processes that underlie physiological changes (Fu *et al.*, 2014; Liu *et al.*, 2019). By reconstructing the bacteriocyte-specific physiological patterns over a cycle of symbiont depletion and symbiont recovery, we could track the breakdown, uptake and storage of symbiont biomass, and identified the repertoire of immunity processes that are triggered by symbiont presence in a bathymodiolin mussel.

Methods

Mussel collection, experimental setup and sample preparation

Bathymodiolus childressi specimens were collected in 2014 next to a brine pool at 652 m depth at the cold seep site Green Canyon 233 (27°43'25.062" N, 91°16'45.834" W) in the Northern Gulf of Mexico during the Nautilus cruise NA043-NA045 (Supplementary Figure 1A). Five mussels were dissected and gill pieces from each mussel were stabilised in different fixatives for later microscopy and nucleotide extractions. The remaining mussels were transferred alive to Kiel, Germany, where they were kept in aquaria with constant supply of methane (Supplementary Figure 1B). After a year of husbandry with influx of 10 µM methane, five individuals were dissected and gill pieces were stabilised in different fixatives for later microscopy and nucleotide extractions. The methane influx was increased to 40 µM for another year, after which another five individuals were dissected and gill pieces were stabilised in different fixatives for later microscopy and nucleotide extractions.

Transmission electron microscopy

For electron microscopy, samples were fixed in 2.5% glutaraldehyde (GA) in PHEM buffer (piperazine-N, N′-bis , 4-(2-hydroxyethyl)-1-piperazineethanesulfonic acid, ethylene glycol-bis(β-aminoethyl ether and MgCl2 for 12 h at 4°C (Montanaro *et al.*, 2016). After fixation, samples were washed with buffer and post fixed with 1% osmium tetroxide (OsO4) for 2 h at 4°C, washed three times with PHEM and dehydrated with an ethanol series (30%, 50%, 70%, 80%, 90% and 100%; v/v) at -10°C, each step lasting 10 min. The samples were then

transferred into 50:50 ethanol and acetone, followed by 100% acetone and infiltrated with low-viscosity resin (Agar Scientific, UK) using centrifugation embedding (McDonald, 2014). Samples were centrifuged for 30 s in resin:acetone mixtures of 25%, 50%, 75% and twice in 100%. Finally, the samples were transferred into fresh resin in embedding moulds and polymerized at 60–65°C for 48 h.

Ultra-thin (70 nm) sections were cut on a microtome (Ultracut UC7 Leica Microsystem, Austria), mounted on formvar-coated slot grids (Agar Scientific, UK) and contrasted with 0.5% aqueous uranyl acetate (Science Services GmbH, Germany) for 20 min and with 2% Reynold's lead citrate for 6 min. Sections were imaged at 20–30 kV with a Quanta FEG 250 scanning electron microscope (FEI Company, USA) equipped with a STEM detector using the xT microscope control software v.6.2.6.3123.

Fluorescence in situ hybridisation and Nile red staining

For correlative fluorescence *in situ* hybridisation (FISH) and Nile red staining, PFA-fixed *B. childressi* gills from wild and aquarium-starved mussels were dehydrated with an increasing ethanol series followed by Roti-Histol. Infiltration and embedding was done using paraffin. A Leica microtome RM2255 (Leica Biosystems, Germany) was used to section the hardened paraffin blocks into 5-10 µm sections. Sections were mounted on polylysine adhesion slides (Thermo Fisher Scientific, USA). The slides were baked in a horizontal position at 60°C for 60 min to enhance adhesion of the sections to the slide, and subsequently de-waxed and rehydrated by immersing them in Roti-Histol and in an ethanol series of decreasing concentration. Sections were air dried and encircled with a liquid blocker (PAP-Pen, Science Services GmbH, Germany).

For the *in situ* hybridization, DOPE-FISH probes were used (Stoecker *et al.*, 2010). The FISH protocol was performed with modifications after Duperron *et al.* (2005). To label the methane-oxidizing symbionts, we used a general probe targeting conserved regions of the 16S rRNA gene in bacteria (EUB I-III; Daims *et al.*, 1999). We applied between 20-300 µl of hybridization mixture per section depending on the section size. Before the mixture was

applied onto the sections, the 8.4 pmol probe stock solution was diluted 1:10 with the hybridization buffer. The hybridisation buffer contained 30-35% of formamide and hybridisations were performed at 46°C for 3h. Pre-warmed (48°C) washing buffer was used to wash the samples for at least 15 min.

The washing step was followed by the Nile red stain. Prior to the Nile red stain a Nile red stock solution of 1 mM was prepared. This stock solution was diluted 1:200 for the Nile red stain. About 50-100 µl of Nile red staining solution was directly applied on each section and incubated at room temperature (RT) for 30 min in the dark. The staining was followed by two washing steps in Phosphate Buffered Saline (PBS) at RT for 10 min. Afterwards the samples were air dried at 30 °C for 30 min. To counterstain the nucleic-acids, samples were incubated with 1 µg DAPI/ml for 10 min at RT in the dark and washed twice in PBS. Afterwards the slides were air-dried at 30°C for 30 min. Finally, the stained gill sections were covered with Invitrogen ProLong™ Glass Antifade Mountant (Thermo Fisher Scientific, USA) and Menzel™ Microscope Coverslips (Thermo Fisher Scientific, USA).

An Olympus BX53 compound microscope (Olympus, Japan) equipped with an ORCA Flash 4.0 (Hamamatsu Photonics K.K, Hamamatsu, Japan) camera and the software cellSens (Olympus, Tokyo, Japan) was used to acquire overview images of the gill sections. Using a 100x Plan-Apochromat oil-immersion objective and the Zen-Black software (Carl Zeiss, Germany) we acquired close-up images on a Zeiss LSM 780 confocal laser-scanning microscope (Carl Zeiss, Germany) equipped with an Airyscan detector (Carl Zeiss, Germany). Raw images from both microscopes were further processed in Fiji v1.52p (Schindelin *et al.*, 2012).

Gill dissection and nucleotide extractions

For nucleotide extractions, gill pieces from all mussels were further dissected to separate the symbiont-containing bacteriocyte gill region and the symbiont-free ciliated edge gill region (Supplementary Figure 2). For nucleotide and protein extractions, gill regions up to 50 filaments were pooled from one individual mussel to obtain sufficient material for DNA and

RNA extractions. All extractions were done using the AllPrep DNA/RNA/Protein Mini Kit (Qiagen, Germany) following the manufacturers guidelines with minor amendments to the protocol: The RNA was incubated in 50 µl RNase-free water at room temperature for 10 min, centrifuged and again incubated with the flow-through along with another 50 µl RNase-free water to increase the RNA yield. Details of nucleotide extractions can be found in Supplementary Table 1.

DNA sequencing, symbiont assembly, binning and metabolic analysis

All metagenome libraries were prepared and sequenced at the Max Planck Genome Centre in Cologne, Germany (https://mpgc.mpipz.mpg.de). Library preparation was done using the TruSeq DNA Library Prep kit (Illumina, USA) and Covaris DNA shearing protocol (Covaris, USA). Libraries were sequenced on a HiSeq3000 system (Illumina, USA) to a minimum depth of 7 million with 150 basepairs (bp) paired-end reads. Symbiont 16S rRNA genes were assembled from all samples, and symbiont abundances were estimated with read counts matching the 16S rRNA gene using phyloFlash (Gruber-Vodicka *et al.*, 2020). The 16S rRNA gene read counts were normalised to the total reads per library and the 18S rRNA gene reads of the host. For symbiont phylogeny reconstruction in Geneious R11.1.5 (https://www.geneious.com), the assembled 16S rRNA genes were blasted against NCBI (accessed on 16th June 2020), and the sequences with their closest hits were aligned with MAFFT multiple alignment v1.4.0 and a tree was calculated using FastTree v2.1.12.

For symbiont binning, sequencing adaptors were removed and reads were quality filtered (Q=2) with BBDuk v38.06 and normalised with BBNorm v38.06 (http://sourceforge.net/projects/bbmap/) to a maximum kmer target of 30. Three concatenated bacteriocyte metagenome libraries from wild mussels were kmer-filtered for the high coverage methane-oxidising symbiont and assembled with SPAdes v3.10.1 (Bankevich *et al.*, 2012). The genome of the methane-oxidising symbiont was binned with Bandage v0.8.0 (Wick *et al.*, 2015) from three concatenated metagenome libraries of wild mussels. The genome bin was quality-checked with CheckM v1.0.7 (Parks *et al.*, 2015) and annotated with

RAST v2.0 (Aziz *et al.*, 2008) using the ClassicRAST annotation pipeline. Effector proteins and their associated secretion systems were predicted with EffectiveDB (Eichinger *et al.*, 2016) including T4SEpre (beta) for predictions of type 4 secretion system effector (T4SS) proteins (accessed 20th July 2020). Metabolic pathways of the symbiont and *Methyloprofundus sedimenti* WF1^T (GenBank accession: GCA_002072955.1) genomes were reconstructed and analysed in Pathway Tools v22.0 (Karp *et al.*, 2002).

RNA sequencing, host de novo transcriptome assembly and functional annotation

All transcriptome libraries were prepared and sequenced at the Max Planck Genome Centre in Cologne, Germany (https://mpgc.mpipz.mpg.de). An aliquot of each RNA sample was subjected to poly-A tail selection for host mRNA enrichment and unselected total RNA library preparation, resulting in two RNA libraries per sample. Poly-A tail mRNAs were enriched using NEBNext poly(A) mRNA Magnetic Isolation Module (New England Biolabs, Germany) and libraries were prepared with NEBNext Ultra Directional RNA Library Prep Kit for Illumina (New England Biolabs, Germany) including 15 cycles of PCR amplification. Total RNA libraries were prepared with NEBNext Ultra Directional RNA Library Prep Kit for Illumina (New England Biolabs, Germany). Library preparation included 10 cycles of PCR amplification. Quality and quantity of all libraries were assessed with capillary electrophoresis using the TapeStation system (Agilent Technologies, USA) and fluorometry using Invitrogen Qubit (Thermo Fisher Scientific, USA). All libraries were immobilized and processed onto a flow cell with cBot (Illumina, USA) and subsequently sequenced on a HiSeq3000 system (Illumina, USA) to a minimum depth of 7 million reads with 1 x 150 bp single reads (Supplementary Table 1).

All libraries were adaptor-trimmed and quality-filtered (Q=2) using BBDuk v38.06 (http://sourceforge.net/projects/bbmap/). Ribosomal RNA was filtered out with BBMap v38.06 using the rRNA database of SortMeRNA (Kopylova *et al.*, 2012). To generate a host *de novo* transcriptome assembly, the poly-A tail enriched libraries were subjected to read normalisation with BBNorm v38.06 to target read depth of 80 reads. The *de novo*

transcriptome was assembled combining all libraries from bacteriocyte and ciliated edge regions using Trinity v2.5.1 (Grabherr *et al.*, 2011). Assembly statistics and completeness were assessed with utility scripts of the Trinity package v2.5.1 (Haas *et al.*, 2013) and BUSCO v3 using the metazoan database odb09 (accessed on 5th February 2019; Simão *et al.*, 2015). To remove redundant sequences, transcripts were clustered to 97 % identity using VSEARCH (Rognes *et al.*, 2016). Contaminating reads were removed with MEGAN6 v6.10.3 (Huson *et al.*, 2016) based on their taxonomic origin (e.g. plants, fungi, non-symbiotic bacteria) determined by the closest hits from NCBI blast v2.2.28 searches against nr (db version 20150811).

For functional annotation of the *B. childressi* gill transcriptome, the annotation pipeline of Trinotate v3.0.1 (https://github.com/Trinotate/Trinotate.github.io/; e.g. Bryant *et al.*, 2017) was applied to the cleaned *de novo* assembly including a prediction for signal peptides and transmembrane proteins. Additionally, a cloud-based InterProScan was run in Blast2GO v5.2.5 (Conesa *et al.*, 2005) using the following databases to assign Gene Ontologies (GOs): CDD (Marchler-Bauer *et al.*, 2017), HAMAP (Pedruzzi *et al.*, 2015), HMMPanther (Mi *et al.*, 2019), HMMPfam (El-Gebali *et al.*, 2019), HMMPIR (Wu *et al.*, 2004), FPrintScan (Attwood *et al.*, 2012), BlastProDom (Servant *et al.*, 2002), ProfileScan (Sigrist *et al.*, 2013), PatternScan (Sigrist *et al.*, 2013), Gene3D (Lewis *et al.*, 2018), SFLD (Akiva *et al.*, 2014), Superfamily (Oates *et al.*, 2015), and MobiDBLite (Piovesan *et al.*, 2018). Gene annotations were based on the top BLAST hits from Blast2GO. Gene names were either newly assigned or copied from UniProt BLAST hits if annotation of genes were at least marked as “Reviewed”.

Symbiont and host gene expression, and gene co-expression analysis

The gene expression of symbionts from wild and symbiont-recovered mussels was quantified with kallisto v0.46.0 (Bray *et al.*, 2016) using the metagenome-assembled symbiont genome as reference. Symbiont expression values represented by transcript per million (TPMs) were added to the metabolic overview reconstructed with Pathway Tools v22.0 (Supplementary Table 2). Host gene expression was quantified with kallisto v0.46.0 (Bray *et al.*, 2016) using

the *B. childressi de novo* transcriptome assembly as reference. Raw gene count matrices were generated with utility scripts of the Trinity v2.5.1 package (Haas *et al.*, 2013) for pairwise comparisons between bacteriocyte regions of "wild" and "symbiont-depleted", "wild" and "symbiont-recovered", and "symbiont-depleted" and "symbiont-recovered" mussels. Relative gene expression changes between conditions represented by $\log_2$ fold-changes ($\log_2$FC) were determined using the centred-log ratios calculated with ALDEx2 v1.14.1 (Fernandes *et al.*, 2013) and median centred-$\log_2$ fold-changes were used to visualise the level of expression.

To avoid bias over choosing the appropriate approach for analysing RNA-seq datasets, we combined two different analyses to determine differential gene expression between sampling conditions with high certainty. Using R v3.5.3, we applied the count-data approach of edgeR v3.24.3 implemented in the utility scripts of the Trinity package v2.8.4 (Haas *et al.*, 2013), and the compositional data approach with ALDEx2 v1.14.1 (Fernandes *et al.*, 2013) to the same gene count matrices. In both cases, statistical significance was accepted at a False-Discovery Rate (FDR) of < 5%. Only genes with significant FDR in both approaches were determined as differentially expressed.

Gene count data from RNA-seq experiments are compositional or relative data (Fernandes *et al.*, 2014), and pairwise correlation between expressed genes are better represented by proportionalities (Quinn *et al.*, 2017). We used propr (Quinn *et al.*, 2017) to determine gene co-expression for both bacteriocyte- and ciliated edge gill regions from gene count matrices. As co-expression between genes is sensitive to random permutations if the number of conditions and replicates included is low (Carter *et al.*, 2004), we used all replicates from the three symbiont-states to generate the gene co-expression network. Only genes with minimum kallisto-estimated gene expression counts of 5 were included in the calculation to reduce the amount of data similar to the approach presented in Quinn *et al.* (2017). A proportionality cut-off of $\rho_p > 0.9$ between genes was chosen so that only highly correlated genes were analysed in the final gene co-expression networks (GCNs). The bacteriocyte- and ciliated edge GCNs were visualised using Cytoscape v3.8.0 (Shannon *et al.*, 2003). By merging both GCNs,

overlapping genes were subtracted resulting in GCNs that only contained highly proportional genes with region-specific co-expression.

Results & Discussion

Methane starvation leads to symbiont and biomass loss in mussel gills

With our experimental setup, we obtained three distinct physiological states of *B. childressi* mussels characterised by the overall symbiont abundance in gill bacteriocytes (Figure 1 and Supplementary Note 1). By acclimatising the mussels to aquaria conditions for one year, we were able to sample steady-states for each methane concentration. Metagenomes and metatranscriptomes, transmission electron microscopy and fluorescent *in situ* hybridisation images revealed high abundances of symbionts in gills of mussels fixed directly after collection from the mussel bed. As expected, mussels held at 10 µM methane showed near complete absence of the symbionts inside the gill. Devoid of symbionts, the bacteriocyte region instead displayed microvilli on all gill cells (Supplementary Note 2). After increasing the methane concentration to 40 µM, the symbiont population recovered but overall, still showed lower abundances than the freshly collected mussels (Figure 1 and Supplementary Figures 3-5). In this state of recovery, no microvilli could be detected on bacteriocytes. We hereon refer to the three physiological states of the mussels as "wild", "symbiont-depleted" and "symbiont-recovered".

Methane is the primary source of carbon and energy for the chemosynthetic symbionts of *B. childressi* (Duperron *et al.*, 2007). At the sampled cold-seep site Green Canyon 233, *B. childressi* colonises patches at a brine pool that is supersaturated with methane (equilibrium concentrations between 53 mM and 102 mM; Joye *et al.*, 2005). In such brine pools in the Gulf of Mexico, methane-oxidising symbionts of bathymodiolin mussels assimilate methane with high efficiency, converting up to 80% of consumed carbon into biomass (Kochevar *et al.*, 1992). The symbionts oxidise methane *via* particulate methane monoxygenase, with all three subunits among the top 25 of highest expressed genes in all conditions (Supplementary Table 2 and Supplementary Figure 6). This is consistent with previous observations that even at methane concentrations below 5 µM, methanotrophic symbionts of *Bathymodiolus* spp.

assimilate methane into biomass (Kochevar *et al.*, 1992). However, since symbiont abundance was highly depleted at 10 µM methane, such low concentrations were likely not sufficient to sustain the energy and carbon demand of the symbiont population at its natural density. Depletion of methanotrophic symbionts has been also observed in the related cold-seep mussel *B. platifrons* after methane supply was diminished for three months (Yu *et al.*, 2019). Short-term methane starvation has been induced in the closely related free-living *M.*

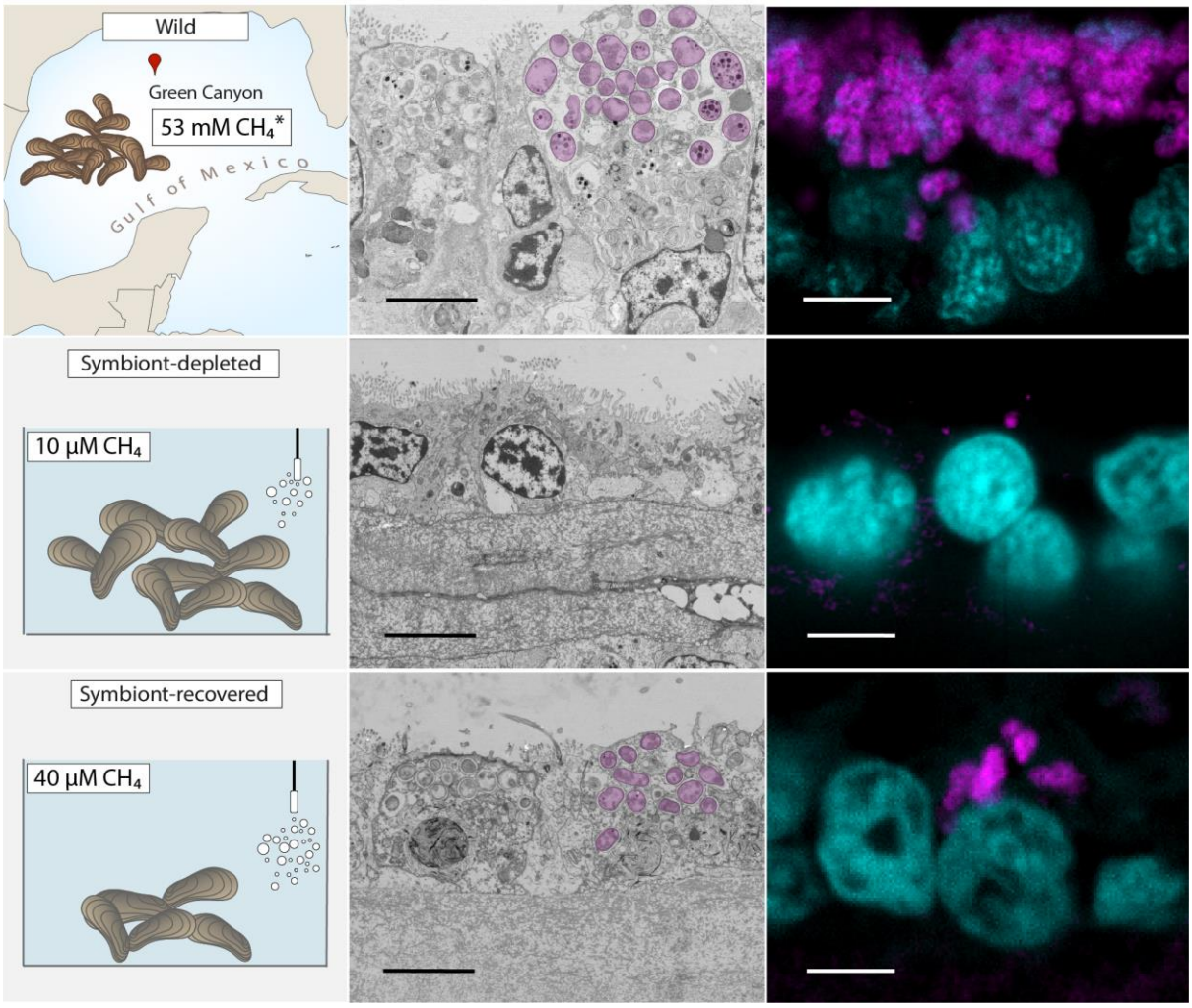

Figure 1: Symbiont loss and recovery in *Bathymodiolus childressi* induced by different methane concentrations in long-term aquaria setups. Mussels were collected from the mussel bed Green Canyon in Northern Gulf of Mexico with ~ 53 mM methane (Joye *et al.*, 2005) and/or placed into aquaria for one year at 10 µM methane, and/or held at increased concentrations of 40 µM methane for another year. Transmission electron microscopy and fluorescence *in situ* hybridisation images of *B. childressi* gill cross-sections from all three sampling conditions show absence/lower abundances of symbionts in aquaria mussels (highlighted in magenta). FISH images show host nuclei in cyan and symbionts in magenta. Scale bars = 5 µm.

sedimenti and inhibited growth of the bacteria over the course of the 96 h experiment. After reintroduction of methane to the cultures, population growth resumed rapidly (Tavormina *et al.*, 2017). This suggests that the symbiont population in our experiment might have quickly recovered after increasing methane to 40 µM, and was in a steady-state at the time of sampling.

Bacteriocyte-specific co-expression patterns reveal host response to symbionts

To systematically evaluate the physiological responses of the host to the three symbiont states, we combined gene co-expression networks (GCNs) and differential gene expression analyses based on a *de novo* host transcriptome assembly. The co-assembly of all samples yielded an almost complete and highly resolved host gill transcriptome. The assembly contained 255,285 genes on 352,557 transcripts with an average transcript length of 507.88 basepairs (N50 = 598 basepairs) and estimated GC content of 34.65%. More than 96% of the BUSCO metazoan gene dataset could be fully assembled with only 30 fragmented and two missing single-copy orthologs. The high number of assembled host transcripts was in accordance with other bivalve *de novo* transcriptome assemblies (Zheng *et al.*, 2017). About one third of the transcriptome assembly can be explained by splice variants that may be expressed under the different sampling conditions that were included in the assembly. Roughly 20% (67,427 transcripts) of all transcripts could be functionally annotated.

With our GCNs based on proportionality (Quinn *et al.*, 2017), we identified host candidate genes and molecular processes that respond to the distinct physiological states in symbiotic and non-symbiotic gill regions (Figure 2). Since we generated the GCNs with replicates from all physiological states, the resulting co-expression of genes reflected non-random correlation and therefore true biological function (examples in Supplementary Note 3). The bacteriocyte-specific GCN contained 1,431 genes, most of which were co-expressed in 34 clusters with at least four linked genes (Supplementary Figure 7A and B). Results of differential gene expression analyses and median $\log_2$ fold-changes complemented the gill region-specific GCNs and revealed clusters of relevant genes (Supplementary Table 3). Functional analyses of co-expressed genes in the bacteriocyte-specific GCN attributed gene groups to five major

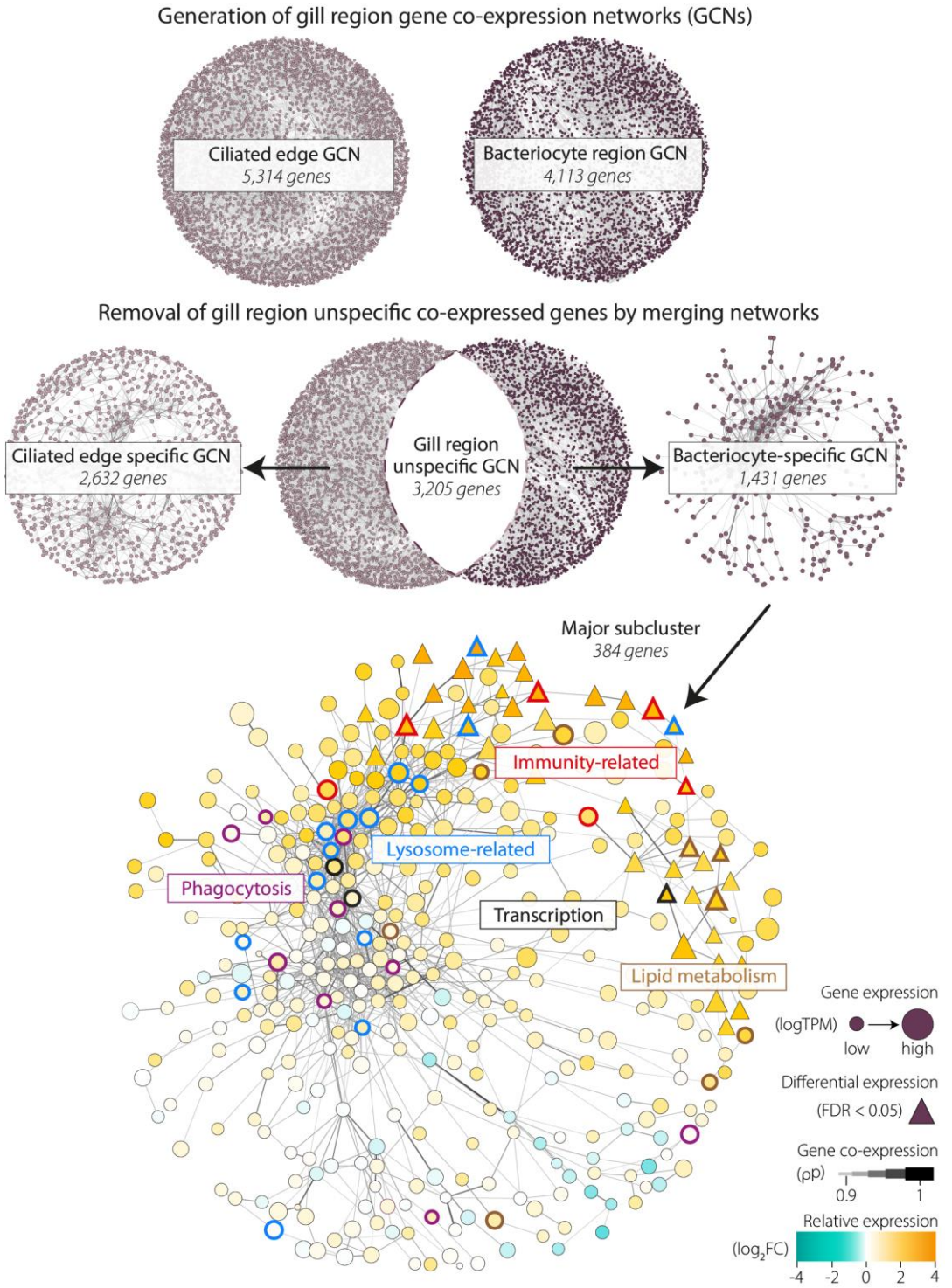

Figure 2: Generation of gill region-specific gene co-expression networks (GCNs). The removal of overlapping co-expressed genes resulted in a ciliated edge specific and a bacteriocytes-specific GCN. Major cluster of the bacteriocyte-specific GCN (edge-weighted spring-embedded layout) overlaid with data from i) expression of genes in wild mussels (node size) ii) relative expression of genes between wild and symbiont-depleted mussels (node colour), and iii) differential gene expression analyses between wild and symbiont-depleted mussels (node shape). Five major groups of genes could be identified in the major cluster: phagocytosis, lysosome-related, immunity-related, transcription and lipid metabolism. Genes of these groups were higher expressed in wild mussels than in symbiont-depleted mussels.

biological processes: phagocytosis, lysosome-related processes, immune-related, transcription, and lipid metabolism. Most genes of these groups were co-expressed in the largest cluster of the bacteriocyte-specific GCN and showed higher expression in the wild mussels compared to symbiont-depleted and symbiont-recovered mussels (Figure 2 and Supplementary Table 3). One of the key strengths of GCN analyses is that regulatory elements can be identified (van Dam *et al.*, 2018). In our case, we detected three transcription factors in the main cluster of the bacteriocyte-specific GCN that likely regulate the expression of members within the cluster.

The symbiont triggers innate immune response in host bacteriocytes

Bathymodiolin mussels are continuously exposed to diverse microorganisms in the surrounding water column. To protect themselves from invaders, the mussel gills are equipped with a range of proteins and metabolites that detect molecular patterns on the bacterial envelope like carbohydrates or lipopolysaccharides (LPS), and induce an innate immune response (Barros, Mendes and Rosa, 2016; Zheng *et al.*, 2017; Ikuta *et al.*, 2019). We identified a mannose-binding C-type lectin (MLEC) that had one of the strongest responses in bacteriocytes of wild mussels with nearly 40-fold higher expression than bacteriocytes of symbiont-depleted mussels (cluster 32 in Supplementary Figure 7A, Supplementary Table 3). Mannose-binding C-type lectins are specific for binding mannose on the surface of bacteria (Bulgheresi *et al.*, 2011). Along with MLEC, we found an LPS-binding bactericidal permeability increasing (BPI) protein that was 2.5-fold higher expressed in wild mussels relative to symbiont-depleted mussels (Figure 3). Such BPIs can lead to the destruction of their microbial target by altering outer membrane integrity, and also trigger the synthesis of immune responsive proteins and metabolites (Canny *et al.*, 2002; Bülow *et al.*, 2018; Domínguez-Andrés *et al.*, 2019). Our data suggest a strong immune detection of abundant symbionts in bacteriocytes of wild mussels through the upregulation of both MLEC and BPI.

We identified *cis*-aconitate decarboxylase (CAD), which mediates the synthesis of itaconate, in the major cluster of the bacteriocyte-specific GCN. Itaconate was found to be among the most abundant metabolites produced in mammalian immune cells during microbial infection and fulfils multiple roles (O'Neill and Artyomov, 2019; Riquelme *et al.*, 2020; Cordes *et al.*, 2020). In the non-symbiotic mussel *Perna canaliculus,* elevated levels of itaconate were measured upon infection with *Vibrio* sp., suggesting that itaconate plays a role in the innate

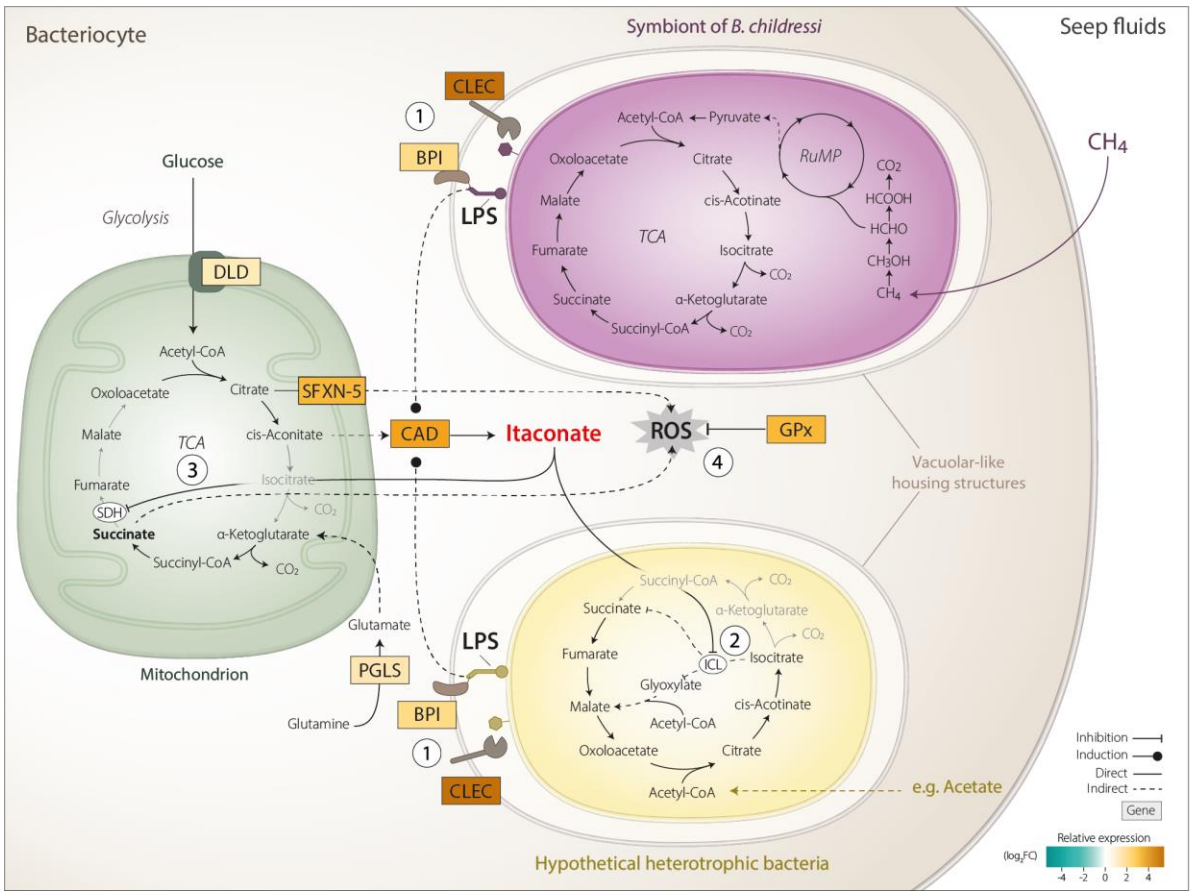

Figure 3: Bacteriocyte-specific innate immunity responds to detection of symbiont LPS inducing inflammatory processes in *B. childressi*. (1) Recognition of symbiont/bacterial lipopolysaccharides (LPS) via bactericidal permeability increasing (BPI) protein and C-type lectin (CLEC) induces expression of cis-aconitate decarboxylase (CAD) to produce metabolite itaconate. (2) Antimicrobial effect of itaconate through inhibition of isocitrate lyase (ICL) in the glyoxylate shunt of TCA cycle in bacteria that must grow on acetate or other carbon sources. Symbionts of *B. childressi* do not have glyoxylate shunt and only grow on methane as sole carbon source. (3) Disbalance of TCA cycle through sideroflexin-5 (SFXN-5) mediated export of citrate and inhibition of succinate decarboxylase (SDH) causing accumulation of succinate and consequent production of reactive oxygen species (ROS). (4) Glutathione peroxidase (GPx) responds to higher levels of ROS and protects cells from oxidative damage.

immunity of mussels (Nguyen and Alfaro, 2019). We found significantly higher expression of CAD in bacteriocytes of wild and symbiont-recovered mussels compared to symbiont-depleted mussels with 8.3-fold and 1.9-fold increase, respectively (Figure 3 and Supplementary Table 3). We hypothesise that symbiont recognition *via* MLEC and BPIs induced the synthesis of itaconate similar to mammalian macrophages (Domínguez-Andrés *et al.*, 2019).

Itaconate has also gained attention for its antimicrobial activity against bacteria in various hosts including marine molluscs (Young *et al.*, 2017; O'Neill and Artyomov, 2019). To overcome competition with the host, many heterotrophic pathogens use the glyoxylate shunt and ensure cell survival by growing on acetate or fatty acids instead of glucose (Ahn *et al.*, 2016). The glyoxylate shunt short-cuts the TCA cycle and is particularly important for heterotrophic bacteria in carbon-limited environment to conserve carbon for gluconeogenesis (Figure 3; Cordes, Michelucci and Hiller, 2015; Dolan and Welch, 2018). Itaconate binds to isocitrate lyase and thereby inhibits the glyoxylate shunt. We hypothesise that this inhibitory effect of itaconate in the bacteriocytes might be involved in regulating the colonisation by heterotrophic bacteria. The symbiont of *B. childressi* do not encode the glyoxylate shunt and their growth is consequently not inhibited by the antimicrobial metabolite itaconate, which might explain why these symbionts can persist in the host environment (Figure 3 and Supplementary Table 2). Because itaconate has been observed in other bivalve species (Nguyen and Alfaro, 2019), we propose that itaconate fulfils a similar role in other bathymodiolin symbioses.

Itaconate inhibits mitochondrial succinate dehydrogenase leading to accumulation of succinate, which subsequently causes formation of reactive oxygen species (Tannahill *et al.*, 2013). We also found 5.4-fold higher expression of mitochondrial citrate export *via* Sideroflexin-5 (SFXN-5) in bacteriocytes of wild mussels (Figure 3). Both mitochondrial succinate and citrate have been correlated with the formation of reactive oxygen species in mammalian inflammatory cells (Tannahill *et al.*, 2013; Williams and O'Neill, 2018). To avoid cellular damage during inflammation, ROS are typically neutralised through glutathione

peroxidases using reduced glutathione as electron donor (Margis *et al.*, 2008; Harijith, Ebenezer and Natarajan, 2014). Glutathione peroxidase was significantly higher expressed in bacteriocytes of wild mussels compared to symbiont-depleted mussels (6.1-fold increase), suggesting that these cells combat high levels of ROS induced by build-up of mitochondrial TCA intermediated succinate and citrate to maintain cellular function functions (Figure 3).

Our results show that high symbiont presence triggers the expression of inflammatory molecular patterns and upregulation of antibacterial compounds in the bacteriocyte region of the host. In mammals, pro-inflammatory immune cells typically reprogram their metabolism to interrupt mitochondrial oxidative phosphorylation of the TCA cycle and upregulate glycolysis for ATP synthesis (Russell *et al.*, 2019). The bacteriocytes of wild mussels show similar pro-inflammatory molecular reprogramming through greater export of citrate, and higher synthesis of itaconate and blocking of succinate dehydrogenase causing accumulation of succinate (Figure 3). While we did not see upregulation of glycolysis-related genes, we propose that the host is supplied with high amounts of glucose for glycolysis through digestion of symbiont glycogen, thus enabling higher synthesis of ATP from glycolysis (Figure 3 and 4; discussed in the next sections).

Bacteriocytes use a tailored set of enzymes for lysosomal symbiont digestion

Epithelial cells, such as the bacteriocytes of *B. childressi,* engage phagocytic processes to engulf and digest invading microorganisms (Günther and Seyfert, 2018). Not only is this process part of the innate immunity of bacteriocytes, but also supports the nutrient acquisition in bathymodiolin hosts to meet their nutritional requirements (Zheng *et al.*, 2017). Such phagolysosomal processes have repeatedly been reported for several bathymodiolin species, but the underlying molecular processes involved in symbiont digestion have not yet been resolved. We found that in wild *B. childressi*, lysosomal digestion of symbionts dominated the cellular processes of bacteriocytes and fuelled the host cellular metabolism. All genes in our bacteriocyte-specific GCN that could be attributed to this process were higher expressed in wild mussels compared to symbiont-depleted mussels (Figure 4 and Supplementary Table 3).

Lysosomes are acidic organelles responsible for the degradation and recycling of intracellular material in phagocytes (Luzio *et al.*, 2020). We found significantly higher expression of genes that play a role in phagocytosis (Supplementary Table 3). The engulfment and cell motility protein 1 (ELMO1) and the actin-related protein 2 (ARP2) appear to play a role in the rearrangement of the actin cytoskeleton to compartmentalise the symbionts (Gumienny *et al.*, 2001; Rotty *et al.*, 2017). The subunits of the AP-2 complex (AP2SU) and AP-3 complex (AP3SU) aid the movement of these likely clathrin-coated phagocytic vesicles (Moretti and Blander, 2014). All of these proteins could be involved in symbiont internalisation into bacteriocytes. We also found the RAB5 activating vesicular sorting protein VPS9, which is likely involved in the maturation of phagosomes before fusion with lysosomes (Luzio *et al.*, 2007). Additionally, we detected significantly higher expression of Syntaxin-7 (STX7) in bacteriocytes of wild mussels, which is a key protein required for membrane fusion of symbiont-engulfed phagosomes with lysosomes (Figure 4; Mullock *et al.*, 2000; Luzio, Pryor and Bright, 2007).

In the following phagolysosome stage, we observed that symbionts were broken down and accessible components were resorbed by the bacteriocytes (Figure 4). The enzymatic attack on engulfed symbionts likely relies on an acidic environment regulated by membrane-bound proton pumps (Luzio *et al.*, 2007). Three of the subunits of the proton pump V-type ATPase were identified in the bacteriocyte-specific GCN (Figure 4c and Supplementary Table 4). We also identified the lysosome membrane-bound protein LAMTOR1 of the Ragulator complex in the bacteriocyte-specific GCN (Figure 4c and Supplementary Table 3). Together with V-type ATPase, LAMTOR1 may form a complex that suppresses innate immune responses similar to anti-inflammatory macrophages (Kimura *et al.*, 2016).

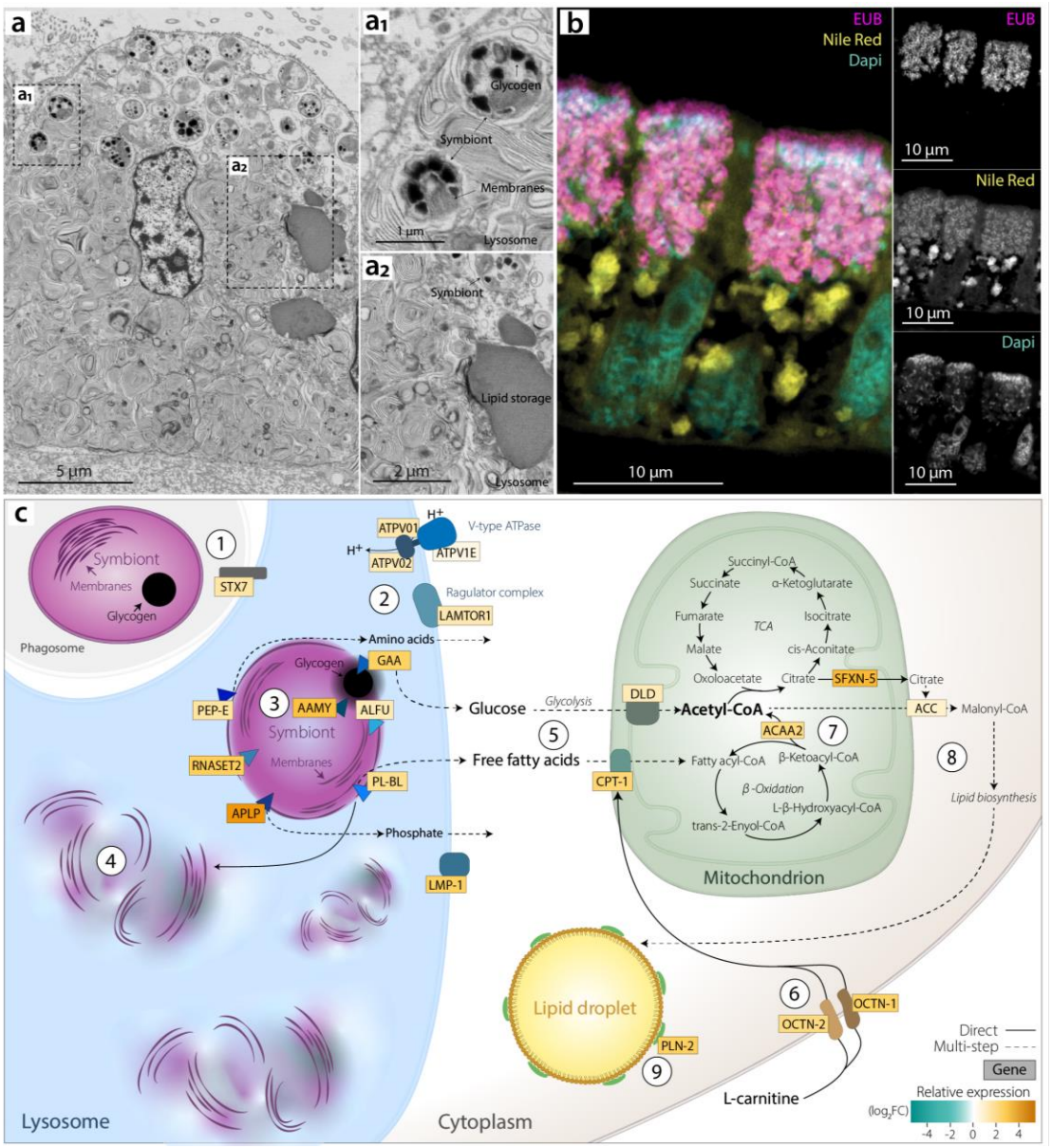

Figure 4: Bacteriocytes of *B. childressi* gills digest and metabolise symbiont-derived products leading to build-up and long-term storage of lipids. a) TEM image of a bacteriocyte from wild mussels showing a large area of the cell occupied by residual bodies with remnants of partially digested symbiont membranes. **b)** FISH combined with Nile red staining of bacteriocytes from wild mussels show large amounts of lipids located toward the basal lamina of the cell below the symbiont layer**. c)** Digestion of symbionts and metabolism of symbiont-derived products. **(1)** Fusion of symbiont-engulfed phagosome with lysosome. **(2)** Acidification of lysosome through V-type ATPase proton pumps. **(3)** Digestion of symbiont cell components through selected set of enzymes to degrade symbiont components such as glycogen and membranes, releasing glucose and fatty acids. **(4)** Build-up of undigested symbiont material. **(5)** Export of glucose and fatty acids from the lysosome for glycolysis and subsequent TCA cycle, and β-oxidation. **(6)** Import of L-carnitine to support fatty acid import into mitochondria. **(7)** Acetyl-CoA synthesis from β-oxidation of symbiont-derived fatty acids. **(8)** Synthesis of malonyl-CoA from acetyl-CoA, which can further metabolised in a range of lipid biosynthesis pathways. **(9)** Long-term storage of lipids in lipid droplets through coating of Perilipin-2.

Once the phagolysosome is acidified, several families of digestive enzymes break down the cellular envelope of the symbionts. We identified a set of such lysosomal proteins that are likely involved in the targeted digestion of the methane-oxidising symbiont. Likely, the most nutritious source accessible to the gills of *B. childressi* are the fatty acids acquired from the lysosomal digestion of the highly abundant symbiont membranes. Besides the cellular envelope, the methane-oxidising symbiont of *B. childressi* contains intracytosolic membrane stacks that enhance methane oxidation (Figure 4; Hanson and Hanson, 1996). We detected phospholipase B (PL-BL) in the bacteriocyte-specific GCN, which was 2-fold higher expressed in wild mussels compared to symbiont-depleted mussels. Upon lysosomal degradation of symbiont membranes by phospholipase B, the host cells have access to a pool of free fatty acids that can be transported into the mitochondria for subsequent β-oxidation (Figure 4).

Glycogen is the second major energy and carbon resource that the host exploits from lysosomal symbiont digestion. The methane-oxidising symbiont of *B. childressi* expressed genes for a complete glycogen synthesis and storage pathway (Supplementary Table 2). As to be expected, the synthesis of symbiont glycogen was higher expressed in wild and symbiont-recovered mussels (Supplementary Table 2). Abundant electron-dense granules detected *via* TEM of the symbiont also support glucose storage in form of glycogen (Figure 4). This symbiont-derived glycogen was likely degraded by the host *via* a lysosomal alpha glucosidase (GAA), which was 3.6-fold higher expressed in wild mussels compared to symbiont depleted mussels (Figure 4c). Upon lysosomal glycogen degradation, glucose is released into the host cytosol, where it can fuel glycolysis and other energy-generating pathways.

Alongside the alpha glucosidase, a putative acid-phosphatase (APLP) was present in the repertoire of lysosomal enzymes, which was more than 11-fold higher expressed in bacteriocytes of wild mussels compared to symbiont-depleted mussels. Acid-phosphatases have been shown to be valuable marker enzymes for lysosomal digestion as well as lysosomal maturation (Streams, Fisher and Fiala-Médioni, 1997; de Duve, 2005; Sun *et al.*, 2008). The extremely high levels of APLP expression are indicative for high rates of pre-lysosome

maturation in bacteriocytes of wild mussels, and imply high levels of phosphate release from symbiont digestion. Additionally, a broad range of digestive enzymes was detected including an alpha-fucosidase (AFLU) and an alpha-amylase (AAMY), a digestive peptidase (PEP-E), and a ribonuclease (RNASET2), and reflect the near-complete degradation of symbiont biomass (Figure 4c). Previously, lysozymes were proposed to play a fundamental role in the digestion of symbionts in *B. azoricus* (Detree *et al.*, 2016). We did not detect lysozymes in the bacteriocyte-specific GCN (more in the Appendix of Chapter III). Lysozymes were also not among the differentially expressed genes between wild and symbiont-depleted bacteriocytes. Instead, we found consistent expression of multiple lysozyme-coding genes in both gill regions across all sampling conditions. This suggests that the expression of lysozymes in *B. childressi* gills is not symbiont-specific but rather part of the general lysosomal digestion processes and the innate immune system across the gill.

The endpoint of lysosomal digestion are packages of indigestible material known as residual bodies or tertiary lysosomes (Walkley, 1998). We repeatedly detected large residual bodies in the bacteriocytes of wild mussels with TEM (Figure 4). Within bacteriocytes, the residual bodies were almost exclusively observed close to the basal lamina of the gill filament and underneath the layer of intact symbiont cells (Figure 4a). The residual bodies predominantly contained what looked like symbiont-derived membranes and often occupied a large area of the 2-dimensional cellular space (example in Figure 4). This built-up of residual bodies is a hallmark for bathymodiolin bacteriocytes and has been observed in several other host species as well (e.g. Fiala-Medioni *et al.*, 1994; Distel, Lee and Cavanaugh, 1995; Streams, Fisher and Fiala-Médioni, 1997).

Fatty acids and sugars from symbiont digestion fuel mitochondria

The release of free fatty acids and glucose from lysosomes into the cytosol likely fuelled the host metabolism in wild mussels (Figure 4c). Within the bacteriocytes-specific GCN, we detected dihydrolipoyl dehydrogenase (DLD), the subunit of the mitochondrial pyruvate dehydrogenase complex to convert pyruvate into acetyl-CoA for the TCA cycle. The higher

expression of DLD in bacteriocytes of wild mussels compared to symbiont-depleted mussels may indicate higher availability of pyruvate resulting from glycolysis. It is not surprising that we did not detect glycolysis-related genes in the bacteriocyte-specific GCN co-expressed with DLD, as glycolysis is the major pathway for generating ATP from glucose for most cell types (Oparina *et al.*, 2013). Nonetheless, glycolysis-related genes were generally higher expressed in bacteriocytes of wild mussels relative to symbiont-depleted and symbiont-recovered mussels, indicating higher ATP synthesis and pyruvate production from symbiont-derived glucose.

Our data showed higher import of free fatty acids into the mitochondria *via* carnitine O-palmitoyltransferase 1 (CPT-1). This suggests an increase of β-oxidation to generate acetyl-CoA. CPT-1 depends on carnitine to transport the fatty acids into the mitochondria (Longo *et al.*, 2016). We found both sodium-dependent high-affinity and low-affinity carnitine translocases (OCTN1 and OCTN2) co-expressed with CTP-1 in the bacteriocyte-specific GCN (Figure 4 and Supplementary Table 3). The expression of both low and high-affinity carnitine translocases suggests variable amounts of carnitine available within a bacteriocyte or across the bacteriocyte gill region. We could not resolve the complete metabolism of symbiont fatty acids with our GCN analyses, but we found higher expression of parts of the mitochondrial β-oxidation in bacteriocytes of wild mussels suggesting high energy yields from symbiont-derived fatty acids. We found 3-ketoacyl-CoA thiolase (ACAA2), the enzyme that catalyses the last step of β-oxidation to produce acetyl-CoA from fatty acids (Germain *et al.*, 2001). Acetyl-CoA is likely exported from the mitochondria to support lipid biosynthesis *via* the acetyl-carboxylase (ACC) in bacteriocytes of wild mussels (Guo *et al.*, 2009). Likewise, the higher export of citrate from mitochondria through SFXN-5 (Figure 3 and 4) may provide an additional resource for lipid biosynthesis in bacteriocytes of wild mussels, which has been observed in pro-inflammatory macrophages (Russell *et al.*, 2019).

These resulting neutral lipids are likely stored in lipid droplets within bacteriocytes, where they can be consumed in nutrient-deprived conditions (Olzmann and Carvalho, 2019). We

found indications for such long-term lipid storage *via* Perilipin-2 (PLIN2) and apolipoprotein L3 (APOL3) in bacteriocytes of wild mussels and hypothesise that these cells are in a state of nutrient surplus. Large lipid droplets in bacteriocytes have been reported multiple times in bacteriocytes of other bathymodiolin mussels with TEM (Fiala-Médioni *et al.*, 1986). Additionally, high abundances of triglycerides, which are components of neutral lipids and lipid droplets, were recently detected in bacteriocytes of *B. childressi* (Geier *et al.*, 2020), supporting our hypothesis that the host metabolises symbiont phospholipids and uses the resulting free fatty acids for lipid biosynthesis and storage. However, lipid droplets might not be the sole component of lipid storage in *B. childressi* bacteriocytes. Rather, we propose that the lysosomes also represent a major lipid store for the bacteriocytes of *B. childressi*. It is possible that the residual bodies themselves serve as storage organelles that contain digestible lipid reserves (e.g. symbiont membranes) that can be accessed *via* phospholipases to produce free fatty acids when needed.

We visualised these lysosomal lipid stores in the bacteriocytes with fluorescence microscopy combining the lipid stain Nile Red with *in situ* hybridisation of the symbionts (Figure 4). In bacteriocytes of wild mussels, large areas of lipid stores were located toward the basal lamina of the gills below the symbiont layer. The lipid staining mirrored our TEM ultrastructure analyses (Figure 4), and supports our interpretations of lipid build-up in bacteriocyte lysosomes. In symbiont-depleted and symbiont-recovered mussels, hardly any bacteriocytes showed Nile Red stained cell components, reflecting the low expression of phospholipase in the bacteriocyte GCN (Supplementary Figure 3 and Supplementary Table 3). The lysosome-contained phospholipids in bacteriocytes of wild mussels may be stored for later use or remain within lysosomes as waste products (Lawrence and Zoncu, 2019). However, lipid storage within residual bodies is not only a rich reservoir of energy and carbon. Build-up of lipid-rich waste in residual bodies could also have detrimental effects for bacteriocytes. In humans, accumulation of excess phospholipids has been linked to the lysosomal storage disease known as phospholipidosis, which assumed to have currently unknown pathological implications (Breiden and Sandhoff, 2019).

Conclusion

We show that unbiased gene co-expression networks provide streamlined access to the most relevant details in the physiology of symbiotic bathymodiolin hosts. Our study identifies the largest cell population on the gill surface as defensive, behaving like phagocytes co-opted into a beneficial and multifunctional symbiotic organ. Besides the symbiosis-specific nutritional insights, this observation opens new avenues in our understanding of bivalve gill physiology and the ecological success of bivalves in environments with heavy bacterial load, especially in ecosystems driven by high primary production.

Mussel immunity is considered to be mediated by hemocytes in the circulating hemolymph that eliminate invading microorganisms (Tame *et al.*, 2015; Yang *et al.*, 2015; Castro *et al.*, 2018). Based on our bacteriocyte-specific GCN analyses, we propose that the bacteriocytes of *B. childressi* gills are main drivers of gill immunity. Depending on symbiont load, the bacteriocytes reflect different stages of immune activity (Figure 5). Under natural conditions with high symbiont load, the bacteriocytes of *B. childressi* show expression patterns that resemble a macrophage-like inflammatory state. These include the upregulation of itaconate synthesis, switch from oxidative phosphorylation in the TCA cycle to ATP production through glycolysis, higher production of ROS, and enhanced phagocytosis (Figure 5, Mills *et al.*, 2016). In bacteriocytes with moderate symbiont load (symbiont-recovered state), the expression of genes involved in these immune responses did not differ from the symbiont-depleted bacteriocytes. Intriguingly, the symbiont-recovered bacteriocytes showed upregulation of the symbiont-recognition proteins MLEC and BPI, which suggests that the bacteriocytes have a fine-tuned ability to sense and respond to symbiont load.

The most prominent feature of bacteriocytes from wild mussels was the high expression of phagocytic pathways and the large amounts of cellular lipid stores. With naturally high abundances of symbionts, *B. childressi* employs a selected set of digestive enzymes to thrive off the symbiont cellular components through lysosomal digestion. This symbiont harvest appears to be dependent on symbiont load, as lysosomal digestion was only higher expressed

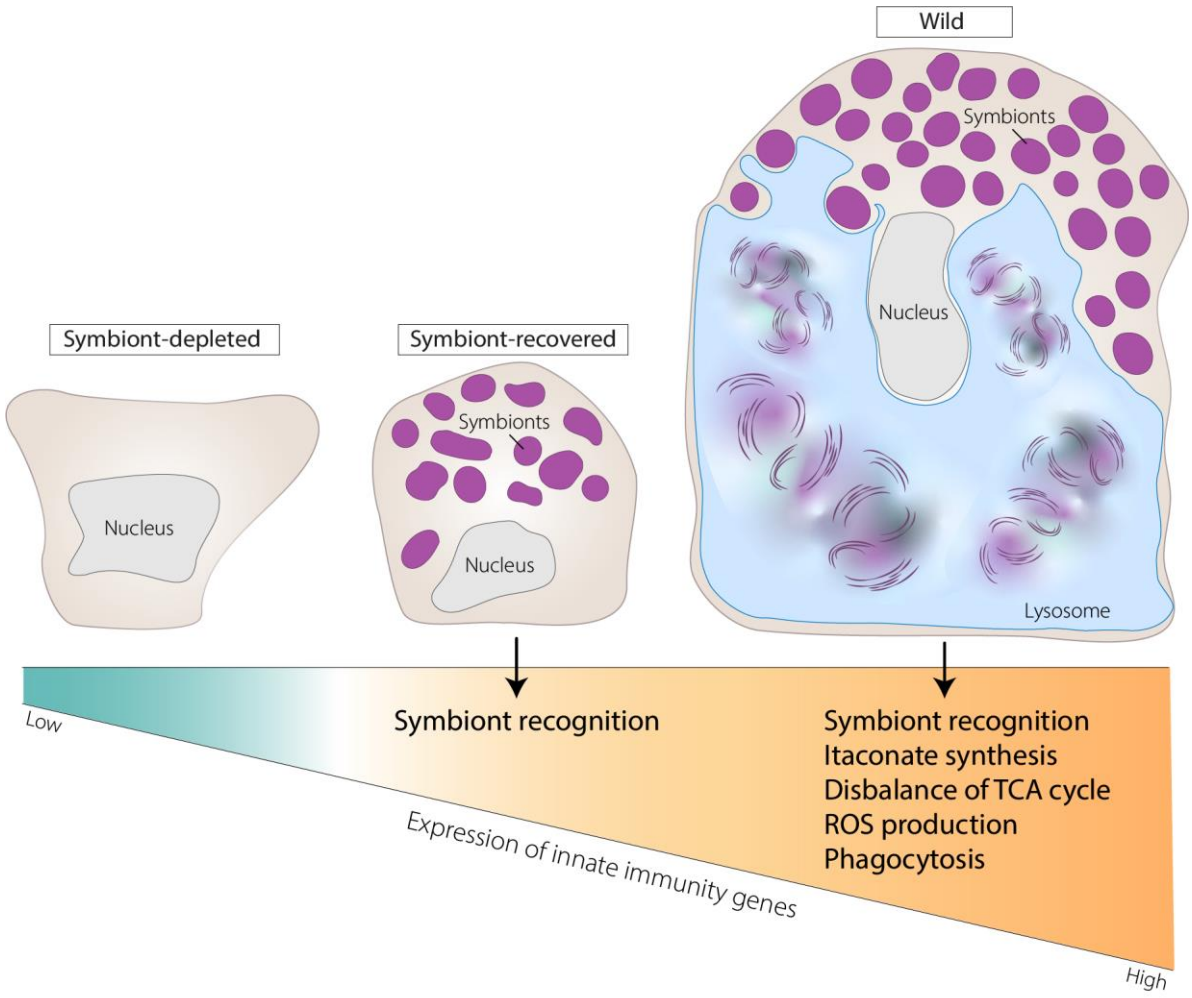

Figure 5: Physiological states of bacteriocytes ordered from low to high innate immune activity reflecting symbiont load. Symbiont-depleted mussels showed lowest expression of innate immune genes. In the symbiont-recovered state, only symbiont recognition *via* MLEC and BPI was higher expressed compared to symbiont-depleted mussels. In wild mussels, symbionts are recognised *via* MLEC and BPI inducing a metabolic shift and upregulation of pro-inflammatory processes. Illustrations are drawn to realistic proportion and are based on TEM images of mussel gills from the corresponding symbiont states.

in wild mussels (Figure 5). However, the digestion of symbionts in wild mussels with high symbiont load may lead to a physiological dilemma in bacteriocytes: Continuous digestion of symbionts leads to a build-up of waste in residual bodies that are expected to increase in volume throughout the bacteriocyte life time ultimately leading to cell death (e.g. through apoptosis), and cell renewal. Future research should aim to investigate the turnover of gill bacteriocytes in mussels with low, moderate and high symbiont load to find out if lysosomal digestion and accumulation of residual bodies influences the renewal of cells.

Acknowledgements

We thank the crew, captain and research team of the Nautilus cruise NA043-045 in 2014 for supporting the sampling of mussels. We particularly thank Samantha (Mandy) Joye and Chuck Fisher for their assistance and support in sample collection, and Jillian Petersen and Corinna Breusing for sample coordination and transfer to the Kiel aquaria. We thank Finn-Ole Petersen for supporting the mussel husbandry throughout the years. Special thanks to Bruno Hüttel and Lisa Czaja-Hasse from the Max Planck Genome Centre in Cologne for supporting the library preparation and sequencing. We also thank the Symbiosis Department, especially Adrien Assié, Antony Chakkiath, Maxim Rubin-Blum and Patric Bourceau for scientific discussions and input.

Chapter III: Supplementary Notes

Supplementary Note 1 - Methane starvation causes symbiont and biomass loss

Methane limitation was the main driver of symbiont loss in *B. childressi*. A depletion of methanotrophic symbionts has been also observed in the related cold-seep mussel *B. platifrons* after methane supply was diminished for three months (Yu *et al.*, 2019). In our study, symbiont populations recovered when we increased the methane concentrations to 40 µM for another year (Figure 1 and Supplementary Figures 3-5) albeit the overall abundance of symbionts was much less than in the wild mussels. In *M. sedimenti*, the recovery of population growth has been observed to occur quickly after reintroduction of methane to the cultures, suggesting that the symbiont population might have quickly recovered from methane starvation and that we always sampled a steady-state for the given methane supply (Tavormina *et al.*, 2017). We hypothesise that symbiont recovery in *B. childressi* resulted from fast re-growth of almost diminished symbiont numbers rather than re-acquisition from the surrounding aquarium water, which is supported by identical 16S rRNA phylotypes in symbiont-recovered mussels compared wild mussels (Supplementary Figure 8).

Inhabiting comparatively shallow cold-seep sites in the Northern Gulf of Mexico, *B. childressi* does not solely rely on symbiont-derived nutrients. Stable isotope analyses recently provided insights into the dependency of *B. childressi* on phototrophic carbon and nutrition via filter-feeding, indicating that even under natural conditions nutrients acquired by the mussels can derive from both chemo- and photosynthesis (Demopoulos *et al.*, 2019). Mussel survival in our aquaria setups was ensured by additional feeding with *Rhodomonas* sp. algae as reported previously for *B. childressi* (Riekenberg *et al.*, 2016). Nonetheless, the overall biomass and cell sizes in the bacteriocyte gill region of symbiont-depleted and symbiont-recovered mussels was much lower than in wild mussels as revealed by TEM images (Figure 1 and Supplementary Figure 4). Overall, gills of aquaria mussels appeared fragile with near transparent colouration compared to their natural dark-brown colour (data not shown), similar to *B. azoricus* mussels that were maintained in aquaria without sulphur- and methane supply (Kádár *et al.*, 2005).

Supplementary Note 2 – Symbiont-induced microvilli loss in gill bacteriocytes

In our study, symbiont presence was linked to the absence of microvilli on host cells in the bacteriocyte region of *B. childressi* gills. In symbiont-depleted mussels, we observed microvilli on all cells of the bacteriocyte gill region, while microvilli were not detectable on symbiont-containing cells of neither wild nor symbiont-recovered mussels (Figure 1 and Supplementary Figure 4). Microvilli, or microfilaments, are commonly found on polarised epithelial cells of nearly all animals and support nutrient acquisition by increasing the cell surface (Sauvanet *et al.*, 2015). These protein- and actin-rich cell protrusions have also been discovered on gill cells of *Bathymodiolus* spp. (Fiala-Médioni *et al.*, 1986). Strikingly, microvilli are absent on all symbiont-containing cells of *Gigantidas* and *Bathymodiolus* spp. gills (Wentrup *et al.*, 2014), but are present on bathymodiolin hosts with ectosymbionts (Lorion *et al.*, 2009) as well as on symbiont-containing gill cells of the vesicomyid clam *Calyptogena magnifica* (Fiala-Médioni and Le Pennec, 1987). While the function of microvilli remains unresolved, we hypothesise that these microvilli likely serve to enhance nutrient acquisition from the environment into the gill cells. It is currently unclear how microvilli loss is linked to symbiont presence in bathymodiolin hosts.

Symbiont colonisation was previously suggested to cause microvilli loss in *Bathymodiolus azoricus*, where the abundance of microvilli was negatively correlated with the abundance of symbionts in developing mussels (Wentrup *et al.*, 2014). Based on our genomic and transcriptomic data, we hypothesise that upon symbiont-colonisation of gill cells, microvilli are disrupted in response to specific effector proteins secreted by the symbionts. The symbionts express a Type 4 Secretion System (T4SS) and several predicted effector proteins that are potentially secreted via the T4SS (Supplementary Table 2). This is comparable to the effector proteins of the enteropathogen *Escherichia coli* strain EPEC that causes microvilli effacement in mammalian gut epithelial cells (Dean and Kenny, 2009; Shifrin *et al.*, 2014). The absence of microvilli may be linked to the high expression of innate immunity genes in the bacteriocytes in *B. childressi* (Figure 3). As electrostatic barrier, the microvilli brush border is considered to minimise bacterial invasion of host cells (Bennett *et al.*, 2014). If this

barrier is diminished, the host must rely on other mechanisms, such as higher expression and subsequent synthesis of immune-related proteins, to protect itself from potential invaders.

Supplementary Note 3 – Examples for gill region specific gene co-expression

Previous studies on host and symbiont physiology in bathymodiolin symbioses mainly focused on differential expression analyses of RNA-seq or qPCR data from gill pieces, and inferred host molecular processes in symbiont-containing cells from single genes. However, gill pieces always contain a consortium of different cell types that share expression of genes that are part of general cellular functions. On top of this, genes rarely function alone and are rather linked to gene networks involved in multiple molecular and cellular processes in eukaryotic organisms (Li *et al.*, 2018). By analysing replicates of mussel states with varying symbiont abundances, the inferred co-expression of genes that is represented by proportionality reflected non-random correlation and therefore true biological function. The annotation with Gene Ontologies (GOs) identified most of the genes from the gill region specific GCNs to be involved in biological processes that are expected to be enriched in cells within these regions. For examples, the majority of genes of the bacteriocyte-specific GCN were attributed to transmembrane transport (Supplementary Figure 9). In bathymodiolin mussels, the symbionts are contained within vacuolar-like structures (Wentrup *et al.*, 2014). Therefore host-symbiont interaction likely occurs *via* the host membrane, and a high abundance of transmembrane proteins in bacteriocytes might be related to the symbiosis. In the ciliated edge specific GCN, a high number of genes were assigned to biological processes that are related to the function of cilia including 'microtubule-based movement' and 'microtubule-based process'. Specifically, we identified a range of dynein-coding genes in the ciliated edge specific GCN, which are the motor proteins of cilia (Cianfrocco *et al.*, 2015; Supplementary Table 3). These genes were absent in the GCN of the bacteriocyte gill region where ciliated cells in between non-ciliated bacteriocytes are much less abundant in symbiotic bathymodiolin mussels (Fiala-Médioni *et al.*, 1986).

References

Ahn, S., Jung, J., Jang, I. A., Madsen, E. L., *et al.* (2016) 'Role of glyoxylate shunt in oxidative stress response', *Journal of Biological Chemistry*, 291, pp. 11928–11938. doi: 10.1074/jbc.M115.708149.

Akiva, E., Brown, S., Almonacid, D. E., Barber, A. E., *et al.* (2014) 'The Structure-Function Linkage Database', *Nucleic Acids Research*, 42, pp. 521–530. doi: 10.1093/nar/gkt1130.

Assié, A., Leisch, N., Meier, D. V., Gruber-Vodicka, H., *et al.* (2020) 'Horizontal acquisition of a patchwork Calvin cycle by symbiotic and free-living Campylobacterota (formerly Epsilonproteobacteria)', *ISME Journal*, 14, pp. 104–122. doi: 10.1038/s41396-019-0508-7.

Attwood, T. K., Coletta, A., Muirhead, G., Pavlopoulou, A., *et al.* (2012) 'The PRINTS database: A fine-grained protein sequence annotation and analysis resource-its status in 2012', *Database*, 2012, pp. 1–9. doi: 10.1093/database/bas019.

Aziz, R. K., Bartels, D., Best, A., DeJongh, M., *et al.* (2008) 'The RAST Server: Rapid annotations using subsystems technology', *BMC Genomics*, 9, pp. 1–15. doi: 10.1186/1471-2164-9-75.

Bankevich, A., Nurk, S., Antipov, D., Gurevich, A. A., *et al.* (2012) 'SPAdes: A new genome assembly algorithm and its applications to single-cell sequencing', *Journal of Computational Biology*, 19, pp. 455–477. doi: 10.1089/cmb.2012.0021.

Barros, I., Divya, B., Martins, I., Vandeperre, F., *et al.* (2015) 'Post-capture immune gene expression studies in the deep-sea hydrothermal vent mussel *Bathymodiolus azoricus* acclimatized to atmospheric pressure', *Fish and Shellfish Immunology*, 42, pp. 159–170. doi: 10.1016/j.fsi.2014.10.018.

Barros, I., Mendes, S. and Rosa, D. (2016) '*Vibrio diabolicus* Immunomodulatory Effects on Bathymodiolus azoricus During Long-term Acclimatization at Atmospheric Pressure', *Journal of Aquaculture Research & Development*, 7. doi: 10.4172/2155-9546.1000464.

Bennett, K. M., Walker, S. L. and Lo, D. D. (2014) 'Epithelial microvilli establish an electrostatic barrier to microbial adhesion', *Infection and Immunity*, 82, pp. 2860–2871. doi: 10.1128/IAI.01681-14.

Bray, N. L., Pimentel, H., Melsted, P. and Pachter, L. (2016) 'Near-optimal probabilistic RNA-seq quantification', 34, pp. 525–527. doi: 10.1038/nbt.3519.

Breiden, B. and Sandhoff, K. (2019) 'Emerging mechanisms of drug-induced phospholipidosis', *Biological Chemistry*, 401, pp. 31–46. doi: 10.1515/hsz-2019-0270.

Bryant, D. M., Johnson, K., DiTommaso, T., Tickle, T., *et al.* (2017) 'A Tissue-Mapped Axolotl De Novo Transcriptome Enables Identification of Limb Regeneration Factors', *Cell Reports*, 18, pp. 762–776. doi: 10.1016/j.celrep.2016.12.063.

Bulgheresi, S., Gruber-Vodicka, H. R., Heindl, N. R., Dirks, U., *et al.* (2011) 'Sequence variability of the pattern recognition receptor Mermaid mediates specificity of marine nematode symbioses', *ISME Journal*, 5, pp. 986–998. doi: 10.1038/ismej.2010.198.

Bülow, S., Zeller, L., Werner, M., Toelge, M., *et al.* (2018) 'Bactericidal/Permeability-Increasing Protein Is an Enhancer of Bacterial Lipoprotein Recognition', *Frontiers in immunology*, 9, p. 2768. doi: 10.3389/fimmu.2018.02768.

Canesi, L., Gallo, G., Gavioli, M. and Pruzzo, C. (2002) 'Bacteria-hemocyte interactions and phagocytosis in marine bivalves', *Microscopy Research and Technique*, 57, pp. 469–476. doi: 10.1002/jemt.10100.

Canny, G., Levy, O., Furuta, G. T., Narravula-Alipati, S., *et al.* (2002) 'Lipid mediator-induced expression of bactericidal/permeability-increasing protein (BPI) in human mucosal epithelia',

Proceedings of the National Academy of Sciences of the United States of America, 99, pp. 3902–3907. doi: 10.1073/pnas.052533799.

Carter, S. L., Brechbühler, C. M., Griffin, M. and Bond, A. T. (2004) 'Gene co-expression network topology provides a framework for molecular characterization of cellular state', *Bioinformatics*, 20, pp. 2242–2250. doi: 10.1093/bioinformatics/bth234.

Castro, J. M., Bianchi, V. A., Pascual, M. M., Almeida, C., *et al.* (2018) 'Immune and biochemical responses in hemolymph and gills of the Patagonian freshwater mussel *Diplodon chilensis*, against two microbiological challenges: Saccharomyces cerevisiae and Escherichia coli', *Journal of Invertebrate Pathology*, 157, pp. 36–44. doi: 10.1016/j.jip.2018.08.005.

Cianfrocco, M. A., Desantis, M. E., Leschziner, A. E. and Reck-Peterson, S. L. (2015) 'Mechanism and Regulation of Cytoplasmic Dynein', *Annual Review of Cell and Developmental Biology*, 31, pp. 83–108. doi: 10.1146/annurev-cellbio-100814-125438.

Conesa, A., Götz, S., García-Gómez, J. M., Terol, J., *et al.* (2005) 'Blast2GO: A universal tool for annotation, visualization and analysis in functional genomics research', *Bioinformatics*, 21, pp. 3674–3676. doi: 10.1093/bioinformatics/bti610.

Cordes, T., Lucas, A., Divakaruni, A. S., Murphy, A. N., *et al.* (2020) 'Itaconate modulates tricarboxylic acid and redox metabolism to mitigate reperfusion injury', *Molecular Metabolism*, 32, pp. 122–135. doi: 10.1016/j.molmet.2019.11.019.

Cordes, T., Michelucci, A. and Hiller, K. (2015) 'Itaconic Acid: The Surprising Role of an Industrial Compound as a Mammalian Antimicrobial Metabolite', *Annual Review of Nutrition*, 35, pp. 451–473. doi: 10.1146/annurev-nutr-071714-034243.

Daims, H., Brühl, A., Amann, R., Schleifer, K.-H., *et al.* (1999) 'The Domain-specific Probe EUB338 is Insufficient for the Detection of all Bacteria: Development and Evaluation of a more Comprehensive Probe Set', *Systematic and Applied Microbiology*, 22, pp. 434–44. doi: https://doi.org/10.1016/S0723-2020(99)80053-8.

van Dam, S., Võsa, U., van der Graaf, A., Franke, L., *et al.* (2018) 'Gene co-expression analysis for functional classification and gene-disease predictions', *Briefings in bioinformatics*, 19, pp. 575–592. doi: 10.1093/bib/bbw139.

Dattagupta, S., Martin, J., Liao, S. M., Carney, R. S., *et al.* (2007) 'Deep-sea hydrocarbon seep gastropod Bathynerita naticoidea responds to cues from the habitat-providing mussel *Bathymodiolus childressi*', *Marine Ecology*, 28, pp. 193–198. doi: 10.1111/j.1439-0485.2006.00130.x.

Dean, P. and Kenny, B. (2009) 'The effector repertoire of enteropathogenic *E. coli*: ganging up on the host cell', *Current Opinion in Microbiology*, 12, pp. 101–109. doi: 10.1016/j.mib.2008.11.006.

Demopoulos, A. W. J., McClain-Counts, J. P., Bourque, J. R., Prouty, N. G., *et al.* (2019) 'Examination of Bathymodiolus childressi nutritional sources, isotopic niches, and food-web linkages at two seeps in the US Atlantic margin using stable isotope analysis and mixing models', *Deep-Sea Research Part I: Oceanographic Research Papers*, 148, pp. 53–66. doi: 10.1016/j.dsr.2019.04.002.

Detree, C., Chabenat, A., Lallier, F. H., Satoh, N., *et al.* (2016) 'Multiple I-type lysozymes in the hydrothermal vent mussel bathymodiolus azoricus and their role in symbiotic plasticity', *PLoS ONE*, 11, pp. 1–19. doi: 10.1371/journal.pone.0148988.

Distel, D. L., Lee, H. K. W. and Cavanaugh, C. M. (1995) 'Intracellular coexistence of methano- and thioautotrophic bacteria in a hydrothermal vent mussel', *Proceedings of the National Academy of Sciences of the United States of America*, 92, pp. 9598–9602. doi: 10.1073/pnas.92.21.9598.

Dolan, S. K. and Welch, M. (2018) 'The Glyoxylate Shunt, 60 Years On', *Annual Review of Microbiology*, 72, pp. 309–330. doi: 10.1146/annurev-micro-090817-062257.

Domínguez-Andrés, J., Novakovic, B., Li, Y., Scicluna, B. P., *et al.* (2019) 'The Itaconate Pathway Is a Central Regulatory Node Linking Innate Immune Tolerance and Trained Immunity', *Cell Metabolism*, 29, pp. 211-220.e5. doi: 10.1016/j.cmet.2018.09.003.

Duperron, S., Nadalig, T., Caprais, J.-C., Sibuet, M., *et al.* (2005) 'Dual Symbiosis in a *Bathymodiolus* sp. Mussel from a Methane Seep on the Gabon Continental Margin (Southeast Atlantic): 16S rRNA Phylogeny and Distribution of the Symbionts in Gills', *Applied and Environmental Microbiology*, 71, pp. 1694–1700. doi: 10.1128/AEM.71.4.1694.

Duperron, S., Sibuet, M., MacGregor, B. J., Kuypers, M. M. M., *et al.* (2007) 'Diversity, relative abundance and metabolic potential of bacterial endosymbionts in three *Bathymodiolus* mussel species from cold seeps in the Gulf of Mexico', *Environmental Microbiology*, 9, pp. 1423–1438. doi: 10.1111/j.1462-2920.2007.01259.x.

Duperron, S., Lorion, J., Samadi, S., Gros, O., *et al.* (2009) 'Symbioses between deep-sea mussels (Mytilidae: Bathymodiolinae) and chemosynthetic bacteria: diversity, function and evolution', *Comptes Rendus - Biologies*, 332, pp. 298–310. doi: 10.1016/j.crvi.2008.08.003.

de Duve, C. (2005) 'The lysosome turns fifty', *Nature Cell Biology*, 7, pp. 847–849. doi: 10.1038/ncb0905-847.

Eichinger, V., Nussbaumer, T., Platzer, A., Jehl, M. A., *et al.* (2016) 'EffectiveDB - Updates and novel features for a better annotation of bacterial secreted proteins and Type III, IV, VI secretion systems', *Nucleic Acids Research*, 44, pp. D669–D674. doi: 10.1093/nar/gkv1269.

El-Gebali, S., Mistry, J., Bateman, A., Eddy, S. R., *et al.* (2019) 'The Pfam protein families database in 2019', *Nucleic Acids Research*, 47, pp. D427–D432. doi: 10.1093/nar/gky995.

Feng, Y., Hurst, J., Almeida-De-Macedo, M., Chen, X., *et al.* (2012) 'Massive human co-expression network and its medical applications', *Chemistry and Biodiversity*, 9, pp. 868–887. doi: 10.1002/cbdv.201100355.

Fernandes, A. D., Macklaim, J. M., Linn, T. G., Reid, G., *et al.* (2013) 'ANOVA-Like Differential Expression (ALDEx) Analysis for Mixed Population RNA-Seq', *PLoS ONE*, 8. doi: 10.1371/journal.pone.0067019.

Fernandes, A. D., Reid, J. N., Macklaim, J. M., McMurrough, T. A., *et al.* (2014) 'Unifying the analysis of high-throughput sequencing datasets: characterizing RNA-seq, 16S rRNA gene sequencing and selective growth experiments by compositional data analysis', *Microbiome*, 2, p. 15. doi: 10.1186/2049-2618-2-15.

Fiala-Medioni, A., Michalski, J. C., Jolles, J., Alonso, C., *et al.* (1994) 'Lysosomic and lysozyme activities in the gill of bivalves from deep hydrothermal vents', *Comptes Rendus de l'Academie des Sciences - Serie III*, pp. 239–244.

Fiala-Médioni, A., Métivier, C., Herry, A. and Le Pennec, M. (1986) 'Ultrastructure of the gill of hydrothermal-vent mytilid Bathymodiolus sp.', 92, pp. 65–72.

Fiala-Médioni, A. and Le Pennec, M. (1987) 'Trophic structural adaptations in relation to the bacterial association of bivalve molluscs from hydrothermal vents and subduction zones', *Symbiosis*, 4, pp. 63–74.

Fu, X., Sun, Y., Wang, J., Xing, Q., *et al.* (2014) 'Sequencing-based gene network analysis provides a core set of gene resource for understanding thermal adaptation in Zhikong scallop *Chlamys farreri*', *Molecular Ecology Resources*, 14, pp. 184–198. doi: 10.1111/1755-0998.12169.

Geier, B., Sogin, E. M., Michellod, D., Janda, M., *et al.* (2020) 'Spatial metabolomics of in situ host-microbe interactions at the micrometer scale', *Nature Microbiology*, 5. doi: 10.1038/s41564-019-0664-6.

Germain, V., Rylott, E. L., Larson, T. R., Sherson, S. M., *et al.* (2001) 'Requirement for 3-ketoacyl-CoA thiolase-2 in peroxisome development, fatty acid β-oxidation and breakdown of triacylglycerol in lipid bodies of *Arabidopsis* seedlings', *Plant Journal*, 28, pp. 1–12. doi: 10.1046/j.1365-313X.2001.01095.x.

González, V. L., Andrade, S. C. S., Collins, T. M., Dunn, C. W., *et al.* (2015) 'A phylogenetic backbone for Bivalvia: an RNA-seq approach', *Proceedings of the Royal Society B: Biological Sciences*, 282, p. 20142332. doi: 10.1098/rspb.2014.2332.

Gosling, E. (2015) *Marine Bivalve Molluscs*. Chichester, UK: John Wiley & Sons, Ltd.

Grabherr, M. G., Haas, B. J., Yassour, M., Levin, J. Z., *et al.* (2011) 'Full-length transcriptome assembly from RNA-Seq data without a reference genome', *Nature Biotechnology*, 29, pp. 644–652. doi: 10.1038/nbt.1883.

Gruber-Vodicka, H. R., Seah, B. K. B. and Pruesse, E. (2020) 'phyloFlash: Rapid Small-Subunit rRNA Profiling and Targeted Assembly from Metagenomes', *mSystems*, 5. doi: 10.1128/msystems.00920-20.

Gumienny, T. L., Brugnera, E., Tosello-Trampont, A. C., Kinchen, J. M., *et al.* (2001) 'CED-12/ELMO, a novel member of the CrkII/Dock180/Rac pathway, is required for phagocytosis and cell migration', *Cell*, 107, pp. 27–41. doi: 10.1016/S0092-8674(01)00520-7.

Günther, J. and Seyfert, H. M. (2018) 'The first line of defence: insights into mechanisms and relevance of phagocytosis in epithelial cells', *Seminars in Immunopathology*, pp. 555–565. doi: 10.1007/s00281-018-0701-1.

Guo, Y., Cordes, K. R., Farese, R. V. and Walther, T. C. (2009) 'Lipid droplets at a glance', *Journal of Cell Science*, 122, pp. 749–752. doi: 10.1242/jcs.037630.

Haas, B. J., Papanicolaou, A., Yassour, M., Grabherr, M., *et al.* (2013) 'De novo transcript sequence reconstruction from RNA-seq using the Trinity platform for reference generation and analysis', *Nature Protocols*, 8, pp. 1494–1512. doi: 10.1038/nprot.2013.084.

Hanson, R. S. and Hanson, T. E. (1996) 'Methanotrophic bacteria', *Microbiological Reviews*, 60, pp. 439–471. doi: 10.1128/mmbr.60.2.439-471.1996.

Harijith, A., Ebenezer, D. L. and Natarajan, V. (2014) 'Reactive oxygen species at the crossroads of inflammasome and inflammation', *Frontiers in Physiology*, 5, pp. 1–11. doi: 10.3389/fphys.2014.00352.

Huson, D. H., Beier, S., Flade, I., Górska, A., *et al.* (2016) 'MEGAN Community Edition - Interactive Exploration and Analysis of Large-Scale Microbiome Sequencing Data', *PLoS Computational Biology*, 12, pp. 1–12. doi: 10.1371/journal.pcbi.1004957.

Ikuta, T., Tame, A., Saito, M., Aoki, Y., *et al.* (2019) 'Identification of cells expressing two peptidoglycan recognition proteins in the gill of the vent mussel, *Bathymodiolus septemdierum*', *Fish and Shellfish Immunology*, 93, pp. 815–822. doi: 10.1016/j.fsi.2019.08.022.

Joye, S. B., MacDonald, I. R., Montoya, J. P. and Peccini, M. (2005) 'Geophysical and geochemical signatures of Gulf of Mexico seafloor brines', *Biogeosciences Discussions*, 2, pp. 637–671. doi: 10.5194/bgd-2-637-2005.

Kádár, E., Bettencourt, R., Costa, V., Santos, R. S., *et al.* (2005) 'Experimentally induced endosymbiont loss and re-acquirement in the hydrothermal vent bivalve *Bathymodiolus azoricus*', *Journal of Experimental Marine Biology and Ecology*, 318, pp. 99–110. doi: 10.1016/j.jembe.2004.12.025.

Karp, P. D., Paley, S. and Romero, P. (2002) 'The pathway tools software', *Bioinformatics*, 18, pp. 225–232. doi: 10.1093/bioinformatics/18.suppl_1.S225.

Kimura, T., Nada, S., Takegahara, N., Okuno, T., *et al.* (2016) 'Polarization of M2 macrophages requires Lamtor1 that integrates cytokine and amino-acid signals', *Nature Communications*, 7, pp. 1–15. doi: 10.1038/ncomms13130.

Kochevar, R. E., Childress, J. J., Fisher, C. R. and Minnich, E. (1992) 'The methane mussel: roles of symbiont and host in the metabolic utilization of methane', *Marine Biology*, 112, pp. 389–401.

Kopylova, E., Noé, L. and Touzet, H. (2012) 'SortMeRNA: Fast and accurate filtering of ribosomal RNAs in metatranscriptomic data', *Bioinformatics*, 28, pp. 3211–3217. doi: 10.1093/bioinformatics/bts611.

Lawrence, R. E. and Zoncu, R. (2019) 'The lysosome as a cellular centre for signalling, metabolism and quality control', *Nature Cell Biology*, 21, pp. 133–142. doi: 10.1038/s41556-018-0244-7.

Lewis, T. E., Sillitoe, I., Dawson, N., Lam, S. D., *et al.* (2018) 'Gene3D: Extensive prediction of globular domains in proteins', *Nucleic Acids Research*, 46, pp. D435–D439. doi: 10.1093/nar/gkx1069.

Li, J., Zhou, D., Qiu, W., Shi, Y., *et al.* (2018) 'Application of Weighted Gene Co-expression Network Analysis for Data from Paired Design', *Scientific Reports*, 8, pp. 1–8. doi: 10.1038/s41598-017-18705-z.

Liu, A. X., Li, B. L., Li, C. A., Li, D. Y., *et al.* (2019) 'Transcriptome and Gene Coexpression Network Analyses of Two Wild Populations Provides Insight into the High-Salinity Adaptation Mechanisms of Crassostrea ariakensis', *Marine Biotechnology*. doi: 10.1007/s10126-019-09896-9.

Longo, N., Frigeni, M., Pasquali, M., Biophys, B., *et al.* (2016) 'Carnitine transport and fatty acid oxidation', *Biochim Biophys Acta*, 1863, pp. 2422–2435. doi: 10.1016/j.bbamcr.2016.01.023.

Lorion, J., Duperron, S., Gros, O., Cruaud, C., *et al.* (2009) 'Several deep-sea mussels and their associated symbionts are able to live both on wood and on whale falls', *Proceedings of the Royal Society B: Biological Sciences*, 276, pp. 177–185. doi: 10.1098/rspb.2008.1101.

Luzio, J. P., Hackmann, Y., Dieckmann, N. M. G. and Griffiths, G. M. (2020) 'The Biogenesis of Lysosomes and Lysosome-Related Organelles', pp. 1–18.

Luzio, J. P., Pryor, P. R. and Bright, N. A. (2007) 'Lysosomes: Fusion and function', *Nature Reviews Molecular Cell Biology*, 8, pp. 622–632. doi: 10.1038/nrm2217.

Marchler-Bauer, A., Bo, Y., Han, L., He, J., *et al.* (2017) 'CDD/SPARCLE: Functional classification of proteins via subfamily domain architectures', *Nucleic Acids Research*, 45, pp. D200–D203. doi: 10.1093/nar/gkw1129.

Margis, R., Dunand, C., Teixeira, F. K. and Margis-Pinheiro, M. (2008) 'Glutathione peroxidase family - An evolutionary overview', *FEBS Journal*, 275, pp. 3959–3970. doi: 10.1111/j.1742-4658.2008.06542.x.

McDonald, K. L. (2014) 'Rapid embedding methods into epoxy and LR white resins for morphological and immunological analysis of cryofixed biological specimens', *Microscopy and Microanalysis*, 20, pp. 152–163. doi: 10.1017/S1431927613013846.

Mi, H., Muruganujan, A., Ebert, D., Huang, X., *et al.* (2019) 'PANTHER version 14: More genomes, a new PANTHER GO-slim and improvements in enrichment analysis tools', *Nucleic Acids Research*, 47, pp. D419–D426. doi: 10.1093/nar/gky1038.

Mills, E. L., Kelly, B., Logan, A., Costa, A. S. H., *et al.* (2016) 'Succinate Dehydrogenase Supports Metabolic Repurposing of Mitochondria to Drive Inflammatory Macrophages', *Cell*, 167, pp. 457-470.e13. doi: 10.1016/j.cell.2016.08.064.

Mogensen, T. H. (2009) 'Pathogen recognition and inflammatory signaling in innate immune defenses', *Clinical Microbiology Reviews*, 22, pp. 240–273. doi: 10.1128/CMR.00046-08.

Montanaro, J., Gruber, D. and Leisch, N. (2016) 'Improved ultrastructure of marine invertebrates using non-toxic buffers', *PeerJ*, 4, p. e1860. doi: 10.7717/peerj.1860.

Moretti, J. and Blander, J. M. (2014) 'Insights into phagocytosis-coupled activation of Pattern Recognition Receptors and Inflammasomes', *Current Opinion in Immunology*, 26, pp. 100–110. doi: 10.1038/jid.2014.371.

Mullock, B. M., Smith, C. W., Ihrke, G., Bright, N. A., *et al.* (2000) 'Syntaxin 7 is localized to late endosome compartments, associates with Vamp 8, and is required for late endosome-lysosome fusion', *Molecular Biology of the Cell*, 11, pp. 3137–3153. doi: 10.1091/mbc.11.9.3137.

Nguyen, T. V. and Alfaro, A. C. (2019) 'Targeted metabolomics to investigate antimicrobial activity of itaconic acid in marine molluscs', *Metabolomics*, 15, pp. 1–12. doi: 10.1007/s11306-019-1556-8.

O'Neill, L. A. J. and Artyomov, M. N. (2019) 'Itaconate: the poster child of metabolic reprogramming in macrophage function', *Nature Reviews Immunology*, 19, pp. 273–281. doi: 10.1038/s41577-019-0128-5.

Oates, M. E., Stahlhacke, J., Vavoulis, D. V., Smithers, B., *et al.* (2015) 'The SUPERFAMILY 1.75 database in 2014: A doubling of data', *Nucleic Acids Research*, 43, pp. D227–D233. doi: 10.1093/nar/gku1041.

Olzmann, J. A. and Carvalho, P. (2019) 'Dynamics and functions of lipid droplets', *Nature Reviews Molecular Cell Biology*, 20, pp. 137–155. doi: 10.1038/s41580-018-0085-z.

Oparina, N. Y., Snezhkina, A. V., Sadritdinova, A. F., Veselovskii, V. A., *et al.* (2013) 'Differential expression of genes that encode glycolysis enzymes in kidney and lung cancer in humans', *Russian Journal of Genetics*, 49, pp. 707–716. doi: 10.1134/S1022795413050104.

Parks, D. H., Imelfort, M., Skennerton, C. T., Hugenholtz, P., *et al.* (2015) 'CheckM: Assessing the quality of microbial genomes recovered from isolates, single cells, and metagenomes', *Genome Research*, 25, pp. 1043–1055. doi: 10.1101/gr.186072.114.

Pedruzzi, I., Rivoire, C., Auchincloss, A. H., Coudert, E., *et al.* (2015) 'HAMAP in 2015: Updates to the protein family classification and annotation system', *Nucleic Acids Research*, 43, pp. D1064–D1070. doi: 10.1093/nar/gku1002.

Petersen, J. M. and Dubilier, N. (2009) 'Methanotrophic symbioses in marine invertebrates', *Environmental Microbiology Reports*, 1, pp. 319–335. doi: 10.1111/j.1758-2229.2009.00081.x.

Piovesan, D., Tabaro, F., Paladin, L., Necci, M., *et al.* (2018) 'MobiDB 3.0: More annotations for intrinsic disorder, conformational diversity and interactions in proteins', *Nucleic Acids Research*, 46, pp. D471–D476. doi: 10.1093/nar/gkx1071.

Ponnudurai, R., Kleiner, M., Sayavedra, L., Petersen, J. M., *et al.* (2017) 'Metabolic and physiological interdependencies in the *Bathymodiolus azoricus* symbiosis', *ISME Journal*, 11, pp. 463–477. doi: 10.1038/ismej.2016.124.

Quinn, T. P., Richardson, M. F., Lovell, D. and Crowley, T. M. (2017) 'Propr: An R-package for Identifying Proportionally Abundant Features Using Compositional Data Analysis', *Scientific Reports*, 7. doi: 10.1038/s41598-017-16520-0.

Riekenberg, P. M., Carney, R. S. and Fry, B. (2016) 'Trophic plasticity of the methanotrophic mussel *Bathymodiolus childressi* in the Gulf of Mexico', *Marine Ecology Progress Series*, 547, pp. 91–106. doi: 10.3354/meps11645.

Riquelme, S. A., Liimatta, K., Wong Fok Lung, T., Fields, B., *et al.* (2020) '*Pseudomonas aeruginosa* Utilizes Host-Derived Itaconate to Redirect Its Metabolism to Promote Biofilm Formation', *Cell Metabolism*, 31, pp. 1091-1106.e6. doi: 10.1016/j.cmet.2020.04.017.

Rognes, T., Flouri, T., Nichols, B., Quince, C., *et al.* (2016) 'VSEARCH: A versatile open source tool for metagenomics', *PeerJ*, 2016, pp. 1–22. doi: 10.7717/peerj.2584.

Rotty, J. D., Brighton, H. E., Craig, S. L., Asokan, S. B., *et al.* (2017) 'Arp2/3 Complex Is Required for Macrophage Integrin Functions but Is Dispensable for FcR Phagocytosis and In Vivo Motility', *Developmental Cell*, 42, pp. 498-513.e6. doi: 10.1016/j.devcel.2017.08.003.

Russell, D. G., Huang, L. and VanderVen, B. C. (2019) 'Immunometabolism at the interface between macrophages and pathogens', *Nature Reviews Immunology*, 19, pp. 291–304. doi: 10.1038/s41577-019-0124-9.

Sauvanet, C., Wayt, J., Pelaseyed, T. and Bretscher, A. (2015) 'Structure, Regulation, and Functional Diversity of Microvilli on the Apical Domain of Epithelial Cells', *Annual Review of Cell and Developmental Biology*, 31, pp. 593–621. doi: 10.1146/annurev-cellbio-100814-125234.

Schindelin, J., Arganda-Carreras, I., Frise, E., Kaynig, V., *et al.* (2012) 'Fiji: an open-source platform for biological-image analysis', *Nature Methods*, 9, pp. 676–682. doi: 10.1038/nmeth.2019.

Servant, F., Bru, C., Carrère, S., Courcelle, E., *et al.* (2002) 'ProDom: automated clustering of homologous domains.', *Briefings in bioinformatics*, 3, pp. 246–251. doi: 10.1093/bib/3.3.246.

Shannon, P., Markiel, A., Ozier, O., Baliga, N. S., *et al.* (2003) 'Cytoscape: A Software Environment for Integrated Models', *Genome Research*, 13, pp. 2498–2504. doi: 10.1101/gr.1239303.metabolite.

Shifrin, D. A., Crawley, S. W., Grega-Larson, N. E. and Tyska, M. J. (2014) 'Dynamics of brush border remodeling induced by enteropathogenic E. coli', *Gut Microbes*, 5, pp. 504–516. doi: 10.4161/gmic.32084.

Sigrist, C. J. A., De Castro, E., Cerutti, L., Cuche, B. A., *et al.* (2013) 'New and continuing developments at PROSITE', *Nucleic Acids Research*, 41, pp. 344–347. doi: 10.1093/nar/gks1067.

Simão, F. A., Waterhouse, R. M., Ioannidis, P., Kriventseva, E. V., *et al.* (2015) 'BUSCO: Assessing genome assembly and annotation completeness with single-copy orthologs', *Bioinformatics*, 31, pp. 3210–3212. doi: 10.1093/bioinformatics/btv351.

Stoecker, K., Dorninger, C., Daims, H. and Wagner, M. (2010) 'Double Labeling of Oligonucleotide Probes for Fluorescence In Situ Hybridization (DOPE-FISH) Improves Signal Intensity and Increases rRNA Accessibility', *Applied and Environmental Microbiology*, 76, pp. 922 LP – 926. doi: 10.1128/AEM.02456-09.

Streams, M. E., Fisher, C. R. and Fiala-Médioni, A. (1997) 'Methanotrophic symbiont location and fate of carbon incorporated from methane in a hydrocarbon seep mussel', *Marine Biology*, 129, pp. 465–476. doi: 10.1007/s002270050187.

Sun, P., Sleat, D. E., Lecocq, M., Hayman, A. R., *et al.* (2008) 'Acid phosphatase 5 is responsible for removing the mannose 6-phosphate recognition marker from lysosomal proteins', *Proceedings of the National Academy of Sciences of the United States of America*, 105, pp. 16590–16595. doi: 10.1073/pnas.0807472105.

Tame, A., Yoshida, T., Ohishi, K. and Maruyama, T. (2015) 'Phagocytic activities of hemocytes from the deep-sea symbiotic mussels *Bathymodiolus japonicus* , *B . platifron*s , and *B . septemdierum'*, *Fish and Shellfish Immunology*, 45, pp. 146–156. doi: 10.1016/j.fsi.2015.03.020.

Tannahill, G. M., Curtis, A. M., Adamik, J., Palsson-Mcdermott, E. M., *et al.* (2013) 'Succinate is an inflammatory signal that induces IL-1β through HIF-1α', *Nature*, 496, pp. 238–242. doi: 10.1038/nature11986.

Tavormina, P. L., Hatzenpichler, R., McGlynn, S., Chadwick, G., *et al.* (2015) '*Methyloprofundus sedimenti* gen. nov., sp. nov., an obligate methanotroph from ocean sediment belonging to the "deep

sea-1" clade of marine methanotrophs', *International Journal of Systematic and Evolutionary Microbiology*, 65, pp. 251–259. doi: 10.1099/ijs.0.062927-0.

Tavormina, P. L., Kellermann, M. Y., Antony, C. P., Tocheva, E. I., *et al.* (2017) 'Starvation and recovery in the deep-sea methanotroph *Methyloprofundus sedimenti*', *Molecular Microbiology*, 103, pp. 242–252. doi: 10.1111/mmi.13553.

Thubaut, J., Puillandre, N., Faure, B., Cruaud, C., *et al.* (2013) 'The contrasted evolutionary fates of deep-sea chemosynthetic mussels (Bivalvia, Bathymodiolinae)', *Ecology and Evolution*, 3, pp. 4748–4766. doi: 10.1002/ece3.749.

Walkley, S. U. (1998) 'Cellular pathology of lysosomal storage disorders', *Brain Pathology*, 8, pp. 175–193. doi: 10.1111/j.1750-3639.1998.tb00144.x.

Wentrup, C., Wendeberg, A., Schimak, M., Borowski, C., *et al.* (2014) 'Forever competent: Deep-sea bivalves are colonized by their chemosynthetic symbionts throughout their lifetime', *Environmental Microbiology*, 16, pp. 3699–3713. doi: 10.1111/1462-2920.12597.

Wick, R. R., Schultz, M. B., Zobel, J. and Holt, K. E. (2015) 'Bandage: Interactive visualization of de novo genome assemblies', *Bioinformatics*, 31, pp. 3350–3352. doi: 10.1093/bioinformatics/btv383.

Williams, N. C. and O'Neill, L. A. J. (2018) 'A role for the krebs cycle intermediate citrate in metabolic reprogramming in innate immunity and inflammation', *Frontiers in Immunology*, 9, pp. 1–11. doi: 10.3389/fimmu.2018.00141.

Wu, C. H., Nikolskaya, A., Huang, H., Yeh, L. S. L., *et al.* (2004) 'PIRSF: family classification system at the Protein Information Resource', *Nucleic Acids Research*, 32, pp. 112D – 114. doi: 10.1093/nar/gkh097.

Xu, T., Feng, D., Tao, J. and Qiu, J. W. (2019) 'A new species of deep-sea mussel (Bivalvia: Mytilidae: Gigantidas) from the South China Sea: Morphology, phylogenetic position, and gill-associated microbes', *Deep-Sea Research Part I: Oceanographic Research Papers*, 146, pp. 79–90. doi: 10.1016/j.dsr.2019.03.001.

Yang, H. S., Hong, H. K., Donaghy, L., Noh, C. H., *et al.* (2015) 'Morphology and Immune-related activities of hemocytes of the mussel *Mytilus coruscus* (Gould, 1861) from East Sea of Korea', *Ocean Science Journal*, 50, pp. 77–85. doi: 10.1007/s12601-015-0006-4.

Young, T., Kesarcodi-Watson, A., Alfaro, A. C., Merien, F., *et al.* (2017) 'Differential expression of novel metabolic and immunological biomarkers in oysters challenged with a virulent strain of OsHV-1', *Developmental and Comparative Immunology*, 73, pp. 229–245. doi: 10.1016/j.dci.2017.03.025.

Yu, J., Wang, M., Liu, B., Yue, X., *et al.* (2019) 'Gill symbionts of the cold-seep mussel *Bathymodiolus platifrons*: Composition, environmental dependency and immune control', *Fish and Shellfish Immunology*, 86, pp. 246–252. doi: 10.1016/j.fsi.2018.11.041.

Zheng, P., Wang, M., Li, C., Sun, X., *et al.* (2017) 'Insights into deep-sea adaptations and host – symbiont interactions : A comparative transcriptome study on *Bathymodiolus* mussels and their coastal relatives', pp. 5133–5148. doi: 10.1111/mec.14160.

Chapter III: Supplementary Tables and Figures

All Supplementary Tables of this chapter are deposited on the provided CD-ROM.

Supplementary Figures

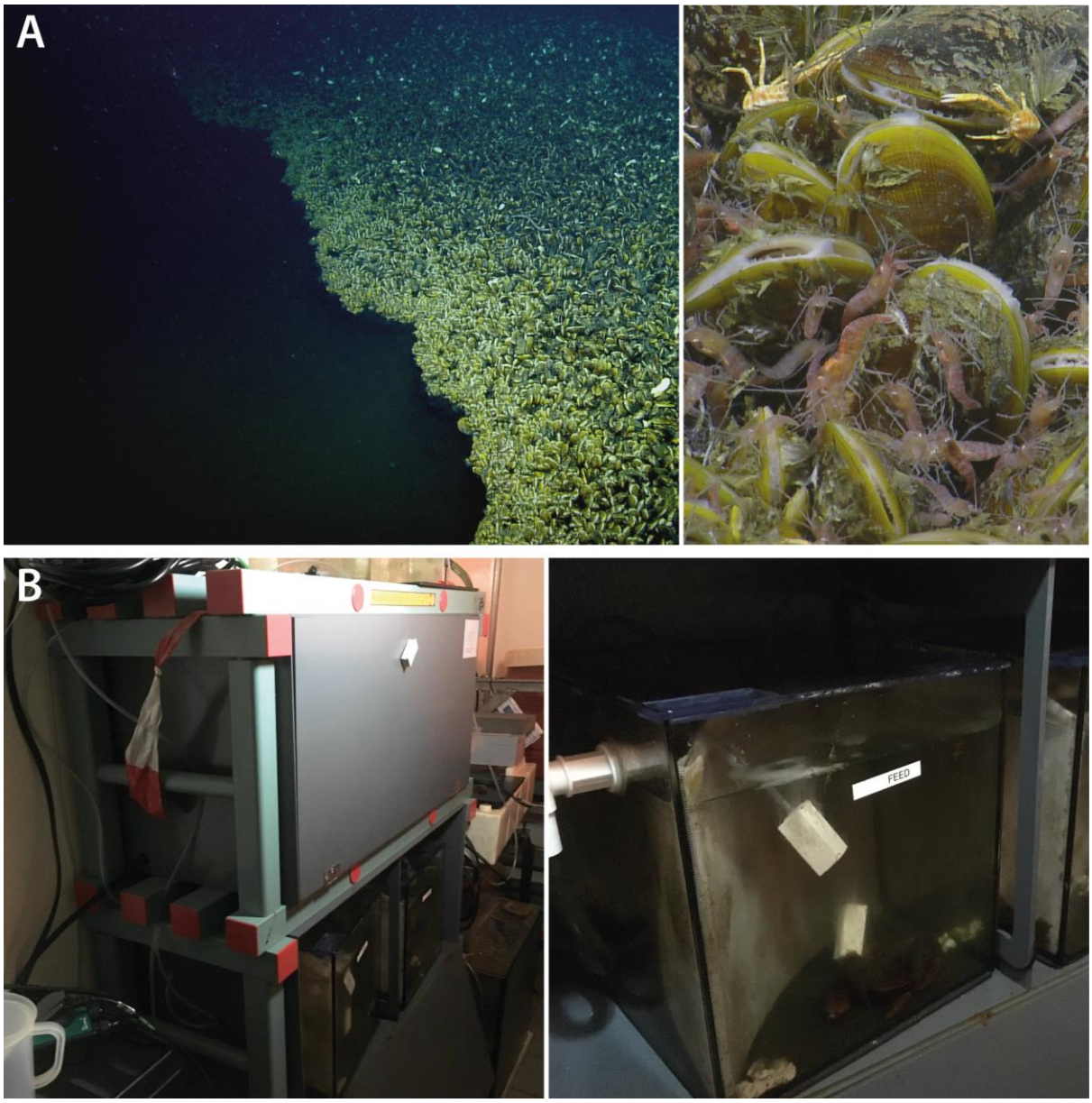

Supplementary Figure 1: Sampling site of *B. childressi* mussels and aquarium husbandry. ***A:*** *Bathymodiolus childressi* in a mussel bed next to a brine pool at the cold seep site Green Canyon 233 in the Northern Gulf of Mexico. Mussels form dense clumps around the brine pool and provide a habitat for other animals including shrimps and crabs. ©Ocean Exploration Trust. ***B:*** *B. childressi* husbandry and experimental setup for aquarium starvation experiment conducted in Kiel, Germany.

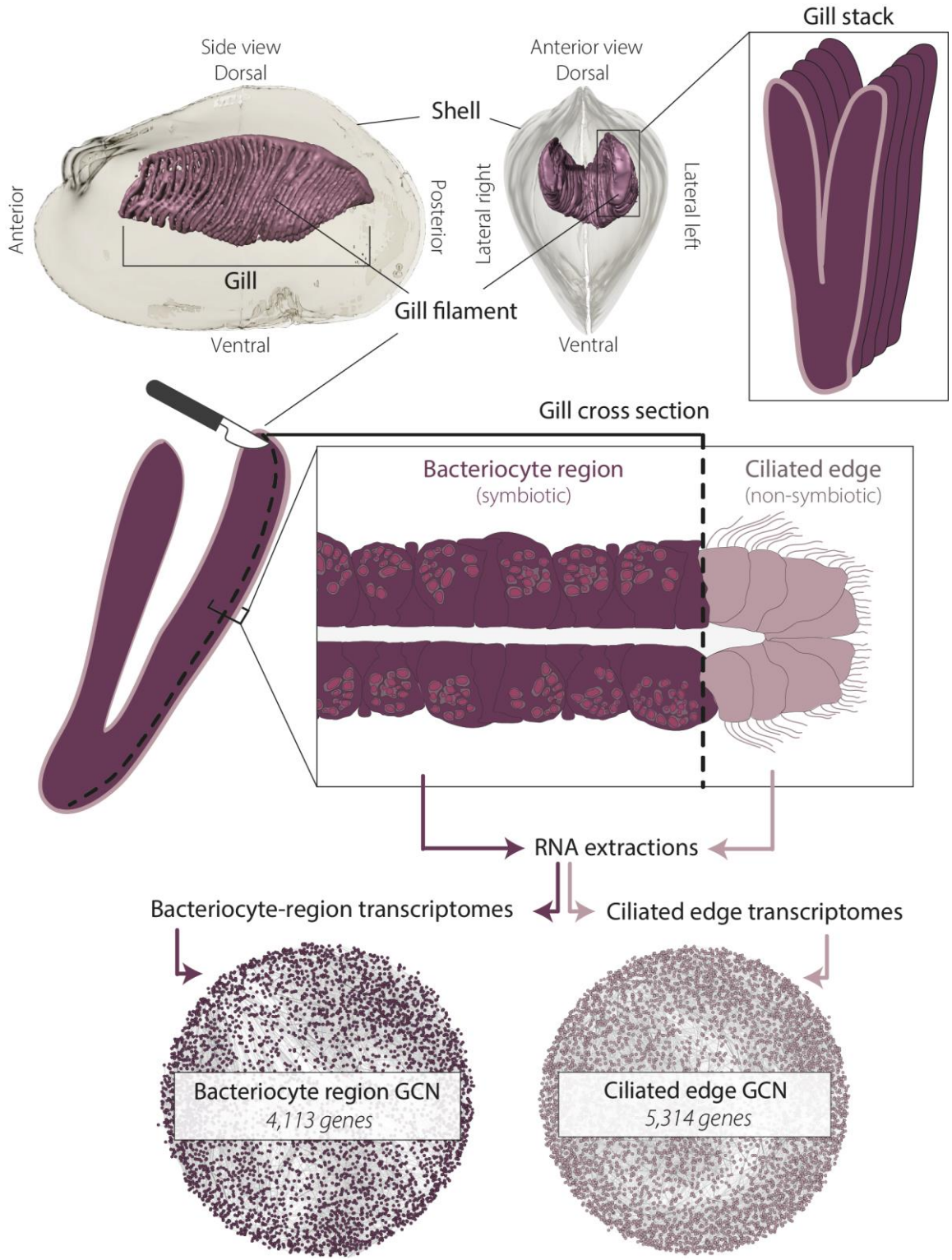

Supplementary Figure 2: Dissection strategy for obtaining gill region specific GCNs. Diagram showing the morphology of *B. childressi* with emphasis on the gills. For obtaining gill region specific GCNs, gill filaments from mussels of all three symbiont states were dissected to separate the symbiont-containing bacteriocyte region from the ciliated edge. For each symbiont state, five mussel gills from different specimens were dissected. RNA was extracted from both regions of the same gills separately. The extracted RNA was sequenced resulting in transcriptomes of each gill region. The transcriptomes were then used to generate the gill region specific GCNs.

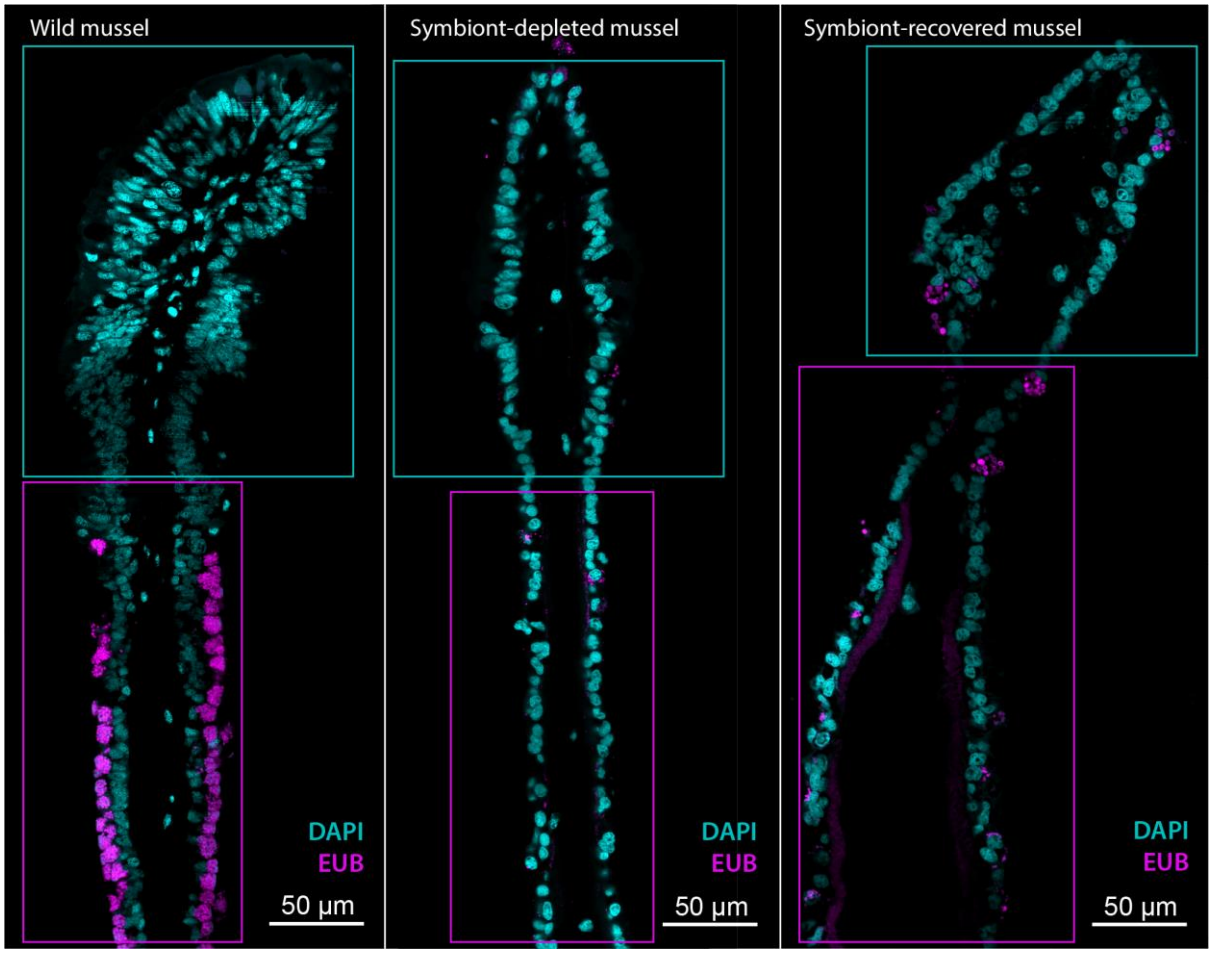

Supplementary Figure 3: Symbiont abundances in gills of the three symbiont-states in *Bathymodiolus childressi*. Fluorescence *in situ* hybridisation images of gill cross sections show symbiont abundances in gills filaments. Symbionts are stained with EUB I-III probe (magenta), host nuclei are stained with DAPI (cyan). Cyan boxes indicate ciliated edge region, magenta boxes indicate bacteriocyte regions of the mussel gills.

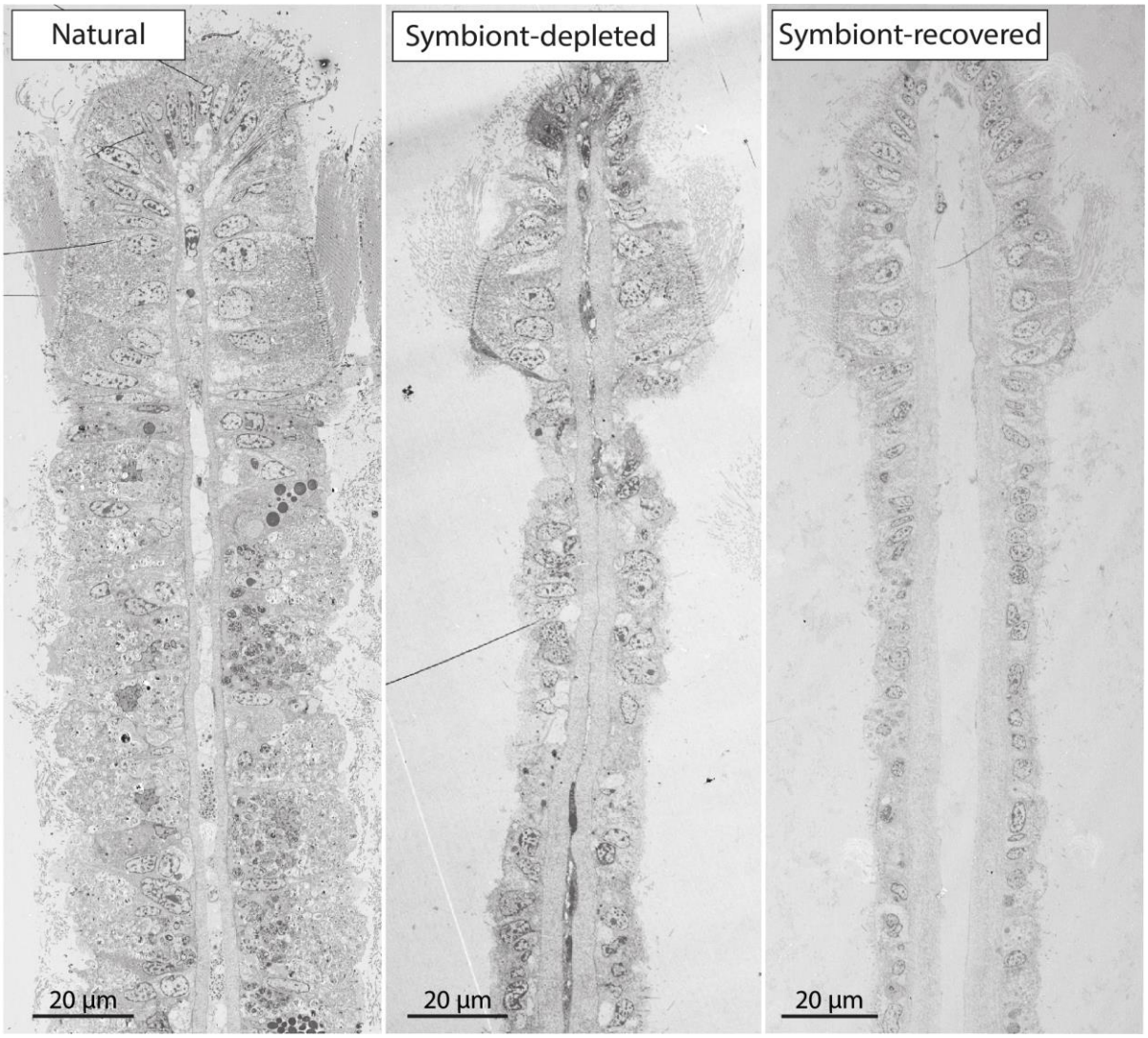

Supplementary Figure 4: Symbiont abundances in gills of the three symbiont-states in *Bathymodiolus childressi*. Transmission electron microscopy images of gill cross sections show symbiont abundances in gills filaments. Cell biomass of wild gills is visibly higher compared to symbiont-depleted and symbiont-recovered gills.

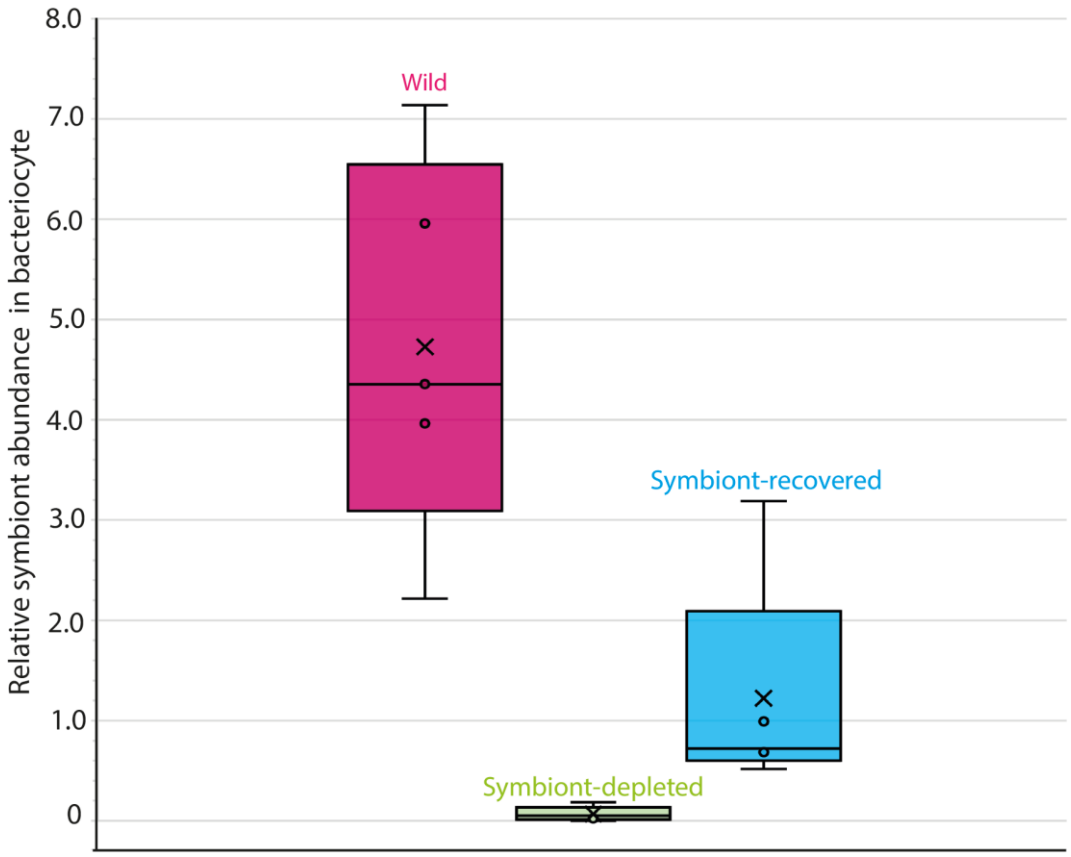

Supplementary Figure 5: Relative symbiont abundance in metagenome libraries from all three symbiont states. Abundances based on ratio between symbiont 16S rRNA gene read counts and host 18S rRNA gene read counts obtained from the metagenomes using phyloFlash. Counts were normalised to library size. Boxplot shows ranges of symbiont abundance and includes replicates (n=5) of bacteriocyte gill samples from wild mussels (red box), symbiont-depleted mussels (green box) and symbiont-recovered mussels (blue box). Medians are indicated by line, means by crosses.

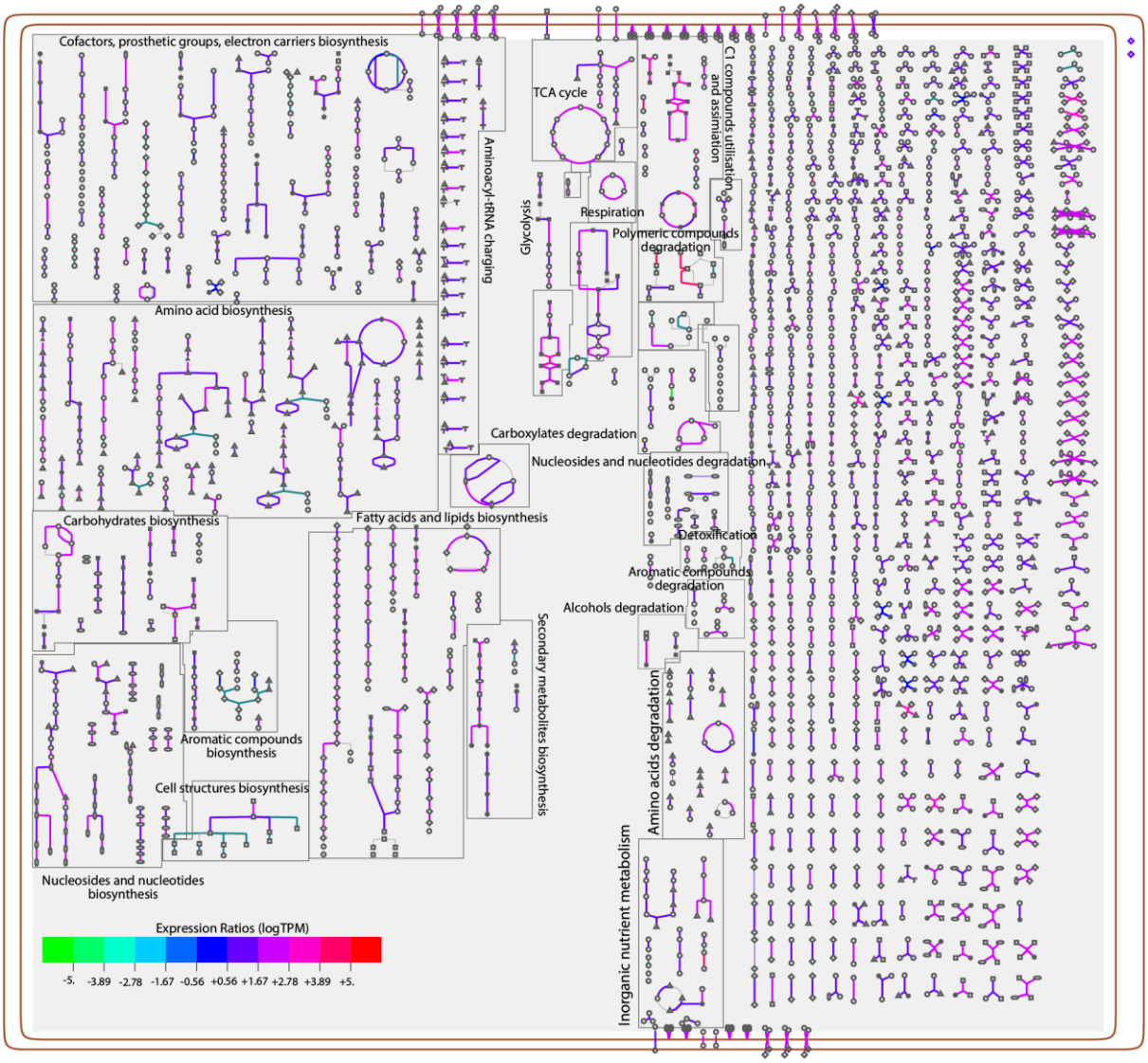

Supplementary Figure 6: Cellular overview of the *B. childressi* symbiont from wild symbiont states. This overview was generated with Pathway Tools v22.0 based on the metagenome-assembled genome and the transcriptome data of symbionts from wild mussels (logTPMs). The most expressed genes were within the C1 compounds utilisation and assimilation pathway (highest = particulate methane monoxygenase for methane oxidation), and polymeric compounds degradation.

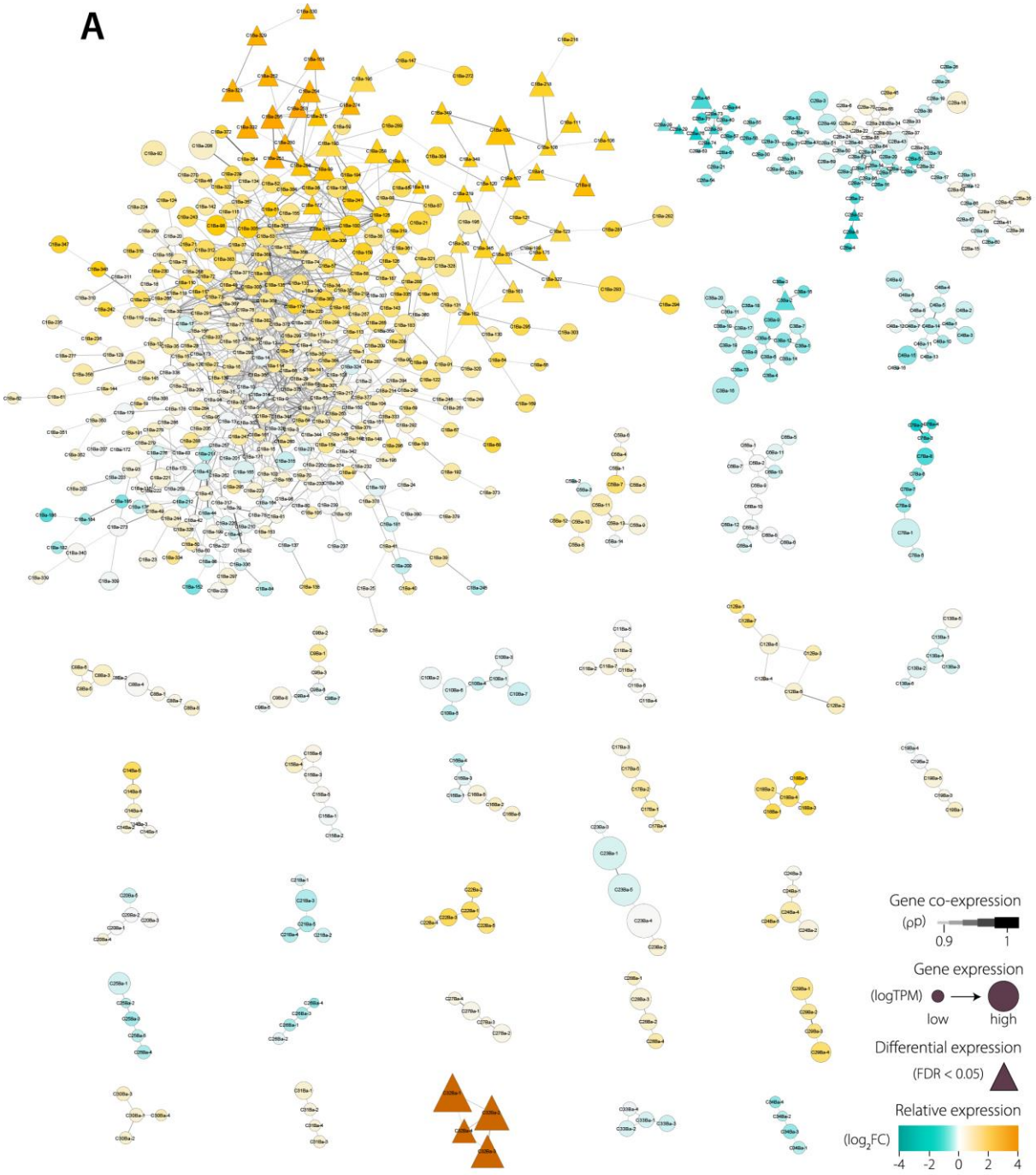

Supplementary Figure 7A: Main clusters of bacteriocyte-specific GCN. GCN was generated with Cytoscape v3.8.0 (yFiles organic layout) overlaid with data from i) expression of genes in wild mussels (node size) ii) relative expression of genes between wild and symbiont-depleted mussels (node colour), and iii) differential gene expression analyses between wild and symbiont-depleted mussels (node shape). Unique node labels correspond to gene identifiers listed in Supplementary Table 3.

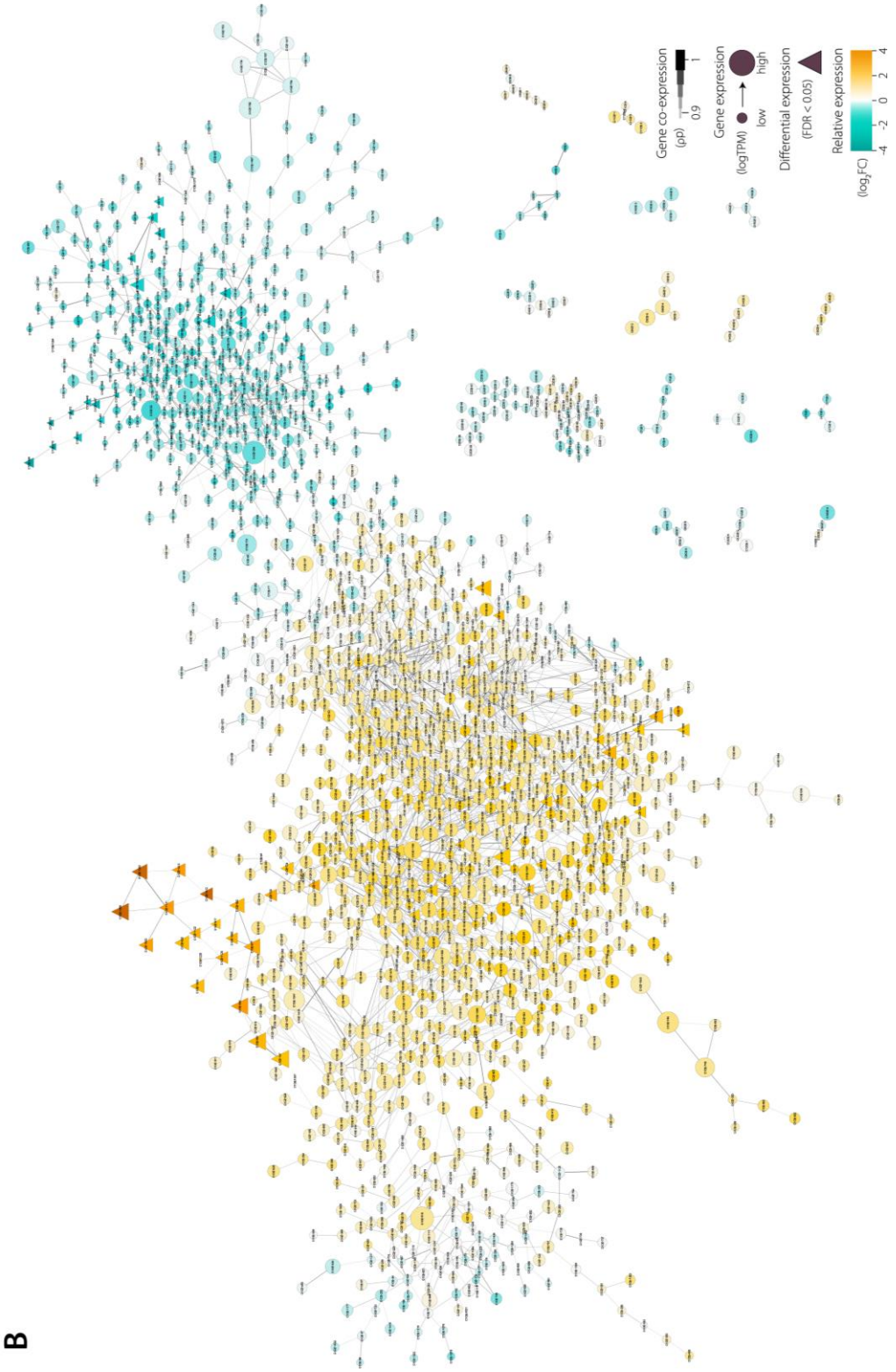

Supplementary Figure 7B: Main clusters of ciliated edge specific GCN. GCN was generated with Cytoscape v3.8.0 (yFiles organic layout) overlaid with data from i) expression of genes in wild mussels (node size) ii) relative expression of genes between wild and symbiont-depleted mussels (node colour), and iii) differential gene expression analyses between wild and symbiont-depleted mussels (node shape). Unique node labels correspond to gene identifiers listed in Supplementary Table 3.

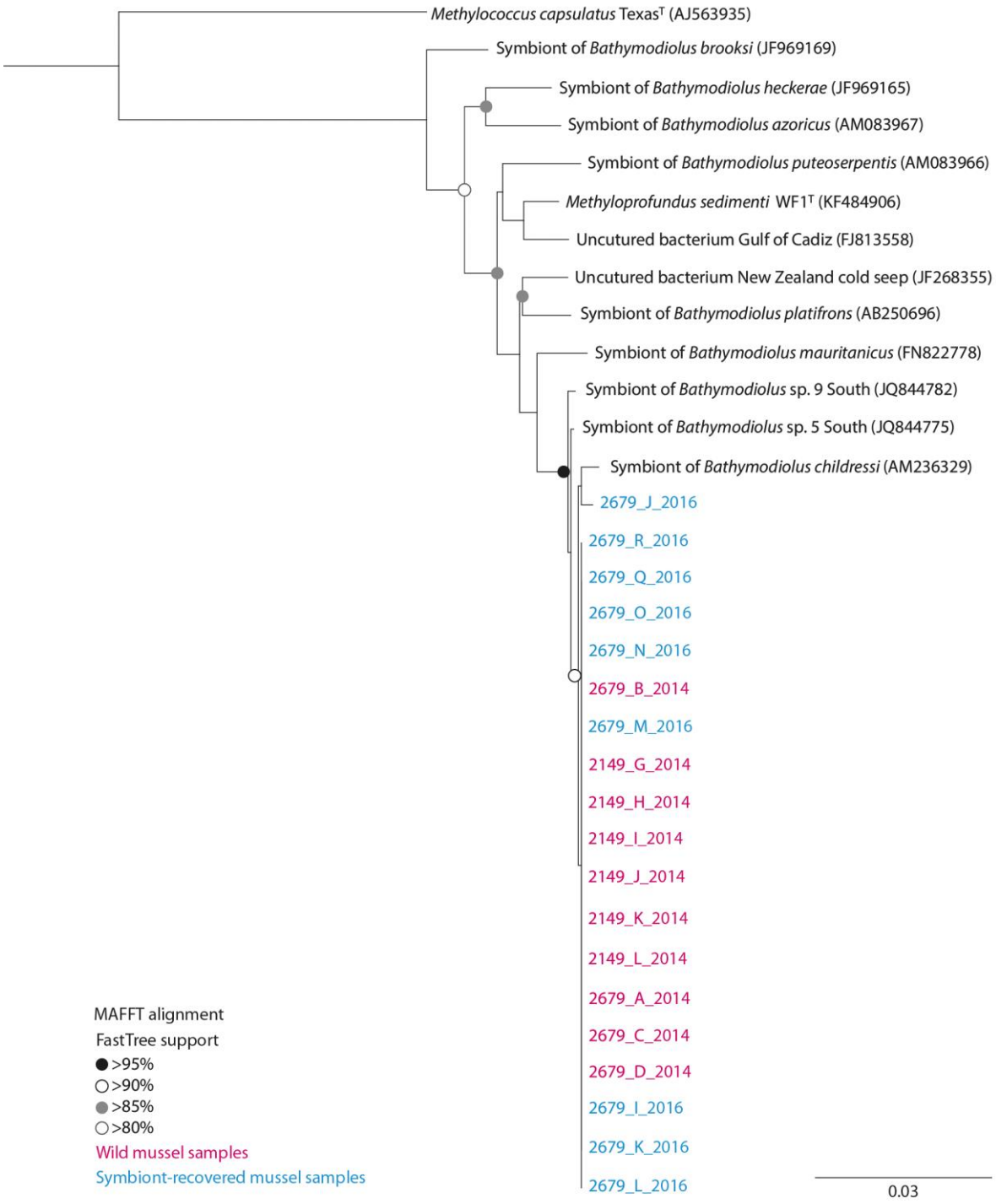

Supplementary Figure 8: 16S rRNA gene phylogeny of the methane-oxidising symbiont from wild and symbiont-recovered mussels. 16S rRNA gene sequences of *B. childressi* symbionts from bacteriocyte samples were assembled with phyloFlash from metagenomes and aligned with 16S rRNA gene sequences of other bathymodiolin mussels alongside their closest free-living relative *Methyloprofundus sedimenti*. The type species of the *Methylococcaceae, Methylococcus capsulatus,* was used as outgroup. Accession numbers of NCBI-obtained sequences indicated in brackets, type strains highlighted by superscript T. Symbionts of wild mussels are coloured in pink, symbionts of symbiont-recovered mussels are coloured in blue. No 16S rRNA gene sequences could be assembled for symbiont-depleted mussels.

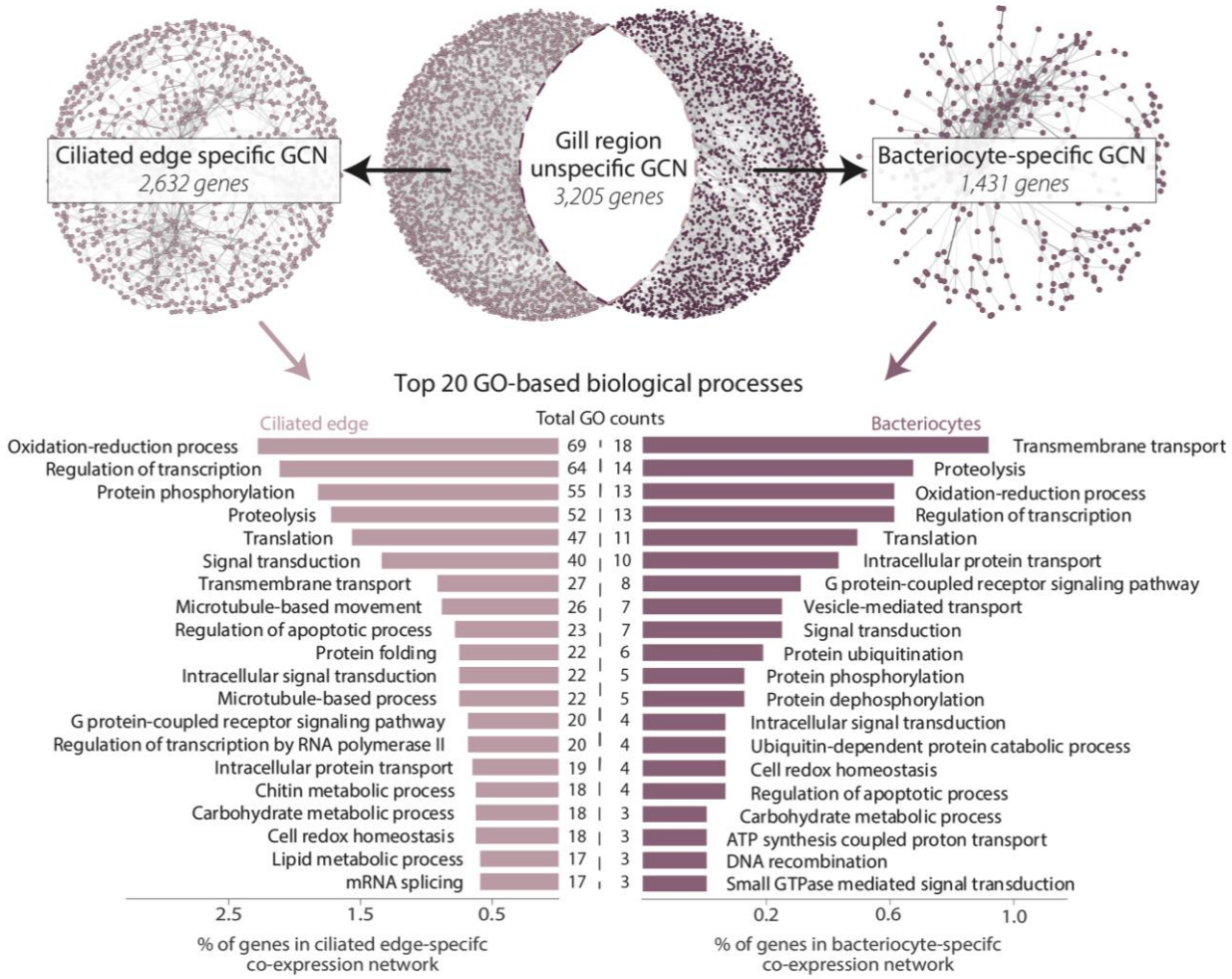

Supplementary Figure 9: Ontologies of genes in the gill region specific co-expression networks. Bar chart shows most abundant gene ontologies (GOs) of biological processes (level 3) in the ciliated edge and bacteriocyte-specific GCNs. More GOs could be attributed to genes in the ciliated edge GCN. GOs were assigned using Blast2GO.

Chapter III: Appendix

"We'll shall hear more about lysozyme." - Alexander Fleming

With his discovery of the lysozyme in 1921, Alexander Fleming has fundamentally contributed to current research (Fleming, 1922; Callewaert and Michiels, 2010). Although lysozymes have been neglected for several decades, they now are considered as key players in animal immunity conserved across the animal kingdom (Ragland and Criss, 2017). In symbiosis research, lysozymes have gained particular interest, and have been associated with regulatory symbiont population control through lysosomal break-down of symbiont cells. For example in the aphid-Buchnera symbiosis, lysozymes were highly expressed in bacteriocytes, the host cells that contain the symbiotic bacteria (Simonet *et al.*, 2018). Similarly, lysozymes have also been proposed to play a key role in controlling symbiont populations in the gills of *Bathymodiolus* mussels (Zheng *et al.*, 2017). In *B. azoricus*, multiple lysozyme isoforms were found to be associated with changing symbiont abundances (Detree *et al.*, 2016).

Using aquarium setups, we were able to keep *B. childressi* mussels over several years and induced changes of symbiont abundances by exposing the mussels to different methane concentrations (see Chapter III Materials & Methods for details on experimental setup). We wanted to investigate the expression changes of lysozyme isoforms comparing wild and symbiont-depleted mussels. We also aimed to resolve in which region of the gills these lysozymes were expressed because previous studies only identified them in whole mussel gill homogenates (Detree *et al.*, 2016). For this, we analysed the lysozyme expression in the bacteriocyte region and the ciliated edge of the same mussel gill filaments.

All transcript isoforms annotated as "lysozyme", "glycoside hydrolase" or "1,4-beta-N-acetylmuramidase" were selected from the *de novo* assembled host transcriptome. We found 29 lysozyme isoforms that all shared highest identity with sequences from the oyster *Crassostrea gigas* in the UniProt database. We obtained the amino acid sequence of each

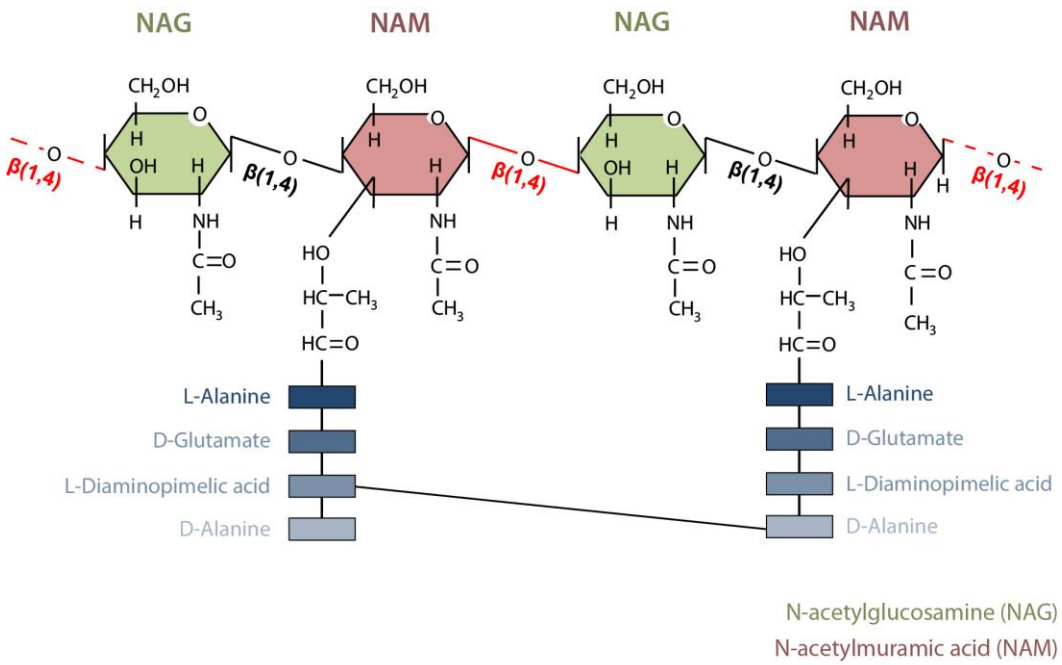

Figure 1: Site of cleavage by lysozymes in the bacterial cell wall peptidoglycan. Lysozymes bind with their catalytic cleft at the NAM-NAG position of the peptidoglycan and hydrolyse the β-1,4-link between the two sugars. Adapted from Callewaert and Michiels (2010).

isoform and aligned them with other lysozymes in the databases. To characterise the lysozyme-type, a preliminary amino acid tree was constructed (Figure 2), and indicated that all *B. childressi* gill lysozyme isoforms resembled invertebrate-type lysozymes. To determine whether *B. childressi* lysozyme isoforms contained the characteristic catalytic cleft of lysozymes (Glu-Asp), we also modelled the 3D structure of two selected lysozymes of our dataset (highlighted in bold in tree of Figure 2) with Phyre 2 and Chimera (Pettersen *et al.*, 2004; Kelley *et al.*, 2015), and revealed that these lysozymes might be functional (Figure 3).

Surprisingly, lysozyme expression was not correlated with symbiont abundance in bacteriocytes of the analysed *B. childressi* dataset. In fact, lysozymes were constitutively expressed in host transcriptomes at similar levels, regardless of the gill region. We hypothesise that lysozymes do not play the key role for maintaining symbiont populations in bacteriocytes of *Bathymodiolus* hosts, which contrasts results of other studies. This suggests that the expression of lysozymes in *B. childressi* gills is not symbiosis-specific but rather part of general digestion processes and of the innate immune system of cells from both gill regions.

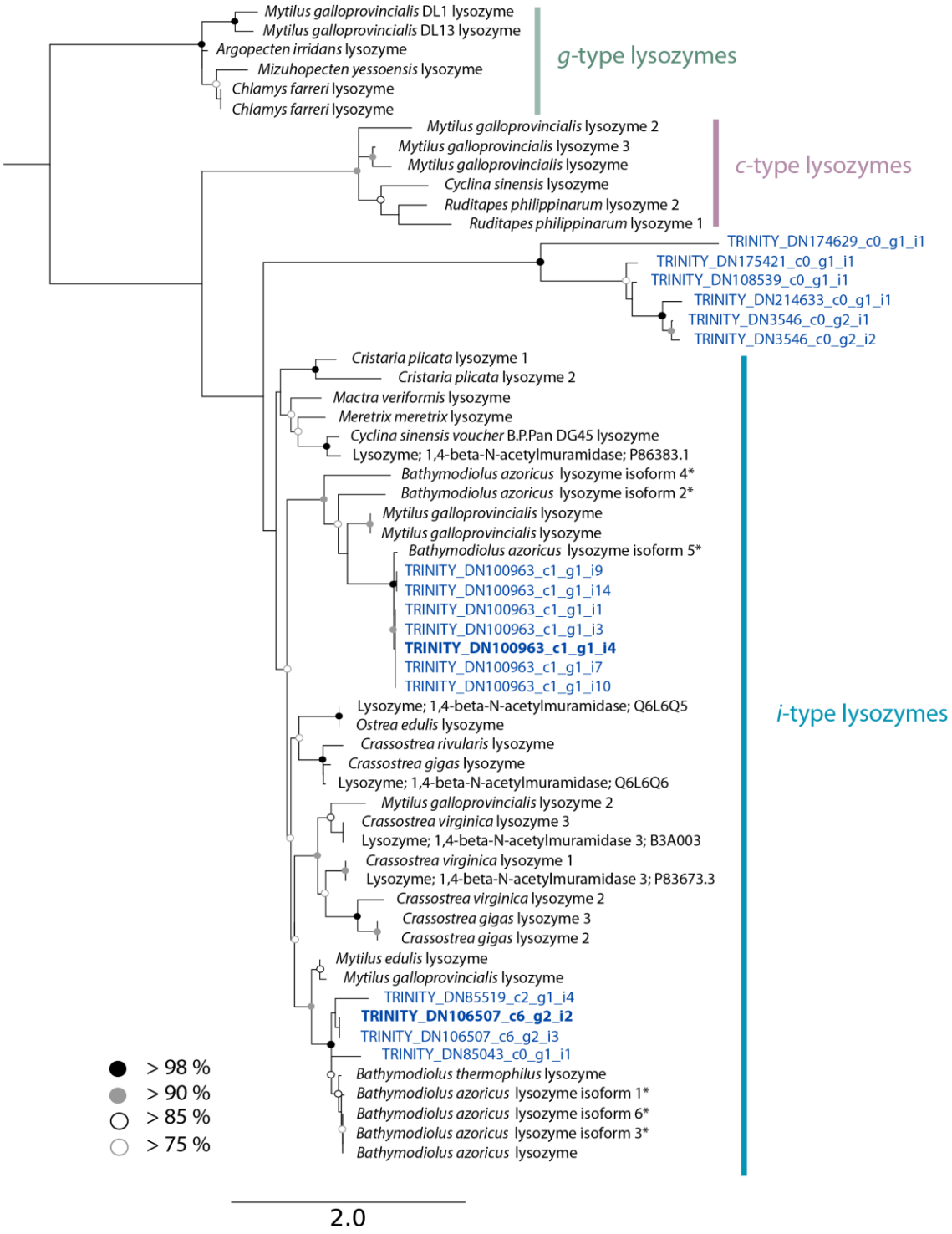

Figure 2: Amino acid tree of lysozyme isoforms expressed in gills of *B. childressi*. The sequences were aligned with MAFFT BLOSUM 80 multiple alignment v1.4.0 and a tree was calculated using FastTree v2.1.12. *B. childressi* sequences are highlighted in blue.

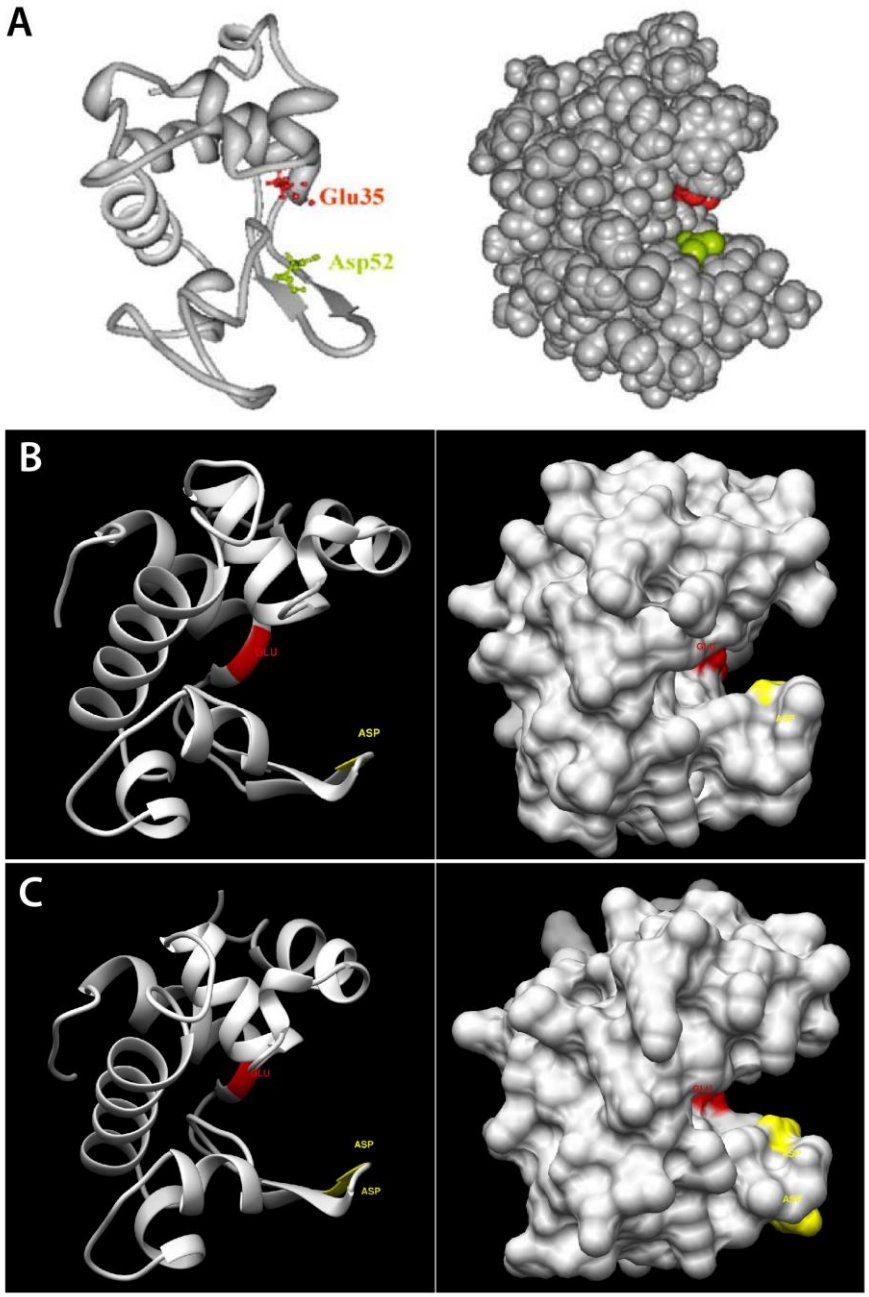

Figure 3: Ribbon and surface structures of lysozyme protein models in *B. childressi*. ***A:*** Protein models show the Glu (red) and Asp (yellow) residues that form the catalytic cleft of the lysozyme. Protein models are based on hen egg-white lysozyme in ***A*** (taken from Callewaert and Michiels; 2010), and from the *B. childressi* gill transcriptome assembly (***B,C***). Proteins models in ***B*** and ***C*** were generated with Phyre2 and Chimera v1.13.

Appendix References

Callewaert, L. and Michiels, C. W. (2010) 'Lysozymes in the animal kingdom', *Journal of Biosciences*, 35(1), pp. 127–160. doi: 10.1007/s12038-010-0015-5.

Detree, C. *et al.* (2016) 'Multiple I-type lysozymes in the hydrothermal vent mussel *Bathymodiolus azoricus* and their role in symbiotic plasticity', *PLoS ONE*, 11(2), pp. 1–19. doi: 10.1371/journal.pone.0148988.

Fleming, A. (1922) 'On a remarkable bacteriolytic element found in tissues and secretions', *Proceedings of the Royal Society B*, 93(9), pp. 306–317.

Kelley, L. A. *et al.* (2015) 'The Phyre2 we portal for protein modeling, prediction and analysis', *Nature Protocols*. Nature Publishing Group, 10(6), pp. 845–858. doi: 10.1038/nprot.2015-053.

Pettersen, E. F. *et al.* (2004) 'UCSF Chimera - A visualization system for exploratory research and analysis', *Journal of Computational Chemistry*, 25(13), pp. 1605–1612. doi: 10.1002/jcc.20084.

Ragland, S. A. and Criss, A. K. (2017) 'From bacterial killing to immune modulation: Recent insights into the functions of lysozyme', *PLoS Pathogens*, 13(9), pp. 1–22. doi: 10.1371/journal.ppat.1006512.

Simonet, P. *et al.* (2018) 'Bacteriocyte cell death in the pea aphid/*Buchnera* symbiotic system', *Proceedings of the National Academy of Sciences*, 115(8), pp. E1819–E1828. doi: 10.1073/pnas.1720237115.

Zheng, P. *et al.* (2017) 'Insights into deep-sea adaptations and host – symbiont interactions : A comparative transcriptome study on *Bathymodiolus* mussels and their coastal relatives', (February), pp. 5133–5148. doi: 10.1111/mec.14160.

Chapter IV

Deep-sea *Bathymodiolus* mussels are resistant to short-term limitations of hydrothermal access

Målin Tietjen[1,2], Christian Borowski[1,2], Nicole Dubilier[1,2] and Harald Gruber-Vodicka[1]

[1]Max Planck Institute for Marine Microbiology, Bremen, Germany

[2]MARUM – Center for Marine Environmental Sciences of the University of Bremen, Germany

Author contributions: *ND, CB, HRGV and MT designed the study, ND and CB coordinated sampling strategy and processed samples on board, MT performed nucleotide extractions, MT and HRGV conceived data analyses, MT performed analyses and wrote the manuscript draft.*

This manuscript (in short communication style) is in preparation and has not been reviewed by all authors.

Abstract

The symbiotic deep-sea mussels of the genus *Bathymodiolus* thrive at hydrothermal vents, where dynamically changing physico-chemical conditions shape the ecosystem. Studying the adaptations of host and symbionts to these fluctuating conditions is challenging because replicating such conditions in the laboratory is almost impossible. We conducted an *in situ* displacement experiment with *B. puteoserpentis* mussels to investigate how the physiology of host and symbionts is affected by limited access to hydrothermal vent fluids. Our results showed that the physiology of the mussel host in the symbiotic gill tissue and the non-symbiotic foot tissues remained largely unaffected, while the symbionts showed a strong physiological response to the environmental conditions at the displacement site. We conclude that deep-sea bathymodiolin mussels are well adapted to cope with short-term fluctuations of environmental conditions, which likely explains their successful colonisation of extreme habitats including hydrothermal vents.

Introduction

Deep-sea *Bathymodiolus* mussels form dense mussel beds at hydrothermal vents along the Mid-Atlantic Ridge (Ponnudurai *et al.*, 2017). In these habitats, *Bathymodiolus* mussels thrive off the biomass produced by chemosynthetic bacteria contained in their gills (Duperron *et al.*, 2016). The symbionts use methane and sulphur compounds from the vent fluids to fuel chemosynthesis (Ponnudurai *et al.*, 2017).

At hydrothermal vents, multiple physical and chemical factors can influence the physiology of organisms. In particular, short-term limitations of chemical energy for the symbionts is expected to occur frequently in these ecosystems due to dynamic mixing of oxygenated seawater with hydrothermal fluids (Seston *et al.*, 2016). Because the natural environmental conditions are not easily simulated in the laboratory, *in situ* experiment can support our understanding of the adaptations of the symbioses to interruptions of the energy source in the symbiosis. In *in situ* experiments with *Bathymodiolus* spp., mussels were translocated from their original mussel bed with hydrothermal fluids access, and re-collected after several days. One of the first translocation experiments was conducted in 1985 with *B. thermophilus* from a hydrothermal vent at the Galapagos Rift (Smith, 1985). Since then, *in situ* experiments with *B. azoricus* revealed major depletion of symbiont populations after few days of displacement (Détrée *et al.*, 2019).

The aim of this experiment was to investigate the effect of limited access to hydrothermal fluids on the gene expression of the symbiotic partners. Because of constraints with symbiont mRNA coverages, we primarily report the transcriptome changes for the mussel host throughout this manuscript. To simulate interruptions of hydrothermal access *in situ,* we removed mussels from their original mussel bed to a location without hydrothermal influence. We re-collected the mussels up to 10 days of displacement, and applied a dual RNA-seq approach to investigate transcriptome changes of symbionts and the host. Our results display the mussel host as sturdy organism that does not show signs of physiological stress induced by changing environmental conditions.

Materials & Methods

Sample collection and experimental setup

We wanted reveal the effects of limited access to hydrothermal fluids on the *Bathymodiolus puteoserpentis* symbiosis. For this, we collected mussels in several mesh cages from the Ash Lighthouse mussel bed of the hydrothermal vent field Semenov-2 (13°30'48.5856"N, 44°57'46.872"W) in the Northern Mid-Atlantic Ridge. These mesh cages were displaced to a site without hydrothermal input, which was approximately 65 m away from the mussel bed (13°30'46.8468"N, 44°57'46.3788"W). We re-collected individual mesh cages from this site after 1, 2, 3, 5, 7, 8 and 10 days after the displacement (Supplementary Figure 1). Samples of day 0 and displacement day 1 and 2 have already been partially analysed in Tietjen, Borowski, *et al.* (2020), and can be identified as "is0", "dis24" and "dis48" samples in the referred study.

To obtain the natural physiological state of host and symbionts as day 0 control, we employed the In Depth Fixation Device (IDEFIX) to fix the nucleotides and proteins of host and symbionts directly at the mussel bed (details in Tietjen, Borowski, *et al.*, 2020). We also fixed mussels from displacement days 1, 2, and 3 with IDEFIX at the displacement site. Mussels from displacement days 5, 7, 8 and 10 were fixed on board approximately 2 hours after collection from the displacement site. The fixed mussels were then stored in individual bags at -80°C until dissection and extraction of nucleic acids and proteins in the laboratory in Bremen, Germany. Sampling details are summarised in Supplementary Table 1.

Specimen dissection and nucleotide extractions

For each displacement day, five mussels were selected for nucleotide extractions. The deep-frozen mussels were dissected quickly while thawing on an ice tray. Pieces of the symbiont-containing gills and the non-symbiotic foot were cut from the mussels. The tissue pieces were immediately placed into the buffering solution of the nucleotide extraction kit. Each sample was subjected to nucleic acid and protein extractions using the AllPrep® DNA/RNA/Protein Mini Kit (QIAGEN, Hilden, Germany) following the manufacturers guidelines with minor

amendments to the protocol: The RNA was incubated in 100 µl RNase-free water at room temperature for 10 min before elution to increase the RNA yield.

Metagenome sequencing and symbiont abundance estimates

DNA library preparation and sequencing were performed at the Max Planck Genome Center Cologne, Germany (https://mpgc.mpipz.mpg.de/home/). For estimating symbiont abundances in gill tissues of displaced mussels, we sequenced the total DNA libraries of gill tissues from the control and the displacement samples. Library preparation was done using the TruSeq DNA Library Prep kit (Illumina, USA) and Covaris DNA shearing protocol (Covaris, USA). Libraries were sequenced on a HiSeq3000 system (Illumina, USA) to a minimum depth of 7 million with 150 basepairs (bp) paired-end reads. The total DNA libraries were then analysed with phyloFlash (Gruber-Vodicka *et al.*, 2020) to quantify host and symbiont SSU reads, and to subsequently estimate relative symbiont abundance in mussel gills.

Transcriptome sequencing, host de novo transcriptome assembly and functional annotation

RNA library preparation and sequencing were performed at the Max Planck Genome Center Cologne, Germany (https://mpgc.mpipz.mpg.de/home/). For host transcriptomics, we sequenced the polyA-tail enriched RNA libraries of gill and foot tissues from the control and the displacement samples (all steps for library preparation summarised in Tietjen, Borowski *et al.,* 2020). PolyA RNA libraries were sequenced on HiSeq3000 system (Illumina, USA) to a minimum depth of 7 million reads as paired-end reads. All libraries were adaptor- and quality-trimmed (Q=2) using BBDuk v38.06 (http://sourceforge.net/projects/bbmap/).

To generate a host *de novo* transcriptome assembly, the polyA-tail enriched libraries were subjected to read normalisation with BBNorm v38.06 with a read kmer-coverage target of 80. We combined both gill and foot libraries to generate a *de novo* transcriptome assembly using Trinity v2.5.1 (Grabherr *et al.*, 2011). Assembly statistics and completeness were assessed

with utility scripts of the Trinity package v2.5.1 (Haas *et al.*, 2013) and BUSCO v3 using the metazoan database odb09 (accessed on 5th February 2019; Simão *et al.*, 2015). Redundant transcripts were removed by clustering the sequencing with minimum identity of 97% with VSEARCH (Rognes *et al.*, 2016). Contaminating reads (e.g. plants, fungi, bacteria) were filtered out with MEGAN6 v6.10.3 (Huson *et al.*, 2016) based on their taxonomic origin determined by the closest hits from NCBI blast v2.2.28 searches against nr (db version 20150811). The cleaned *B. puteoserpentis* transcriptome was annotated following the annotation pipeline of Trinotate v3.0.1 (https://github.com/Trinotate/Trinotate.github.io/; e.g. Bryant *et al.*, 2017). Additionally, InterProScan was run in Blast2GO v5.2.5 (Conesa *et al.*, 2005) using all databases listed in Tietjen, Borowski *et al.* (2020), to assign Gene Ontologies (GOs) to transcripts of the assembly.

Gene quantification and differential gene expression

Host gene expression was quantified with kallisto v0.46.0 (Bray *et al.*, 2016) using the cleaned mRNA reads of the polyA libraries, and the *B. puteoserpentis de novo* transcriptome assembly as reference. A gene was considered expressed when the expression, represented by transcripts per million values (TPMs), was greater than 0. For subsequent differential gene expression analyses, raw gene count matrices were generated with utility scripts of the Trinity v2.5.1 package (Haas *et al.*, 2013) for pairwise comparisons between gill and foot samples of day 0 mussels and displacement day 1, 2, 3, 5, 7, 8 and 10. To identify differentially expressed genes with highest certainty, we applied a two-part approach for differential gene expression analyses using R v3.5.3 (R Core Team, 2019). We used the count-data approach by edgeR v3.24.3 implemented in the utility scripts of the Trinity package v2.8.4 (Haas *et al.*, 2013). We also applied the compositional data approach by ALDEx2 v1.14.1 (Fernandes *et al.*, 2013). Statistical significance was accepted at false-discovery rates (FDRs) below 0.05.

Results & Discussion

Stable symbiont abundances in displaced mussels

Within the framework of an *in situ* displacement experiment, we wanted to gain insights into physiological adaptations of host and symbionts in response to sudden limitation of hydrothermal fluid access. An indicator for potential metabolic changes in the symbiosis is symbiont abundance, because it can influence the gene expression of the host (Barros *et al.*, 2015). Symbiont loss was shown to occur in bathymodiolin mussels when the energy sources for symbionts are low (e.g. Kádár *et al.*, 2005; Tietjen, Leisch, *et al.*, 2020). To investigate if symbiont numbers decreased over the course of the experiment, we used the 16S rRNA gene read counts in the metagenomes to infer the relative symbiont abundance in the host gills. To account for potential biases introduced by the amount of host tissue in each metagenome library, we calculated the ratio of symbiont 16S and host 18S rRNA gene reads. This ratio was normalised to the total number of reads sequenced in each library. We found that the relative abundance of the methanotrophic and thiotrophic symbionts in *B. puteoserpentis* remained at a stable level until displacement day 8. Symbiont numbers only showed considerable decrease towards the end of the experiment at displacement day 10 (Figure 1). The slight symbiont decrease observed for displacement day 1, 2 and 3 are likely caused by naturally occurring variations in symbiont abundance between bathymodiolin mussels of the same species (Duperron *et al.*, 2007).

Interruption of access to chemical energy sources has been simulated in multiple bivalves with chemosynthetic symbionts. In nearly all of these studies, the limitation of energy sources induced a loss of symbionts after varying number of days. For example, in the symbiotic shallow-water clam *Thyasira flexuosa,* a gradual decrease of the sulphur-oxidising symbionts was observed after 18 days of aquarium starvation experiments (Dufour and Felbeck, 2006). Similarly, aquarium-based sulphide starvation induced symbiont loss in the shallow-water clam *Codakia orbiculata,* which was observed after 3 months (Gros *et al.*, 2012).

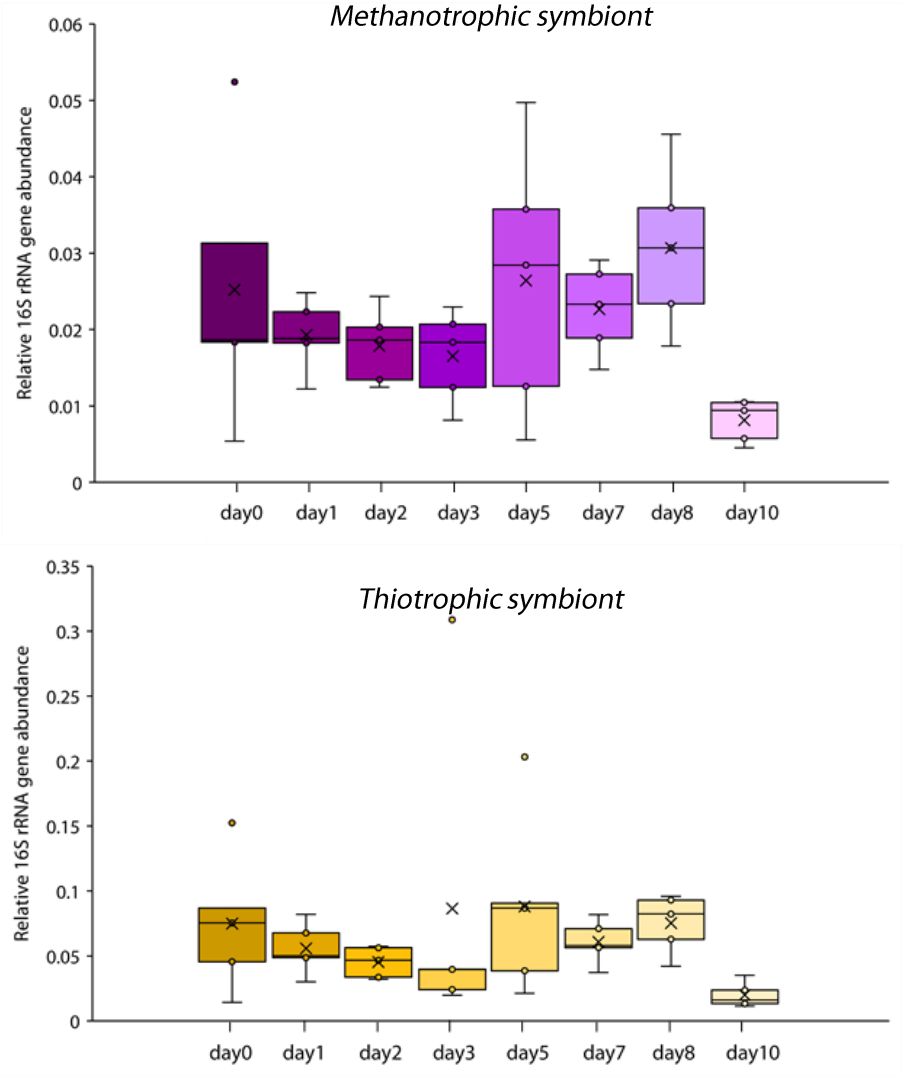

Figure 1: Relative symbiont abundance in *B. puteoserpentis* gills of displaced mussels. Boxplot shows the range of symbiont 16S rRNA gene read counts relative to host 18S rRNA gene reads (normalised to library size, n=5). Overall abundance of the thiotrophic symbiont was higher than the methanotrophic symbiont. Median indicated by a line, mean indicated by a cross in each displacement day.

In the deep-sea mussel *B. azoricus*, apparent symbiont loss was observed in mussels that were kept in aquaria for 14 and 30 days (Kádár *et al.*, 2005; Barros *et al.*, 2018). The same observation was made in an *in situ* translocation experiment with *B. azoricus*, where mussels showed major depletion of symbiont populations already after 7 days (Détrée *et al.*, 2019). Our results are in agreement with previous aquarium-based and *in situ* experiments with *B. azoricus* that showed symbiont loss to occur within days of removals from the symbiont energy source. This symbiont loss appears to occur much faster in *Bathymodiolus* mussels than in

shallow-water relatives, which may be explained by different capabilities of the symbionts to tolerate limitations of the chemical energy resources. Future comparative genomics of selected shallow-water clam symbionts and deep-sea mussel symbionts could uncover whether the clam symbionts are more adapted to low concentrations of chemical energy, for instance through mixotrophy and the presence of high-affinity transporters for substrates.

The methanotrophic and thiotrophic symbionts of *Bathymodiolus* spp. mussels rely on methane and sulphur compounds to maintain cellular processes (Ponnudurai *et al.*, 2017). To date, it is unclear whether the symbionts actively escape the mussel tissues upon removal of the energy source, or whether the mussels control symbiont populations. Escaping the host tissues has been proposed for symbionts of the hydrothermal vent tubeworm *Riftia pachyptila* (Klose *et al.*, 2015). Such an escape of host tissues is also a possible scenario for the symbionts of *Bathymodiolus* mussels that also acquire their symbionts from the environment (Wentrup *et al.*, 2014). However, it is also likely that symbiont populations are controlled by intracellular digestion of symbionts *via* lysosomes (e.g. Tietjen, Leisch, *et al.*, 2020). Upon removal of energy sources for the symbionts, the symbionts may not be capable of outgrowing intracellular digestion rates of their mussel host. Symbiont populations can also re-populate the symbiotic host tissues when the energy sources are re-established. This re-acquisition of symbionts has been demonstrated for *Bathymodiolus* mussels in laboratory experiments (Kádár *et al.*, 2005; Tietjen, Leisch, *et al.*, 2020), and also in *in situ* experiments with mussels that have been displaced from and re-located back to the mussel bed (Fink, 2011). Interestingly, the methanotrophic symbiont showed a significant increase after four days of re-location, while the thiotrophic population did not recover within 7 days. Fluorescence *in situ* hybridisation or transmission electron microscopy would be necessary to confirm symbiont loss in the displaced mussels in our study.

Displacement of mussels induced metabolic changes in both symbionts

Sufficient sequencing coverage was only available for the day 0 control and for displacement day 1 and 2 that allowed meaningful transcriptome analyses for the symbionts. For these displacement days, differential gene expression analyses have been conducted in a previous study, and showed a high number of genes that different significantly from day 0 control samples in both symbionts (in Tietjen, Borowski, *et al.,* 2020: Supplementary Figure 4 and Supplementary Tables 3 and 4). In the methanotrophic symbiont, nearly 20% (581 genes) of the total number of genes showed significant expression changes after 2 days of displacement from the vent fluids. The number of differentially expressed genes was lower in the thiotrophic symbiont with roughly 10% (240 genes) of the total number of genes, showing significant expression changes compared to the day 0 control samples. The high number of differentially expressed genes in both symbionts indicates a strong physiological response of both symbionts to the environmental conditions at the displacement site.

Among these were genes that are part of the primary energy metabolism for the methanotrophic and the thiotrophic symbiont, methane oxidation and sulphur oxidation, respectively (data available in Tietjen, Borowski, *et al.,* 2020: Supplementary Tables 3 and 4). In the methanotrophic symbiont, we observed significantly higher expression of the particulate methane monoxygenase subunit PmoC, but not PmoA and PmoB, in day 1 and day 2 samples. As hypothesized for on-board stored *B. puteoserpentis* mussels in Tietjen, Borowski, *et al.* (2020), the higher expression of methane oxidation genes might indicate an adaptation of the methanotrophic symbiont to scavenge traces of methane in the mussel tissues in the absence of hydrothermal fluids. In the thiotrophic symbiont, genes for thiosulphate oxidation *via* the Sox-complex showed significantly lower expression in displacement day 1 (SoxX, SoxY and SoxA) and day 2 (SoxY and SoxA). In contrast, genes for hydrogen sulphide oxidation *via* the reverse-acting dissimilatory sulphite reductase complex (Dsr-complex) were significantly higher expressed in displacement day 1 (DsrM, DsrP and DsrK) and day 2 (DsrM and DrsK). Higher expression of the Dsr-complex genes could be

linked to higher availability of hydrogen sulphide through a turnover of elemental sulphur stores in the cells (Tietjen, Borowski, *et al.*, 2020).

In addition to this, both symbionts showed changes in the expression of genes involved in nitrate respiration (in Tietjen, Borowski, *et al.,* 2020: Supplementary Tables 3 and 4). In displacement days 1 and 2, we found significantly higher expression of genes encoding NarK, and dissimilatory nitrate reduction *via* NarG and NarH. As suggested for the on-board stored samples in Tietjen, Borowski, *et al.* (2020), upregulation of genes involved in nitrate respiration may be a response to limitations of oxygen for the use of nitrate as alternative electron acceptor. In the thiotrophic symbiont, two genes for nitrate respiration, NarG and NarH, were significantly lower expressed in both displacement day 1 and 2. Instead, genes for assimilatory nitrate reductase were significantly higher expressed. Our results suggest that oxygen concentrations in displacement day 1 and 2 were lower compared to the day 0 control samples, but not critically low to invoke upregulation of alternative respiratory pathways *via* nitrate in the thiotrophic symbiont. The higher expression of nitrate respiration genes in the methanotrophic symbiont reveals high oxygen dependency, e.g. for methane oxidation, and likely represent a typical response of this symbiont to changing environmental conditions. Although we could not analyse gene expression changes of the symbionts for later displacement days, we hypothesise that the symbionts also display a strong physiological response in samples that have been removed from their energy sources even longer.

The mussel host maintains stable transcriptomes in body tissues

We wanted to investigate if the symbiotic gill tissue of the host was affected by the displacement from the hydrothermal vent fluids. To verify whether potential changes in the mussel gills were be related to the symbiosis with the chemosynthetic bacteria, we also analysed the gene expression changes of the mussel foot. Gene expression analyses of foot samples may also provide information on mussel behaviour at the displacement site. For example, higher expression of proteins involved in locomotion and muscle contraction could indicate attempts to move away from the displacement site. Such an escape has been

previously postulated to optimise the positioning closer to the vent fluids for symbiont access to their energy sources (Boutet *et al.*, 2009).

The basis for host tissue analyses was the transcriptome *de novo* assembly that included gill and foot tissues of all mussels in our experiment. The *de novo* assembly consisted of 105,251 transcribed genes, out of which 65% could be functionally annotated. Genes without annotation are hereon after referred to as "hypothetical" genes. In the combined transcriptome of all replicates, 59,619 genes were expressed in the gills (cumulative, TPM > 0), whereas 52,827 genes (cumulative, TPM > 0) were expressed in the foot samples. In gill samples, 18,703 genes were uniquely expressed (cumulative, TPM > 0), while 11,911 genes were only expressed in the foot samples. To investigate if the genes that were only expressed in one tissue reflected the expected expression of genes functioning in the respective tissues, we analysed the distribution of gene ontologies (GOs) for biological processes that could be detected in these samples (Supplementary Figure 2). The distribution of GOs for biological processes were highly similar in both tissues (level 2 and level 3), and did not provide a comprehensive insight into distinct tissue functions. Therefore, we focused on in-depth investigations of the function of genes that showed significant expression changes in displaced mussels compared to day 0 control mussels.

Unlike their symbionts, the mussel hosts showed only minor transcriptome changes in our displacement experiment. We compared the gill and foot transcriptomes of the day 0 control samples with the transcriptomes of all subsequent displacement samples, and analysed expression changes with differential gene expression analyses. We could not detect significant gene expression changes based on analyses with ALDEx2. Analyses with edgeR revealed few genes that were differentially expressed compared to the day 0 control samples. The majority of these genes could not be functionally annotated. For the gills, we only detected significant gene expression changes in displacement days 5, 7 and 8 (Supplementary Table 2). In all other displacement days (1, 2, 3, and 10), we could not detect differential gene expression in the gill tissues compared to the day 0 control samples. With the exception of one hypothetical gene,

all genes with significant statistical support were higher expressed in the displacement samples. Similar to the gill transcriptomes, significant expression changes in foot samples could only be detected with edgeR. The number of differentially expressed genes was equally low as in the gill samples, however all genes detected with edgeR were lower expressed compared to day 0 control samples (Supplementary Table 3). For displacement days 2 and 3, we only detected single genes that were differentially expressed and that had an unknown function. In displacement days 5, 7, 8 and 10, several genes were differentially expressed compared to day 0 control samples. Overall, the number of differentially expressed genes in both gill and foot samples was low in relation to the total number of genes in the respective transcriptomes. We hypothesise that the low number of differentially expressed genes in both host tissues reflect a physiological stability in the displacement experiment

Functional specialisation of different mussel tissues, such as the gill and the foot, should be reflected by distinct transcriptomes profiles as revealed in other mytilid mussels (e.g. Gerdol *et al.*, 2017). Based on this, we wanted to validate if the lack of differentially expressed genes in both tissues was not caused by a bias introduced during sample preparation or sequencing. We therefore also compared the expression of gill and foot tissues with differential gene expression analyses using edgeR. When including all displacement samples of both tissues, we observed distinct transcriptome profiles in gill and foot tissues indicated by clustering of samples from these tissues (Supplementary Figure 3). In addition, replicates of all displacement days showed intermixing within their respective tissue, which illustrates homogenous transcriptomes across the displacement experiment. Based on our data, we conclude that the mussel host did not respond on a molecular, and thus physiological, level to the limitation of hydrothermal fluid access.

Increased respiratory activity and decreased byssus synthesis in displaced mussels

We wanted to gain insights into potential physiological changes in gill and foot samples over the course of the displacement experiment. Because we only detected significant changes for few genes, we extrapolated potential metabolic changes from these genes. Among the genes

with functional annotation, we detected significantly higher expression of genes coding for key proteins of the mitochondrial respiratory chain in the gill samples (Supplementary Table 2). These included cytochrome b (Cytb) of Complex III, cytochrome c oxidase subunit I and III (COX I and COX III) of Complex IV, and F0 subunit 6 (ATP6) of the ATP synthase (Figure 2). Upregulation of genes for mitochondrial respiration indicated higher oxygen consumption

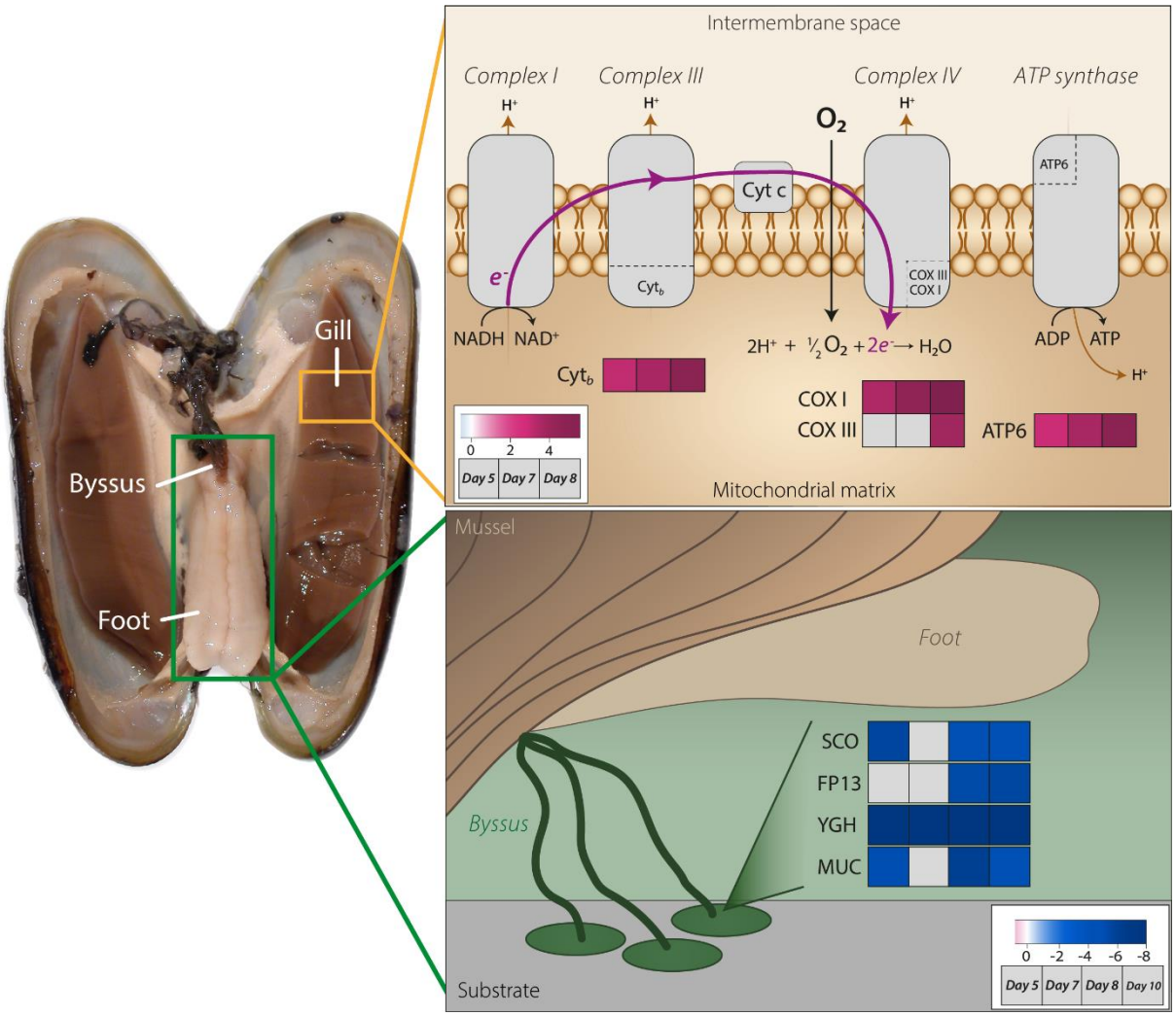

Figure 2: Physiological responses of gill and foot transcriptomes in displaced *Bathymodiolus* mussels. Simplified schematic of inferred physiological changes in gill and foot samples of displaced mussels. Upper reconstruction shows proteins encoded by genes that were significantly higher expressed in gill samples of displacement day 5, 7 and 8 compared to day 0 control samples. Lower reconstruction indicates significantly lower expressed genes in the foot samples in displacement day 5, 7, 8 and 10 samples compared to the day 0 control samples. These included genes coding for proteins with putative function in the adhesion of mussels to substrates *via* byssus. Heatmap indicated the relative expression changes (log_2FCs) of the respective displacement day compared to day 0 control samples. Grey boxes indicate non-differential expression.

through increased respiration rates in the displaced mussels. In a translocation experiment with *B. thermophilus,* higher respiration rates were found in mussels that were close to a vent and mytilids at several meters from this vent (Smith, 1985). This suggests that higher oxygen concentrations in the surroundings of the displacement site was not related to higher oxygen consumption in these mussels.

Among the differentially expressed genes in foot samples of the displacement samples, we detected multiple proteins that were annotated functions typical for the mussel foot (Figure 2 and Supplementary Table 3). These included genes coding for "YGH-rich protein (YGH), SCO-spondin like protein (SCO), foot protein 13 (FP13), which have been identified as components of mussel foot transcriptomes and that play a role in byssus formation (Gerdol *et al.*, 2017). All of these genes were significantly lower expressed in the displaced mussels compared to the day 0 control samples. In the ventral groove of the mussel foot, byssus proteins are produced for the adhesion to hard substrates (Waite, 2017). We also found mucin (MUC) included in the list of genes that showed significantly lower expression in foot samples of the displaced mussed. Mucin has been identified as part of the pedal mucus in the gastropod *Patella vulgata* that supports adhesion to substrates in these limpets (Kang *et al.*, 2020). Lower expression of genes involved in attachment to substrates *via* byssus secreted from the foot gland may indicate a non-sedentary adaptation to the displacement from the vent fluids.

Overall, we only detected minor transcriptome changes in gill and foot tissues of displaced mussels. Our data rather suggests that the physiology of the mussel host remains unchanged. We hypothesise that *Bathymodiolus* mussels are likely undisturbed by the sudden environmental changes, which suggests a resistance to short-term fluctuations of physico-chemical conditions, and explains their ecological success in these habitats.

Acknowledgements

We thank the Deutsche Forschungsgemeinschaft (DFG, German Research Foundation) for funding under Germany's Excellence Strategy EXC-2077-390741603. Special thanks go to the captain, crew and research team from the Meteor M126 research cruise in 2016, and particularly to Volker Ratmeyer and the remaining ROV team from the MARUM for excellent operation of the ROV during IDEFIX fixation and displacement of mussels. We thank Bruno Hüttel und Lisa Czaja-Hasse from the Max Planck Genome Center in Cologne for their great technical support during library preparation and sequencing. We thank Rebecca Ansorge, Silke Wetzel, and Dolma Michellod for their assistance during sample collection and processing, and the Symbiosis Department for scientific input and discussions.

References

Barros, I., Divya, B., Martins, I., Vandeperre, F., *et al.* (2015) 'Post-capture immune gene expression studies in the deep-sea hydrothermal vent mussel *Bathymodiolus azoricus* acclimatized to atmospheric pressure', *Fish and Shellfish Immunology*, 42, pp. 159–170. doi: 10.1016/j.fsi.2014.10.018.

Barros, I., Froufe, H., Marnellos, G., Egas, C., *et al.* (2018) 'Metatranscriptomics profile of the gill microbial community during *Bathymodiols azoricus* aquarium acclimatization at atmospheric pressure', *AIMS Microbiology*, 4, pp. 240–260. doi: 10.3934/microbiol.2018.2.240.

Boutet, I., Jollivet, D., Shillito, B., Moraga, D., *et al.* (2009) 'Molecular identification of differentially regulated genes in the hydrothermal-vent species *Bathymodiolus thermophilus* and Paralvinella pandorae in response to temperature', *BMC Genomics*, 10. doi: 10.1186/1471-2164-10-222.

Bray, N. L., Pimentel, H., Melsted, P. and Pachter, L. (2016) 'Near-optimal probabilistic RNA-seq quantification', *Nature Biotechnology*, 34, pp. 525–527. doi: 10.1038/nbt.3519.

Bryant, D. M., Johnson, K., DiTommaso, T., Tickle, T., *et al.* (2017) 'A Tissue-Mapped Axolotl De Novo Transcriptome Enables Identification of Limb Regeneration Factors', *Cell Reports*, 18, pp. 762–776. doi: 10.1016/j.celrep.2016.12.063.

Conesa, A., Götz, S., García-Gómez, J. M., Terol, J., *et al.* (2005) 'Blast2GO: A universal tool for annotation, visualization and analysis in functional genomics research', *Bioinformatics*, 21, pp. 3674–3676. doi: 10.1093/bioinformatics/bti610.

Détrée, C., Haddad, I., Demey-thomas, E., Vinh, J., *et al.* (2019) 'Global host molecular perturbations upon in situ loss of bacterial endosymbionts in the deep-sea mussel *Bathymodiolus azoricus* assessed using proteomics and transcriptomics', pp. 1–14.

Dufour, S. C. and Felbeck, H. (2006) 'Symbiont abundance in thyasirids (Bivalvia) is related to particulate food and sulphide availability', *Marine Ecology Progress Series*, 320, pp. 185–194. doi: 10.3354/meps320185.

Duperron, S., Sibuet, M., MacGregor, B. J., Kuypers, M. M. M., *et al.* (2007) 'Diversity, relative abundance and metabolic potential of bacterial endosymbionts in three *Bathymodiolus* mussel species from cold seeps in the Gulf of Mexico', *Environmental Microbiology*, 9, pp. 1423–1438. doi: 10.1111/j.1462-2920.2007.01259.x.

Duperron, S., Quiles, A., Szafranski, K. M., Léger, N., *et al.* (2016) 'Estimating Symbiont Abundances and Gill Surface Areas in Specimens of the Hydrothermal Vent Mussel *Bathymodiolus puteoserpentis* Maintained in Pressure Vessels', *Frontiers in Marine Science*, 3, pp. 1–12. doi: 10.3389/fmars.2016.00016.

Fernandes, A. D., Macklaim, J. M., Linn, T. G., Reid, G., *et al.* (2013) 'ANOVA-Like Differential Expression (ALDEx) Analysis for Mixed Population RNA-Seq', *PLoS ONE*, 8. doi: 10.1371/journal.pone.0067019.

Fink, D. (2011) *Dynamics in Symbiont Abundance in Bathymodiolin Deep-Sea Symbioses*. University of Bremen.

Gerdol, M., Fujii, Y., Hasan, I., Koike, T., *et al.* (2017) 'The purplish bifurcate mussel Mytilisepta virgata gene expression atlas reveals a remarkable tissue functional specialization', *BMC Genomics*, 18, pp. 1–24. doi: 10.1186/s12864-017-4012-z.

Grabherr, M. G., Haas, B. J., Yassour, M., Levin, J. Z., *et al.* (2011) 'Full-length transcriptome assembly from RNA-Seq data without a reference genome', *Nature Biotechnology*, 29, pp. 644–652. doi: 10.1038/nbt.1883.

Gros, O., Elisabeth, N. H., Gustave, S. D. D., Caro, A., *et al.* (2012) 'Plasticity of symbiont acquisition

throughout the life cycle of the shallow-water tropical lucinid Codakia orbiculata (Mollusca: Bivalvia)', *Environmental Microbiology*, 14, pp. 1584–1595. doi: 10.1111/j.1462-2920.2012.02748.x.

Gruber-Vodicka, H. R., Seah, B. K. B. and Pruesse, E. (2020) 'phyloFlash: Rapid Small-Subunit rRNA Profiling and Targeted Assembly from Metagenomes', *mSystems*, 5. doi: 10.1128/msystems.00920-20.

Haas, B. J., Papanicolaou, A., Yassour, M., Grabherr, M., *et al.* (2013) 'De novo transcript sequence reconstruction from RNA-seq using the Trinity platform for reference generation and analysis', *Nature Protocols*, 8, pp. 1494–1512. doi: 10.1038/nprot.2013.084.

Huson, D. H., Beier, S., Flade, I., Górska, A., *et al.* (2016) 'MEGAN Community Edition - Interactive Exploration and Analysis of Large-Scale Microbiome Sequencing Data', *PLoS Computational Biology*, 12, pp. 1–12. doi: 10.1371/journal.pcbi.1004957.

Kádár, E., Bettencourt, R., Costa, V., Santos, R. S., *et al.* (2005) 'Experimentally induced endosymbiont loss and re-acquirement in the hydrothermal vent bivalve *Bathymodiolus azoricus*', *Journal of Experimental Marine Biology and Ecology*, 318, pp. 99–110. doi: 10.1016/j.jembe.2004.12.025.

Kang, V., Lengerer, B., Wattiez, R. and Flammang, P. (2020) 'Molecular insights into the powerful mucus-based adhesion of limpets (Patella vulgata L.): Molecular insights into limpets adhesion', *Open Biology*, 10. doi: 10.1098/rsob.200019rsob200019.

Klose, J., Polz, M. F., Wagner, M., Schimak, M. P., *et al.* (2015) 'Endosymbionts escape dead hydrothermal vent tubeworms to enrich the free-living population', 112, pp. 11300–11305. doi: 10.1073/pnas.1501160112.

Ponnudurai, R., Kleiner, M., Sayavedra, L., Petersen, J. M., *et al.* (2017) 'Metabolic and physiological interdependencies in the *Bathymodiolus azoricus* symbiosis', *ISME Journal*, 11, pp. 463–477. doi: 10.1038/ismej.2016.124.

R Core Team (2019) *R: A language and environment for statistical computing*., *R Foundation for Statistical Computing, Vienna, Austria*.

Rognes, T., Flouri, T., Nichols, B., Quince, C., *et al.* (2016) 'VSEARCH: A versatile open source tool for metagenomics', *PeerJ*, 2016, pp. 1–22. doi: 10.7717/peerj.2584.

Seston, S. L., Beinart, R. A., Sarode, N., Shockey, A. C., *et al.* (2016) 'Metatranscriptional response of chemoautotrophic Ifremeria nautilei endosymbionts to differing sulfur regimes', *Frontiers in Microbiology*, 7, pp. 1–18. doi: 10.3389/fmicb.2016.01074.

Simão, F. A., Waterhouse, R. M., Ioannidis, P., Kriventseva, E. V., *et al.* (2015) 'BUSCO: Assessing genome assembly and annotation completeness with single-copy orthologs', *Bioinformatics*, 31, pp. 3210–3212. doi: 10.1093/bioinformatics/btv351.

Smith, K. L. (1985) 'Deep-Sea Hydrothermal Vent Mussels : Nutritional State and Distribution at the Galapagos Rift', *Ecological Society of America*, 66, pp. 1067–1080.

Tietjen, M., Borowski, C., Leisch, N., González Porras, M. Á., *et al.* (2020) *In situ fixation reveals (dis)similar survival strategies in two endosymbionts of a deep-sea mussel host*. Manuscript in prep.

Tietjen, M., Leisch, N., Franke, M., Hiebenthal, C., *et al.* (2020) *Lysosomal digestion of symbionts shapes innate immunity and fuels the metabolism of bacteriocytes in a deep-sea mussel host*. Manuscript in prep.

Waite, J. H. (2017) 'Mussel adhesion - Essential footwork', *Journal of Experimental Biology*, 220, pp. 517–530. doi: 10.1242/jeb.134056.

Wentrup, C., Wendeberg, A., Schimak, M., Borowski, C., *et al.* (2014) 'Forever competent: Deep-sea bivalves are colonized by their chemosynthetic symbionts throughout their lifetime', *Environmental Microbiology*, 16, pp. 3699–3713. doi: 10.1111/1462-2920.12597.

Chapter IV: Supplementary Tables and Figures

Supplementary Tables

***Supplementary Table 1** of this chapter is deposited on the provided CD-ROM.*

Supplementary Table 2: Differentially expressed genes of gill samples in displaced mussels. List of genes in gills that were differentially expressed (FDR < 0.05) compared to day 0 control samples. Values indicate the centred, relative expression changes (log_2FCs) compared to day 0 samples. Blank cells in annotation column represent hypothetical genes; blank cells in the displacement columns indicate non-significant gene expression changes.

Gill								
Gene	**Annotation**	**Day 1**	**Day 2**	**Day 3**	**Day 5**	**Day 7**	**Day 8**	**Day 10**
TRINITY_DN11878_c0_g1							3.23	
TRINITY_DN15190_c0_g1	Cytochrome c oxidase subunit III						3.75	
TRINITY_DN17712_c0_g1							3.40	
TRINITY_DN18989_c0_g1	Vitelline envelope zona pellucida					3.89		
TRINITY_DN19212_c6_g1	Cytochrome oxidase subunit I				3.51	4.60	5.44	
TRINITY_DN2169_c1_g1							4.98	
TRINITY_DN23436_c0_g1					2.09	3.41	4.85	
TRINITY_DN24520_c0_g1						2.57	4.17	
TRINITY_DN28558_c4_g1							3.74	
TRINITY_DN28558_c4_g2					3.18	3.85	5.04	
TRINITY_DN31531_c3_g1					4.24	4.08	6.92	
TRINITY_DN32856_c0_g2						2.51		
TRINITY_DN32856_c0_g6						3.91		
TRINITY_DN36013_c3_g1					4.31	2.32		
TRINITY_DN38275_c3_g1					2.50	3.28	3.53	
TRINITY_DN38955_c2_g1					7.34	8.42	9.15	
TRINITY_DN39044_c1_g2						4.63		
TRINITY_DN39224_c0_g1						3.45		
TRINITY_DN39224_c0_g3						4.84		
TRINITY_DN39313_c0_g1						3.65		
TRINITY_DN44208_c0_g2						3.69		
TRINITY_DN44655_c2_g1						5.92	7.11	
TRINITY_DN44707_c5_g1							7.02	
TRINITY_DN45098_c2_g4							3.04	
TRINITY_DN45875_c36_g1	Cytochrome b				2.96	3.57	4.82	
TRINITY_DN45875_c37_g1	ATP synthase F0 subunit 6				2.70	3.60	4.84	
TRINITY_DN46277_c1_g1	Neuralized pats1						0.44	
TRINITY_DN6141_c0_g1							4.84	
TRINITY_DN8752_c0_g1							7.17	
TRINITY_DN9127_c2_g1						-3.83		

Supplementary Table 3: Differentially expressed genes of foot samples in displaced mussels. List of genes in foot samples that were differentially expressed (FDR < 0.05) compared to day 0 control samples. Values indicate the centred, relative expression changes (log_2FCs) compared to day 0 samples. Blank cells in annotation column represent hypothetical genes; blank cells in the displacement columns indicate non-significant gene expression changes.

Foot								
Gene	**Annotation**	**Day 1**	**Day 2**	**Day 3**	**Day 5**	**Day 7**	**Day 8**	**Day 10**
TRINITY_DN23638_c0_g1					-9.61		-8.27	
TRINITY_DN24076_c0_g1								-7.41
TRINITY_DN25591_c0_g1					-8.83			
TRINITY_DN28054_c3_g1	Mucin-17 isoform X10				-5.22		-5.80	-4.53
TRINITY_DN28054_c3_g2	SCO-spondin like				-5.65		-4.77	-4.75
TRINITY_DN29457_c5_g1								-8.22
TRINITY_DN33818_c0_g1					-7.87		-7.57	-7.81
TRINITY_DN33818_c1_g1					-7.33	-7.31	-7.02	-7.27
TRINITY_DN33818_c1_g3					-7.82	-7.80	-7.51	-7.76
TRINITY_DN34484_c1_g3								-6.66
TRINITY_DN34817_c2_g3							-5.41	-5.59
TRINITY_DN37063_c1_g1							-5.50	-5.68
TRINITY_DN37495_c0_g3	Foot protein 13						-5.54	-5.72
TRINITY_DN40363_c1_g1					-6.06		-5.60	-3.92
TRINITY_DN41510_c1_g1					-6.57	-6.56	-6.34	-6.53
TRINITY_DN42094_c3_g1	Extracellular matrix protein A						-5.13	-4.29
TRINITY_DN42754_c1_g2					-5.38		-4.56	-5.27
TRINITY_DN43652_c1_g2			-8.70					
TRINITY_DN43652_c1_g3				-9.13				-9.18
TRINITY_DN44123_c1_g1								-6.96
TRINITY_DN44907_c5_g1							-5.45	-5.63
TRINITY_DN44907_c5_g2					-8.78	-8.76	-8.47	-8.71
TRINITY_DN44907_c5_g5	YGH-rich protein-1				-7.99	-7.97	-7.68	-7.93
TRINITY_DN45187_c5_g5							-7.75	
TRINITY_DN45699_c2_g1	Peptidyl-prolyl cis-trans isomerase-like				-5.54		-4.45	-4.80
TRINITY_DN46214_c0_g1	Metalloproteinase inhibitor 3-like							-6.46
TRINITY_DN51930_c0_g1	Metalloproteinase inhibitor 1							-7.89

Supplementary Figures

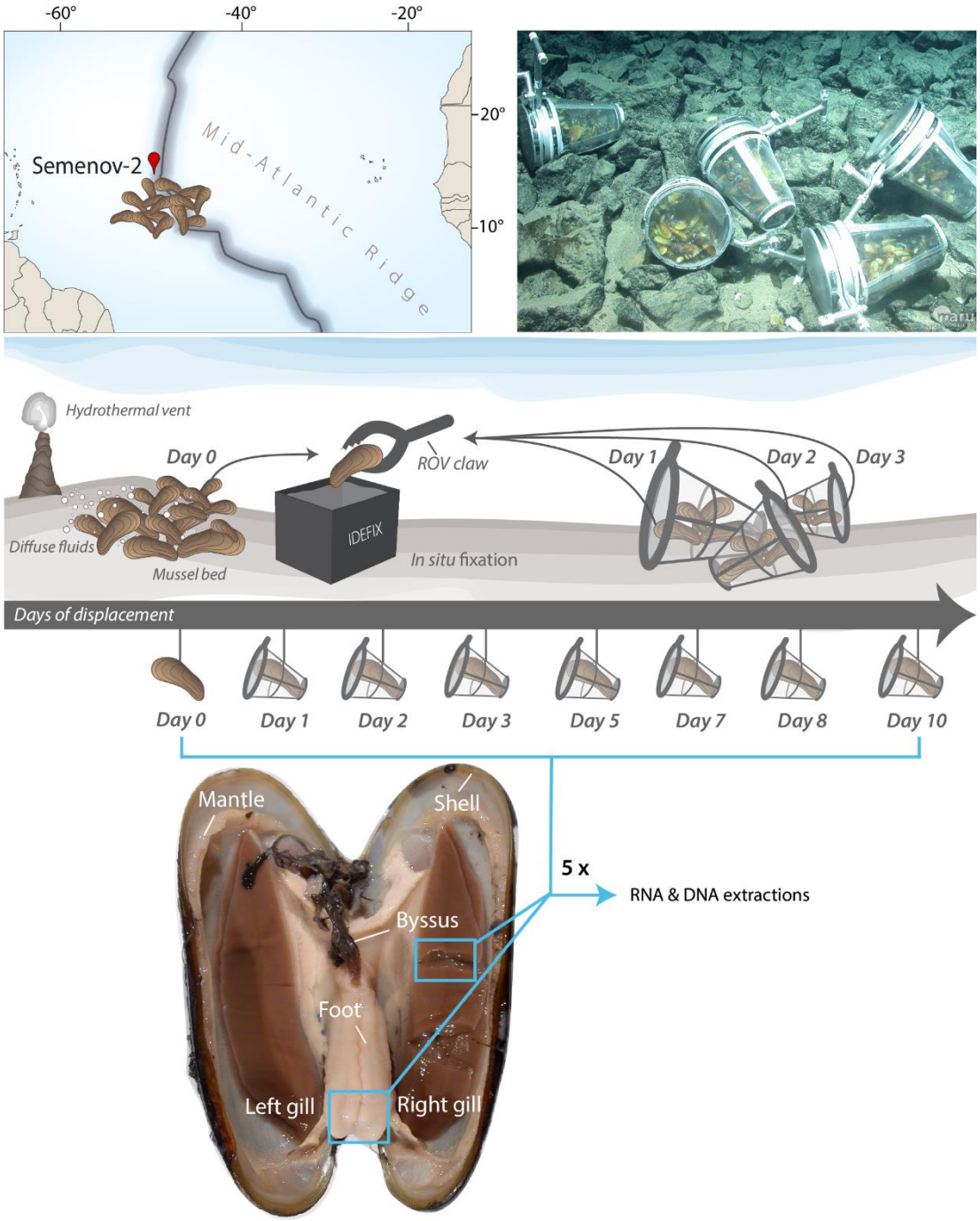

Supplementary Figure 1: Experimental setup and sampling strategy. The displacement experiment was conducted around the Semenov-2 vent field at the Mid-Atlantic Ridge. The mussel were collected in mesh cages and displaced to a site without access to hydrothermal fluids. For each displacement day, five mussels were dissected and pieces of the gill and foot were subjected to nucleotide extractions and subsequent sequencing.

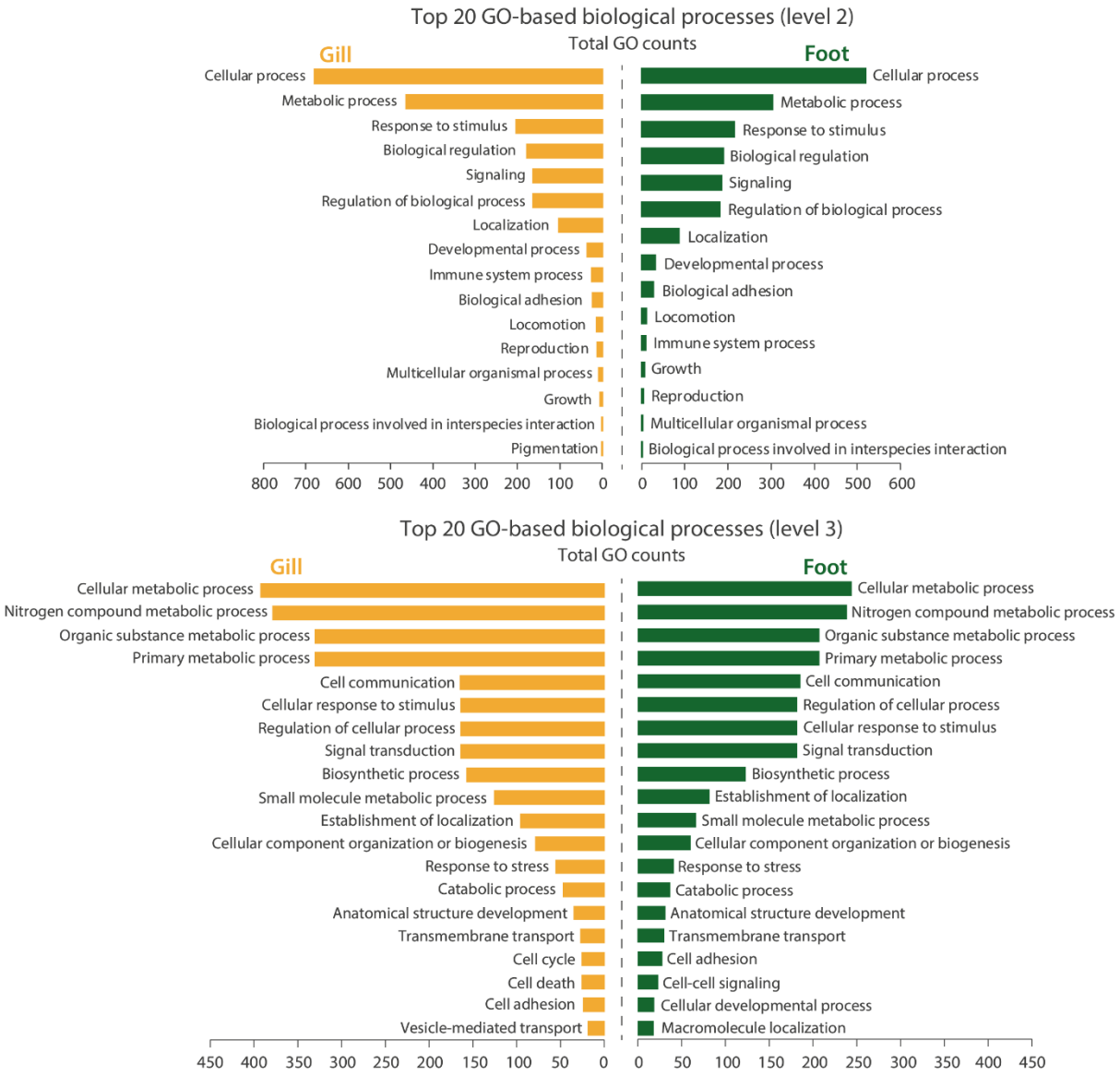

Supplementary Figure 2: Distribution of Gene Ontologies in gill and foot samples. Bar charts indicate total gene counts for each Gene Ontology (GO) category. Lists of genes for GO distribution included only uniquely expressed genes for the gill and foot tissue (18,703 and 11,911, respectively). Represented here are most abundant (GOs) of biological processes (level 2 and level 3) in the gill and foot samples. GO distributions were highly similar in gill and foot samples, however more genes of the gill transcriptome could be attributed to a GO. GOs were assigned using Blast2GO.

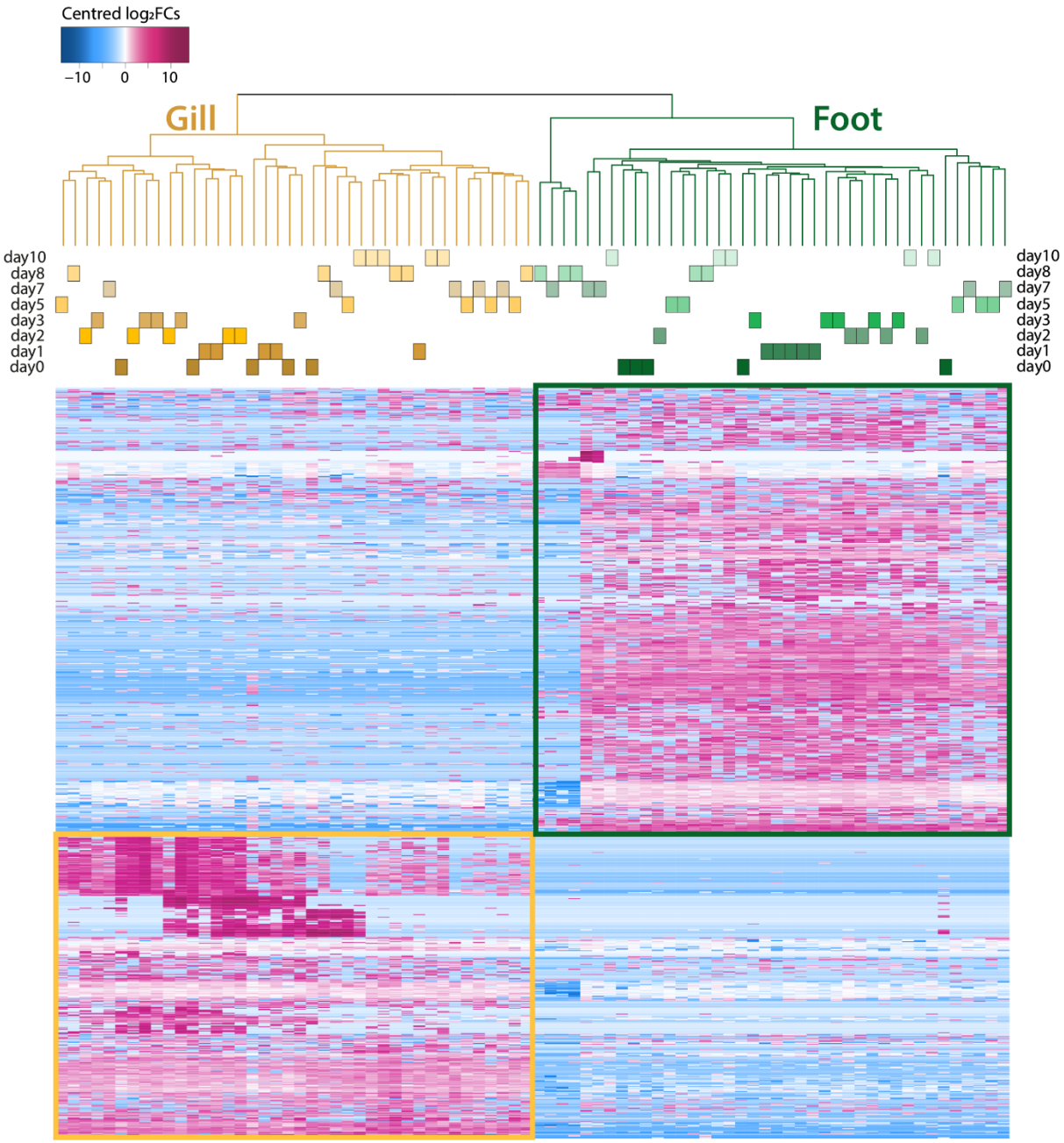

Supplementary Figure 3: Differentially expressed genes of gill and foot samples. Heatmap was generated with Trinity utility scripts for edgeR analyses and shows significant (FDR < 0.05) gene expression changes (centred log2FCs) between gill and foot samples in all displacement samples. Gill samples are indicated by yellow bars, foot samples are represented by green bars. Yellow box in heatmap indicates genes that were higher expressed in gill samples, green box highlights genes that were generally higher expressed in foot tissues. Distinct clustering of gill and foot samples suggest different transcriptome profiles for these tissues. Replicates of the same displacement day showed high intermixing, suggesting minor transcriptome differences between displacement days of the same tissue.

Chapter V | Discussion

Hydrothermal vents and cold seeps are highly dynamic ecosystems, in which the physico-chemical conditions can fluctuate over short periods of time. In these ecosystems, deep-sea mussels of the species *Bathymodiolus* are able to tolerate the supposedly harsh environmental conditions and represent one of the most successful animals. The results I presented within this thesis contribute substantially to our understanding of the physiological adaptations of host and symbionts to short- and long-term limitations of chemical energy supply for the symbiosis. Within the framework of my research aims, I uncovered the metabolic flexibility of the methanotrophic and thiotrophic symbiont reflected by strong gene expression changes in response to sample recovery from the deep sea (Chapter II) and the restriction of hydrothermal vent access (Chapter IV). I also revealed that the mussel host sustains a stable metabolism in short-term changing environmental conditions. However, in long-term starvation conditions, the mussel host displays a distinct physiological state as a result of symbiont loss (Chapter III). My doctoral studies were guided by three major questions that I will elaborate in the following paragraphs.

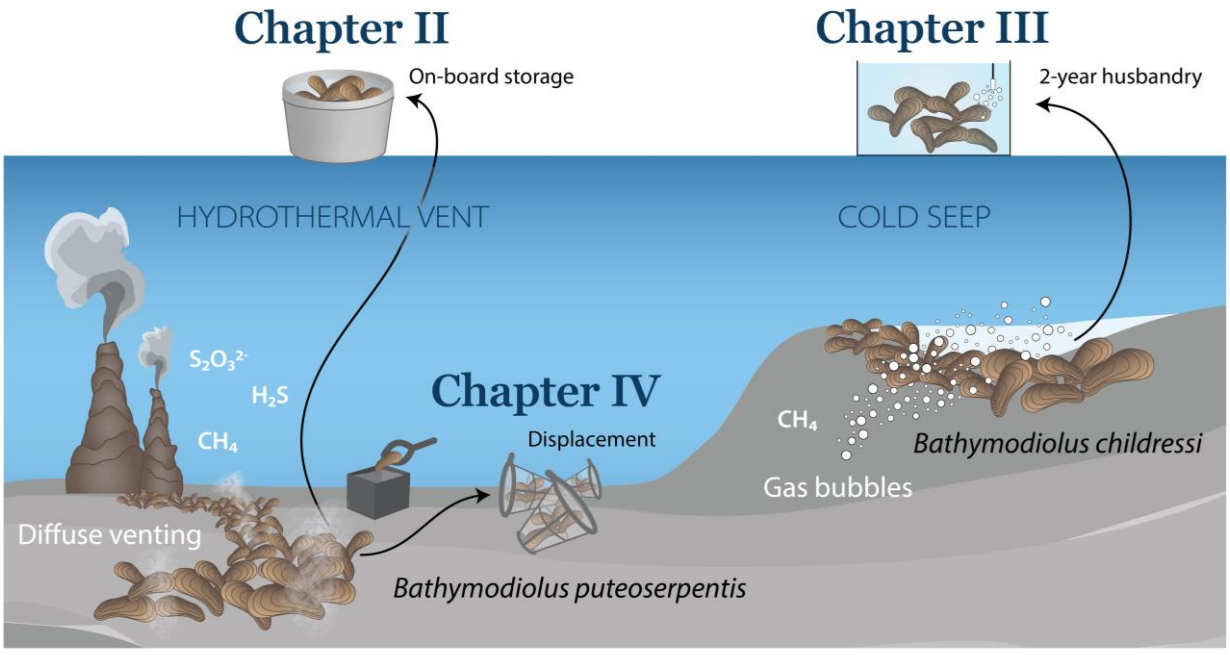

Figure 1: Overview of experimental setup in each chapter of this thesis.

Do the transcriptomes of on-board fixed deep-sea organisms reflect their natural physiology?

As deep-sea organisms are typically collected from great depths and processed on board, the time between sample collection and stabilisation of the organism can often take hours, potentially affecting gene expression profiles. Before I started my doctoral studies, it was unclear if on-board stabilised transcriptomes of deep-sea organisms reflect the physiology in their natural habitat. Our data showed that the physiology of the mussel host was unaffected by the conditions introduced during sample recovery. In contrast, we observed strong physiological responses in both symbionts that indicated survival strategies for naturally occurring interruptions of energy-rich water flow in the system.

What are the long-term effects of limitation of the energy source for the symbiosis?

Using aquarium setups, we simulated long-term methane limitation in the symbiosis of *B. childressi* from the Gulf of Mexico. The exposure to low methane concentrations for one year caused near-complete loss of symbionts, a decrease of gill biomass and resulted in a shift of the physiological state of the host gills. Even though the symbiont populations were diminished, the mussel host could re-acquire a moderate symbiont abundance with slightly increased methane concentrations, and regained a similar transcriptome profile as in the wild mussels. Our findings are in agreement with other studies that showed symbiont re-acquisition after re-introducing symbiont energy source (Gros *et al.*, 2012). However, even after re-establishment of symbiont populations, the gill biomass showed equally low gill biomass, which could indicate biomass loss might be irreversible.

How do host and symbionts cope with short-term fluctuations of hydrothermal access?

Several laboratory-based and *in situ* experiments have shed light onto physiological adaptations of bathymodiolin symbioses to various physical and chemical challenges that may occur naturally at hydrothermal vents. Such studies included also translocations experiments conducted with different *Bathymodiolus* species such as *B. thermophilus* (Smith, 1985) from

the Galapagos Rift, and *B. azoricus* (Détrée *et al.*, 2019) from the Mid-Atlantic Ridge. We wanted to investigate the response of host and symbionts to short-term interruptions of hydrothermal fluid access in an *in situ* displacement experiment. We found that the host physiology is largely unaffected by the temporal environmental changes. This is in contrast to the translocation study with *B. azoricus* that revealed significant expression changes of over 1,000 genes in mussel gills after 7 days (Détrée *et al.*, 2019). The discrepancy between the translocation experiment with *B. azoricus* and our displacement experiment may be related to different environmental settings of the mussel habitats, which may have an influence on their physiological plasticity and thus response to changing environmental conditions. Preliminary data revealed strong physiological responses of both the methanotrophic and the thiotrophic symbiont that were highly similar to the responses observed in the *in situ* fixation experiment suggesting similar environmental stimuli for the symbionts.

The applicability of transcriptome analyses for bathymodiolin symbioses

Transcriptomics is a state-of-the-art approach to explore physiological processes of organisms and their responses to various abiotic conditions that enable life in the their respective habitats (reviewed in Evans, 2015). The rationale of transcriptome-based studies is that observed gene expression changes, represented by mRNA abundances or reads counts of genes, are linked to changing metabolic processes in the organisms. Yet, no "gold-standard" for transcriptome analyses have been developed, which lead me to define the most optimal procedure applying two different transcriptomic tools that will be explained in more detail in the following section.

One way to examine gene expression changes are so-called differential gene expression analyses (Conesa *et al.*, 2016). The term "differentially expressed" signifies expression changes of genes between conditions (ideally between a control and a treatment sample) with statistical support. Multiple bioinformatics tools exist to conduct differential gene expression analyses (Schurch *et al.*, 2016). Throughout my studies, I came across two distinct mathematical assumptions used to calculate differential gene expression: the "count data" approach and the

"compositional data" approach. A common method used for testing differential gene expression is based on the assumption that mRNA counts are true count data. For example, the tool edgeR uses this as basis for calculating differential expression (Robinson *et al.*, 2010). In contrast, it is argued that expression data from RNA-Seq experiments are compositional and not count data (Fernandes *et al.*, 2013). By definition, datasets are compositional when the sum of values (or mRNA reads) obtained for each sample (or mRNA library) is pre-defined, like the set number of reads to reach a target sequencing depth. The tool ALDEx2 calculates differential gene expression based on data compositionality (Fernandes *et al.*, 2013). In transcriptomic studies, both techniques are well accepted but differ in their mathematical assumption of RNA-Seq data.

To obtain the most reliable results in my studies, I investigated which of the two approaches, edgeR or ALDEx2, should be applied on my datasets. To my surprise, only a small number of overlapping genes was identified as differentially expressed by both methods when I included three replicates per condition, and the majority of genes were only identified as statistically significant in one or the other approach (data not shown). I repeated the same analyses with a range of replicates, and found that including five replicates per sample condition increased the number of differentially expressed genes that could be detected by both methods. However, since I wanted to avoid bias introduced by choosing one method over the other, I generally only accepted differential gene expression if the same genes were detected by both methods to increase confidence in the data analyses.

Selecting the most suitable approaches for standard operating procedures to analyse the transcriptomes is particularly important for host studies. It is well-recognised that eukaryotic organisms have highly coordinated and complex transcription systems compared to bacteria. In addition, the genomes of eukaryotic organisms contain roughly 10-fold higher numbers of genes than bacteria. In the case of the *Bathymodiolus* host, the lack of a reference genome complicates such analyses, because mRNA abundance is estimated from *de novo* transcriptome assemblies. The host transcriptome assemblies that I generated contained more

than 100,000 thousand gene transcripts (105,251 predicted genes for *B. puteoserpentis,* Chapter IV*;* and for 255,285 predicted genes in *B. childressi*). With such large datasets, and provided the knowledge that the animals use complex transcription systems to regulate gene expression, differential gene expression analyses alone were not as meaningful as for the symbionts.

In addition to investigating differential gene expression, I analysed the host transcriptomes with gene co-expression networks. The rational of this approach was to identify gene clusters rather than only highlighting single genes, allowing deeper insights into ongoing physiological processes by unravelling a larger piece of the metabolic puzzle. Gene co-expression networks (GCNs) are powerful tools for investigating globally coordinated gene expression patterns to environmental changes in complex eukaryotic organisms (van Dam *et al.*, 2018; Carter *et al.*, 2004). So far, few RNA-Seq based studies have employed GCNs to systematically identify and evaluate gene clusters, and of these, only a few were performed in symbiosis research. One of these examples have revealed specific physiological responses of the plant *Medicago truncatula* colonised by the arbuscular mycorhizobial fungus *Rhizophagus irregularis* to potassium deprivation (Garcia *et al.*, 2017).

I applied GCNs to reveal the molecular processes in specific gill regions of the non-model *Bathymodiolus* host, and demonstrated that these analyses fundamentally complement differential gene expression analyses (Chapter III). Yet, GCNs are not applicable for all host transcriptome datasets. While GCNs were highly advantageous for analysing functional differences between cell types (ciliated edge and bacteriocyte region) of the same tissue, they did not provide useful information for analysing whole tissues. I also aimed to identify gene clusters of gill and foot samples for the dataset of Chapter IV that respond to the displacement of the mussels. However, the expression of host genes in neither gill nor foot tissues showed significant changes (as revealed by differential gene expression analyses, Chapter IV), so that co-expression of genes could not be reconstructed. Based on the host transcriptome analyses,

I found that distinct datasets and experiments had different optimal methods for gene expression analysis.

Taken together, I showed that transcriptome analyses of mussel gills (of host and symbionts) are highly informative in combination with a thorough experimental design and sophisticated approaches to minimise transcriptional noise. The ultimate goal for studying host-symbiont interactions would be to perform single-cell transcriptomics of bacteriocytes, preferentially from mussels exposed to different environmental conditions. However, transcriptome-based studies have been criticised for poor correlations between mRNA and protein levels, and raised concerns about the use of gene expression analyses alone for profiling physiological processes (Evans, 2015). For both, the *Bathymodiolus* mussel host and its symbionts, I showed that observations of biological processes, such as cell elongation in the methanotrophic symbiont (Chapter II) and lysosomal digestion in host cells (Chapter III), were reflected by the gene expression analyses. Ideally, transcriptome studies should always be complemented with omics-based techniques like e.g. proteomics, metabolic imaging and microscopy-based methods such as TEM and FISH, to validate biological interpretations made with gene expression data.

Preliminary results and future directions

Symbiont manipulation via secretion systems in the methanotrophic symbiont

In the interaction between bacteria and hosts, bacterial protein secretion is assumed to play a key role (Eichinger *et al.*, 2016). Several secretion systems have been characterised in recent years, and are categorised into different types depending on their structure and function (Costa *et al.*, 2015). Among these are the Type II and Type IV (T2SS and T4SS) that have been associated with bacteria-host interactions predominantly in bacterial pathogens and intracellular mutualistic symbionts (Masui *et al.*, 2000; Hay *et al.*, 2017). The T2SS is responsible for secreting folded proteins from the periplasm across the outer membrane into the extracellular environment (Costa *et al.*, 2015). This secretions system encompasses between 12 and 15 proteins (Korotkov and Sandkvist, 2019), all of which I detected in the genome of the methanotrophic symbiont of *B. puteoserpentis*. The proteins of the T2SS are mostly referred to as "general secretion proteins" (Gsp). In mussels from the *in situ* fixation experiment (Chapter II), I detected significantly higher expression of genes that are part of the T2SS in the methanotrophic symbiont of on-board fixed mussels compared to the *in situ* transcriptome. For example, I detected significantly higher expression of the GspF-encoding gene in ob2 samples, and in the subsequent on-board stored samples, I found significantly higher expression of genes encoding GspF, GspJ and GspK. Although the other Gsp-encoding genes were not differentially expressed, I observed generally higher expression values in all on-board stored samples compared to the *in situ* transcriptomes. In the methanotrophic symbiont of on-board stored mussels, I also detected significantly higher expression of genes coding for the type IV pilus assembly FimV related transmembrane protein, alongside genes encoding the type IV pilus proteins PilY1, PilN and PilQ. These pilus proteins are part of the T2SS (Hay *et al.*, 2017). In chemosynthetic symbionts of siboglinid tubeworms, the detected bacterial T2SS was postulated to be involved in the establishment of the symbiosis with their host (Li *et al.*, 2018). The upregulation of T2SS proteins could indicate higher secretion of folded proteins into the extracellular space.

In freshly collected *B. childressi* mussels (Chapter III), I detected high expression of symbiont genes that are part of the Type IV Secretion System (T4SS). The T4SS can transport macromolecules, including proteins and DNA, across the bacterial cell envelope into another cell (Wallden *et al.*, 2010; Costa *et al.*, 2015). The T4SS could be the main mode for the symbionts to manipulate the host environment as described for several pathogens (Costa *et al.*, 2015). In the case of the methanotrophic symbiont of *B. childressi,* bacterial proteins could be secreted into the host bacteriocyte. A symbiont genome-based prediction of proteins that could be secreted *via* the T4SS resulted in a set of more than 70 proteins. Among these were a few proteins with inferable roles in the interaction with the host bacteriocytes. Other genes only had hypothetical functions, but may also be involved in the interaction with the host. For example, I found the chitin-degrading enzyme chitinase in this set of secreted proteins, which was also highly expressed in the methanotrophic symbiont transcriptome. Intriguingly, chitin synthase was highly expressed in the host transcriptome of wild *B. childressi* mussels and part of the bacteriocyte-specific GCN. In a recent doctoral thesis, chitin has been proposed as main source for nutrition in the intranuclear parasite *Ca.* Endonucleobacter childressi (González Porras *et al.*, 2020). A chitinase-encoding gene was also detected in the genomes of siboglinid tubeworm symbionts, and was proposed to enable migration through the host tissues (Li *et al.*, 2018). In *Bathymodiolus* gills, chitin is likely concentrated in the secretory cells between the ciliated edge and the bacteriocyte regions (González Porras, 2020). It is possible that the methanotrophic symbionts of *Bathymodiolus* spp. mussels also access host-produced chitin for nutrition.

It is possible that the symbionts also modulate host cellular processes such as the phagocytic pathway through the T4SS. The near complete loss of methane-oxidising symbionts under low methane concentrations, however, suggests that the symbionts cannot completely evade the phagocytic response of the colonised host cells in contrast to some intracellular pathogens (Canesi *et al.*, 2002). It is, however, tempting to speculate that the symbionts manage to shift the balance between growth and phagocytosis using the T4SS, particularly under low methane concentrations. This could explain the disproportional re-growth of the symbiont population

in our symbiont-recovered state with only slight methane increase that was substantially lower than the concentrations at the mussel bed. A deceleration of phagocytosis through the symbiont T4SS could be a particularly useful stabilising strategy in the symbiosis under highly fluctuating methane conditions in the natural environment. Based on the genomic and transcriptomic data that I analysed together with my colleagues, we hypothesise that upon symbiont-colonisation of gill cells, microvilli are disrupted in response to specific effector proteins secreted by the symbionts (Chapter III).

To further understand host-symbiont interactions, future studies should address the presence of secretion systems in *Bathymodiolus* symbionts, particularly in the methanotrophic symbiont. The genome and transcriptome data support the involvement of T4SS and T2SS in the interaction of the methanotrophic symbiont with its host, but further evidence would be necessary to determine that these secretion systems are indeed functional. Such evidence and a greater understanding of macromolecular secretion could be gathered through the investigation of secretion systems using microscopy-based techniques (e.g. with cryo-electron microscopy).

Bathymodiolus symbioses as non-model model-systems

Most model systems for studying host-symbiont interactions are based on cultivable organisms, in which the systems are easily manipulated. From the marine realm, such model systems include the Hawaiian bobtail-squid *Euprymna scolopes* and its bioluminescent bacteria *Vibrio fischeri* (e.g. Bosch *et al.*, 2019). From a classical point of view, the *Bathymodiolus* system does not represent such an ideal model system for several reasons: i) neither host nor symbionts can be cultivated, ii) the maintenance of 'healthy' animals in aquaria is difficult, and iii) the retrieval of *Bathymodiolus* mussels from the deep-sea is very time-consuming and costly. In addition to this, symbiont-free (aposymbiotic) mussels have so far only been obtained through the experimental manipulation of chemical energy sources for the symbionts. Although all of these aspects represent challenges for studying the physiology of host and symbionts and their interaction, the data presented in my thesis demonstrate that

the non-model *Bathymodiolus* system actually has the potential to reveal processes like a model system would do.

Long-term aquarium husbandry of *B. childressi* with low methane influx has provided us with transcriptome profiles of aposymbiotic mussel gills that reflected a stable physiological state (Chapter III). This represents a promising basis for studying host-symbiont interactions in a non-model system. With these mussels, we could reveal several aspects related to symbiont presence on the function and physiology of host cells. For example, symbiont-depleted *B. childressi* mussels displayed a re-established microvilli brush border on the cells of the bacteriocyte gill region, while microvilli could not be observed on symbiont-containing cells. In developing mussels, microvilli loss has been observed before in *Bathymodiolus* host cells, and was has been associated with symbiont colonisation, where symbiont abundance negatively regulated the abundance of microvilli (Wentrup *et al.*, 2014). The manipulation of host cell microvilli has been linked to pathogens (e.g. microvilli effacement in *Escherichia coli* strain EPEC; Dean and Kenny, 2009; Shifrin *et al.*, 2014), and is likely also triggered by the symbionts in *Bathymodiolus* mussels upon colonisation. In addition to this, I found specific genes involved in immune responses of *B. childressi* bacteriocytes that were highly expressed when symbionts were present and were lower expressed when symbionts were absent.

In addition to establishing aposymbiotic mussel tissues for physiological investigations of the host, aquarium-based experiments could also be beneficial to induce physiological changes in the so far uncultivable symbionts. Unexpectedly, I found evidence for cell elongation in the methanotrophic symbiont of *B. puteoserpentis* in response to changing environmental conditions induced during sample recovery and on-board storage (Chapter II). While the triggers for cell elongation remain elusive, it is likely that the starvation of methane, the primary energy and carbon source for the symbiont, causes such cellular responses, because similar expression changes were observed in the methanotrophic symbiont of displaced mussels (Chapter II). We previously hypothesised that cell elongation may be advantageous to induce a fast re-growth upon replenishment of methane to the system. In a transplantation

and re-transplantation experiment with *B. azoricus*, the methanotrophic symbiont showed a much faster re-growth to normal population sizes than the thiotrophic symbiont (Fink, 2011). Interestingly, cell elongation was not reported for methane-starved *Methyloprofundus sedimenti,* the free-living and cultivable close relative of the methanotrophic symbiont in *Bathymodiolus* mussels (Tavormina *et al.*, 2017). In fact, literature searches have uncovered a lack of reports for cell elongation in other Type I methanothrophs (only in Williams and Shimmin, 1978), or in other chemosynthetic endosymbionts, suggesting that this is a rather understudied and 'new' physiological response discovered in this group of bacteria.

In our aquarium-starvation experiment with *B. childressi* (Chapter III), we sampled mussels in one-year intervals, and obtained stable physiological states of the mussels for the respective methane concentrations. To investigate if cell elongation occurs also in other *Bathymodiolus* species besides *B. puteoserpentis,* I propose to repeat an aquarium-based manipulation of methane concentrations with *B. childressi*. To track cell size variations related to methane concentrations, decreasing and increasing methane concentrations over shorter periods should be employed. In addition to this, microscopy imaging (e.g. FISH or TEM) of the mussels from the displacement experiment conducted with *B. puteoserpentis* (Chapter IV) could be performed. The results might reveal whether cell elongation only represents an artefact of physiological stress imposed on the symbiont during sample recovery and on-board storage, or if it represents a true physiological adaptation to limitations of access to their energy source. Although we are currently unable to cultivate *Bathymodiolus* hosts and their symbionts, I demonstrated that long-term aquarium husbandry, but also short-term environmental manipulations, are promising alternatives that allow us to investigate different physiological states of the mussel host and its symbionts. It is an exciting thought that we are able to discover so far unknown physiological responses and host-symbiont interactions using cultivation-independent *in situ* or laboratory-based experiments of deep-sea organisms.

Concluding remarks

The data presented in my thesis provide a comprehensive overview of the metabolism and thus physiology of the deep-sea *Bathymodiolus* mussel host and its symbionts. I uncovered that the mussel host is largely unaffected by short-term changes of environmental condition in an ecosystem with naturally dynamic physico-chemical conditions. The symbionts on the other hand are highly responsive to environmental changes. The results of my thesis indicate that the environmental conditions have a major effect on the physiology of the symbionts. The long-term consequences of energy depletion, however, shifts the physiology of the mussel host to an aposymbiotic state, in which host biomass is low.

Although *Bathymodiolus* mussels may not yet represent the most ideal system for traditional physiological studies conducted with model organisms, the features of the mussel host are an ideal prerequisite experimentally induce physiological changes. On one hand, the location of symbionts in distinct regions of the mussel gill tissue is beneficial to isolate symbiont-containing cells. On the other hand, the bathymodiolin symbioses represents a highly specialised system, in which only two primary symbiont types co-occur in host cells in nature. On top of this, *Bathymodiolus* mussels are hardy animals that can survive periods of variable physico-chemical conditions without alterations of the gene expression, which likely enabled their ecological success.

References

Bosch, T. C. G., Guillemin, K. and McFall-Ngai, M. (2019) 'Evolutionary "Experiments" in Symbiosis: The Study of Model Animals Provides Insights into the Mechanisms Underlying the Diversity of Host–Microbe Interactions', *BioEssays*, 41, pp. 1–8. doi: 10.1002/bies.201800256.

Canesi, L., Gallo, G., Gavioli, M. and Pruzzo, C. (2002) 'Bacteria-hemocyte interactions and phagocytosis in marine bivalves', *Microscopy Research and Technique*, 57, pp. 469–476. doi: 10.1002/jemt.10100.

Carter, S. L., Brechbühler, C. M., Griffin, M. and Bond, A. T. (2004) 'Gene co-expression network topology provides a framework for molecular characterization of cellular state', *Bioinformatics*, 20, pp. 2242–2250. doi: 10.1093/bioinformatics/bth234.

Conesa, A., Madrigal, P., Tarazona, S., Gomez-Cabrero, D., *et al.* (2016) 'A survey of best practices for RNA-seq data analysis', *Genome Biology*, 17, p. 13. doi: 10.1186/s13059-016-0881-8.

Costa, T. R. D., Felisberto-Rodrigues, C., Meir, A., Prevost, M. S., *et al.* (2015) 'Secretion systems in Gram-negative bacteria: Structural and mechanistic insights', *Nature Reviews Microbiology*, 13, pp. 343–359. doi: 10.1038/nrmicro3456.

van Dam, S., Võsa, U., van der Graaf, A., Franke, L., *et al.* (2018) 'Gene co-expression analysis for functional classification and gene-disease predictions', *Briefings in bioinformatics*, 19, pp. 575–592. doi: 10.1093/bib/bbw139.

Dean, P. and Kenny, B. (2009) 'The effector repertoire of enteropathogenic *E. coli:* ganging up on the host cell', *Current Opinion in Microbiology*, 12, pp. 101–109. doi: 10.1016/j.mib.2008.11.006.

Détrée, C., Haddad, I., Demey-thomas, E., Vinh, J., *et al.* (2019) 'Global host molecular perturbations upon in situ loss of bacterial endosymbionts in the deep-sea mussel *Bathymodiolus azoricus* assessed using proteomics and transcriptomics', pp. 1–14.

Eichinger, V., Nussbaumer, T., Platzer, A., Jehl, M. A., *et al.* (2016) 'EffectiveDB - Updates and novel features for a better annotation of bacterial secreted proteins and Type III, IV, VI secretion systems', *Nucleic Acids Research*, 44, pp. D669–D674. doi: 10.1093/nar/gkv1269.

Evans, T. G. (2015) 'Considerations for the use of transcriptomics in identifying the "genes that matter" for environmental adaptation', *Journal of Experimental Biology*, 218, pp. 1925–1935. doi: 10.1242/jeb.114306.

Fernandes, A. D., Macklaim, J. M., Linn, T. G., Reid, G., *et al.* (2013) 'ANOVA-Like Differential Expression (ALDEx) Analysis for Mixed Population RNA-Seq', *PLoS ONE*, 8. doi: 10.1371/journal.pone.0067019.

Garcia, K., Chasman, D., Roy, S. and Ané, J. M. (2017) 'Physiological responses and gene co-expression network of mycorrhizal roots under K+deprivation', *Plant Physiology*, 173, pp. 1811–1823. doi: 10.1104/pp.16.01959.

González Porras, M. Á. (2020) '*Molecular biology and evolution of the bacterial intranuclear parasite Ca . Endonucleobacter*'.

González Porras, M. Á., Assié, A., Tietjen, M., Jensen, M., *et al.* (2020) *The hungry nucleus: The nutritional demands of a chitinolytic intranuclear parasite trigger its host cell to upregulate sugar import*. Manuscript in prep.

Gros, O., Elisabeth, N. H., Gustave, S. D. D., Caro, A., *et al.* (2012) 'Plasticity of symbiont acquisition throughout the life cycle of the shallow-water tropical lucinid *Codakia orbiculata* (Mollusca: Bivalvia)', *Environmental Microbiology*, 14, pp. 1584–1595. doi: 10.1111/j.1462-2920.2012.02748.x.

Hay, I. D., Belousoff, M. J. and Lithgow, T. (2017) 'Structural basis of type 2 secretion system engagement between the inner and outer bacterial membranes', *mBio*, 8, pp. 1–6. doi: 10.1128/mBio.01344-17.

Korotkov, K. V. and Sandkvist, M. (2019) 'Architecture, Function, and Substrates of the Type II Secretion System', *EcoSal Plus*, 8, pp. 227–244. doi: 10.1128/ecosalplus.esp-0034-2018.

Li, Y., Liles, M. R. and Halanych, K. M. (2018) 'Endosymbiont genomes yield clues of tubeworm success', *ISME Journal*, 12, pp. 2785–2795. doi: 10.1038/s41396-018-0220-z.

Masui, S., Sasaki, T. and Ishikawa, H. (2000) 'Genes for the type IV secretion system in an intracellular symbiont, *Wolbachia*, a causative agent of various sexual alterations in arthropods', *Journal of Bacteriology*, 182, pp. 6529–6531. doi: 10.1128/JB.182.22.6529-6531.2000.

Robinson, M. D., Mccarthy, D. J. and Smyth, G. K. (2010) 'edgeR : a Bioconductor package for differential expression analysis of digital gene expression data', *Bioinformatics*, 26, pp. 139–140. doi: 10.1093/bioinformatics/btp616.

Schurch, N. J., Schofield, P., Gierliński, M., Cole, C., *et al.* (2016) 'How many biological replicates are needed in an RNA-seq experiment and which differential expression tool should you use?', *Rna*, 22, pp. 839–851. doi: 10.1261/rna.053959.115.

Shifrin, D. A., Crawley, S. W., Grega-Larson, N. E. and Tyska, M. J. (2014) 'Dynamics of brush border remodeling induced by enteropathogenic *E. coli*', *Gut Microbes*, 5, pp. 504–516. doi: 10.4161/gmic.32084.

Smith, K. L. (1985) 'Deep-Sea Hydrothermal Vent Mussels : Nutritional State and Distribution at the Galapagos Rift', *Ecological Society of America*, 66, pp. 1067–1080.

Tavormina, P. L., Kellermann, M. Y., Antony, C. P., Tocheva, E. I., *et al.* (2017) 'Starvation and recovery in the deep-sea methanotroph *Methyloprofundus sedimenti*', *Molecular Microbiology*, 103, pp. 242–252. doi: 10.1111/mmi.13553.

Wallden, K., Rivera-Calzada, A. and Waksman, G. (2010) 'Type IV secretion systems: Versatility and diversity in function', *Cellular Microbiology*, 12, pp. 1203–1212. doi: 10.1111/j.1462-5822.2010.01499.x.

Wentrup, C., Wendeberg, A., Schimak, M., Borowski, C., *et al.* (2014) 'Forever competent: Deep-sea bivalves are colonized by their chemosynthetic symbionts throughout their lifetime', *Environmental Microbiology*, 16, pp. 3699–3713. doi: 10.1111/1462-2920.12597.

Williams, E. and Shimmin, M. A. (1978) 'Radiation-induced filamentation in obligate methylotrophs', 4, pp. 137–141.

“There are still a lot of unanswered questions.”

Personal contribution to each manuscript

Manuscript 1 (Chapter II)

***In situ* fixation reveals (dis)similar survival strategies in two endosymbionts of a deep-sea mussel host**

Conceptual design: 50%
Data acquisition and experiments: 50%
Analysis and interpretations of results: 80%
Preparation of figures and tables: 90%
Writing the manuscript: 80%

Manuscript 2 (Chapter III)

Lysosomal symbiont digestion shapes innate immunity and fuels the metabolism of bacteriocytes in a deep-sea mussel host

Conceptual design: 50%
Data acquisition and experiments: 50%
Analysis and interpretations of results: 70%
Preparation of figures and tables: 80%
Writing the manuscript: 70%

Manuscript 3 (Chapter IV)

Deep-sea *Bathymodiolus* mussels are resistant to short-term limitations of hydrothermal access

Conceptual design: 50%
Data acquisition and experiments: 50%
Analysis and interpretations of results: 90%
Preparation of figures and tables: 100%
Writing the manuscript: 100%

Acknowledgements

This thesis would not have been possible without the support of several people.

My sincerest thank you, **Prof. Dr. Nicole Dubilier,** for accepting me as a PhD student in your group and giving me the opportunity to conduct this research. I am very grateful for all experiences throughout the years including a research cruise, workshops and conferences that I could attend, and for all the people I met over the years. Also, thank you for reviewing this thesis.

Thank you, **Prof. Dr. Ute Hentschel Humeida,** for reviewing this thesis, for making the time to join the examination committee, and for your participation and input at my thesis committee meetings. I also thank **Prof. Dr. Michael Friedrich** and **Dr. Marcus Elvert** for joining the examination committee.

Special thanks to **Dr. Harald Gruber-Vodicka, Harald**, for being such great supervisor throughout my doctoral studies. You gave me the freedom to develop my skills and provided feedback when necessary. It was very enjoyable to work with you on my projects and manuscripts, and I appreciate the bioinformatical, scientific and writing skills I learned from you. Thank you also for joining the examination committee.

Thank you to **Dennis Jacob** for being part of my examination committee, and for your genuine interest in reading my thesis.

I also thank the other members of my thesis committee meetings **Nikolaus Leisch, Thorsten Reusch, Manuel Kleiner,** for the lively discussion, your feedback and scientific input that helped proceed to this stage.

I would also like to thank all of my co-authors **Maximilian Franke, Nikolaus Leisch, Thorsten Reusch, Claas Hiebenthal, Frank Melzner, Miguel Ángel González Porras, Rebecca Ansorge, Christian Borowski, Nicole Dubilier** and **Harald Gruber-Vodicka** for your great expertise, and your work and effort that you contributed to the research projects.

Thank you **Dr. Christiane Glöckner**, for your immense help on so many levels. I am grateful for all of your support during this important part of my career.

Prof. Dr. Colin Munn, **Colin,** thank you so much for guiding me on this academic path, and for your moral support over the years.

I would have been lost without the constant supply of research papers from **Bernd Stickfort**. Thank you very much for every single request you immediately answered. Thank you **Susanne Krüger, Ulrike Tietjen, Tina Peters, Martina Patze and Ralf Schwenke** for all administrative support.

I would like to thank the **Symbiosis Department** for everything I learned and all the experience I gained in the last years. I am grateful for the great scientific input and discussions that helped me grow as a scientist.

Thank you to our "Team Blue", **Tina** and **Anna**, for the fun discussions and the constructive feedback throughout the years.

Miguel, thank you for all the fun we had over the last years like organising the fall retreat, and for the awesome cooking recipes (especially the tomatoes).

Thank you **Benedikt**, for the being the partner-in-crime on the SO253 cruise, for all the fun and the constructive discussions.

Thank you **Christian**, for everything you taught us on the SO253 cruise, the New Caledonia trip, and for being the "to-go-to" person for all things "Bathy". I enjoyed learning from you, and appreciate your efforts and support to be available when needed.

Thank you for all the Bathy-specialists and former members of the Department, **Liz, Maxim, Adrien** and **Antony**. Thank you for all scientific input, in particular in the first period of my studies! Huge thanks also to the technicians **Silke, Martina** and **Miriam** for all the support during the laboratory work and the organisational help in preparation of SO253 cruise.

Special thanks also go to my "new" office, to **Merle and Janine**, for your friendship, your support and all the great discussions we had. I miss our office and the daily conversations, and cannot wait until the restrictions are lifted. Thank you for everything! Thank you also to my former office 2244**, Brandon, Antony, Yui** and **Svenja** for the great conversations and the good times.

I thank all former members of the Symbiosis Department that I am lucky to call my friends. Thank you **Rebecca**, for your support, advice, positivity, and for fun the game nights. **Rahel,** thank you for the great times and your friendship. I also thank **Anne-Christin** and **Juliane,** for all discussions, advice and support, and for the fun game nights.

Ich danke meiner **Familie** von ganzem Herzen für die permanente Unterstützung und Motivation seit Beginn meines Studiums. Gerade in dieser Zeit merkt man wie wichtig Familie ist, und ich bin dankbar für diese Stütze. Diese Arbeit widme ich meinen Großeltern, und vor allem **Opa**, der es kaum erwarten konnte einen Doktor in der Familie zu haben. Leider konntest du dies so kurz vor Ende nicht mehr miterleben. Wir vermissen dich.

Danke **Oliver**, vor allem für deine Geduld, dein gutes Zureden und auch für deine wissenschaftlichen Ratschläge. Danke **Mama, Papa und Malte** – ihr habt mir den Rücken gestärkt haben und meinen Traum vom Meeresbiologie-Studium unterstützt. Sorry Malte, aber Haie fand ich halt einfach nicht so cool. Vielleicht kann ich dich mit dieser Arbeit überzeugen, dass Muscheln auch ganz okay sind.

Ort, Datum: *Bremen, den 22.12.2020*

Versicherung an Eides Statt

Ich, *Målin Tietjen, Bgm.-Deichmann-Str. 63,* (Vorname, Name, Anschrift, Matr.-Nr.)
28217 Bremen

.

versichere an Eides Statt durch meine Unterschrift, dass ich die vorstehende Arbeit selbständig und ohne fremde Hilfe angefertigt und alle Stellen, die ich wörtlich dem Sinne nach aus Veröffentlichungen entnommen habe, als solche kenntlich gemacht habe, mich auch keiner anderen als der angegebenen Literatur oder sonstiger Hilfsmittel bedient habe.
Ich versichere an Eides Statt, dass ich die vorgenannten Angaben nach bestem Wissen und Gewissen gemacht habe und dass die Angaben der Wahrheit entsprechen und ich nichts verschwiegen habe.
Die Strafbarkeit einer falschen eidesstattlichen Versicherung ist mir bekannt, namentlich die Strafandrohung gemäß § 156 StGB bis zu drei Jahren Freiheitsstrafe oder Geldstrafe bei vorsätzlicher Begehung der Tat bzw. gemäß § 161 Abs. 1 StGB bis zu einem Jahr Freiheitsstrafe oder Geldstrafe bei fahrlässiger Begehung.

Bremen, den 22.12.2020